



UNIVERSITAT DE
BARCELONA

Pathophysiological understanding of acute decompensated heart failure: a proteomic approach

Elisa Diaz Riera

ADVERTIMENT. La consulta d'aquesta tesi queda condicionada a l'acceptació de les següents condicions d'ús: La difusió d'aquesta tesi per mitjà del servei TDX (www.tdx.cat) i a través del Dipòsit Digital de la UB (diposit.ub.edu) ha estat autoritzada pels titulars dels drets de propietat intel·lectual únicament per a usos privats emmarcats en activitats d'investigació i docència. No s'autoritza la seva reproducció amb finalitats de lucre ni la seva difusió i posada a disposició des d'un lloc aliè al servei TDX ni al Dipòsit Digital de la UB. No s'autoritza la presentació del seu contingut en una finestra o marc aliè a TDX o al Dipòsit Digital de la UB (framing). Aquesta reserva de drets afecta tant al resum de presentació de la tesi com als seus continguts. En la utilització o cita de parts de la tesi és obligat indicar el nom de la persona autora.

ADVERTENCIA. La consulta de esta tesis queda condicionada a la aceptación de las siguientes condiciones de uso: La difusión de esta tesis por medio del servicio TDR (www.tdx.cat) y a través del Repositorio Digital de la UB (diposit.ub.edu) ha sido autorizada por los titulares de los derechos de propiedad intelectual únicamente para usos privados enmarcados en actividades de investigación y docencia. No se autoriza su reproducción con finalidades de lucro ni su difusión y puesta a disposición desde un sitio ajeno al servicio TDR o al Repositorio Digital de la UB. No se autoriza la presentación de su contenido en una ventana o marco ajeno a TDR o al Repositorio Digital de la UB (framing). Esta reserva de derechos afecta tanto al resumen de presentación de la tesis como a sus contenidos. En la utilización o cita de partes de la tesis es obligado indicar el nombre de la persona autora.

WARNING. On having consulted this thesis you're accepting the following use conditions: Spreading this thesis by the TDX (www.tdx.cat) service and by the UB Digital Repository (diposit.ub.edu) has been authorized by the titular of the intellectual property rights only for private uses placed in investigation and teaching activities. Reproduction with lucrative aims is not authorized nor its spreading and availability from a site foreign to the TDX service or to the UB Digital Repository. Introducing its content in a window or frame foreign to the TDX service or to the UB Digital Repository is not authorized (framing). Those rights affect to the presentation summary of the thesis as well as to its contents. In the using or citation of parts of the thesis it's obliged to indicate the name of the author.



UNIVERSITAT DE
BARCELONA



HOSPITAL DE LA
SANTA CREU I
SANT PAU
UNIVERSITAT AUTÒNOMA DE BARCELONA



santpau
Institut
Investigació Biomèdica | Barcelona

Tesi doctoral

Pathophysiological understanding of acute decompensated heart failure: a proteomic approach

Memòria de tesi doctoral presentada per

Elisa Diaz Riera

**per optar al grau de doctora per la Universitat de
Barcelona**

Dirigida per:

Dra Teresa Padró Capmany

Prof Lina Badimon Maestro

Programa ICCV Cardiovascular – Institut de Recerca Hospital de
la Santa Creu i Sant Pau; IIB Sant Pau; Barcelona

Tutor:

Dr Julià González Martín

Servei de Microbiologia-CDB, Hospital Clínic de Barcelona;
Barcelona

**PROGRAMA DE DOCTORAT MEDICINA I RECERCA
TRANSLACIONAL**

**FACULTAT DE MEDICINA I CIÈNCIES DE LA SALUT.
UNIVERSITAT DE BARCELONA**

Març 2022

**Pathophysiological understanding of acute
decompensated heart failure:
A proteomic approach**

Memòria de tesi doctoral presentada per

Elisa Diaz Riera

per optar al grau de doctora per la Universitat de Barcelona

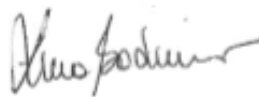
**Programa Cardiovascular ICC – Institut de Recerca
IIB Sant Pau Hospital de la Santa Creu i Sant Pau**

La directora



Dra Teresa Padró Capmany

La codirectora



Prof Lina Badimon Maestro

La doctoranda



Elisa Diaz Riera

Barcelona, 2022

Agraïments

Aquesta tesi no s'ha pogut completar si no hagués estat per l'ajuda, influència, i aportacions de moltes persones.

Primer de tot voldria donar les gràcies a la Dra Teresa Padró per donar-me l'oportunitat de participar en aquest projecte i per guiar-me al llarg d'aquests anys. Han estat moltes hores en el seu despatx fent, desfent i refent molts *abstracts*, figures, pòsters, manuscrits, i finalment la tesi, i també en trens per anar a recollir mostres, tot i que també va donar temps a fer alguna partida de cartes. També voldria donar les gràcies a la Prof. Lina Badimon per donar-me l'oportunitat de treballar al laboratori, i pel seu suport i consells al llarg d'aquests anys.

A la Fundació La Marató de TV3, i a tots els seus donants, que han fet possible la realització d'aquest projecte que espero que pugui, en un futur, ajudar a molts pacients.

També voldria agrair a la Maisa qui sempre ha estat disposada a ajudar-me, ensenyar-me coses noves, anar a recollir mostres al departament de Cardiologia pel projecte, passar estones fent *zip-tip* per preparar mostres pel MALDI, i moltes coses més: *Muuuuchas gracias!*

No em voldria oblidar de la Loli, qui m'ha ensenyat tot el que sé sobre la 2DE i la millor companya de debats sobre patinatge: *Muchas gracias! Se te echa de menos por el lab!*

A la Montse, qui m'ha ensenyat el món dels WB i dels ELISAs, qui m'ha acompanyat un munt de vegades a buscar mostres al biobanc: Moltes i moltes gràcies!

Voldria agrair el suport de tots aquells companys amb qui hem compartit tot tipus d'experiències bones i no tan bones: a la Soumaya per totes les estones i dubtes que m'ha resolt al llarg d'aquests anys. A l'Alba, la meva correctora particular, per llegir, corregir manuscrits i aquesta

mateixa tesi, per les estones al gimnàs i per molt més. Altra vegada a l'Alba i ara també a la Natàlia per totes les hores que hem passat de viatge en tren, passejant per les ciutats, jugant a cartes i, que no falti, processant mostres. A l'Àlex, per seguir-me les bromes i jocs de paraules amb les que a vegades deixem a més d'una persona sense entendre res. També voldria donar les gràcies tots els altres companys i companyes que han anat arribant i marxant al llarg dels anys: Hue, Vicky, Tomeu, Pablo, Aureli, Leonie, Carmen, Anna i Sebastià. Amb ells i elles he compartit nits de trasplantaments, partides de pàdel, discussions preparant pòsters, manuscrits i presentacions, incomptables esmorzars i dinars, i un cop acabada la jornada laboral, moltes tardes jugant a jocs de taula. Tots ells han estat grans fitxatges que han fet que aquests anys hagin passat més ràpid. A tots vosaltres: Moltes gràcies! Sembla que acabar la tesi queda molt lluny, però ja queda menys! Molts ànims!

També estic molt agraïda a l'Esther, l'Olaya, la Sonia, la Mari, la Mònica, la Nerea, el Rafael, les Roses, i a tota la resta de personal del laboratori per la seva ajuda amb experiments i suport al llarg d'aquests anys.

També voldria donar les gràcies a tots els qui han participat per part de l'hospital: al Dr Xavier Garcia-Moll i la Dra Laura López principalment, però també a tots els residents que han participat al llarg de l'estudi. Però, sobretot, a tot l'equip d'infermeria de B3: Dani, María José, les Laures i Marines, etc que, a part d'aconseguir mostres per l'estudi i algun *suc de poma*, també m'han convidat a esmorzar en diverses ocasions els caps de setmana. I també a tots aquells infermers i infermeres de l'hospital que també hagin participat en algun moment. Sense la seva participació realment no s'hauria pogut dur a terme aquest projecte.

Voldria agrair l'oportunitat de participar en les jornades a la Fundació d'Hipercolesterolèmia Familiar. Però sobretot a la Raquel amb qui

també hem passat moltes estones recollint mostres, passejant per les ciutats, buscant imants, sopant, mirant i discutint d'Eurovisió. A tots ells: *Muuuchas gracias!*

No em puc oblidar dels meus amics de sempre: Cris, Laura, Arantxa, Lórien, Àngels, Èric, Isma, Dani, Àlex, Andrea, Bernat, Jaume, Eli i Ari. Han estat molts i molts anys compartint un munt d'hores jugant, viatjant, resolent *escape rooms*, rient, saltant i, que no falti, estudiant, però mai ha faltat el seu suport durant aquesta tesi.

També voldria agrair el seu suport incondicional a tots els meus familiars: la meva àvia, Isabel, Reina, Jaume, Olga, Lali, i els meus cosins Jordi, Joan, Dario i Ton. Tots ells i elles m'han procurat amb el eu suport incondicional i amb moltes i moltes carmanyoles. Als meus éssers preferits que m'han fet descansar quan ho necessitava (i quan no també) i sempre han estat contents que fos allà: la Mel, el Sol i la Mia.

Last but not least, estaré eternament agraïda als meus pares per tot el seu suport. Gràcies a ells estic on estic avui i he pogut realitzar aquesta tesi.

Index

AGRAÏMENTS	IV
INDEX	VII
LIST OF FIGURES	X
LIST OF TABLES	XI
ABBREVIATIONS	XII
ARTICLES PUBLICATS	XVIII
RESUM	XX
ABSTRACT	XXIII
1. INTRODUCTION	2
1.1. EPIDEMIOLOGY OF HEART FAILURE	2
1.2. CLINICAL RELEVANCE OF HEART FAILURE	3
1.3. ADHF PATHOPHYSIOLOGY	7
1.3.1. <i>Renin-angiotensin-aldosterone system</i>	9
1.3.2. <i>Immune system and inflammation</i>	11
1.3.2.1. Interleukins, cytokines & growth factors	12
1.3.2.2. Complement system.....	15
1.3.3. <i>Haemostasis imbalances</i>	17
1.3.3.1. Hypercoagulability.....	18
1.3.3.2. Endothelial dysfunction	18
1.3.3.3. Blood flow stasis.....	19
1.3.4. <i>Extracellular matrix remodelling</i>	19
1.3.5. <i>Other mechanisms</i>	20
1.4. ADHF AS A MULTIORGAN DISORDER	21
1.4.1. <i>Cardiorenal syndrome</i>	23
1.4.1.1. <i>Cardiorenal syndrome type 1</i>	25

1.5.	PROTEIN BIOMARKERS	27
1.5.1.	<i>Biomarkers in acute heart failure</i>	27
1.5.1.1.	Acute heart failure	28
1.5.1.2.	Kidney function evaluation in AHF	31
1.5.2.	<i>Plasma/serum and urine as matrices for biomarker analysis in acute heart failure</i>	36
1.5.2.1.	Urine as a sample	36
1.5.3.	<i>Urinary proteomics in heart and kidney failure</i>	38
1.5.4.	<i>Proteomic approaches to identify and characterise differential proteomic signatures</i>	41
1.6.	PROTEOMIC APPROACHES	42
1.6.1.	<i>Two-dimensional electrophoresis</i>	42
1.6.2.	<i>Mass spectrometry</i>	45
1.7.	FUTURE PERSPECTIVES.....	47
2.	HYPOTHESIS	49
3.	OBJECTIVES	51
4.	MATERIALS AND METHODS	53
4.1.	EXPERIMENTAL DESIGN	53
4.2.	PATIENTS	54
4.2.1.	<i>ADHF study</i>	54
4.2.2.	<i>Patients of the mechanistic study</i>	59
4.3.	SAMPLING	61
4.4.	BIOCHEMICAL VARIABLES.....	61
4.5.	TWO-DIMENSIONAL ELECTROPHORESIS	62
4.5.1.	<i>2DE urine sample preparation</i>	63
4.5.2.	<i>First dimension</i>	63
4.5.3.	<i>Second dimension</i>	65
4.6.	DIFFERENTIAL ANALYSIS	66
4.7.	PROTEIN IDENTIFICATION	66
4.8.	MASS SPECTROMETRY	67

4.9.	VALIDATION TECHNIQUES	68
4.9.1.	<i>Western Blot</i>	69
4.9.2.	<i>ELISA immunoassay</i>	71
4.10.	METHODS FOR MECHANISTIC STUDIES.....	73
4.10.1.	<i>Vascular smooth muscle cells</i>	73
4.10.2.	<i>Cell adhesion and wound healing</i>	73
4.10.3.	<i>Confocal microscopy</i>	74
4.11.	STATISTICAL ANALYSIS	74
5.	RESULTS.....	77
5.1.	ARTICLE 1	78
5.2.	ARTICLE 2	111
5.3.	ARTICLE 3	145
5.4.	ARTICLE 4	190
6.	DISCUSSION.....	215
7.	CONCLUSIONS	223
8.	REFERENCES	226

List of figures

FIGURE 1: EPIDEMIOLOGY OF HEART FAILURE.	3
FIGURE 2: SCHEMATIC ADHF PATHOPHYSIOLOGY.....	7
FIGURE 3: PATHOPHYSIOLOGICAL MECHANISMS AFFECTING HEART FAILURE.....	8
FIGURE 4: RAAS ACTIVATION PATHWAY AND ITS ADVERSE EFFECTS.....	10
FIGURE 5: CYTOKINES AND CRP EFFECTS ON THE HEART.....	14
FIGURE 6: SIMPLIFIED COMPLEMENT SYSTEM PATHWAY.	15
FIGURE 7: MAIN ORGANS AFFECTED IN HEART FAILURE.	22
FIGURE 8: MECHANISMS INVOLVED IN CARDIORENAL SYNDROME.....	24
FIGURE 9: URINE PRODUCTION.....	37
FIGURE 10: PROTEOMIC TECHNIQUES SUMMARISED.....	42
FIGURE 11: REPRESENTATIVE 2DE GEL.....	43
FIGURE 12: MALDI-TOF MASS SPECTROMETER PRINCIPLE.....	45
FIGURE 13: EXPERIMENTAL DESIGN.	54
FIGURE 14: SUMMARISED 2DE WORKFLOW.....	62
FIGURE 15: SUMMARISED MASS SPECTROMETRY WORKFLOW	67
FIGURE 16: SANDWICH ELISA STEPS.....	71

List of tables

TABLE 1: COMMON HEART FAILURE COMORBIDITIES.....	4
TABLE 2: HEART FAILURE CLASSIFICATION ACCORDING TO LEFT VENTRICULAR EJECTION FRACTION.	5
TABLE 3: CARDIORENAL SYNDROME CLASSIFICATION	25
TABLE 4: ESTABLISHED AND POTENTIAL BIOMARKERS IN AHF.	28
TABLE 5: EXPERIMENTAL AND CLINICAL STUDIES CONCERNING URINARY PROTEOMICS	40
TABLE 6: CLINICAL CHARACTERISTICS OF ADHF PATIENTS.....	57
TABLE 7: CLINICAL CHARACTERISTICS OF 2DE PATIENTS.	58
TABLE 8: DEMOGRAPHIC AND CLINICAL CHARACTERISTICS OF FAMILIAL HYPERCHOLESTEROLAEMIA POPULATION.	60
TABLE 9: ISOELECTRIC FOCUSING STEPS AND THEIR CHARACTERISTICS..	64
TABLE 10: ANTIBODIES USED FOR WESTERN BLOT.....	70
TABLE 11: ELISAS USED TO ANALYSE URINE SAMPLES.	72
TABLE 12: ELISAS USED TO ANALYSE BLOOD SAMPLES.....	72

Abbreviations

ACE	angiotensin-converting enzyme
ACN	acetonitrile
ACS	acute coronary syndrome
ADHF	acute decompensated heart failure
ADQI	Acute Dialysis Quality Initiative
agLDL	aggregated LDL
AHF	acute heart failure
AKI	acute kidney injury
AKIN	Acute Kidney Injury Network
AMBIC	ammonium bicarbonate
ApoB	apolipoprotein B
ARB	angiotensin II type I receptor blockers
ARSA	aryl sulphatase A
AT	atherosclerosis
ATTR	transthyretin amyloidosis
AT3	antithrombin III
AUC	area under the curve
AZGP1	zinc- α_2 -glycoprotein
BNP	brain natriuretic peptide
BSA	bovine serum albumin
B2M	β_2 -microglobulin
CAD	coronary artery disease
CE-MS	capillary electrophoresis mass spectrometry
CFH	complement factor H
CHAPS	3-[(3-cholamidopropyl)dimethylammonio]-1-propanesulfonate
CHF	chronic heart failure
CKD	chronic kidney disease

COPD	chronic obstructive pulmonary disease
CRP	C reactive protein
CRS	cardiorenal syndrome
CS	cardiogenic shock
CTA	computed tomographic angiography
cTn	cardiac troponin
cTnT	cardiac troponin T
CTSD	cathepsin D
CysC	cystatin C
C3	complement C3
C3a	complement C3 activated
C3a R	activated C3 receptor
C5	complement C5
DAMPs	damage-associated molecular patterns
DIGE	difference gel electrophoresis
DTT	dithiothreitol
ECM	extracellular matrix
EDTA	ethylene diamine tetraacetic acid
ELISA	enzyme-linked immunosorbent assay
FCS	foetal calf serum
FDR	false discovery rate
FGG	fibrinogen γ -chain
FH	familial hypercholesterolaemia
Gal-3	galectin 3
GC-MS	gas chromatography mass spectrometry
GFR	glomerular filtration rate
GO	Gene Ontology
GPCRs	G protein-coupled receptors
HCCA	α -cyano-4-hydroxycin-namic acid

HDL	high density lipoprotein
HF	heart failure
HFmrEF	HF with mildly reduced ejection fraction (41-49%)
HFpEF	HF with preserved ejection fraction ($\geq 50\%$)
HFrEF	HF with reduced ejection fraction ($\leq 40\%$)
HS	healthy subjects group
HT	hypertension
H-FABP	heart-type fatty acid binding protein
hVSMCs	human vascular smooth muscle cells
ICAT	isotope-coded affinity tag
IEF	isoelectric focusing
IGFBP7	insulin-like growth factor-binding protein 7
IgG	immunoglobulin G
IL	interleukin
IPG	immobilised pH gradient
IQR	interquartile range
iTRAQ	isobaric tag for relative and absolute quantitation
I/R	ischaemia / reperfusion
KDIGO	Kidney Disease Improving Global Outcomes
KIM-1	kidney injury molecule 1
KNG	kininogen 1
LC-MS	liquid chromatography mass spectrometry
LDL	low density lipoprotein
LLT	lipid-lowering therapy
Lp(a)	lipoprotein (a)
LRG1	leucine rich α -2-glycoprotein (LRG1)
LV	left ventricle
LVDP	left ventricular diastolic pressure
LVEF	left ventricular ejection fraction

L-FABP	liver fatty acid binding protein
MAC	membrane attack complex
MALDI	matrix-assisted desorption ionisation
MALDI-ToF	matrix-assisted desorption ionisation time of flight
MASP1/2	mannan-binding lectin serine protease 1/2
MDRD-4	Modification of Diet in Renal Disease
MI	myocardial infarction
MPAs	monocyte-platelet aggregates
MR-proANP	mid-regional pro atrial natriuretic peptide
MS	mass spectrometry
NAG	N-acetyl- β -D-glucosaminidase
NFκB	nuclear factor kappa-light-chain-enhancer of activated B cells
NGAL	neutrophil gelatinase-associated lipocalin
NO	nitric oxide
noRI	group of ADHF patients did not develop renal injury
NRF	group of ADHF patients with normal renal function
NP	natriuretic peptides
NT-proBNP	N-terminal prohormone of brain natriuretic peptide
OPG	osteoprotegerin
ORM1	Orosomucoid-1
PAI-1	plasminogen activator inhibitor 1
PAMPs	pathogen-associated molecular patterns
pAT3	plasma antithrombin III
PBS	phosphate buffered saline
PCR	polymerase chain reaction
pCRP	plasma C reactive protein
pC3	plasma complement C3
PGBM	basement membrane-specific heparan sulphate proteoglycan core protein

pI	isoelectric point
PMF	peptide mass fingerprinting
PO	pulmonary oedema
PPI	protein-protein interaction
PRR	pattern-recognition receptors
pTTR	plasma transthyretin
PTM	posttranslational modification
RAAS	renin-angiotensin-aldosterone system
RBP4	retinol binding protein 4
RD	group of ADHF patients with renal disease
RI	group of ADHF patients who developed renal disease
RIFLE	Risk, Injury, Failure, Loss of kidney function, and End-stage kidney disease
ROC	receiver operating characteristic
ROS	reactive oxygen species
RT-PCR	reverse transcription polymerase chain reaction
sCr	serum creatinine
SDS	sodium dodecyl sulphate
SDS-PAGE	sodium dodecyl sulphate polyacrylamide gel electrophoresis
SELDI	surface-enhanced laser desorption/ionisation
SELDI-ToF	surface-enhanced laser desorption-ionisation time of flight
SEM	standard error of the mean
SERPINA1	α -1-antitrypsin
SMC	smooth muscle cell
sST2	soluble suppression of tumorigenicity 2
SWATH-MS	sequential window acquisition of all theoretical mass.
TAT	thrombin-antithrombin complex
TBS	TRIS buffered saline

TBS-T	TRIS buffered saline with tween
TFA	trifluoroacetic acid
TGF-β	transforming growth factor β
TIMP2	tissue inhibitor of metalloproteinase-2
TLRs	toll-like receptors
TNF	tumour necrosis factor
TnI	troponin I
tPA	tissue plasminogen activator
TRIS	tris(hydroxymethyl)aminomethane
TTR	transthyretin
uAT3	urinary antithrombin III
uC3	urinary complement C3
uTTR	urinary transthyretin
VCAM-1	vascular cell adhesion molecule 1
VDBP	vitamin D binding protein
VDR	vitamin D receptor
VP	vasopressin
VSMC	vascular smooth muscle cell
WB	western blot
WRF	worsening renal function
1DE	one dimensional electrophoresis
2DE	two dimensional electrophoresis
2DE-MS	two dimensional electrophoresis coupled to mass spectrometry

Articles publicats

Tesi en format de compendi d'articles:

Article 1:

Urinary proteomic signature in acute decompensated heart failure: advances into molecular pathophysiology

Elisa Diaz-Riera; Maísa García Arguinzonis; Laura López; Xavier Garcia-Moll; Lina Badimon; Teresa Padro

Published: International Journal of Molecular Sciences

Int. J. Mol. Sci. 2022, 23, 2344. <https://doi.org/10.3390/ijms23042344>

Impact Factor 2020: 5.924

Article 2:

Vitamin D Binding Protein and renal injury in acute decompensated heart failure

Elisa Diaz-Riera; Maisa García Arguinzonis; Laura López; Xavier Garcia-Moll; Lina Badimon; Teresa Padro

Accepted: Frontiers in Cardiovascular Medicine

Front. Cardiovasc. Med. DOI: 10.3389/fcvm.2022.829490

Impact Factor 2020: 6.050

Article 3:

Alternative C3 Complement System: Lipids and Atherosclerosis

Maisa García-Arguinzonis; **Elisa Diaz-Riera**; Esther Peña; Rafael Escate; Oriol Juan-Babot; Pedro Mata; Lina Badimon; Teresa Padró

Published: International Journal of Molecular Sciences

Int. J. Mol. Sci. 2021, 22, 5122. <https://doi.org/10.3390/ijms22105122>

Impact Factor 2020: 5.924

Resum

Pathophysiological understanding of acute decompensated heart failure: a proteomic approach

Introducció: La insuficiència cardíaca és una condició patològica dinàmica que presenta freqüentment episodis aguts d'empitjorament, coneguts com insuficiència cardíaca aguda descompensada (*acute decompensated heart failure, ADHF*, per les seves sigles en anglès). Es tracta d'una síndrome clínica complexa que pot afectar diversos òrgans i que involucra diferents mecanismes fisiopatològics, els efectes dels quals no es coneixen completament. L'ADHF està relacionada amb la disfunció renal, la qual afecta l'evolució de la malaltia i dona lloc a un major risc de complicacions. La nostra hipòtesi és que la identificació i una millor caracterització, mitjançant un enfocament proteòmic, de les proteïnes associades amb la descompensació aguda de la insuficiència cardíaca contribuiria a comprendre la fisiopatologia de la malaltia, aportaria un fenotip més precís i permetria identificar millor els pacients amb una pitjor evolució de la malaltia.

Objectius: L'objectiu d'aquesta tesi va ser identificar i caracteritzar la signatura proteica diferencial a l'orina de pacients amb ADHF en associació amb funcions moleculars i processos biològics relacionats amb la progressió de la malaltia.

Mètodes: A l'estudi s'hi van incloure pacients admesos a l'Hospital de la Santa Creu i Sant Pau. Les mostres d'orina es van analitzar mitjançant un enfocament no dirigit d'espectrometria de masses, i es van comparar amb les d'un grup d'individus sans a través d'electroforesi bidimensional acoblada a espectrometria de masses (MALDI-ToF/ToF). Es van realitzar anàlisis *in silico* i es van seleccionar proteïnes per a estudis de validació posteriors mitjançant immunoassaigs específics (ELISA), en mostres d'orina i plasma/sèrum. Els grups de comparació

d'ADHF es van definir per la filtració glomerular i la fracció d'ejecció del ventricle esquerre (FEVE). Es va utilitzar un grup d'individus sans per determinar el rang normal. La capacitat de les proteïnes per identificar els pacients ADHF segons la seva patologia, severitat de la malaltia i pronòstic es va obtenir mitjançant l'anàlisi de la corba característica operativa del receptor (ROC curve en anglès) i l'anàlisi de corba de supervivència de Kaplan-Meier. També es van realitzar estudis de mecanismes de la funció cel·lular.

Resultats: La signatura diferencial va mostrar 26 proteïnes (amb canvis de més d'1.5 vegades), la majoria d'origen hepàtic. Aquestes proteïnes estan associades a funcions i processos moleculars, com ara el transport, l'hemostàsia i la immunitat. Cal destacar que es van observar nivells elevats a l'orina de l'ingrés hospitalari de transtiretina (TTR), antitrombina III (AT3), complement C3 (C3) i la proteïna transportadora de la vitamina D (VDBP) en comparació amb individus sans. Els nivells elevats de pèrdua en orina de proteïnes com la TTR i la proteïna d'unió al retinol 4 (*retinol binding protein 4*, RBP4, en anglès) podrien tenir un impacte perjudicial en l'evolució de la malaltia, donant lloc a un elevat risc de complicacions. A més, els nivells elevats d'AT3 a l'orina i al plasma van permetre identificar els pacients amb ADHF amb disfunció renal i FEVE conservada o lleugerament reduïda. Més enllà del seu paper en la coagulació, l'AT3 es correlaciona amb C3, un dels principals components de la immunitat innata, independentment de la inflamació sistèmica. Curiosament, C3 es localitza a la matriu extracel·lular vascular i estimula funcions cel·lulars com l'adhesió, la migració i la reorganització del citoesquelet. Els nivells de VDBP, juntament amb els de cistatina C i KIM-1 (*kidney injury molecule 1* en anglès), podrien ajudar a estratificar els pacients d'ADHF amb major risc de desenvolupar dany renal durant l'hospitalització.

En conclusió, els resultats d'aquesta tesi mostren una signatura de proteïnes en orina en pacients d'ADHF molt diversa però, a la vegada, diferent a la d'individus sans. Els resultats obtinguts suggereixen un impacte perjudicial de la signatura diferencial de proteïnes en l'evolució de la malaltia, donant lloc a un major risc de complicacions després de l'alta hospitalària. Són necessaris més estudis en poblacions més grans per validar la rellevància de la signatura de proteïnes diferencials identificada en la fisiopatologia de l'ADHF.

Abstract

Pathophysiological understanding of acute decompensated heart failure: a proteomic approach

Introduction: Heart failure is a dynamic pathological condition that frequently presents episodes of acute worsening, recognised as acute decompensated heart failure (ADHF). This is a complex clinical condition that may affect different organs and involve several pathophysiological mechanisms that remain incompletely understood. ADHF is often related to kidney dysfunction, which impacts disease evolution resulting in higher risk for adverse outcomes. It is our hypothesis that identification and better characterisation by proteomic approaches of proteins associated with heart failure decompensation would contribute to gain understanding of the disease pathophysiology, support a more accurate disease phenotyping, and better identify patients with poor disease evolution.

Objectives: The aim of this thesis was to identify and characterise the differential protein signature in urine of ADHF patients in association with molecular functions and biological processes related to disease progression.

Methods: ADHF patients admitted to the emergency room at Hospital de la Santa Creu i Sant Pau were included in the study. Urine samples were analysed by an untargeted mass spectrometry approach and compared with a group of healthy subjects by 2 dimensional electrophoresis coupled to mass spectrometry (MALDI-ToF/ToF). *In silico* analysis was performed and proteins selected for further validation studies using specific immunoassays (ELISA), in urine and plasma/serum samples. ADHF comparison groups were defined by the glomerular filtration rate and left ventricular ejection fraction (LVEF). Healthy subjects were used to determine the normal range. Protein

power to discriminate ADHF patients according to their pathology, disease severity, and prognosis was achieved by Receiver operating curve (ROC) and Kaplan-Meier survival curve analysis. Cell function mechanistic studies were also performed.

Results: A differential signature of 26 proteins (more than 1.5 fold), mostly of hepatic origin, was identified. These proteins relate to molecular functions and processes, such as transport, haemostasis, and immunity. Of note, we observed elevated levels in urine at hospital admission of transthyretin (TTR), antithrombin III (AT3), complement C3 (C3) and vitamin D binding protein (VDBP) when compared to HS. The increased urinary loss of proteins, such as TTR and retinol binding protein 4 (RBP4) may have a harmful impact on disease evolution resulting in higher risk for adverse outcomes after hospital discharge. Furthermore, high AT3 levels in urine and plasma identified those ADHF patients with renal dysfunction and preserved and mildly reduced LVEF. AT3, beyond its role in coagulation, correlates with C3, a key component of innate immunity, independently of systemic inflammation. Interestingly, C3 is localised in vascular extracellular matrix and stimulates cell functions such as adhesion, migration and cytoskeletal reorganisation. Levels of VDBP, along with cystatin C and KIM-1, could help to stratify ADHF patients at higher risk of developing kidney injury during hospitalisation.

In conclusion, the results of this thesis show a urinary protein signature in ADHF patients highly diverse yet different from healthy individuals. The obtained results suggested a harmful impact of the differential protein signature on disease evolution resulting in a higher risk for adverse outcomes after hospital discharge. Future studies in larger populations are needed to validate the relevance of the identified differential protein signature in ADHF pathophysiology.

CHAPTER I: INTRODUCTION

1. Introduction

1.1. Epidemiology of heart failure

Heart failure (HF) is one of the most important causes of morbidity and mortality in the industrialised world. Heart failure is defined as a clinical syndrome with signs and/or symptoms caused by functional and/or structural abnormalities in the heart that leads to abnormal cardiac function, with impaired ventricular filling or ejection of blood, elevated natriuretic peptides and/or evidence of pulmonary or systemic congestion (1,2).

The prevalence of symptomatic HF is estimated to range from 0.4 to 2.0% in general the European population, and over 10% among the elder population (3–6). A recent Spanish study indicates that HF incidence ranges <1% in the younger population (18-44 years old), 2.1% between 45-64 years old, 3.5% between 65-79 years old and 8.7% in the elder population (>80 years old) (7), as shown in **Figure 1**. While it is the first cause of hospitalisation of people over 65 years old, it represents 3% of hospital admissions and 2.5% of health care costs (8). Despite the discovery and development of several new therapeutic strategies, many patients do not respond well to guidelines therapy, and their prognosis remains poor (9).

Heart failure is often divided in two different presentations: chronic heart failure (CHF) and acute heart failure (AHF), that can be presented as a decompensation (ADHF) of a CHF patient or *de novo*, that is as a new occurrence in the patient.

Acute heart failure is the first cause of hospitalisation in the elderly population (>65 years old) in industrialised countries, and is associated with high mortality and rehospitalisation rates (1), with in-hospital

mortality ranging from 4-10% (10–12), 60 to 90 day mortality ranging from 7% to 11%, and 60 to 90 day rehospitalisation rate from 25% to 30% (13) despite the therapeutic advances. In Spain, about 100.000 hospitalisations annually occur for this reason, and it is the main determinant of the huge expenditure related to AHF.

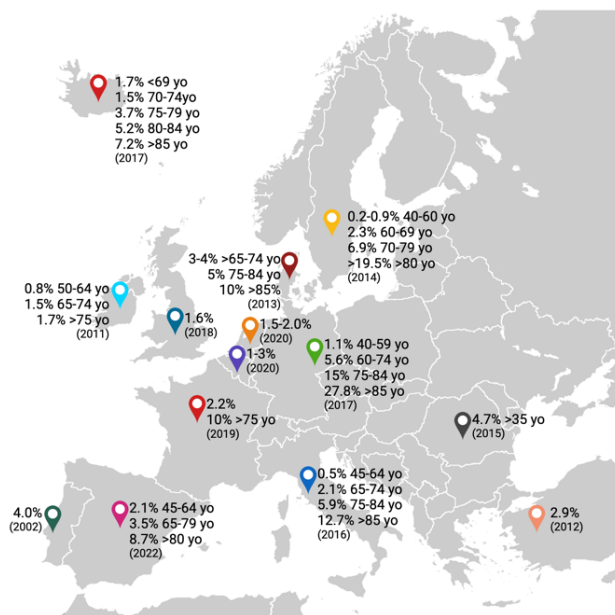


Figure 1: Epidemiology of heart failure.

Heart failure prevalence of several European countries. yo refers to years old; data obtained from several sources (7,14–23).

1.2. Clinical relevance of heart failure

Heart failure is mainly characterised by the impaired ejection of blood or ventricular filling (24). However, it also presents a great variety of signs and symptoms such as dyspnoea, elevated jugular venous pressure, as well as pulmonary congestion (an abnormal amount of fluid in the lungs or other organs), or tachycardia that can be caused by a structural and/or functional abnormality in the heart, resulting in a reduced cardiac output and/or elevated intracardiac pressures during stress or at rest (4,5).

Currently, HF diagnosis is restricted to stages with apparent clinical symptoms. Asymptomatic, structural or functional cardiac abnormalities, which are HF precursors, can already be present in patients before clinical symptoms appear (5,25). HF is usually caused by a myocardial abnormality that causes systolic and/or diastolic ventricular dysfunction. However, it can also be caused by abnormalities in the pericardium, endocardium, heart rhythm, or valves. It is essential to determine the underlying cause, as each pathology requires specific treatment, such as valve replacement, heart rhythm reduction, or specific pharmacological options. Furthermore, HF is often complicated by common comorbidities such as atrial fibrillation, diabetes, or chronic kidney disease (**Table 1**).

Table 1: Common heart failure comorbidities.

	Characteristics	Effect
Atrial fibrillation (AF)	Main arrhythmia in heart failure (up to 25% prevalence) Elevated heart rate at rest and exaggerated response to exercise Loss of ventricular response and atrial contractile function	Exacerbates HF Persistent tachycardias eventually precipitate HF
Chronic kidney disease (CKD)	High prevalence, 30-50% in HF patients Established risk factor for adverse events	Activation of vicious cycles that advance heart and kidney deterioration Complicates decongestive therapy
Chronic obstructive pulmonary disease (COPD)	Loss and remodelling of bronchiolar architecture 9-41% prevalence in Europe More prevalent in men and in urban areas Mainly caused by smoking history	Present 4.5x higher risk to develop HF
Coronary artery disease (CAD)	Atherosclerotic disease due to accumulation of lipoprotein droplets May present genetic origin, such as familial hypercholesterolaemia	Unstable angina, myocardial infarction, cardiac sudden death
Diabetes	Insulin resistance, also associated with independent predictor of HF May induce inflammation, fibrosis, ROS cascade	2x risk of developing HF Worse prognosis and increased severity

Adapted from several sources (26–39).

According to the 2021 Guidelines by European Society of Cardiology, heart failure patients are usually stratified in three different groups based on the contractile function of the left ventricular myocardium as outlined in **Table 2**, this includes HF with reduced ejection fraction (HFrEF), HF with preserved ejection fraction (HFpEF) (40), and the most recent category of HF with mildly reduced ejection fraction (HFmrEF) (1).

Table 2: Heart failure classification according to left ventricular ejection fraction.

Ejection fraction		Characteristics	Comorbidities
Reduced EF (HFrEF)	≤40%	Deficient pump volume Deficient cardiac output Progressive dilation Adverse cardiac remodel of left ventricle >75 years old Black population	Atrial fibrillation Kidney dysfunction Diabetes Coronary artery disease
Mildly reduced (HFmrEF)	41-49%	Elevated BNP and NT-proBNP Structural heart disease Very similar to HFrEF	Elevated incidence of coronary artery disease
Preserved (HFpEF)	≥50%	Cardiac amyloidosis Hypertrophic cardiomyopathy Shrinkage of left ventricle Older population Primarily female	Atrial fibrillation Chronic kidney disease Other non-cardiovascular

Adapted from 2021 Guidelines (1).

Different cardiovascular and non-cardiovascular factors can cause or precipitate the deterioration of heart function, and possibly lead to hospitalisation (1). Among cardiovascular causes are acute coronary syndrome, bradycardia (slow heart rate), tachycardia (rapid heart rate), myocarditis, or aortic dissection, among others. Non-cardiovascular factors such as anaemia, kidney dysfunction, pregnancy, excessive physical exercise, hyperthyroidism, or hypothyroidism, among others, can also precipitate AHF. Moreover, poor compliance with medication, drugs and/or alcohol abuse, as well as excessive salt or fluid intake can also cause AHF (13).

Currently, AHF diagnosis depends on several factors: patient history, and signs and symptoms. Signs and symptoms are analysed by several techniques including, but not limited to, echocardiography, chest X-ray, electrocardiogram, and elevated natriuretic peptides levels in blood (1).

AHF is treated with both pharmacological and non-pharmacological strategies, and it must be started promptly and parallelly. Intravenous diuretics are crucial in ADHF treatment, such as furosemide or torasemide, are characterised by their rapid onset and efficacy, thus being commonly used to avoid or diminish congestion. Once the patients are stable, they are transitioned to oral diuretics. However, depending on their condition they may require a combination of diuretics, and their doses may be reassessed depending on their kidney function (1).

Several different manifestations of AHF have been defined. However, the most common are *de novo* (or new onset) heart failure, or worsening or a decompensation of CHF, commonly known as acute decompensated heart failure (ADHF), which is the type concerning this project. Other phenotypes are cardiogenic shock (CS), right-sided HF, pulmonary oedema (PO), and acute coronary syndrome (11).

Fluid status and cardiac output define the kinds of ADHF presentation and their treatment. Patients are classified depending on whether they are congested (wet) or not congested (dry), and on whether they exhibit adequate perfusion (warm) or poor perfusion (cold) (41). Thus, venous congestion is defined as elevated left ventricular diastolic pressure (LVDP), that is related to dyspnoea, oedema or abnormal lung sounds, all of which are hallmark signs and symptoms of ADHF (42). High LVDP in HF patients without apparent clinical congestion was coined as *haemodynamic congestion*, which can anticipate clinical congestion by several days or even weeks (42,43). Haemodynamic congestion can activate neurohormones, and lead to subendocardial ischaemia, resulting in myocardial necrosis, fibrosis or apoptosis, further

deteriorating heart function (42,44). However, a lot remains to be unravelled.

1.3. ADHF pathophysiology

Acute decompensated heart failure is a complex clinical condition that affects different organs and involves several pathophysiological mechanisms. Until now, the underlying biological processes have not been completely elucidated (45), emphasising the need for a deeper understanding of the molecular functions and pathways associated to the ADHF pathophysiology (**Figure 2**).

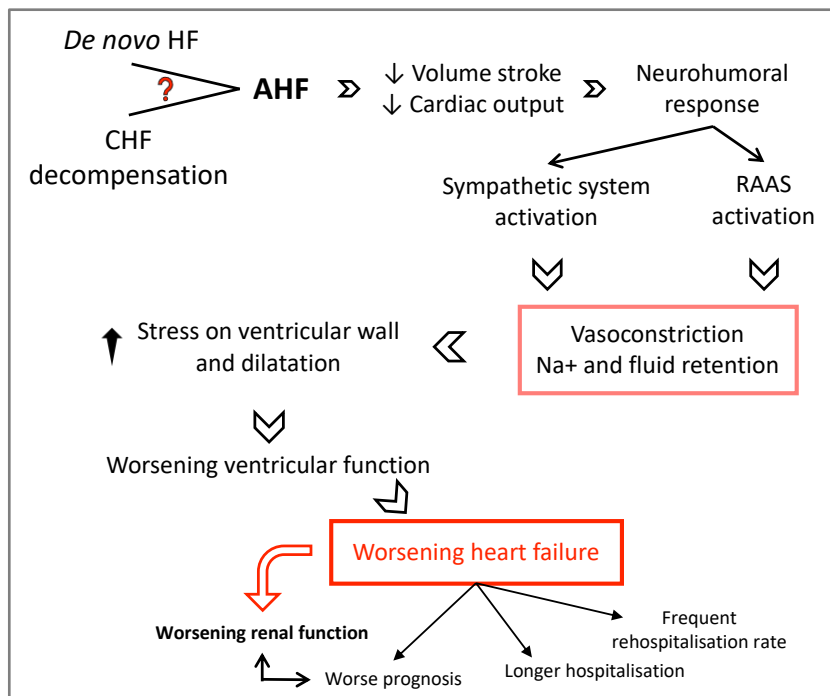


Figure 2: Schematic ADHF pathophysiology.

AHF: acute heart failure; CHF: chronic heart failure; RAAS: renin-angiotensin-aldosterone system. Adapted from Jackson *et al.* (46).

In the heart, the elevation of ventricular filling pressure leads to increasing ventricular wall tension, myocardial stretching and

remodelling, which contributes to progressive worsening in cardiac contractility, valvular regurgitation and systemic congestion (47), this can also emerge from growing accumulation of fluid through other mechanisms, such as sodium retention from kidney disease, noncompliance with medication or diet, arrhythmias, infections, uncontrolled hypertension, cardiac ischaemia, or pulmonary embolisms among others (45,48). Systemic congestion is present in most AHF patients, and, in addition to impaired cardiac function, other organs participate in the development and propagation of congestion. Therefore, congestion is one of the most important pathophysiological mechanisms of damaged organ function in ADHF. If present, hypoperfusion can cause further deterioration of organ function, which is associated with increased mortality. Decongestive therapies have been associated with reduced mortality risk, thus, prevention and treatment are essential therapeutic targets in ADHF patients (47).

Within ADHF pathophysiology, several mechanisms have been suggested to be dysregulated, contributing to the disease severity and progression. This includes alterations in renin-angiotensin-aldosterone system, inflammatory and immune system, the haemostatic pattern, in the extracellular matrix, and natriuretic peptides (**Figure 3**).

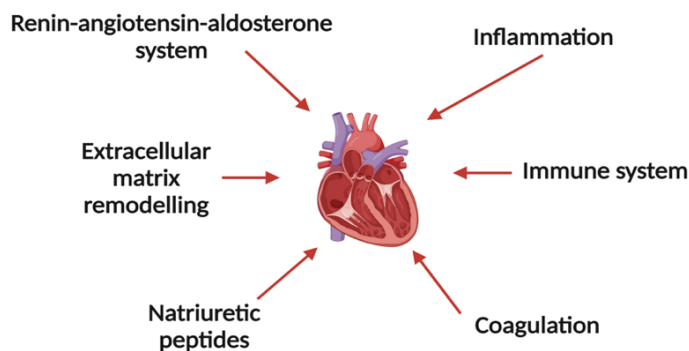


Figure 3: Pathophysiological mechanisms affecting heart failure.

1.3.1. Renin-angiotensin-aldosterone system

The renin-angiotensin-aldosterone system (RAAS) was the first mechanism to be studied in HF due to its pivotal role in systemic vasoconstriction (49). The initial body response to impaired cardiac function is the activation of the neurohumoral system including RAAS, among others (4). Baroreceptors found in the afferent arteriole wall respond to diminished perfusion pressure by triggering renin release from secretory granules (50) in the juxtaglomerular cells. Renin cleaves ten amino acids from angiotensinogen to form angiotensin I, which is cleaved by angiotensin-converting enzyme (ACE) to form angiotensin II. Chymase, a protease, is also involved in angiotensin I into angiotensin II conversion (51).

Angiotensin II mainly acts through the AT₁ receptor, which activates several cardiovascular and renal processes (49). Although angiotensin II is a general vasoconstrictor, there is a notable effect on the renal efferent arterioles, which stimulates aldosterone release, inducing noradrenalin excretion and inhibiting the vagal tone (4). Angiotensin II also stimulates the reabsorption of sodium and water (49). This results in the rise of intraglomerular pressure and glomerular filtration, and the decline of hydrostatic pressure and increase of oncotic pressure. Due to passive mechanisms, sodium is eventually reabsorbed (4). Moreover, as described in **Figure 4**, angiotensin II promotes vascular smooth muscle contraction as well as aldosterone release from adrenal glands and prostaglandins, which hamper excessive vasoconstriction in the systemic and renal circulation (49). These actions are translated into an increase of renal tubular sodium storage and an increase in circulating aldosterone (49). In case of decreased renal perfusion, the glomerular filtration rate is preserved by an increase in efferent arteriolar resistance (49).

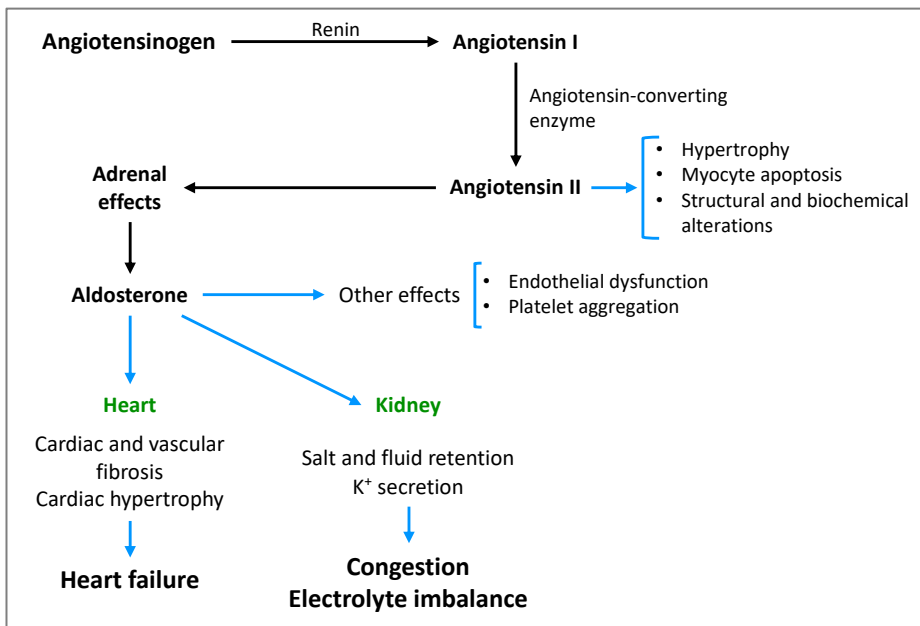


Figure 4: RAAS activation pathway and its adverse effects.
Adapted from Tanai E & Frantz S (4).

As a remarkable drawback, angiotensin II is cardiotoxic. Independently of systemic vasoconstriction, angiotensin II produces myocyte hypertrophy and stimulates fibroblast hypertrophy, as well as collagen deposition. Eventually it leads to myocardial fibrosis and apoptosis (52–54). Furthermore, it is associated with cardiac dysfunction severity and prognosis (54). RAAS activation also leads to noradrenalin increase, is associated with mortality in advanced heart failure patients (55), and can lead to arrhythmias and worsen myocardial ischaemia (4). Moreover, aldosterone may stimulate collagen synthesis and ACE levels in the heart, further increasing angiotensin II levels, as it was observed in studies in adult rat cardiac fibroblasts (56).

Besides aldosterone adrenal production, angiotensin II may also promote myocardial production of aldosterone, as it has been observed that aldosterone receptor density is upregulated, which would suggest an increase in local aldosterone production due to RAAS activation (57).

The roles of RAAS and adrenergic system in HF are known, in contrast, the roles in ADHF are not completely understood (44), although, elevated levels of renin, aldosterone, endothelin-1 and noradrenalin have been reported (58,59). In advanced HF patients, Biegus *et al.* (60) suggested that elevated RAAS levels are related to low glomerular filtration rate (GFR) and natriuresis, which would lead to lower decongestive strength and poorer outcome (60).

In addition, angiotensin II maintains an intricate relationship with vasopressin (VP) (61), a nonapeptide hormone, also known as antidiuretic hormone, that plays a pivotal role in cardiovascular homeostasis and HF progression. VP is synthesised in supraoptic and paraventricular hypothalamic nuclei by neurons to respond to osmotic or hypovolemic stimuli (62). A reduction of 3% of plasma volume triggers VP release (62). VP acts through specific G protein-coupled receptors (GPCRs) stimulation, which are classified into three different types: V1-vascular, V2-renal, and V3-pituitary. VP is mainly responsible for vasoconstriction and cardiac remodelling through V1a receptor activation in smooth blood vessels, however, excessive direct myocardial stimulation can lead to inappropriate ventricular remodelling, increased diastolic wall stress, fluid retention and hyponatraemia (63).

1.3.2. Immune system and inflammation

The innate immune system is responsible for inflammatory responses in HF (4). Since the discovery that tumour necrosis factor (TNF) was elevated in HFrEF (64), many other cytokines have been identified in chronic and acute HF (65), suggesting the contribution of inflammatory response in both HF manifestations.

As a response to tissue injury, both innate and adaptive immune responses are activated (65). While the adaptive immune system provides highly specific response mediated by B and T cells, the innate

immune system produces a general, non-specific defence against tissue injury and pathogens (65). However, this response can become uncontrolled, which can lead to collateral left ventricle (LV) myocardial damage.

Pattern-recognition receptors (PRRs) are expressed on the surface of cardiomyocytes and recognise specific ligands known as pathogen-associated molecular patterns (PAMPs) and damage-associated molecular patterns (DAMPs) (66). Within PRRs, toll-like receptors (TLRs) play a vital role in the innate immune system, with TLR4 being the most expressed in the heart. Regarding HF, TLR4 contributes to myocardial inflammation, among others (67). The interaction between TLR4 and DAMPs or PAMPs triggers a signalling cascade that leads to inflammasome activation and the expression of several proinflammatory mediators and genes, such as TNF- α , interleukin 6 (IL-6) or nuclear factor kappa-light-chain-enhancer of activated B cells (NF κ B) (67,68). An excessive and long-term TLR4 signalling becomes maladaptive and results in proinflammatory cytokines and adhesion molecules expansion, encouraging adverse cardiac remodelling and recruitment of inflammatory cells (66).

1.3.2.1. Interleukins, cytokines & growth factors

Elevated levels of proinflammatory cytokines, such as interleukin 1 β (IL-1 β), TNF, and chemokines have been detected in hearts of both ischaemic and dilated cardiomyopathy, but not in healthy hearts (69,70), however, the reasoning and clinical meaning is not clear yet (71). TNF- α is a ubiquitous cell signalling protein mainly produced by macrophages although it has been observed that, to a lesser extent, cardiomyocytes also produce this protein (72) (**Figure 5**).

Several interleukins have been found to be associated with the failing heart, such as IL-1 β , IL-6, or IL-18 (70). These interleukins have been

found to be involved in ischaemia/reperfusion (I/R) injury, while IL-1 β , IL-4, IL-10 and IL-18 have been previously involved in acute myocarditis (70). IL-6 and IL-1 β also play a role in dilated cardiomyopathy; whereas IL-4, IL-6 and IL-18 have been reported in association with cardiac fibrosis and HF (70) (**Figure 5**).

C-reactive protein (CRP) is an acute phase inflammatory protein produced by hepatocytes in response to IL-6 signalling (73,74). CRP has been found elevated in ADHF patients at hospital admission, however their levels were not always associated with increased risk of rehospitalisation or death (73,75). Thus, it is necessary to further study its mechanisms to be able to better interpret its levels. Elevated CRP levels have been observed in myocardial infarction (MI) patients with structural heart disease and more severe HF patients (76). Moreover, elevated levels of CRP have been associated with 30 day mortality in MI patients and increased HF development risk (77).

Furthermore, ADHF patients have also been observed to present elevated levels of proinflammatory markers such as interleukins (78) and TNF- α (44), which could facilitate a proapoptotic and prothrombotic environment and be involved in HF progression (79,80).

Transforming growth factor β (TGF- β) family is composed of four main members (TGF- β 1-4), although there are 26 other members (70). Myocardial TGF- β has been found to be persistently upregulated in animal models of heart failure and involved in cardiac remodelling (81). Furthermore, elevated expression of TGF- β has also been found to be involved in myocardial hypertrophy and cardiac fibrosis in animal models (70,81) (**Figure 5**). Moreover, TGF- β was elevated during hypertrophic growth in rats undergoing pressure overload (82).

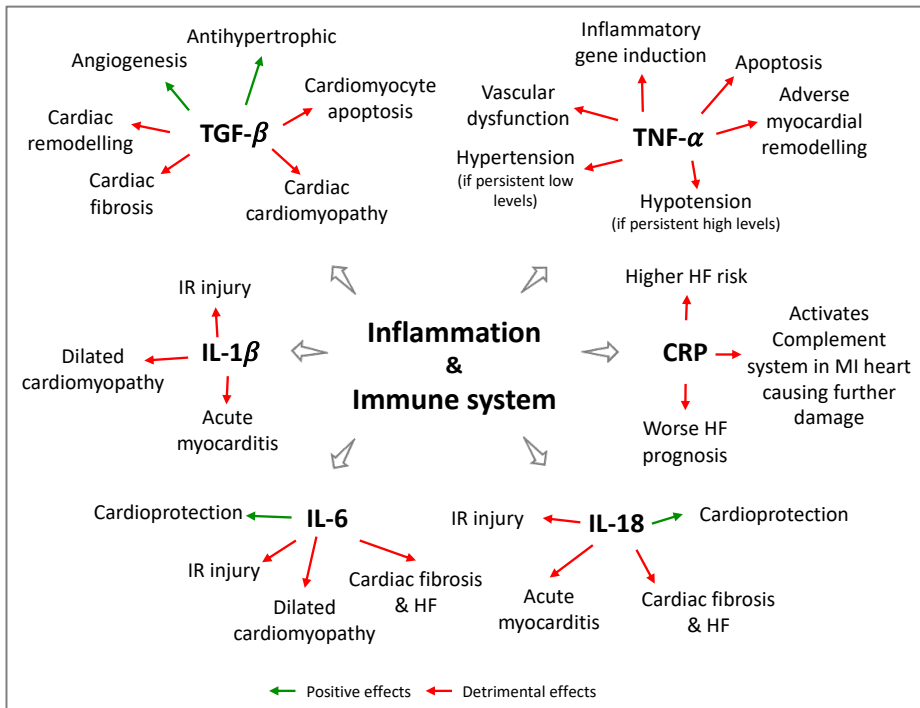


Figure 5: Cytokines and CRP effects on the heart.

TGF- β : transforming growth factor β ; TNF- α : tumour necrosis factor α ; CRP: C reactive protein; IL: interleukins; HF: heart failure; IR ischaemia/reperfusion; MI: myocardial infarction. Adapted from Bartekova *et al.* (70).

A proinflammatory milieu at the coronary microvascular endothelium can lead to impaired nitric oxide and elevated reactive oxygen species (ROS) production (83), which can drive to cardiomyocytes stiffening and hypertrophy and collagen production through local fibroblasts activation that eventually lead to HF (84). Endothelial inflammation can originate other adverse effects, such as expression of vascular cell adhesion molecule 1 (VCAM-1) and E-selection adhesion molecules, which attract and activate monocytes, leading to interstitial collagen deposition (85), proliferation of fibroblasts and myofibroblasts, capillary rarefaction and impaired microvascular vasodilation (66,83,86).

1.3.2.2. Complement system

The complement family is an essential part of the innate immune system and is comprised of more than 30 proteins (87). The complement cascade presents different roles, from identifying foreign organisms, generation of potent inflammatory mediators (anaphylatoxins C3a, C4a and C5a), coating of pathogenic surface or formation of the membrane attack complex (MAC) to destroy cells (87,88). The complement system can be activated through three different sub-pathways (**Figure 6**):

- Classical pathway: activation by antigen-antibody immune complex.
- Lectin pathway: activation by binding of mannose-binding lectin to mannose residues on bacterial surface.
- Alternative pathway: active under inhibitory activity of complement regulators.

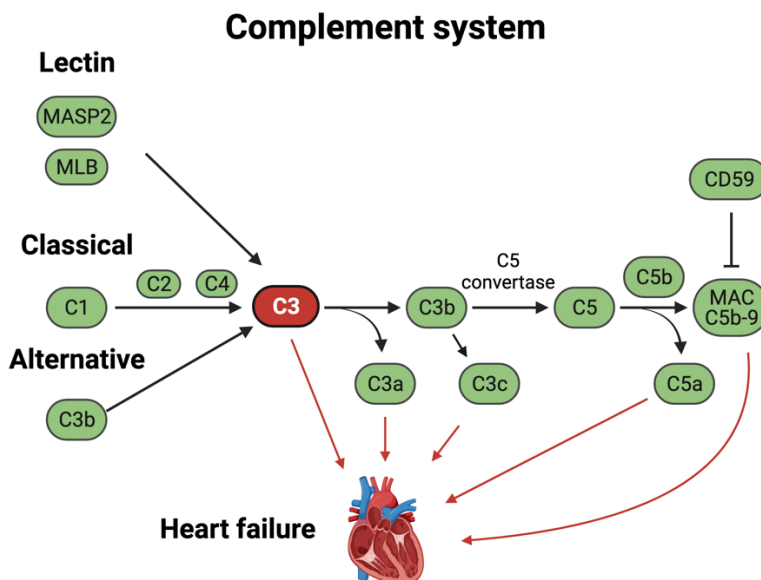


Figure 6: Simplified complement system pathway.

However, all three arms converge at complement C3 (C3) cleavage and present a common effector phase, which involves accumulation of potent opsonin in C3b, proinflammatory molecules (C3a, C4a, C5a), and lysis of target cell via MAC (C5b-9) (87). The complement system, though, is tightly regulated by several complement proteins, including Factor I, Factor H, or membrane cofactor protein (89).

Huber-Lang *et al.* (90) discovered that there is another complement activation via direct activation of C5 without previous C3 activation. This new activation route leads to the common C3 and C5 activation and followed by the terminal pathway with anaphylatoxin C5a release and terminal C5b-9 complex formation (90).

Aukrust *et al.* (91) reported, in 2001, increased complement system activation in HF patients. While, previously, del Balzo *et al.* (92) found in 1985 that activated C3 (C3a) caused tachycardia, left ventricular contractile function, atrioventricular conduction dysfunction and histamine release in the heart after injection into hearts of isolated guinea pigs.

The uncontrolled complement activation, be that by acute or chronic tissue damage, transplants, biomaterials or effect of age, attacks host cells and participates in inflammatory disorders (93). Elevated C3a levels were associated with rehospitalisation and mortality (94), as they were also associated with inflammation and acute-phase response, endothelial cell activation and cellular stress response, while lower C3c and C4c levels were associated with higher risk of death in HF patients (95). In addition, Frey *et al.* (88) suggested that elevated C3c levels were associated with lower adverse remodelling and better survival in HF patients.

Furthermore, the kidney is sensitive to complement damage, which is depicted by its role in several renal diseases (C3 glomerulonephritis as

an example), as well as in haemodialysis and kidney transplant complications (93).

Zhang *et al.* (96) discovered that hypertensive mice presented elevated complement system levels. They found that C3a and C5a were statistically elevated, and that C5a receptor expression was also increased. While they also observed elevated C5a levels in humans, they did not observe elevated C3a levels. Moreover, it has been suggested (97) that lack of functional C5a leads to heart distress and cardiac dysfunction predisposition if faced with additional injury.

MAC of the complement system activates TNF- α and other proteins, which may participate in further HF progression by cellular remodelling and apoptosis, when anchored to the eukaryotic cell membrane. Therefore, if MAC is present in the hearts of HF patients, it may contribute to HF progression, as Oliveira *et al.* (98) suggested. They also reported that complement inhibition could become another potential therapeutic strategy in HF patients.

1.3.3. Haemostasis imbalances

Heart failure can often be complicated by coagulation disturbances, and current epidemiological data associate HF to an increased risk of thrombosis leading to increased risk of ischaemic stroke, systemic and/or venous thromboembolism, and sudden death (99). It is known that HF is more prone to arterial and venous thromboembolism, which occurs to about 30% of the patients (99). While stroke incidence has been reported to be 18‰ during the first year after HF diagnosis, it increases to 47‰ incidence within five years of diagnosis (99). Furthermore, with a prevalence of 25%, atrial fibrillation is the most common arrhythmia within HF patients, and their combination is associated with even higher coagulation irregularities and higher risk of thromboembolism than either pathology alone (27).

For many years it has been acknowledged that thrombi formation is precipitated by endothelial dysfunction, blood flow stasis and hypercoagulability (99). The combination of these components increases thrombosis risk in HF patients (100,101).

1.3.3.1. Hypercoagulability

Hypercoagulability in HF is mediated by chronic inflammation, defective fibrinolysis, platelet hyperreactivity and increased procoagulants levels (100). D-dimer, plasminogen activator inhibitor (PAI-1) antigens and tissue plasminogen activator (tPA) levels were elevated in HFpEF patients in the study performed by Jug *et al.* (102), which manifested impaired fibrinolysis. Markers of platelet activation have also been found to be elevated in HF patients, which would indicate an intense platelet activation (100). Moreover, platelet interaction with monocytes can lead to monocyte-platelet aggregates (MPAs), which also serve as a platelet activity marker, and were found to be elevated in HF patients by Wrigley *et al.* in 2013 (103).

1.3.3.2. Endothelial dysfunction

The main characteristics of endothelial dysfunction are the prothrombotic and proinflammatory states, as well as reduced vasodilation (100), mediated by impaired nitric oxide (NO) availability. Furthermore, endothelium damage caused by oxidative stress (eg ROS) and inflammatory background (eg CRP) associates to a higher permeability, which could allow toxins to pass into the underlying tissues, such as the myocardium and the heart (104). Moreover, damaged endothelium initiates platelet adhesion cascade, activation and aggregation to form an occlusive thrombus (100). Within HF, however, endothelial dysfunction is mainly depicted by the elevated formation of superoxide radicals, which contributes to heart dysfunction

development and progression (105). Evidence of the endothelial dysfunction relevance in HF patients was provided by Fischer *et al.* (106), who reported that endothelium-mediated vasodilation independently predicts increased hospitalisation incidence, heart transplant, or death in chronic patients.

1.3.3.3. Blood flow stasis

Debilitated contractility, abnormal regional vessel walls and dilated chambers can lead to low blood flow, which in turn, lead to thrombi formation in the left ventricles (100). In case of HF with atrial fibrillation, the ineffective and disorganised atrial activity leads to greater risk of thromboembolism (32), especially in the left atrial appendage (100).

1.3.4. Extracellular matrix remodelling

Heart failure is characterised by abnormal function, structure, rhythm, or conduction (107). An abnormal structure is caused by alterations in the extracellular matrix (ECM), which is a very dynamic 3-dimensional network present in most tissues with a relevant role in tissue remodelling in association to haemostasis and disease. In the heart, its main role as a mechanical scaffold is to maintain cardiac geometry, at the time that may transduce important regulating signals to cardiomyocyte and to non-myocyte cells (108). ECM structure is regularly degraded and rebuilt by non-myocyte cells, being in normal conditions tightly regulated in order to preserve tissue homeostasis (109). In the heart, cardiac fibrosis is depicted by ECM expansion and is found in many myocardial diseases, although myocardial fibrosis is not always the initial dysfunction cause (110).

The ECM can undergo two different and important dynamic changes that can have a critical impact on the heart function deriving in heart failure. The activation of a reparative process in response to

cardiomyocyte injury following MI can lead to cardiac fibrosis (110). On the other hand, the process of the accumulation of ECM proteins, such as amyloids, is known to derive in an extensive remodelling intimately associated with deleterious outcome (109,110). Cardiac amyloidosis is represented by two main examples: immunoglobulin light chain amyloidosis, usually acquired, and transthyretin amyloidosis (ATTR), that can be inherited in younger individuals but acquired in older population (111). ATTR is increasingly being recognised as a possible heart failure origin (112).

Fibroblasts are crucial in creating new ECM, wound healing, and breaking down fibrin clot (113). During the inflammatory phase following an injury process, fibroblasts are activated. In the heart after a myocardial injury, fibroblasts are differentiated into myofibroblasts, which produce ECM proteins, especially collagen, in an attempt to preserve structural integrity and avoid cardiac rupture (114). However, the excessive ECM remodelling and collagen deposition leads to cardiac fibrosis, ventricle stiffness and disrupts heart contractility (115).

1.3.5. Other mechanisms

Natriuretic peptides (NP) are endogenous peptide hormones that are released from the heart during myocardial stretch due to pressure or volume overload. NP main biological effects in the heart are the reduction in preload that leads to a drop in cardiac output and the inhibition of cardiac remodelling. Moreover, other NP functions are vasorelaxation and RAAS, VP and endothelin inhibition. More specifically in the kidney, NP induce vasodilation of the afferent arterioles and vasoconstriction of the efferent arterioles to increase glomerular filtration rate increase; Na⁺ and water reabsorption inhibition, and reduce renin secretion (116).

1.4. ADHF as a multiorgan disorder

Cardiac dysfunction and the causes leading to it have been studied for several years now and the main characteristics of HF are congestion and hypoperfusion, which often drive to multi-organ injury. The most common organs affected are the kidney, lungs, liver, brain and intestine (**Figure 7**), and injury in either organ is associated with increased mortality (117). Unfortunately, organ injury pathophysiology remains poorly elucidated and understood, especially if it affects another organ (117).

A very common complication in acute and chronic HF patients is the development of worsening renal function (WRF), known as cardiorenal syndrome, which affects 20-30% of acute HF patients (118). Even though the pathophysiology behind cardiorenal syndrome is not completely clear, it has been divided in two different subtypes: WRF associated to increased central venous and right heart pressure and venous renal congestion. Whereas the second subtype is associated with low cardiac output and arterial underfilling, which would lead to renal blood flow hypoperfusion, and systemic and renal artery afferent vasoconstriction (119). Decongestive treatment is the first step in acute HF, however, it is still very difficult to predict and detect WRF in acute HF patients undergoing decongestive treatment (117).

Liver dysfunction is a frequent complication in HF patients (120) and can affect 20-30% of acute HF patients (121,122), and they often coexist due to systemic disorders that involve both organs, such as inflammation, infections, alcohol or drug abuse, or autoimmunity (123). Furthermore, HF may lead to liver disease, but prior liver disease can also drive towards HF, in any case, the development of either dysfunction complicates management and worsens patient prognosis (123).

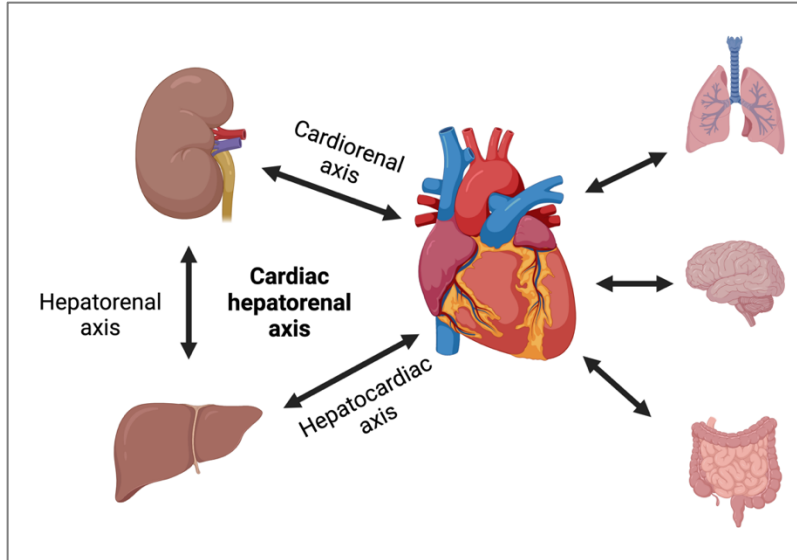


Figure 7: Main organs affected in heart failure.

Hepatic congestion and hepatic hypoperfusion are two pivotal pathophysiological mechanisms and are involved in both cardiogenic liver injury and hepatic congestion. Hepatic I/R injury in heart failure triggers the early activation of Kupffer cells, late activation of polymorphonuclear cells, intracellular calcium overload, oxidative stress, cytokines and chemokines, mitochondrial damage, and liver microcirculation disruption (123). As described earlier, elevated levels of cytokines, chemokines and oxidative stress can lead to adverse cardiac effects.

Cardiohepatic and cardiorenal syndromes (**Figure 7**) have already been studied extensively from a clinical point of view, however, it has only recently been observed that there may be a three-way relationship between heart, kidney, and liver. Dysfunction of both kidney and liver are related to HF severity and independently correlated with adverse prognosis, according to Poelzl *et al.* results (124). Nevertheless, the pathophysiological processes behind this relationship remain poorly

understood. A better understanding is pivotal to better stratify risk of HF patients and ameliorate patient outcome.

1.4.1. Cardiorenal syndrome

ADHF is a complex syndrome that affects all organs, especially the kidney, with which it has a very intertwined and bidirectional relationship (125). Elevated central venous pressure leads to venous hypertension, which increases renal interstitial pressure. If the hydrostatic pressure exceeds the intratubular hydrostatic pressure, it can result in the collapse of tubules, thus, reducing glomerular filtration rate (47). Ten to forty per cent of ADHF patients develop worsening renal failure (125–128), which is associated with a poorer clinical outcome. This wide range can be attributed to the different threshold values of renal failure.

A very frequent complication of ADHF is the development of acute kidney injury (AKI). The National Heart, Lung and Blood Institute defined in 2004 in a *working group* meeting the cardiorenal syndrome (CRS), wherein *therapy to relieve congestive symptoms of heart failure is limited by further decline in renal function*, as heart dysfunction often occurs along with kidney dysfunction, overlapping one another. Both organs are heavily involved in basic physiology, and their functions are strongly intertwined, when either organ fails, the other organ frequently suffers as well (129). The classic interpretation of renal dysfunction in HF was that low renal plasma flow signals the kidneys to retain water and sodium, which would lead to refilling and improved perfusion to other essential organs (130). Recently, however, it became evident that kidney hemodynamic adaptations and other related pathophysiological mechanisms could be independent of cardiac hemodynamic (131) (**Figure 8**).

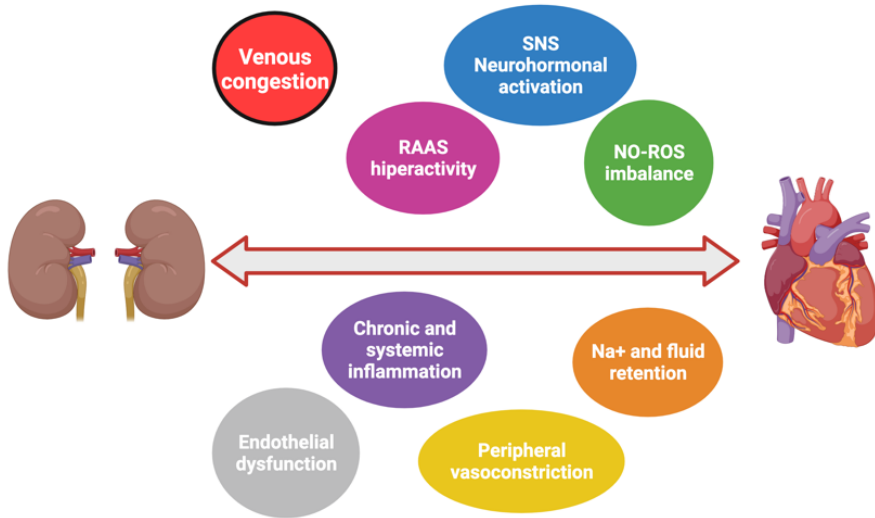


Figure 8: Mechanisms involved in cardiorenal syndrome.

Chronic heart failure is characterised as the attempt to preserve GFR and low renal plasma flow, which results in an increased filtration rate. An increase in efferent arteriolar resistance and glomerular capillary hydrostatic pressure maintains GFR until cardiac function is dangerously impaired. An Acute Dialysis Quality Initiative (ADQI) conference in 2008 proposed a novel classification for CRS depending on the inciting organ (128,132) as outlined in **Table 3**.

Acute heart failure is mainly involved in cardiorenal syndrome type 1; however, it may also be a consequence in cardiorenal syndrome type 3 and 5.

Table 3: Cardiorenal syndrome classification

	Characteristics	Aetiology / examples
CRS type 1 Acute CRS	Rapid worsening of cardiac function leading to AKI	Acute MI with cardiogenic shock, acute valvular insufficiency
CRS type 2 Chronic CRS	Chronic abnormalities in cardiac function leading to CKD	Chronic inflammation, long-term RAAS and SNS activation, chronic hypoperfusion
CRS type 3 Acute renocardiac syndrome	Acute worsening of renal function leading to cardiac dysfunction (HF, arrhythmias, etc)	Uraemia causing impaired contractility, elevated K ⁺ levels causing arrhythmias, volume overload causing PO
CRS type 4 Chronic renocardiac syndrome	Chronic worsening of renal function leading to worsening cardiac function	CKD leading to left ventricular hypertrophy, coronary disease and calcification, diastolic dysfunction
CRS type 5	Acute or chronic systemic disease leading to both cardiac and renal dysfunction	Diabetes mellitus, amyloidosis, vasculitis, sepsis

CRS: Cardiorenal syndrome; AKI: acute kidney injury; CKD: chronic kidney disease; PO: pulmonary oedema.

Adapted from Cole *et al.* (133).

1.4.1.1. Cardiorenal syndrome type 1

Acute cardiorenal syndrome, the type of CRS that concerns this project, is characterised by the acute worsening of cardiac function, that is ADHF, that leads to acute kidney injury (128). Worsening renal function greatly impacts treatment, monitoring and the prognosis of the patient, affecting between 30-40% of hospitalised ADHF (132). WRF/AKI development has been associated with short and long term all-cause and cardiovascular mortality, longer hospitalisation, increased readmission rates, increased progression to chronic kidney disease (CKD) stages 4-5 (134), and higher healthcare expenditure (135).

Even though aggressive decongestive treatment is the first step in ADHF patients with loop diuretics, it might lead to the development of WRF or AKI. WFR refers to the acute and/or subacute changes in renal function that occur during decongestion and treatment of ADHF (119). However, the definition can vary across different studies, as it can be associated with different biomarkers (estimated GFR, serum creatinine,

or cystatin C), but it is also important to notice the magnitude of said change (136). Even though the term AKI refers to an increase in serum creatinine levels, there are three different criteria sets to assess AKI severity: Risk, Injury, Failure, Loss of kidney function, and End-stage kidney disease (RIFLE), Kidney Disease Improving Global Outcomes (KDIGO), and Acute Kidney Injury Network (AKIN). According to the 2010 consensus, RIFLE and AKIN criteria are applied in type 1 cardiorenal syndrome (132). In any case, the development of CRS can severely complicate patient management, lengthen hospital stay, and worsen their prognosis.

Recently, cardiorenal syndrome type 1 has been divided in two different subtypes: WRF associated to increased central venous and right heart pressure, right cardiac dysfunction, with its consequent tubular collapse, venous renal congestion, and tubuloglomerular feedback that leads to further salt and water retention (congestional WRF). While, the second subtype is associated with low cardiac output and arterial underfilling, which would lead to renal blood flow hypoperfusion, and systemic and renal artery afferent vasoconstriction (119).

Currently, AKI is assessed by creatinine and GFR levels, however, these are affected by several factors (137). According to Metra *et al.* (138) creatinine and GFR levels can overestimate renal damage in advanced renal dysfunction and are not sensitive to tubular damage. Furthermore, to date there is a lack of an early biomarker that indicates high risk of developing AKI in AHF patients, which further complicates treatment and worsens patient prognosis.

1.5. Protein biomarkers

Biomarkers are measurable and quantifiable biological parameters that are used as indices for physiology and patient's health assessments. It is important that biomarkers include disease risk and diagnosis (139). A good biomarker is characterised by its accuracy, reproducibility, its easy obtention, easy interpretation by clinicians, and more importantly, its high sensitivity and high specificity, and that it can be used as a substitute marker for disease and its severity (139,140).

Most current molecular biomarkers are found in blood, as blood carries thousands of molecules that reflect what is happening in the body, although other fluids can also be used, such as urine, cerebrospinal fluid, or bronchoalveolar lavage, among others. However, molecular biomarkers are not the only kind as other types exist. For example, histology reflects biochemical and molecular alterations in tissues, cells, or fluids; physiologic biomarkers measure body processes, while radiographic biomarkers are obtained from imaging studies.

Most protein biomarkers are indicative of present disease, such as creatinine for kidney dysfunction, troponins for MI, however, genetic biomarkers are used to study predisposition to different diseases (141).

1.5.1. Biomarkers in acute heart failure

Over the last years, several biomarkers have been described to be used in the evaluation of both heart failure and kidney function. However, these biomarkers have several flaws as described below, thus exposing urgent unmet needs regarding diagnosis and risk stratification in HF. Moreover, identification of new molecules associated to these pathologies would contribute to better understand the underlying mechanisms.

Table 4 summarises the current gold biomarkers (in bold) for evaluation of HF and kidney dysfunction, as well as other molecules that have emerged during the last years associated to HF pathophysiology, and those proposed as biomarkers for heart or kidney dysfunction.

Table 4: Established and potential biomarkers in AHF.

Heart		
Myocardial damage	Myocardial stretch	BNP, NT-proBNP , MR-proANP
	Myocardial injury	Troponins T and I
Neurohormonal activation	RAAS	Renin, angiotensin II, aldosterone
	Sympathetic nervous system	Noradrenaline
	Arginine vasopressin	Vasopressin
Remodelling	Inflammation	CRP, TNF- α , ILs, osteoprotegerin
	Hypertrophy	Soluble ST2, galectin 3, matrix metalloproteinases
Kidney		
Worsening renal function	Kidney function evaluation	Creatinine, GFR , urea, cystatin C
	Proximal tubule damage	KIM-1, NAG
	Distal tubule damage	NGAL

In bold the established biomarkers for acute heart failure (NT-proBNP) and kidney deterioration (creatinine and glomerular filtration rate or GFR).

Adapted from Gaggin & Januzzi (142).

1.5.1.1. Acute heart failure

Natriuretic peptides

Currently, ADHF diagnosis work-up is performed by patient history and signs and symptoms analyses. The diagnosis gold standards are, currently, elevated natriuretic peptides (BNP and NT-proBNP), which are indicative of an acute heart failure event. To notice, plasma NT-proBNP has lower threshold levels for younger patients, that is, levels

above 450 pg/mL is considered ADHF if the patient is <55 years old, above 900 pg/mL for patients 55-75 years old, and 1800pg/mL and higher for patients >75 years old, according to 2021 ESC Guidelines (1). BNP and NT-proBNP levels are also used to evaluate prognosis and long-term mortality in ADHF patients (143–146). On the one hand, it has been observed that BNP was an independent predictor for short-term mortality (143,146) as well as long-term mortality (145). On the other hand, NT-proBNP was also an independent predictor for short-term mortality (147), while in an another study, predischage NT-proBNP levels were associated with better short-term outcomes (148). Nonetheless, natriuretic peptides several limitations as it can be affected by other factors such as sex (149,150), age (150), body mass (151), and medication (152,153), kidney dysfunction (154), anaemia, pulmonary heart disease, among others (142). Therefore, it is important to consider how these factors can affect patient diagnosis and prognosis.

Soluble suppression of tumorigenicity 2

Soluble suppression of tumorigenicity 2 (sST2) is a member of the IL-1 receptor-like family of proteins that are expressed on fibroblasts and cardiomyocytes in response to mechanical stress and cardiac overload (155,156).

Borovac *et al.* (157) found elevated sST2 and catestatin in ADHF patients. Furthermore, their results indicated that patients who died during hospitalisation presented higher sST2 and CST levels than patients alive at discharge. Additionally, patients with sST2 levels >35ng/mL were at higher risk for adverse events (157). Another study by Januzzi *et al.* (158) also found elevated sST2 levels in patients complaining of dyspnoea and later being diagnosed with AHF, although, NT-proBNP levels were superior at acute HF diagnosis. They also reported that sST2 levels strongly predicted mortality after one year, and

that sST2 levels could complement NT-proBNP levels for diagnosis and prognosis. However, a study by Mueller *et al.* (159) reported that the addition of sST2 levels to BNP levels did not improve AHF diagnosis. A recent review (160) and a meta-analysis (161) examined sST2 levels and its use in AHF diagnosis and patient prognosis. They concluded that, even though sST2 has good potential, a lot remains to be elucidated, such as when and how it should be analysed, which cut-off value should be used, or what is the sST2 role in AHF (160,161).

High sensitivity cardiac troponin

Cardiac troponins (cTn) are specific of the myocardium and have become the gold standard biomarker for MI diagnosis since their levels rise 3-4h after cardiac symptoms of MI. Cardiac troponins are released upon myocardium damage such as cardiomyocyte injury or necrosis (156), but not its damage mechanism (162). However, it has been observed that they are also elevated in other cardiac disorders (142).

Xue *et al.* (163) reported that small cTn elevation had been seen in AHF patients. They analysed troponin I (TnI), and their results indicated that TnI levels were associated with elevated 90-day mortality in HF-related rehospitalisation; and that serial increases TnI levels were associated with higher mortality than decreasing or stable TnI levels. The combination of TnI and BNP levels resulted in better risk stratification (163). Whereas, Pascual-Figal *et al.* (164) study revealed that the combination of cardiac troponin T (cTnT), NT-proBNP and sST2 enhanced prognostic ability. In a recent meta-analysis by Aimò *et al.* (165) it was revealed that high sensitivity cTnT was a strong independent predictor of adverse outcome in HF, be that cardiovascular rehospitalisation, cardiovascular and all-cause death, independently of sex, age, systolic and renal function, and NT-proBNP levels.

Galectin-3

Galectin-3 (Gal-3) is a member of the galectin superfamily that plays pivotal roles in cell growth and differentiation, cell adhesion, inflammation, tumour progression, angiogenesis and fibrogenesis, and apoptosis (166). It is mainly expressed in macrophages and damaged cardiomyocytes (166) and increases cardiac fibroblasts proliferation, collagen deposition stimulation and ventricular dysfunction (156).

Even though Gal-3 levels are elevated in AHF patients (167), a recent study performed by Stoica *et al.* (168) reported that although their patients presented higher Gal-3 levels than healthy individuals, its levels capability of AHF diagnosis were similar to those of NT-proBNP (168), however the combination of both molecules led to better diagnostic value. However, Mueller *et al.* (159) reported in 2016 that Gal-3 and BNP were equally useful at AHF diagnosis, and that the combination of both molecules did not lead to better patient diagnosis.

Other potential AHF biomarkers

Other potential biomarkers are being studied such as adiponectin, osteoprotegerin (OPG), heart-type fatty acid binding protein (H-FABP), among others, however with controversial results (156).

1.5.1.2. Kidney function evaluation in AHF

Creatinine is the main kidney function biomarker currently, however due to its drawbacks (see below) a search for new and better renal function biomarkers is ongoing. Cystatin C, kidney injury molecule 1, and neutrophil gelatinase-associated lipocalin are the most remarkable, among others, as of these last years.

Creatinine and glomerular filtration rate

Kidney function is nowadays evaluated using serum creatinine (sCr) levels and estimated GFR, which can be calculated using different sCr-based models (169). However, creatinine is not a perfect biomarker as its levels can be influenced by several factors such as advanced age, sex, excessive protein intake, muscle mass, medication, or intense exercise (137,169). Another inconvenient of creatinine is that its elevation is indicative of *present* kidney injury, not that the patient is at high risk of developing kidney injury. Kidney dysfunction, though, is very difficult to reverse.

Cystatin C

Cystatin C (CysC) is a small (13KDa), non-glycosylated protein. It is freely filtered in the glomerulus and reabsorbed and catabolised, but not secreted, by the proximal tubules (170). It is produced by all human nucleated cells and its plasma levels seem to be altered only by dysfunctional glomerular filtration (170). It has been shown to be particularly superior to creatinine or estimation of GFR to identify mild renal insufficiency. CysC levels has had very good results at predicting kidney injury as several studies have found (171). Recently, serum CysC levels have been associated with prognostic in patients with ADHF (172).

However, Bredihart *et al.* (173) study concluded that CysC did not adequately predict AKI in their ADHF patients. Furthermore, altered levels of CysC have been found in preeclampsia (174), breast cancer (175), and migraine (176). Stephan *et al.* (177) suggested in their study that subjective age, especially in the older population, could lead to increased CysC levels. Musaimi *et al.* (178) studied whether CysC levels were affected by non-renal disorders, and their results reveal that statistically significant CysC levels were found between

hyperthyroidism, diabetes and cardiac dysfunction than healthy individuals. Maahs *et al.* (179) also suggested that there might be a relationship between age, sex and CysC levels in adolescents. CysC role, be that in blood or in urine, to predict onset or mechanism of renal dysfunction in ADHF patients remains unexplored and requires further evaluation. Therefore, it is vital to understand why CysC levels are altered.

Kidney injury molecule 1

Kidney injury molecule 1 (KIM-1) is a 38.7 KDa cell membrane glycoprotein (180) and very low levels of KIM-1 are expressed in healthy kidneys (181), which would be ideal to detect kidney injury. According to data, it was suggested that KIM-1 expression was protective only during early injury, but not in chronic states (182). KIM-1 may play a role in kidney proximal epithelial cells transformation into phagocytes, which would mean that in the clearance of dead cells increases to protect the kidney after early injury (183). It also may play a role in innate immune response modulation in AKI patients (183). Urinary KIM-1 levels have been studied as a possible AKI biomarker and it has yielded several good results, for example Huang *et al.* study (184). Unfortunately, there are not many studies with ADHF patients and AKI. One example is Verbrugge *et al.* study (185), however, they reported that urinary KIM-1 was only a modest AKI predictor, and actually being outperformed by IL-18. Similarly, urinary KIM-1 levels were not able to predict AKI in ADHF patients in the study performed by Atici *et al.* (186).

Even though KIM-1 may be an ideal biomarker due to its low levels in healthy kidneys, its performance in ADHF levels require further evaluation as they have not been as promising as in other clinical settings.

Neutrophil gelatinase-associated lipocalin

Neutrophil gelatinase-associated lipocalin, or commonly known as NGAL, is a 25 KDa glycoprotein (187). NGAL exists in two other forms: a homodimer (45KDa) and an heterodimer conjugated with gelatinase (135KDa) (181). NGAL is encoded by the *LCN2* gene (188) and secreted in kidneys (189), liver (190), as well as lungs, breast, bone marrow and trachea, among others (191)

Both urinary and blood NGAL levels have been studied in AKI settings, although with controversial results. The same study performed by Verbrugge *et al.* (185) also revealed that urinary NGAL levels were not able to predict AKI in AHF patients nor persistent renal impairment, and also being outperformed by IL-18 levels. Legrand *et al.* (192) evaluated urinary NGAL levels but their results also revealed that NGAL levels were not able to predict WRF. Breidhart *et al.* (193) evaluated plasma NGAL levels in AHF patients, however, their results revealed that plasma alone was not able to predict AKI, and, additionally, neither in combination with sCr levels. Serial NGAL measurements did not add predictive power of plasma NGAL at admission. Whereas Aghel *et al.* (194) found elevated serum NGAL levels in ADHF at day 3 of hospitalisation and their NGAL levels were associated with adverse clinical outcomes as well. A study concerning serum NGAL reported that NGAL levels were also not able to predict AKI in AHF patients (195).

To notice, altered NGAL levels have also been found in other pathologies such as diabetes and different types of tumours and cancers (endocrine gland, gastrointestinal tumours, breast, nervous system, etc) (196–198). Thus, it is crucial to know how these pathologies can affect NGAL levels and its interpretation in AKI, especially in ADHF patients.

N-acetyl- β -D-glucosaminidase

N-acetyl- β -D-glucosaminidase is commonly known as NAG and formed in the lysosomes of proximal tubule cells. Given NAG large size of 140 KDa it is unlikely that its origin is non-renal (199). Elevated urine levels have been previously associated with proximal tubule injury with lysosomal integrity loss (199). According to PubMed search in January 2022 there is only one study concerning NAG and AHF/cardiorenal syndrome, where Legrand *et al.* (192) found that urinary NAG levels were not able to predict WRF in cardiorenal syndrome patients.

Other potential biomarkers

Liver fatty acid binding protein (L-FABP), IL-18, the combination of urinary tissue inhibitor of metalloproteinase-2 and insulin-like growth factor-binding protein 7 (TIMP2/IGFBP7), among others, have also been proposed as AKI biomarkers. These molecules might have very interesting results in other pathologies, but due to the complex pathophysiology of AKI in AHF or cardiorenal syndrome it their specificity or sensitivity might not be enough to detect early changes consistently. Furthermore, there aren't many studies performed in ADHF or cardiorenal syndrome type I patients from where definitive conclusions can be drawn (185,192,200–203) as Fu *et al.* recently reviewed (204).

Final remarks

After evaluating the current potential biomarkers, it is clear that there are no candidate biomarkers able to consistently detect early AKI, before the increase in creatinine, in ADHF. Furthermore, the pathophysiology of both ADHF and AKI remains poorly understood, which further complicates the discovery of novel and better biomarkers. It is crucial to discover the underlying mechanisms behind both pathologies to better stratify high risk patients and to find novel biomarkers with a higher

sensitivity, less susceptibility to patients' characteristics, and an earlier change to that of creatinine.

1.5.2. Plasma/serum and urine as matrices for biomarker analysis in acute heart failure

As mentioned earlier, there are several matrices used to study biomarkers, such as plasma and serum, urine, saliva and cerebrospinal fluid. Nevertheless, plasma and serum have been the main biological matrix for heart failure studies for many years. In the last few years, urine has emerged as a promising biofluid to study not only heart failure, but many other disorders.

Blood samples contain a wide amount of information, including proteins, ions and salts, other molecules (O₂, CO₂, lipids, carbohydrates, etc) that are transported between tissues (205). Therefore, blood samples require subfractionation prior to analysis. Urine, on the other hand, is a much simple body fluid. It contains lower content of components, thus no subfractionation is required. Differing from plasma/serum where endogenous proteases may be activated generating breakdown products during blood sample collection and handling, urine is a much more stable sample that enables larger and more recurrent sampling without causing discomfort to the patient (206).

1.5.2.1. Urine as a sample

Urine is produced by the kidney, where the glomeruli filter plasma resulting in primitive urine, and it permits the body to dispose of waste products from the blood through glomerular filtration (**Figure 9**) (206). However, besides glomerular filtrate, urine composition also results from urogenital tract secretions and renal tubule extraction that can reflect the

patient's pathophysiologic and metabolic state (207). In healthy subjects, 30% of the urinary protein content comes from glomerular filtration, while the remaining 70% of urinary proteins come from the kidney or urogenital tract. Given that urine is formed by waste from all over the body, effects of drugs or environmental toxins can be studied as well (208).

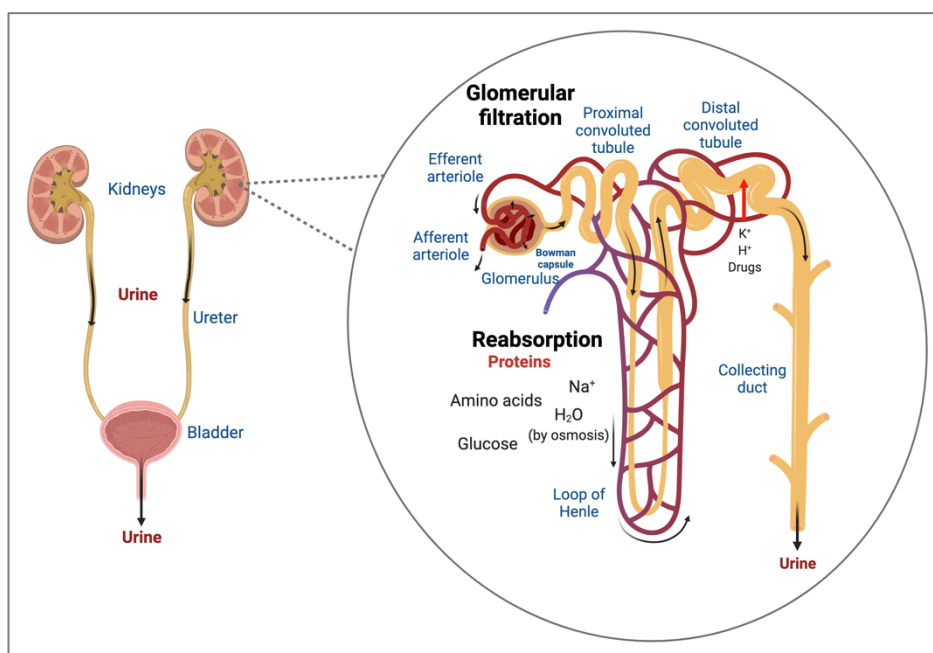


Figure 9: Urine production.

Given these characteristics, and that urine can be collected by non-invasive techniques and relatively large volumes, urine has become a highly desirable biospecimen. Usually, adults excrete 1.5-1.6L of urine in 24h, typically ranging 0.6-2L daily.

Usually, urine contains very low levels of protein, up to 150mg ever 24h or 10mg/dL. The most abundant protein, albumin, represents a third of the urinary protein content, while the remaining is composed by small

globulins. In healthy individuals, small plasma proteins are able to cross the glomeruli and later the most part of filtered protein is reabsorbed by receptor-mediated processes, leaving only a small quantity of protein in urine (209).

Several studies suggest that urinary biomarkers are able to detect a pathological state even before it is observed in the affected organ, as seen by Wu *et al.* (210).

The main urinary disadvantage is that its protein concentration varies depending on daily fluid intake, which complicates reproducibility if normalisation is not considered.

1.5.3. Urinary proteomics in heart and kidney failure

Proteomics is the study of the proteins in different samples at a given moment, also known as the proteome (211). Therefore, proteome alterations reflect the development or on-going of different biological processes. The proteome is defined as the science that characterises and quantifies cellular and molecular effectors that reflect the genic expression (212). Proteins and their levels can be used for diagnosis as well as prognostic and therapeutic targets. The proteome has become a crucial tool to study the protein amino acid sequence, structure, possible modifications, and the functional pathways in the cell where it may play a role. Modifications in their structure and expression levels might indicate presence of a disease (213).

Differential proteomic patterns and signatures can be achieved by using different proteomic approaches, be that different sample types and analytical strategies. A large number of proteome studies are performed in blood samples, while urine remains under-represented, with less than 10% of publications, regarding the search of biomarkers with either blood, plasma or serum (214).

Urine has been used primarily to study renal diseases, and so far different biomarkers have been found for acute kidney injury after cardiopulmonary bypass (215), diabetic nephropathy (216), and bladder cancer (217). Nevertheless, urinary proteome has been studied to see whether it changes before and after exercise (218), changes in menstrual cycle and in women taking estro-progestin pills (219), and Parkinson's disease (220), among others. Several reviews also evaluate the different potential urinary biomarkers for different pathologies in humans, such as lupus nephritis (221), renal cell carcinoma (222), familial nephrolithiasis (223), as well as Alzheimer's and Parkinson's diseases (224). Therefore, urine samples have been used to study many different pathologies.

However, there are not many studies concerning urinary proteome of HF. Farmakis *et al.* (225) studied the urinary proteome in HFREF patients and chronic kidney disease (CKD). Even though they did not have a very large patient cohort, 62 HF patients, which is similar to this project's cohort, they were able to identify 107 urinary peptides specific to HFREF with CKD as complicating factor.

Proteomic studies in kidney and heart pathologies are not limited to human patients and, for example, Templeton and colleagues (226) investigated the proteome in kidney samples of adult sheep with ADHF in search for novel AKI biomarker. Furthermore, Malagrino *et al.* (227) studied the serum and urine proteome in swine with AKI. Additionally, Ferlizza *et al.* (228) studied the urinary proteome and metabolome in dogs with CKD. Even though there are considerable differences between humans, sheep, swine and dogs, their studies offer new possible targets that could be useful in human studies and new insights into the pathophysiology of HF and kidney disease.

Table 5: Experimental and clinical studies concerning urinary proteomics

Experimental studies					
Article	Pathology	Animal	Sample	Analysis	Results
Melenovsky <i>et al.</i> 2018	CRS in CHF	Male HanSD rats	Frozen kidney	LC-MS/MS	41 proteins 1.8x↑ 5 proteins 1.8x↓
Büttner <i>et al.</i> 2021	HFpEF	Obese and lean ZSF1 rats	Urine and serum	LC-MS and GC-MS	Arginine, nitrite and nitrate concentrations altered in obese ZSF1 rats.
Ferlizza <i>et al.</i> 2020	CKD	Dogs	Urine	SDS-PAGE-MS	Significant alterations in uromodulin and albumin
Templeton <i>et al.</i> 2022	AKI in ADHF	Adult Coopworth ewes (sheep)	Kidney, plasma, serum and urine	SWATH-MS	17 protein candidates of AKI in ADHF
Malagrino <i>et al.</i> 2017	AKI	Swine	Kidney, urine, and serum	LC-ESI-MS/MS	49 differential urinary proteins
Baskal <i>et al.</i> 2021	HFpEF	ZSF1 rats	Urine	GC-MS	Higher lysine and cysteine metabolites
Clinical studies					
Article	Pathology	Patients	Study type	Analysis	Results
Zhang <i>et al.</i> 2017	HF	57 HF at admission, 38 developed. 192 HS	Prospective study	CE-MS	The comparative analysis depicted potentially HF-specific peptides
Farmakis <i>et al.</i> 2016	HFpEF	59 HFpEF and 67 HS	Case-control study	CE-MS	107 discriminatory peptides
He <i>et al.</i> 2021	HF	993 HF patients, 3977 HS	Case-control study	CE-MS	577 peptides associated with HF
Rossing <i>et al.</i> 2016	HFpEF (LVEF<45%)	33 HFpEF and 29 non-HFpEF	Case-control	CE-MS	103 peptides differentially excreted
Cooper <i>et al.</i> 2022	HF	25 patients	Prospective study	Olink	Significant differences in urine B2M and NGAL
Hou <i>et al.</i> 2014	Early CHF	Discovery: 15 CHF, 15 HS. Total: 197 CHF	Prospective study	2DE-MS	Significant changes in ORM1, 20 other differential proteins
He <i>et al.</i> 2020	AKI in CKD	2707 patients	Prospective study	CE-MS	SC and pIgr associated with kidney disease severity.
Kuznetsova <i>et al.</i> 2012	HT in LV dysfunction	Discovery: 19 patients and 19 HS	Pilot study	CE-MS	85 peptides differentially excreted
Nguyen <i>et al.</i> 2006	AKI in open heart surgery	15 paediatric patients 15 matched controls	Prospective study	SDS-PAGE SELDI-ToF	Significant changes in several molecules

ADHF: acute decompensated heart failure; AKI: acute kidney injury; CE-MS: capillary electrophoresis-mass spectrometry; CHF: chronic heart failure; CKD: chronic kidney disease; CRS: cardiorenal syndrome; GC-MS: gas chromatography-mass spectrometry; HF: heart failure; HFpEF: HF with preserved ejection fraction; HFREF: HF with reduced ejection fraction; HT: hypertension; LC-MS: liquid chromatography-mass spectrometry; LV: left ventricle; LVEF: left ventricular ejection fraction; ORM1: Orosomucoid-1; SELDI-ToF: surface-enhanced laser desorption/ionisation – time of flight; SWATH-MS: sequential window acquisition of all theoretical mass. Adapted from (225–239).

1.5.4. Proteomic approaches to identify and characterise differential proteomic signatures

In proteomic studies there are two different working strategies: top-down and bottom-up, nevertheless, both strategies can be combined to obtain more detailed results. On the one hand, bottom-up methodology requires sample proteolysis, which destroys information on protein size and connectivity between peptide fragments (240). On the other hand, the top-down approach, main strategy of this thesis, is based on the analysis of the intact proteins by mass spectrometry (MS). This methodology enables the identification of protein isoforms and possible post-translational modifications (PTM) of proteins since it utilises molecular and fragment ion mass data.

An important step in top-down strategies is the separation method. There are several separation techniques that can be coupled with MS. In this thesis we have focused on isoelectric focusing (IEF) of proteins followed by electrophoresis, resulting in 2 dimensional electrophoresis (2DE) coupled to MS (2DE-MS). In this technique, proteins are separated according to their isoelectric point in the first step, followed by separation according to molecular weight in the second step. 2DE-MS allows proteins in a large molecular weight range to be studied. Even though this methodology requires longer time of analysis is difficult to automate, its results are highly specific (240).

1.6. Proteomic approaches

Proteomic techniques are based on the combination of different technologies for sample preparation, protein separation, proteomic pattern analysis and protein identification and characterisation by mass spectrometry (**Figure 10**). With the information obtained, *in silico* analyses are performed to determine the pathways wherein these proteins are involved and if they can become possible targets.

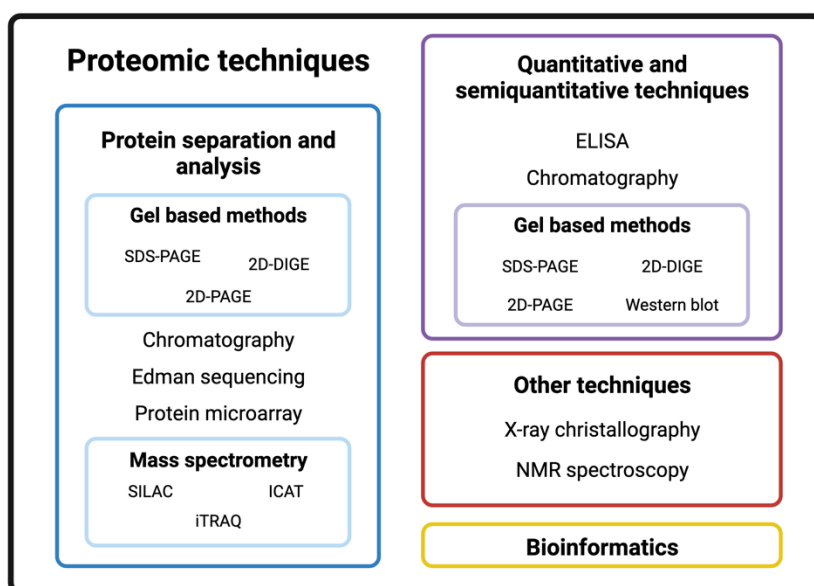


Figure 10: Proteomic techniques summarised.

ELISA: enzyme-linked immunosorbent assay; ICAT: isotope-coded affinity tag; iTRAQ: isobaric tag for relative and absolute quantitation; SDS-DIGE: sodium dodecyl sulphate difference gel electrophoresis; SDS-PAGE: sodium dodecyl sulphate polyacrylamide gel electrophoresis; SILAC: stable isotope labelling by/with amino acids in cell culture 2D-PAGE: 2 dimensional polyacrylamide gel electrophoresis. Adapted from Aslam *et al.* (241).

1.6.1. Two-dimensional electrophoresis

Within the nowadays accepted proteomic protocols there is 2DE (242). After several modifications and improvements (243,244), the definitive approach was described in 1975 by Patrick O'Farrell (245), when he combined a first dimension of IEF by separating proteins by their

isoelectric point (pI, charge). And, a second dimension where proteins are separated by molecular weight in a polyacrylamide gel with sodium dodecyl sulphate (SDS-PAGE), which was chosen due to its high resolution based on protein size (245). This new technique was deemed crucial for protein separation as the double separation of proteins, by charge and molecular weight, allows for better visualisation of protein concentration and distribution, as it can be observed in **Figure 11**.

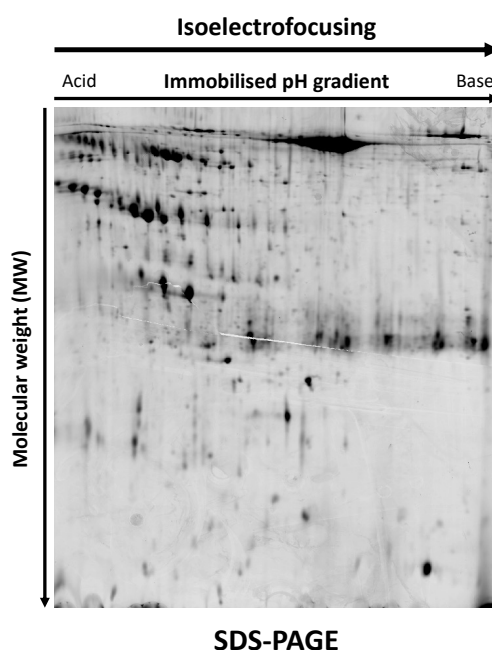


Figure 11: Representative 2DE gel

Although several improvements have been accomplished since then, the protocol has remained unaltered. Within these improvements it is important to notice the development of immobilised pH gradients (IPG strips), which replaced the carrier ampholyte-based pH gradient in tube gels (244). Furthermore, these IPG strips allow now for separation by lineal or non-lineal pH gradient. Another improvement was the

development of new chaotropes and detergents that increased hydrophobic proteins solubility (244).

The following step is protein staining, for which several options have been developed. Coomassie brilliant blue has good linearity and accuracy but only moderate sensitivity (ng level). This option is based on the dye binding to aromatic amino acids by electrostatic and hydrophobic interactions. Silver staining, another option, is more sensitive (pg level) but with worse linearity and accuracy (246), furthermore, it is not completely adapted for mass spectrometry. Fluorescent staining solutions such as Sypro Ruby and Flamingo combine high linearity, high sensitivity (pg-ng level) and compatibility with mass spectrometry (247). Additionally, fluorescent staining allows performing multiplexing samples on 2DE gels, which is called difference gel electrophoresis (DIGE). This combination allows the user to perform 2DE of different samples in the same gel (248).

The resulting proteomic pattern can be analysed using specific software, which allows the protein quantification and comparison to other performed gels from the same or different groups for differential analysis (249).

Differential proteomic analysis is based on the comparison of different proteomic profiles from different samples in order to identify differences between them, which can be between different patients and groups or from a same patient but different time points (249). The analysis of differential protein profiles from 2DE allows investigating not only changes in quantity of the proteins, but also whether these proteins have undergone post-translational modifications, such as oxidations, glycosylation, or acetylation, among others.

1.6.2. Mass spectrometry

Identification of the proteins, or other molecules, obtained by mass spectrometry (MS). There are different MS technologies, however Matrix-assisted desorption ionisation time of flight (MALDI-ToF MS) was the technology used for this study (**Figure 12**).

MALDI-ToF is one of the main techniques for protein ionisation. Michael Karas *et al.* (250) in 1985 described protein ionisation, and later in 1988 it was experimentally demonstrated by Tanaka *et al.* (251) for the first time, which led to the Chemistry Nobel prize in 2002.

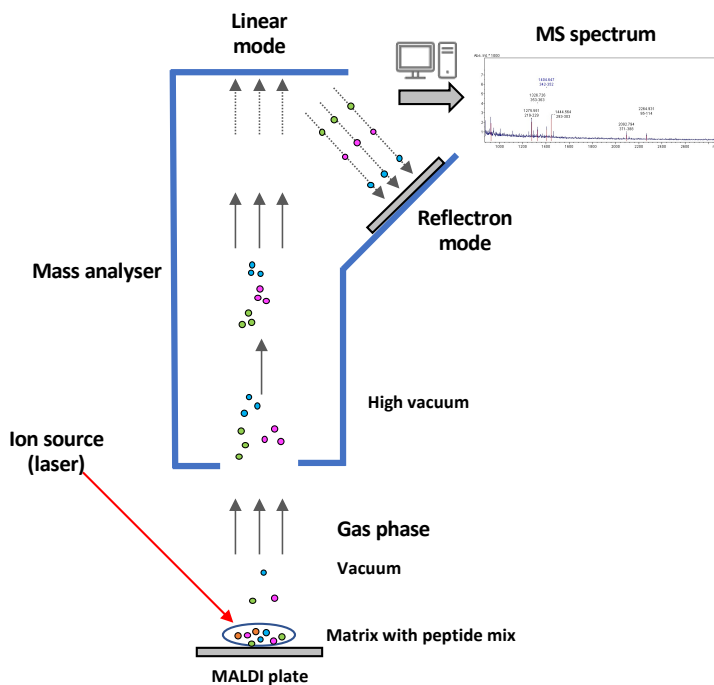


Figure 12: MALDI-ToF mass spectrometer principle.
Adapted from several sources (252,253).

MALDI-ToF is a very accurate and sensitive technique (254). To analyse samples in a MALDI-ToF, they need to be mixed in a matrix solution that will be applied to the MALDI target, in many cases a stainless-steel plate

(**Figure 12**). This solution, containing the sample and the matrix, is crystallised and introduced into the mass spectrometer. A very small amount of sample is required (approximately 1 μ L) for the analysis, thus, several samples can be applied to the MALDI plates each occupying a unique location. One by one, the dried samples are irradiated with a pulsed laser beam generating ions that are accelerated down the ToF analyser and detector. The abundance and time of flight of each ion are recorded. These results are converted to mass spectrum, which is a vertical bar graph with the position of each peak on the abscissa axis representing m/z of an ion, while the height of each bar indicates the relative abundance (255). The obtained peptide results are compared to theoretical mass from databases in order to potentially identify the molecules analysed. MALDI-ToF mass spectrometers can perform analyses for large molecules up to 100KDa (255).

For a more reliable protein identification, peptide mass fingerprinting (PMF) was developed. The protein separated by 2DE is extracted from the gel and digested by trypsin, usually. Trypsin, a protease, cuts the C-terminal of lysine (L) and arginine (K) amino acids. This process leads to the obtention of the protein peptides. PMF analyses and measures the m/z of the peptides obtained and compares the resulting mass list of peptide m/z to databases. One or more proteins are suggested alongside a probability score (252). If the ionisation source is attached to ToF-ToF mass analysers in tandem, as is the set-up for this work, the peptides are fragmented into two other ions (B and Y), and along with the peptide mass, a more accurate identification can be obtained (256).

1.7. Future perspectives

Nowadays, ADHF is one of the leading causes of morbidity and mortality in the industrialised world and it mainly affects the older population (>65 years old). Moreover, ADHF patients often develop AKI during hospitalisation. The combination of these pathologies complicates treatment, lengthens hospital stay, and worsens patient prognosis. Furthermore, these patients usually present, or develop, concomitant comorbidities such as arterial hypertension, type 2 diabetes mellitus, dyslipidaemia, atrial fibrillation, and cardiovascular disease, which further aggravates patient outcomes. Many pathways have been studied within heart failure; however, the pathophysiology and molecular drivers behind ADHF and AKI remain poorly understood.

Currently, renal function is assessed using serum creatinine levels and GFR. But, the increase of creatinine levels, or decrease in GFR, is indicative of present kidney dysfunction, which, unfortunately, is difficult to revert, and conditions a worsened cardiac function at short and long-term. Several potential molecules have been proposed as early AKI biomarkers; however, their consistency and usefulness are controversial.

Therefore, it is crucial to elucidate the pathophysiology of ADHF and AKI in order to improve the detection and stratification of ADHF patients at a higher risk of developing AKI before its onset and creatinine levels increase. A greater pathophysiology knowledge could help us understand the main triggers behind both disorders and target new proteins, individually or in combination, as potential biomarkers. An early AKI biomarker in ADHF patients would enable personalised treatment strategies according to their AKI risk. As for the patient, an early biomarker(s) would translate into shorter hospital stay, diminished risk for kidney injury development, lower risk of rehospitalisation, and overall, a better quality of life.

CHAPTER II: HYPOTHESES

2. Hypothesis

Acute decompensated heart failure (ADHF) is one of the main causes of hospital admission, especially in the elderly. It is a life-threatening condition characterised by the rapid onset of signs and symptoms of heart failure, requiring urgent evaluation and usually hospitalisation. It is often accompanied by kidney function deterioration, which worsens patients' prognosis.

Even though many studies have been conducted on ADHF, its pathophysiology and the underlying triggers remain elusive. Because of the clinical link of ADHF with kidney function deterioration, it was our **hypothesis** that the mapping of the urinary proteomic signature could provide key novel information to advance our understanding of ADHF pathophysiology.

CHAPTER III: OBJECTIVES

3. Objectives

The specific objectives proposed to prove the hypothesis were:

Objective 1: To comprehensively identify, using an untargeted mass spectrometry approach, the differential protein signature related to acute decompensation of heart failure (ADHF) at hospital admission:

- To investigate the differential proteomic profile of urine from ADHF patients as compared to healthy individuals using 2 dimensional electrophoresis.
- To identify and validate the differential proteins associated with ADHF.

Objective 2: To investigate whether changes in differential protein signature relate to biological functions underlying the pathophysiology of ADHF and cardiovascular disease, and associate with kidney dysfunction and/or cardiorenal syndrome.

Objective 3: To examine the pathophysiological link between changes in selected proteins and disease progression in ADHF.

Objective 4: To unveil early changes in the urine protein signature associated with kidney function deterioration in patients hospitalised due to ADHF.

CHAPTER IV:
MATERIALS
&
METHODS

4. Materials and methods

4.1. Experimental design

This study was performed mainly in a well-controlled cohort of patients with ADHF, consecutively recruited during hospitalisation according to inclusion / exclusion criteria indicated below.

Patients and biological samples (urine, plasma/serum) were studied at hospital admission and at three days after hospitalisation. This included determination of clinical variables, biochemical variables, and a proteomic-based approach to identify differential urine protein signature to identify and characterise the differential urinary protein profile in ADHF patients at hospital admission in comparison with healthy subjects used as reference group and relate it to mechanistic processes associated with the pathophysiology of ADHF and disease progression.

Based on *in silico* analysis and available literature, several proteins with differential pattern in ADHF patients were selected and further investigated both in urine and plasma in association with disease pathophysiology: renal dysfunction by GFR and cardiac function defined by the LVEF hospital at admission, disease severity (kidney function deterioration during hospitalisation) and progression during 18-month follow-up after hospital discharge.

Mechanistic studies were performed in cultured human vascular smooth muscle cells.

Figure 13 shows a flow-diagram of the study design used for identification and validation of the differential protein signature in ADHF patients.

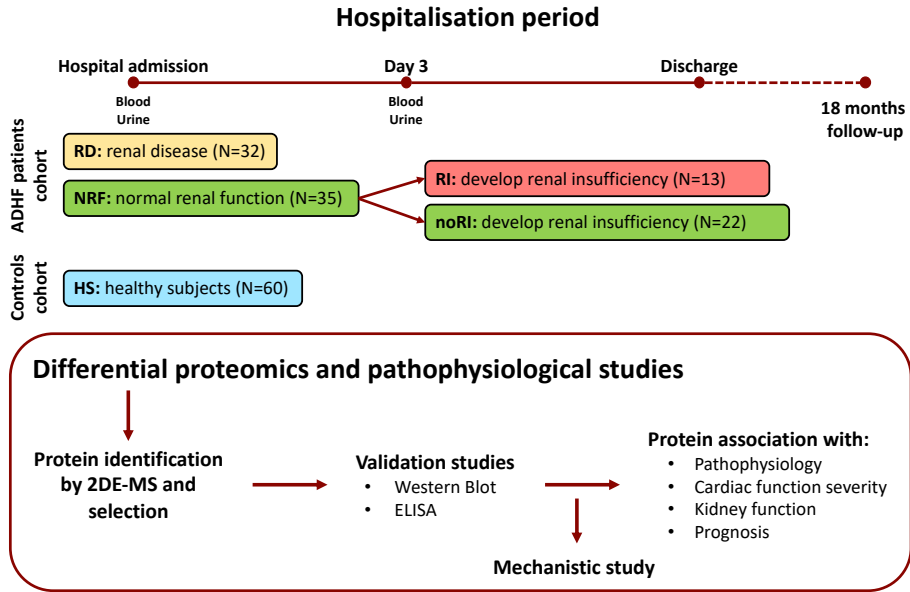


Figure 13: Experimental design.

4.2. Patients

Two different sets of patients were used for this thesis. The first, and main, group is the ADHF group with their healthy individuals (*Manuscripts 1-3*). The second set includes familial hypercholesterolaemia patients, and their respective healthy individuals, for the mechanistic study (*Manuscript 4*).

4.2.1. ADHF study

The ADHF study includes **67 patients** (71 [65-77] years old) hospitalised at the Hospital de la Santa Creu i Sant Pau (HSCSP) in Barcelona. A group of healthy subjects (HS, N=60, 49.0 [44.5-53.5] years old) was used to establish the urine and plasma normal range for the different studied proteins (*Manuscripts 1, 2, and 3*).

ADHF patients were separated in two different groups based on their GFR levels at hospital admission. Patients' renal function was

calculated using MDRD-4 formula, which is based on serum creatinine, age, race, and sex of the patient. Levels below 60mL/min/1.73 m² were considered pathological.

- **NRF group:** ADHF patients with normal renal function (MDRD-4 83.0 [68.9-99.0] ml/min/1.73m²) at hospital admission (N=35, 69 [58-75] years old, 29% female). Three days after admission, NRF patients were subgrouped depending on the evolution of their kidney function:
 - **noRI group:** ADHF patients who maintained normal renal function (N=22, 62 [54-70] years old, 32% female).
 - **RI group:** ADHF patients who developed kidney injury, usually after day 5 of hospitalisation (N=13, 74 [69-77] years old, 23% female).
- **RD group:** ADHF patients with renal disease (MDRD-4 39.7 [31.3-45.0] ml/min/1.73m²) at admission (N=32, 74 [69.5-77.5] years old, 38% female).

Inclusion criteria: men and women, at least 18 years old, and hospitalised due to acute decompensated heart failure (ADHF).

Exclusion criteria: chemotherapy patients, pregnant or post-delivery ischemic heart syndrome women, patients younger than 18 years old, *de novo* HF patients with other causes of acute episode (myocardial infarction, myocarditis, or toxic aetiology), or patients already defined for organ transplantation. Medication was not considered as exclusion criteria except those required in oncological treatment (who were already excluded).

Main baseline characteristics of the ADHF patients included in the study for demographic and clinical characteristics are shown in **Table 6**.

Untargeted proteomic studies were performed in a representative and randomly taken subgroup of ADHF patients (76% male, 72 [69-76] years old) that referred to the 25% of the total ADHF study population. As

shown in the **Table 7**, the subgroup used in the urine proteomic studies (2DE group) did not statistically differ from the total study group (Validation Group) regarding demographic characteristics (sex, age), kidney and cardiac function markers and risk factors including hypertension and pulmonary hypertension, diabetes type 2 and dyslipidaemia. No major differences were observed concerning background medication.

ADHF patients had plasma NT-proBNP values above the pathological cut-off defined by the European Society of Cardiology's most recent Guidelines (1). Forty per cent of ADHF patients had reduced left ventricular ejection fraction (LVEF $\leq 40\%$: 32 [21-35]%), and 42% had a LVEF $\geq 50\%$ (60 [56-61]%) at admission. The remaining group of patients (18%) presented mildly reduced LVEF, with values between 41-49% (45 [44-47]%), as per the most recent Guidelines by the European Society of Cardiology (1). Mean hospitalisation time was 10.8 ± 5.3 days for all patients.

The Ethics Committee of the Santa Creu i Sant Pau Hospital in Barcelona, Spain, in March 2016 (reference number 16/022), approved this project and all studies were performed according to principles of Helsinki's Declaration. All patients signed informed consent prior being included in the study.

Table 6: Clinical characteristics of ADHF patients.

	All patients N=67	NRF N=35	RD N=32	P-value
DEMOGRAPHIC CHARACTERISTICS				
Female/male, N	22/45	10/25	12/20	0.603
Age, years	71.0 [65.0-77.0]	69.0 [58.0-75.0]	74.0 [69.5-77.5]	0.008
Weight, kg	73.0 [61.6-86.8]	70 [61.2-86.6]	77.2 [62.0-88.6]	0.543
KIDNEY FUNCTION MARKERS				
Creatinine, µmol/L	105.0 [78.0-147.0]	78.0 [67.0-97.0]	147.0 [122.5-194.0]	<0.001
Glomerular filtration (MDRD-4) ^a	61.0 [40.9-83.3]	83.0 [68.9-99.0]	39.7 [31.3-45.0]	<0.001
Urea, mmol/L	10.2 [6.8-16.1]	7.0 [5.8-9.2]	16.5 [13.0-22.9]	<0.001
CARDIAC FUNCTION MARKERS				
NT-proBNP, ng/L	4.0 [2.3-8.6]	3.2 [1.9-6.4]	4.5 [2.8-14.7]	0.026
Left ventricular ejection fraction (LVEF), %	45.0 [33.0-58.0]	38.0 [33.0-57.0]	51.0 [35.5-59.5]	0.225
Reduced LVEF ≤40%, N (%)	29 (43)	19 (54)	10 (31)	0.125
Mid-range LVEF 41-49%, N (%)	10 (15)	5 (14)	5 (16)	
Preserved LVEF ≥50%, N (%)	28 (42)	11 (31)	17 (53)	
Atrial fibrillation, N (%)	32 (48)	16 (47)	16 (50)	>0.999
Cardiovascular disease, N (%)	23 (34)	11 (31)	12 (38)	0.618
OTHER BIOCHEMICAL MARKERS				
Haemoglobin, g/L	122 [101-138]	128 [114-142]	110 [95-124]	0.004
RISK FACTORS; N (%)				
Active smoking	10 (15)	8 (23)	2 (6)	0.086
Hypertension	49 (74)	21 (62)	28 (88)	0.024
Pulmonary hypertension	16 (24)	8 (23)	8 (25)	>0.999
Diabetes mellitus type 2	30 (45)	11 (32)	19 (59)	0.047
Dyslipidaemia	46 (70)	20 (59)	26 (81)	0.063
BACKGROUND MEDICATION; N (%)				
Diuretics	49 (73)	21 (60)	28 (88)	0.014
Statins	43 (64)	18 (51)	25 (78)	0.040
Anticoagulants	27 (40)	14 (40)	13 (41)	>0.999
Antiplatelet agents	38 (57)	19 (54)	19 (59)	0.806
Beta-blockers	46 (69)	21 (60)	25 (78)	0.124
Antiarrhythmic agents	7 (10)	4 (11)	3 (9)	>0.999
Antidiabetics	27 (40)	8 (26)	19 (59)	0.003
Insulin	12 (18)	2 (6)	10 (31)	0.010
Oral antidiabetic agents	22 (33)	8 (23)	14 (44)	0.117
ACE inhibitor/ARB	43 (66)	26 (74)	17 (57)	0.189

^aMDRD-4 levels expressed in mL/min/1.73m²; Quantitative values were given in median [Q1-Q3]. P values of categorical variables were calculated with Fisher exact test, except for LVEF where χ^2 was used. LVEF classification according to 2021 Guidelines by the European Society of Cardiology. P values of numerical data were calculated with Mann-Whitney, except for LVEF where Kruskal-Wallis was used. Diuretics: hydrochlorothiazide, furosemide, eplerenone, and spironolactone. Statins: atorvastatin, pravastatin, simvastatin, ezetimibe. Anticoagulants: warfarin, acenocumarol, bempiparin, heparin, dabigatran, rivaroxaban, edoxaban, and apixaban. Antiplatelet agents: acetylsalicylic acid and clopidogrel. Beta-blockers: bisoprolol and carvedilol. Antiarrhythmic agents: amiodarone. Oral antidiabetic agents: metformin and repaglinide. Angiotensin-converting enzyme inhibitors (ACEI) include: captopril, enalapril, and ramipril. Angiotensin receptor blockers (ARB): losartan, olmesartan, and valsartan.

Table 7: Clinical characteristics of 2DE patients.

	2DE group N=17	All patients N=67	P value
DEMOGRAPHIC CHARACTERISTICS			
Female/male, n	3/14	22/45	0.565
Age, years	72 [69-76]	71 [65-77]	0.624
Weight, kg	76 [66-87]	73 [62-89]	0.583
CARDIAC FUNCTION MARKERS			
NT-proBNP, µg/L	2.4 [1.7-4.6]	4.0 [2.3-8.6]	0.160
Left ventricular ejection fraction (LVEF), %	48 [33-56]	45 [33-58]	0.738
Reduced LVEF ≤40%, N (%)	6 (35)	27 (40)	0.916
Mildly reduced LVEF 41-49%, N (%)	3 (18)	12 (18)	
Preserved LVEF ≥50%, N (%)	8 (47)	28 (42)	
Atrial fibrillation	12 (71)	32 (48)	0.283
Cardiovascular disease	4 (24)	23 (34)	0.563
KIDNEY FUNCTION MARKERS			
Creatinine, µmol/L	101 [73-131]	105.0 [78.0-147.0]	0.693
Glomerular filtration, MDRD-4 ^a	68 [43.2-81.7]	61.0 [40.9-83.3]	0.476
Urea, mmol/L	9.0 [5.8-13.1]	10.2 [6.8-16.1]	0.367
OTHER BIOCHEMICAL MARKERS			
Haemoglobin, g/L	122 [106-139]	122 [101-138]	0.889
RISK FACTORS; N (%)			
Active smoking	3 (18)	10 (15)	0.721
Hypertension	12 (71)	49 (74)	>0.999
Pulmonary hypertension	6 (35)	16 (24)	0.364
Diabetes mellitus type 2	6 (35)	30 (45)	0.586
Dyslipidaemia	11 (65)	46 (70)	>0.999
BACKGROUND MEDICATION; N (%)			
Diuretics	11 (65)	49 (73)	0.253
Statins	9 (53)	43 (64)	0.415
Anticoagulants	10 (59)	27 (40)	0.415
Antiplatelet agents	7 (41)	38 (57)	0.286
Beta-blockers	11 (65)	46 (69)	0.777
Antiarrhythmic agents	0 (0)	7 (10)	0.335
Antidiabetics	4 (24)	27 (40)	0.265
Insulin	3 (18)	12 (18)	>0.999
Oral antidiabetics	3 (18)	22 (33)	0.373
ACE inhibitor/ARB	13 (76)	43 (66)	0.562

4.2.2. Patients of the mechanistic study

Subjects (N=49, 38.6±11.3 years old, 36% female) with genetic diagnosis of heterozygous familial hypercholesterolemia (FH) and, thus, lifelong exposure to high LDL cholesterol plasma levels and high risk of premature atherosclerosis from the SAFEHEART cohort were included in the mechanistic study. A group of young healthy volunteers (non-FH subjects, N=28, 24.5±4.6, 57% female) from the same cohort was used as reference group to establish the normal plasma range of C3 levels in a healthy population, at very low risk of presenting subclinical atherosclerosis (**Table 8**) (Details in *manuscript 4*).

This part of the study was approved by the Local Ethics Committee for Clinical Investigation in the Fundación Jimenez Diaz (CEIC-FJD; Madrid, Spain) [protocol's number: 01/09], was conducted according to the Declaration of Helsinki (2013) and a written in-formed consent was obtained from all participants.

Table 8: Demographic and clinical characteristics of familial hypercholesterolaemia population.

	Familial Hypercholesterolaemia N=49	Healthy Subjects N=28
DEMOGRAPHIC CHARACTERISTICS; mean ± SEM		
Female/male, N	18/31	16/12
Age, years	38.6±11.3	24.5±4.6
RISK FACTORS; N (%)		
Smokers	14 (29)	12 (43)
Hypertension	1 (2)	0 (0)
Diabetes mellitus	0 (0)	0 (0)
Dyslipidaemia	48 (98)	0 (0)
BIOCHEMICAL DATA, mean ± SEM		
Total cholesterol, mg/dL	282±72	170±20
Triglycerides, mg/dL	104±67	77±35
HDL cholesterol, mg/dL	47±11	56±15
LDL cholesterol, mg/dL	221±78	99±15
Apo A1, mg/dL	135±20	139±29
Apo B, mg/dL	134±41	61±10
Lipoprotein(a), mg/dL	42±35	18±21
Glucose, mg/dL	89±9	78±9
C-reactive protein, mg/L	1.86±2.6	0.73±0.2
SUBCLINICAL ATHEROSCLEROTIC DISEASE; (%)		
Plaque burden, %	23.5±6.3	-
Calcium burden, %	2.2±2.5	-
Non-calcium burden, %	21.3±5.3	-
BACKGROUND MEDICATION; N (%)		
Angiotensin-converting-enzyme inhibitors	0 (0)	0 (0)
Angiotensin II receptor blockers	1 (2)	0 (0)
β-blockers	0 (0)	0 (0)
Diuretics	2 (4)	0 (0)
Statins*	39 (80)	0 (0)

SEM: standard error of the mean; HDL: high density lipoprotein; LDL: low density lipoprotein. Statins include: rosuvastatin, ezetimibe, atorvastatin, simvastatin, lovastatin, pravastatin, fluvastatin, pitavastatin, resins, and fibrates. Healthy subject population was used to establish the C3 range in a healthy group.

4.3. Sampling

Urine and blood (serum / plasma EDTA) samples were collected from ADHF patients at hospital admission and at day 3 of hospitalisation. From healthy subjects, FH patients and their controls, samples were collected at first time in the morning after 10–14h fasting. All samples were processed within 30 minutes of obtention.

Urine samples were stabilised with the protease inhibitor cComplete Mini (Roche, Basel, Switzerland) to avoid protease activity. Urine samples were centrifuged for 10 minutes at 1200g and at room temperature to precipitate debris. The supernatant was aliquoted for 4 mL and 1 mL aliquots and stored at -80°C until further analysis.

Serum was obtained after incubation of 30 minutes at 37°C, 30 minutes at 4°C, followed by 30 minutes centrifugation at 4°C and 1800 g, aliquoted and stored at -80°C until analysed. Plasma EDTA was obtained after centrifugation of blood samples at 1600g (20 minutes, room temperature), aliquoted and stored at -80°C until analysed.

4.4. Biochemical variables

Blood creatinine (Jaffe reaction), haemoglobin, urea (kinetic urease), and NT-proBNP (electroquimioluminescence), were analysed by standard laboratory methods as part of the patients' routine analyses in the hospital. Glomerular filtrate was calculated using MDRD-4 formula with each patient's blood creatinine levels, age, sex, and race (176). Total protein and creatinine in urine were analysed using Gernon kits (RAL S.A., Barcelona, Spain) for creatinine and total protein (Variables for *Manuscript 1, 2, and 3*; see manuscript 1 for further details).

For lipid profile, total cholesterol, triglycerides, and HDL cholesterol were measured by standardised enzymatic methods; serum LDL cholesterol concentration was calculated using the Friedewald formula;

and lipoprotein (a) levels were measured using a turbidimetric method. Genetic diagnosis of FH was performed using a DNA-microarray (LIPOCHIP), described in Alonso *et al.* (257) (Variables in *Manuscript* 4).

4.5. Two-dimensional electrophoresis

Two-dimensional electrophoresis (2DE) experiments in ADHF patients and healthy subjects are based on three main steps: preparation of urine samples, isoelectric focusing (IEF) of the total protein extracts (1st dimension) and electrophoresis (2nd dimension) that are described below (**Figure 14**).

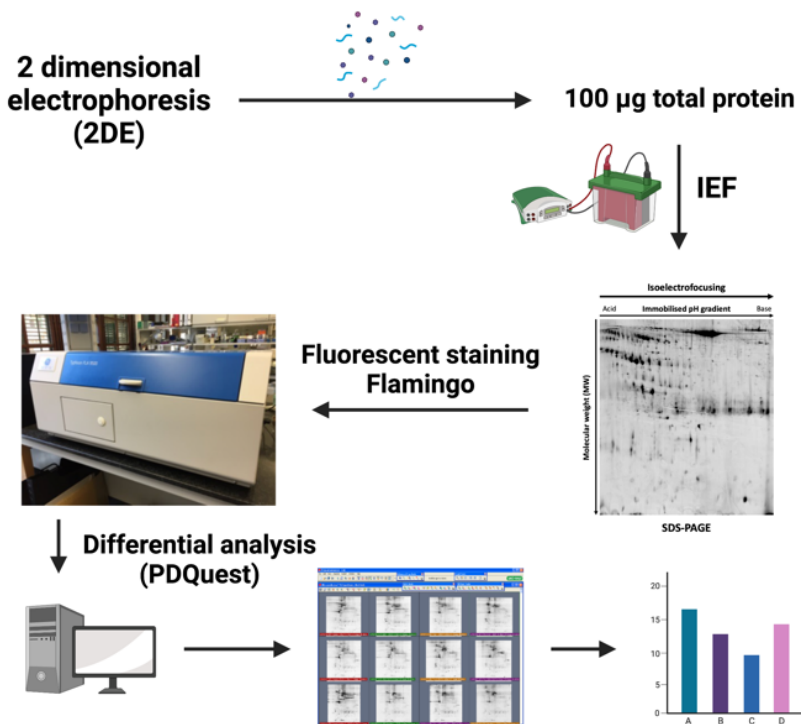


Figure 14: Summarised 2DE workflow.

4.5.1. 2DE urine sample preparation

Urine protein samples of ADHF patients and healthy controls (4-5mL) were centrifuged with Amicon Ultra-4 centrifugal filters units (3KDa cut-off, MilliporeSigma, Burlington MA, USA) to deplete our samples of smaller proteins for 30 minutes, at 3220g and 10°C. Tris-HCl 100mM was added to lower samples pH, and it was centrifuged once again in the same conditions.

The next step involved the depletion of albumin and IgGs from urine samples using ProteoExtract Albumin/IgG Removal Kit (Calbiochem, San Diego, CA, USA). The column buffer, which included the kit buffer and urine sample for a total of 2-3mL, was changed by centrifuging the samples with 9 mL of 2DE buffer (7M urea, 2M thiourea, 2% CHAPS) at 3220g and room temperature, to a final volume of 400µL of every sample. These sample extracts were quantified using 2D Quant Kit (GE Healthcare, Chicago, IL, USA) and aliquots containing 100µg of total protein per aliquot were prepared and frozen at -80°C until further analysis.

4.5.2. First dimension

The first dimension of 2DE experiments involves the separation of proteins based on their isoelectric point (pI) in commercial acrylamide strips with an immobilised pH gradient (IPG strip).

Before the first dimension step, protein samples were added:

- 1% ampholytes pH 3-10 of a commercial solution (Bio-Rad, CA, USA) to help proteins migrate towards their pI,
- 1% of 0.2% bromophenol blue,
- 100mM dithiothreitol to break disulphide bonds,
- And 2DE buffer (7M urea, 2M thiourea, 2% CHAPS) to final volume of 300µL.

Solubilised samples were separated by 17cm IEF ReadyStrips IPG strips (Bio-Rad, CA, USA) 4 to 7 linear using PROTEAN i12 IEF system (Bio-Rad, CA, USA) for the first dimension using the recommended protocol by the provider.

Before the protocol begins, the strips needed to be hydrated for protein separation. For this thesis' samples, the active hydration was performed, which involved 100V for 12h in a constant manner to facilitate proteins absorption by the strip. Once hydrated, different currents are applied so that the proteins are properly separated along the strip according to their pI (**Table 9**).

During steps 1 and 2, proteins move along the strip towards their pI, whereas during step 3 all the molecules of each protein focus forming a protein cluster. While steps 1 and 2 have set timings, 30 minutes and 2 hours, respectively; step 3 lasts until 43000 Vh are accumulated, which for these samples usually lasted 3-4 additional hours. Step 4, the *maintenance* step, is an optional step that protects the proteins from diffusion in-between the end of step 3 and extraction of the strips for storage or further analysis. Even though the strips can be kept in step 4 for several hours, the strips from ADHF patients and HS were never left in step 4 for more than two hours.

Table 9: Isoelectric focusing steps and their characteristics.

Step	Voltage	Gradient	Current	Duration
Hydration	100	Hold		12:00 h
1	250	Rapid	50	00:30 h
2	10000	Gradual	50	2:00 h
3	10000	Rapid	50	43000 Vh
4	1000	Hold	50	

Voltage in volts (V), current in micro amperes (μ A); duration: hour (h) and volt hour (Vh).

4.5.3. Second dimension

The second dimension of 2DE experiment is based on the separation of proteins according to their molecular weight in SDS-PAGE gels, also known as electrophoresis.

After IEF and before the electrophoresis, strips needed to be equilibrated using a reducing solution (50mM Tris-HCl pH 8.8, 6M urea, 2% SDS, 30% glycerol, and 2% dithiothreitol (DTT)) and an alkylating solution (50mM Tris pH 8.8, 6M urea, 2% SDS, 30% glycerol, and 2% iodoacetamide). Each step lasted 15 minutes in order to protect proteins from oxidation and to avoid vertical lines in the gel, also known as *streaking*.

For the electrophoresis, samples strips were transferred onto 12% SDS-PAGE gels where two different electric current steps were applied. The first step was set to a slow current (current applied depends on number of gels) for 30 minutes to enable the proteins enter the gel, and a second step with higher current where proteins were separated. This second step was left running at a constant current, although the amount depended on the number of gels analysed, until the sample front reached the end of the gel. This last step usually lasted 4-5h.

Once the electrophoresis was finished, gels were fixed for two hours (40% ethanol, 10% acetic acid), and stained with a fluorescent commercial solution, Flamingo (Bio-Rad, CA, USA), overnight for protein visualisation. At the end of the process, protein visualisation was performed using Typhoon FLA 9500 (GE Healthcare, Chicago, IL, USA) to obtain the protein profile of each sample.

In the discovery phase, two different kinds of gels were prepared: *analytical gels* where 100µg of total protein was loaded. These gels were used in the comparison step between patients and healthy individuals. And *preparative gels* contained 300µg of total protein was loaded to facilitate protein identification by mass spectrometry.

4.6. Differential analysis

All samples were handled the same way to minimise variability between samples and groups. The proteomic patterns were compared using PDQuest analysis software (version 8.0, Bio-Rad, CA, USA). A master gel is created in which all gels are included and used to compare with each individual sample. The program assigns every protein spot a relative value, according to the total sum of protein spots, after background subtraction. After that, ADHF patients and HS gels were compared manually so that the equivalent spots of each gel are compared between them, also known *matching*.

4.7. Protein identification

After differential analysis, the spot proteins were analysed by MS (**Figure 15**). To prepare the spots for MS the following protocol was followed:

1. Protein spots were excised and separated automatically using Ettan Spot Picker (GE Healthcare, Chicago, IL, USA).
2. The excised protein spots were washed with 25mM ammonium bicarbonate (Ambic) solution for 20 minutes.
3. Protein spots were dehydrated first with 25mM Ambic / 50% acetonitrile (ACN, three times 20 minutes each time) and 100% ACN.
4. The samples were dried in a vacuum program using Concentrator Plus (Eppendorf International, Hamburg, Germany).
5. The dried gel pieces were rehydrated with 0.2ng/ μ l of trypsin Gold (Promega Corporation, Madison, WI, USA) in 25nM ammonium bicarbonate and incubated overnight at 30°C.
6. The trypsin activity was stopped by the addition of 100% ACN for 15 min at 37°C.

7. The protein peptides were extracted with 0.2% trifluoroacetic acid (TFA) 30min at room temperature and concentrated using μ C18-Zip Tips (MilliporeSigma, Burlington, MA, USA).
8. Samples and calibrant were mixed 1:1 with α -cyano-4-hydroxycinnamic acid (HCCA) matrix (0.7mg/mL) and were applied to Anchor Chip plates (BrukerDaltonics, Billerica, MA, USA) for MS analysis, which is described below.

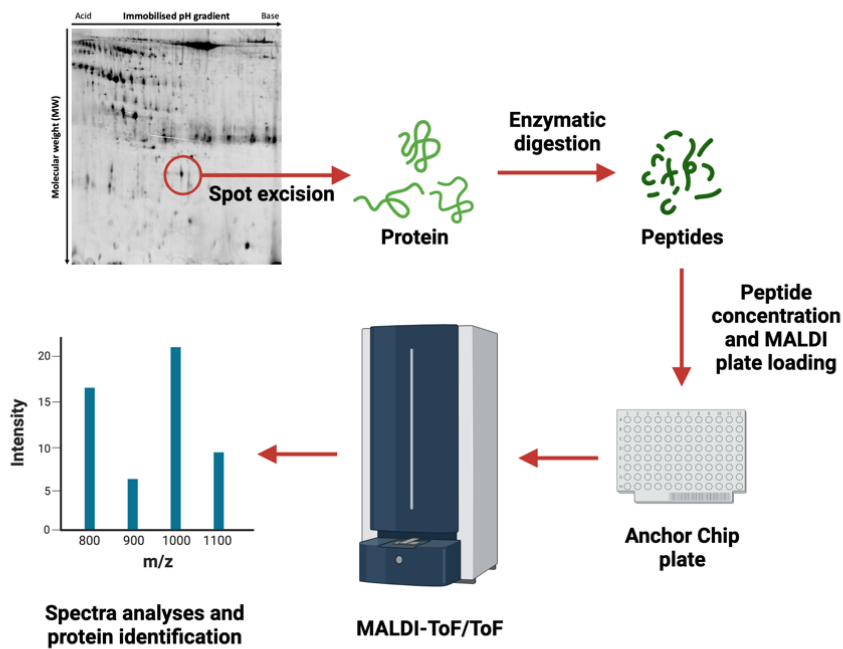


Figure 15: Summarised mass spectrometry workflow

4.8. Mass spectrometry

Proteins were identified after by matrix-assisted laser desorption /ionisation time-of-flight (MALDI-ToF) using an AutoFlex III Smart beam MALDI-ToF/ToF (Bruker Daltonics, Billerica, MA, USA), as previously described (**Figure 15**) (258).

Mass spectra were obtained with flexControl on reflectron mode, (mass range m/z 850–4,000; reflectron 1, 21.06 kV; reflectron 2, 9.77 kV; ion source 1 voltage, 19 kV; ion source 2, 16.5kV; detection gain, 2.37 \times) with an average of 3500 added shots at a frequency of 200 Hz. Samples were analysed with flexAnalysis (version 3.0, Bruker Daltonics, Billerica, MA, USA) considering a signal-to-noise ratio >3 , eliminating background peaks, and applying statistical calibration.

After processing, spectra were sent to the BioTools software (version 3.2, Bruker Daltonics, Billerica, MA, USA) and MASCOT search on Swiss-Prot 57.15 database for protein identification. For this search the following parameters were selected:

- Taxonomy: Homo sapiens taxonomy
- Mass tolerance: 50 to 100 ppm
- Maximum of two trypsin miss cleavages
- Global modification: carbamidomethyl (C) and variable modification: oxidation (M)

Protein identification was carried out by peptide mass fingerprinting (PMF) where MASCOT scores >56 and at least five matched peptides was accepted. Confirmation of identified protein was performed by peptide fragmentation working on the LIFT mode (MS/MS) (258,259).

4.9. Validation techniques

The validation of the proteomic results obtained by 2DE in manuscripts 1-3 was performed using two different techniques: Western Blot and ELISA.

4.9.1. Western Blot

Western blot (WB) is a semi-quantitative method where one single protein is detected using a specific antibody against that protein and the relative amount this protein is measured.

For the studies in ADHF patients (*manuscripts 2 and 3*), pool samples (5 representative patients) were prepared by the following protocol. A total of 4 mL of pool urine samples were centrifuged for 30 minutes, at 10°C and 3220g. Filtrate was discarded, and 100mM Tris-HCl (pH 7.6) was added to lower sample pH. Samples were once again centrifuged with the same conditions. Then, albumin and IgGs were depleted using ProteoExtract Albumin/IgG Removal Kit (Calbiochem, San Diego, CA). Proteins in the filtrate were precipitated overnight with 100% acetone. The following day samples were centrifuged for 30 minutes, at 4°C and 16200g to precipitate the protein content. The supernatant was removed, and the pellet obtained resuspended with 400µL of 100mM Tris-HCl (pH 7.6).

These samples were quantified using 2D Quant Kit (GE Healthcare, Chicago, IL, USA). The equivalent amount of 15 µg of total protein were precipitated with 100% acetone, centrifuged, and resuspended with 20µL of 100mM Tris-HCl (pH 7.6) and 4µL of sample buffer 6x with reducing conditions (with 6% β-mercaptoethanol), boiled at 95°C for 5 minutes before unidimensional electrophoresis in 12% SDS-PAGE gels. The separated proteins were transferred to a nitrocellulose membrane (Bio-Rad, CA, USA) for 2 hours, 400 mA and 4°C. To confirm the proper transfer of proteins, the membranes were stained with Ponceau solution (0.1M Tris, 1M NaCl, 0.05% Tween and pH 7.4).

These membranes were later incubated for 1h at room temperature and gentle agitation with a blocking solution (5% of non-fat dried milk or bovine serum albumin (BSA) in Tris buffer with 20% of Tween (TBS-T), to avoid non-specific binding. Next, membranes were incubated

overnight with gentle agitation at 4°C with primary antibodies, whose characteristics are detailed **Table 10: Antibodies used for Western Blot.** The following morning, membranes were washed with TBS-T and incubated for 1h at room temperature with the corresponding secondary antibody.

After two additional washing steps with TBS-T and two with TBS, protein signal was detected by chemiluminescence using peroxidase reaction (SuperSignal chemiluminescence system, Pierce), and the image was obtained with Chemidoc™ XRS system (Bio Rad). Obtained bands were normalised with total protein from Ponceau staining.

Western blots for mechanistic studies (*Manuscript 4*) were performed for each independent cell extract and ECM-extracts (Details in methods Manuscript 4, page 13) using following human primary antibodies against C3, C5, C3aR, C11b, and C18. Human β -actin and total protein (Ponceau staining) were used as loading controls.

Table 10: Antibodies used for Western Blot.

Primary antibodies					Secondary antibodies			
Antigen	Brand	Reference	Species	Dilution	Solution	Antibody	Dilution	Manuscript
AT3	Abcam	ab124808	Rabbit	1:500	BSA 5%	Anti-rabbit	1:5000	Manuscript 2
CD11b	Abcam	ab133357	Rabbit	1:1000	Blotto 5%	Anti-rabbit	1:5000	Manuscript 4
CD18	Abcam	ab119830	Rat	1/500	Blotto 5%	Anti-rat	1:5000	Manuscript 4
C3	Abcam	ab200999	Rabbit	1:1000	BSA 5%	Anti-rabbit	1:10000	Manuscript 2, 4
C3a R	Abcam	ab126250	Rabbit	1:1000	BSA 5%	Anti-rabbit	1:10000	Manuscript 4
C5	Abcam	ab11876	Mouse	1:500	BSA 3%	Anti-mouse	1:10000	Manuscript 4
TAT	Abcam	ab191378	Mouse	1:500	BSA 3%	Anti-mouse	1:10000	Manuscript 2
VDBP	Abcam	ab81307	Rabbit	1:5000	Blotto 5%	Anti-rabbit	1:2000	Manuscript 3
β -actin	Abcam	ab8226	Mouse	1:5000	BSA 3%	Anti-mouse	1:5000	Manuscript 4

AT3: antithrombin III; C3: complement C3; C3aR: complement C3a receptor; TAT: thrombin-antithrombin complex; VDBP: Vitamin D binding protein; BSA: bovine serum albumin in Tris buffer with 20% of Tween; blotto: non-fat dried milk in Tris buffer with 20% of Tween.

4.9.2. ELISA immunoassay

The Enzyme-Linked ImmunoSorbent Assay (ELISA) is a quantitative method that enables the measurement of one single protein concentration in a sample. All the ELISAs were performed using commercial kits known as *sandwich ELISA* where the plate contains the specific antibody against the desired protein. The proteins of the sample are held back by the antibody once added to the plate. A second antibody that recognises the antigen is added to the plate where it binds to the protein-antibody. This second antibody contains an enzyme that will react with another specific substrate leading to a colour change detectable by colourimetry (**Figure 16**).

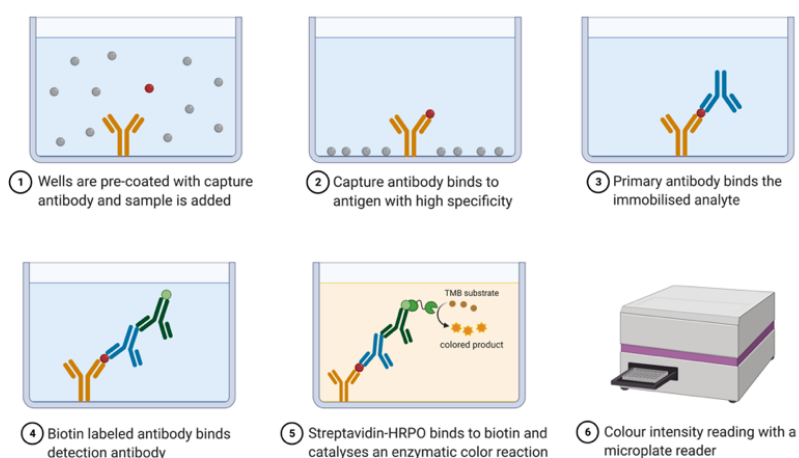


Figure 16: Sandwich ELISA steps

Adapted from "Sandwich ELISA", by BioRender.com (2022). Retrieved from <https://app.biorender.com/biorender-templates>

Specific quantitative sandwich enzyme immunoassays were used to quantify levels of different selected proteins in urine and plasma-EDTA, including TTR and RBP4 (Manuscript 1), AT3, C3, TAT, and CRP

(Manuscript 2 and Manuscript 4), and VDBP, Cystatin C, and KIM-1 (Manuscript 3), as described in **Table 11** and **Table 12**.

Table 11: ELISAs used to analyse urine samples.

Protein	Brand	Reference	Dilution	Detection limit	Intra-assay CV (%)	Inter-assay CV (%)	Manuscript
AT3	AssayPro	EA3301-1	1:3 – 1:10	9.93 ng/mL	<5.9	<9.8	<i>Manuscript 2</i>
C3	AssayPro	EC3201-7	1:5	0.30 ng/mL	<4.3	<9.8	<i>Manuscript 2</i>
CysC	Biovendor	RD191009100	1:20	0.25 ng/mL	<3.4	<6.9	<i>Manuscript 3</i>
KIM-1	Abcam	ab235081	1:5	1.28 pg/mL	<2.2	<4.8	<i>Manuscript 3</i>
RBP4	Abcam	ab196264	1:1000	2.60 pg/mL	<5.1	<8.9	<i>Manuscript 1</i>
TTR	Immundiagnostik	K6331	-	0.93 ng/mL	<3.4	<5.6	<i>Manuscript 1</i>
VDBP	R&D Systems	DVDBP0B	1:2 – 1:8	0.34 ng/mL	<1.9	<3.6	<i>Manuscript 3</i>

AT3: antithrombin III; C3: complement C3; CysC: cystatin C; KIM-1: kidney injury molecule-1; RBP4: retinol binding protein 4; TTR: transthyretin; VDBP: vitamin D binding protein; CV: coefficient of variation

Serum and plasma EDTA samples of ADHF and FH patients, and all healthy subjects were analysed for several other proteins and described in **Table 12**.

Table 12: ELISAs used to analyse blood samples.

Protein	Brand	Reference	Sample	Dilution	Detection limit	Intra-assay CV (%)	Inter-assay CV (%)	Manuscript
AT3	AssayPro	EA3303-1	P-EDTA	1:300	51 ng/mL	<5.6	<10.4	<i>Manuscript 2</i>
CRP	AssayPro	EC1001-1	P-EDTA	1:4000	0.11 ng/mL	<3.9	<9.2	<i>Manuscript 1, 2</i>
C3	AssayPro	EC2101-1	P-EDTA	1:1500	77 ng/mL	<5.6	<9.5	<i>Manuscript 2, 4</i>
TAT	AssayPro	ET1020-1	P-EDTA	-	0.78 ng/mL	<6.2	<9.9	<i>Manuscript 2</i>
TTR	Immundiagnostik	K6331	P-EDTA	1:10000	0.933 ng/mL	<3.4	<5.6	<i>Manuscript 1</i>
VDBP	R&D Systems	DVDBP0B	Serum	1:5000	0.338 ng/mL	<1.9	<3.6	<i>Manuscript 3</i>

AT3: antithrombin III; CRP: C reactive protein; C3: complement C3; TAT: thrombin-antithrombin complex; TTR: transthyretin; VDBP: vitamin D binding protein; P-EDTA: plasma EDTA; CV: coefficient of variation

Each kit was performed following respective instruction manuals. Concentration trials were performed to determine appropriate urine concentration for each ELISA kit, usually based on instruction manual recommendations.

4.10. Methods for mechanistic studies

The detailed methods used for the mechanistic study can be found in Manuscript 4 (pages 11-14).

4.10.1. Vascular smooth muscle cells

For the mechanistic study, primary cultures of human vascular smooth muscle cells (VSMC, Cell Application, Inc. San Diego CA, USA) derived from umbilical vein (pool of 10 donors) were used to study expression of C3 and C3-mediated mechanisms of cell migration and adhesion.

These VSMC were cultured in M199 complete medium (Gibco - Thermo Fisher Scientific, Waltham, MA, USA) and incubated at 37°C in a humidified atmosphere with 5% CO₂. Culture medium was replaced every 48 hours and used between passages four and eight. (See details Manuscript 4, page 12).

4.10.2. Cell adhesion and wound healing

Migration studies in the mechanistic study were performed with human VSMCs seeded in a culture insert (ibidi 2-well culture insert, ibidi GmbH, Martinsried, Germany) and left in M-199 with 10% foetal calf serum (FCS) with or without 100 µg/mL aggregated LDL (agLDL) until desired cell confluence was achieved. C3a (10 nM) or iC3b (100 nM) were added to the culture medium 1h before stimulation with agLDL and maintained during the assay when indicated. After culture inserts removal, VSMCs were washed with phosphate buffered saline (PBS) and maintained in M199 migration medium with 10% FCS with its corresponding treatment for a total of 8h.

Migration on the cell-depleted area was controlled using an inverted microscope and evolution images were taken every 2h. During migration, cells were also maintained at 37°C in a humidified

atmosphere of 5% CO₂. Cell attachment studies were performed as previously described (260); however, more detailed information is found in manuscript 4 (page 13-14).

4.10.3. Confocal microscopy

For confocal studies, VSMCs fixed with 4% paraformaldehyde were permeabilised (0.5% Tween with PBS), blocked with BSA, immunolabeled for F-actin, and analysed by confocal microscopy, as previously described by this group (261–263) using Alexa Fluor 633 or 488 phalloidin (Molecular Probes, Eugene, OR, USA) on a Leica TCS SP2-AOBS inverted fluorescence microscope (Leica Microsystems, Heidelberg GmbH, Mannheim, Germany). Fluorescent images were acquired in a scan format of 1024 × 1024 pixels at 0.1 mm intervals (20 slides) and processed with the TCS-AOBS software (Leica Microsystems, Heidelberg GmbH, Mannheim, Germany). Maximal intensity projection values were calculated using the LASAF Leica Software (Leica Microsystems, Heidelberg GmbH, Mannheim, Germany) and given as AU/mm².

4.11. Statistical analysis

Data are expressed as median ± interquartile range (IQR) for ADHF study, and mean ± SEM (standard error of the mean) for mechanistic study, except when indicated. N indicates the number of subjects tested. The normal distribution was determined via Kolmogorov-Smirnov test. Statistic differences between groups for non-normally distributed continuous variables were analysed by non-parametric tests, including Mann-Whitney or Kruskal-Wallis tests. Frequencies of categorical variables were compared by Fisher exact and Chi-square analyses. Correlations between variables were determined using Spearman rank correlation and pictured by single regression models. Due to the

exploratory character of the proteomic study, determination of the sample size was based on past experience with similar studies (258). The variability observed in the data (ADHF patients with and without renal dysfunction at hospital admission) from the proteomic studies served to guide sample size in the validation quantitative analysis (ELISA method). Sample size was validated using the JavaScript based method for simple power and sample size calculation when two independent groups are compared, that are provided in <http://www.stat.ubc.ca/~rollin/stats/ssize/n2.html> (258).

Receiver operating characteristic (ROC) curve estimations and their corresponding C statistics [area under the curve (AUC) with their 95% CI] were calculated to determine the power to discriminate ADHF patients according to heart dysfunction severity and kidney function.

Kaplan-Meier survival (free of adverse outcomes) analysis was performed after including the study variables in a logistic rank analysis to evaluate the value of the studied parameters for predicting disease progression (adverse outcome incidence) in ADHF patients. In case of multiple events, only the first one was considered for Kaplan-Meier analysis.

Adjustments for multiple testing in the discovery proteomic study were performed by the false discovery rate (FDR) using two-stage sharpened method described by Benjamin *et al.* (264). The results of the calculated adjusted q values (FDR adjusted) indicate the probability of false positives for the identified proteins considered to be significant.

Statistical analysis was performed using Stata (version 15, StataCorp., College Station, TX, USA) and SPSS (version 26, IBM Corp, Armonk NY, USA) and StatView (Abacus Concepts). A P value ≤ 0.05 was considered statistically significant.

CHAPTER IV:

RESULTS

5. Results

The results of this thesis include four different articles.

ARTICLE 1:

Urinary Proteomic Signature in Acute Decompensated Heart Failure: Advances into Molecular Pathophysiology

Published: International Journal of Molecular Sciences. (Impact Factor 2020: 5.924)

Int. J. Mol. Sci. 2022, 23, 2344. DOI: 10.3390/ijms23042344

ARTICLE 2:

Association between Antithrombin III and Complement C3 in Acute Decompensated Heart Failure

Submitted: Thrombosis and Haemostasis (Impact Factor 2022: 5.249)

ARTICLE 3:

Vitamin D Binding Protein and renal injury in acute decompensated heart failure

Accepted: Frontiers in Cardiovascular Medicine (Impact Factor 2020: 6.050)

Front. Cardiovasc. Med. DOI: 10.3389/fcvm.2022.829490

ARTICLE 4:

Alternative C3 Complement System: Lipids and Atherosclerosis

Published: International Journal of Molecular Sciences (Impact Factor 2020: 5.924)

Int. J. Mol. Sci. 2021, 22, 5122. DOI: 10.3390/ijms22105122

5.1. Article 1

Urinary proteomic signature in acute decompensated heart failure: Advances into molecular pathophysiology

Elisa Diaz-Riera; Maisa García Arguinzonis; Laura López; Xavier Garcia-Moll; Lina Badimon; Teresa Padró

Published: International Journal of Molecular Sciences

Int. J. Mol. Sci. 2022, 23, 2344. <https://doi.org/10.3390/ijms23042344>

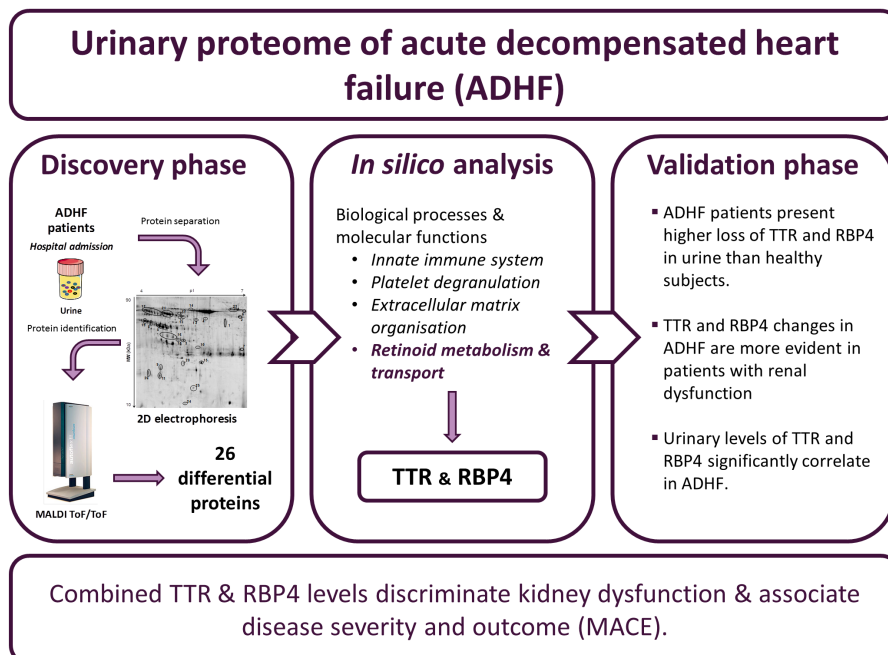
Objective: To identify and characterise the urinary protein pattern of ADHF patients at hospital admission and study the associations between the identified proteins and ADHF pathophysiology.

Highlights:

- A urinary profile of 26 differential proteins is identified in ADHF patients compared to healthy individuals.
- Most of the identified proteins are mainly produced in the liver.
- The identified proteins in urine relate to different biological functions and molecular processes, with retinoid metabolism and transport among them.
- Transthyretin, the main transporter for retinoid, presents elevated urinary levels but low plasma levels compared to healthy individuals.
- Urinary loss of transthyretin correlates with urinary loss of retinol binding protein 4.

- The combination of transthyretin and RBP4 levels discriminate kidney dysfunction and are associated with disease severity and adverse outcome.

Graphical abstract



Article

Urinary Proteomic Signature in Acute Decompensated Heart Failure: Advances into Molecular Pathophysiology

Elisa Diaz-Riera ^{1,2}, Maïsa García-Arguinzonis ¹, Laura López ³, Xavier Garcia-Moll ^{3,4}, Lina Badimon ^{1,4,5} and Teresa Padro ^{1,4,*}

- ¹ Cardiovascular-Program ICCV, Research Institute—Hospital Santa Creu i Sant Pau, IIB-Sant Pau, 08041 Barcelona, Spain; ediazr@santpau.cat (E.D.-R.); mgarciaar@santpau.cat (M.G.-A.); lbadimon@santpau.cat (L.B.)
- ² Faculty of Medicine, Universitat de Barcelona, 08036 Barcelona, Spain
- ³ Cardiology Department, Hospital Santa Creu i Sant Pau, 08025 Barcelona, Spain; llopezl@santpau.cat (L.L.); xgarcia-moll@santpau.cat (X.G.-M.)
- ⁴ Centro de Investigación Biomédica en Red Cardiovascular (CIBERCV), Instituto de Salud Carlos III, 28029 Madrid, Spain
- ⁵ Cardiovascular Research Chair, UAB, 08025 Barcelona, Spain
- * Correspondence: tpadro@santpau.cat; Tel.: +34-935565886; Fax: +34-935565559



Citation: Diaz-Riera, E.; García-Arguinzonis, M.; López, L.; Garcia-Moll, X.; Badimon, L.; Padro, T. Urinary Proteomic Signature in Acute Decompensated Heart Failure: Advances into Molecular Pathophysiology. *Int. J. Mol. Sci.* **2022**, *23*, 2344. <https://doi.org/10.3390/ijms23042344>

Academic Editor: Paolo Iadrola

Received: 3 February 2022

Accepted: 18 February 2022

Published: 20 February 2022

Publisher's Note: MDPI stays neutral with regard to jurisdictional claims in published maps and institutional affiliations.



Copyright: © 2022 by the authors. Licensee MDPI, Basel, Switzerland. This article is an open access article distributed under the terms and conditions of the Creative Commons Attribution (CC BY) license (<https://creativecommons.org/licenses/by/4.0/>).

Abstract: Acute decompensated heart failure (ADHF) is a life-threatening clinical syndrome involving multi-organ function deterioration. ADHF results from multifaceted, dysregulated pathways that remain poorly understood. Better characterization of proteins associated with heart failure decompensation is needed to gain understanding of the disease pathophysiology and support a more accurate disease phenotyping. In this study, we used an untargeted mass spectrometry (MS) proteomic approach to identify the differential urine protein signature in ADHF patients and examine its pathophysiological link to disease evolution. Urine samples were collected at hospital admission and compared with a group of healthy subjects by two-dimensional electrophoresis coupled to MALDI-TOF/TOF mass spectrometry. A differential pattern of 26 proteins (>1.5-fold change, $p < 0.005$), mostly of hepatic origin, was identified. The top four biological pathways ($p < 0.0001$; in silico analysis) were associated to the differential ADHF proteome including retinol metabolism and transport, immune response/inflammation, extracellular matrix organization, and platelet degranulation. Transthyretin (TTR) was the protein most widely represented among them. Quantitative analysis by ELISA of TTR and its binding protein, retinol-binding protein 4 (RBP4), validated the proteomic results. ROC analysis evidenced that combining RBP4 and TTR urine levels highly discriminated ADHF patients with renal dysfunction (AUC: 0.826, $p < 0.001$) and significantly predicted poor disease evolution over 18-month follow-up. In conclusion, the MS proteomic approach enabled identification of a specific urine protein signature in ADHF at hospitalization, highlighting changes in hepatic proteins such as TTR and RBP4.

Keywords: proteomics; 2DE-MS/MS; acute decompensated heart failure; urine samples; pathophysiology

1. Introduction

Heart failure (HF), a pathological condition characterized by the inability of the heart to pump enough blood and oxygen to support the metabolic demands of other organs [1], is nowadays a leading cause of morbidity and mortality worldwide [2]. HF is a progressive pathology with recurrent episodes of acute worsening or decompensation [3]. Hence, acute decompensated heart failure (ADHF) is a distinct clinical syndrome with a multifaceted and still incompletely understood pathophysiology, thus leaving potential for discovery of new targets to cover unmet clinical needs regarding more accurate patient risk stratification and novel preventive and therapeutic interventions. ADHF is frequently associated with

diminished renal function, an important risk factor for poor outcomes [4,5]. Kidney dysfunction in HF has generally been considered a result of impaired renal blood flow in the setting of depressed cardiac function [6]. However, increasing evidence suggests a more complex and multifactorial process [7], stressing the need to gain a better understanding of the pathophysiological mechanisms linking the failing heart and the kidney.

Human body fluids containing disease-associated proteins that reflect ADHF pathophysiology might assist clinicians in early diagnosis, risk stratification, and management of the patients. More specifically, protein signals can themselves be mediators of the ADHF phenotype and represent both causal and secondary pathways leading to the development and progression (or remission) of the disease. In this respect, urine contains proteins from the kidney and urinary tract, but also from distant organs and tissues [8]. Therefore, urine proteins are particularly suitable to gain better understanding of dysfunctional processes involving these organs.

Differential proteome signatures between normal and disease states can be determined by using targeted and untargeted mass spectrometry (MS)-based proteomic approaches [9,10]. MS analysis has emerged as a powerful tool in proteomics to identify and characterize proteins and protein complexes in biological samples including blood, urine, tissues, and cells. MS can be used for high-throughput identification of proteins in complex mixtures or after protein separation by different methods including two-dimensional gel electrophoresis (2DE) [11,12]. In previous studies, we used a top-down strategy (analysis of intact protein) based on 2DE coupled to matrix-assisted laser desorption and ionization time of flight (MALDI-TOF/TOF) mass spectrometry to describe changes of the plasma proteome in early stages of acute myocardial infarction [13,14] or in isolated platelets of subjects with metabolic disorders [15]. Here, we focused on a similar 2DE-MS-based approach to characterize the differential urinary protein profile in ADHF patients at hospital admission in comparison with healthy subjects used as reference group. In silico analysis was performed to highlight the most representative differential proteins and gain better insight into the biological processes and molecular functions associated with the pathophysiology of ADHF and its association with kidney dysfunction and/or the cardiorenal syndrome.

2. Results

2.1. Clinical Characteristics of the ADHF Patient Population

The study included 67 patients who were hospitalized due to ADHF at Hospital de la Santa Creu i Sant Pau (HSCSP) in Barcelona. Baseline demographic and clinical characteristics of the studied population are given in Supplementary Table S1. ADHF patients had a median glomerular filtration rate of 61.0 (40.9–83.3) mL/min/1.73 m², with 47% of patients presenting values within the pathological range (41 (31–45) mL/min/1.73m²). Median percentage of ventricular ejection fraction in the study population was 45 (33–58)%, with values of <40% in 27 of the 67 ADHF patients.

For the 2DE-MS studies, a subgroup representing 25% of the ADHF patients was randomly selected (76% male, 72 (69–76) years old). As shown in the Supplementary Table S2, the subgroup used in the urine proteomic studies (2DE-MS group) did not statistically differ from the total study group (Validation Group) regarding demographic characteristics (sex, age), kidney and cardiac function markers, and risk factors including hypertension and pulmonary hypertension, diabetes type 2, and dyslipidaemia. No major differences were observed concerning background medication.

2.2. Urine Protein Signature in ADHF Patients by 2DE Mass Spectrometry

Urine samples of ADHF patients at hospital admission depicted a differential pattern of 47 protein spots compared to healthy subjects when analyzed by 2D electrophoresis (2DE) gel within a pH range of 4 to 7 and molecular weight between 10 and 80 kDa (Figure 1A and Supplementary Figure S1). After in-gel tryptic digestion of the spots, 26 non-redundant proteins were identified by mass spectrometry MALDI-TOF/TOF, as described below.

Among them, 19 proteins were detected as one, single spot; two were detected as a two-spot protein, while the other five proteins showed a multi-spot pattern (Figure 1A).

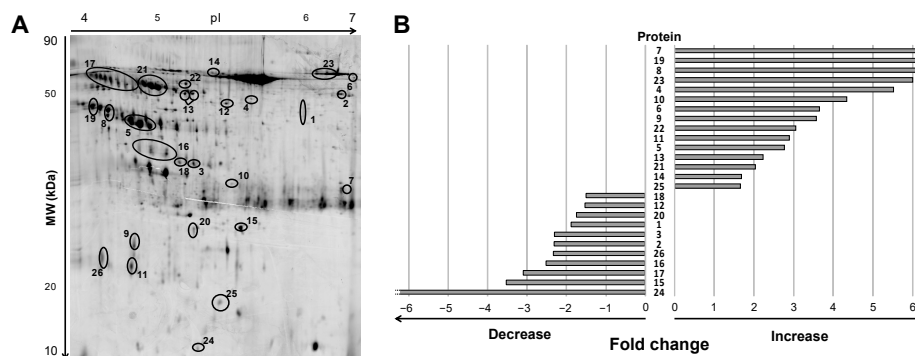


Figure 1. Differential protein signature by 2DE-MS in urine of ADHF patients at hospital admission. (A) Representative 2DE-PAGE gel of an ADHF patient depicting proteins with >1.5-fold change compared to healthy subjects. Urine proteins were separated on IPG strips (pH 4–7) in the first dimension followed by 12% SDS-PAGE in the second dimension 2D gel electrophoresis. Proteins were stained with fluorescent flamingo and images were captured with blue laser (excitation 512 nm and emission 535 nm) using a Typhoon FLA9500. (B) Bars refer to fold change increase/decrease labeling intensity for each protein highlighted in panel A (ID Gel spot number), in ADHF patients compared to healthy group. To note, spots identified as the same protein by MS are shown under the same ID number, and fold change in panel B was calculated by adding the individual spot intensities.

Of this 19-protein subset, 15 had >1.5-fold higher levels in urine of ADHF patients than in healthy subjects, while 11 proteins presented >1.5-fold lower intensity in the ADHF group (Figure 1B). Consistency for these findings (>1.5-fold change in intensity between ADHF patients and healthy subjects across all gels) was higher than 82% for 16 proteins, 7 other proteins depicted a consistency >75%, and for 3 proteins (ID number: 12, 14, 18) it was between 58–65%.

Protein identification of the MALDI-TOF/TOF spectra was obtained using the MASCOT Server search engine on the monoisotopic mode, allowing a maximum of 100 ppm peptide tolerance and a maximum of 2 trypsin missed cleavages against the SwissProt database (see Section 4 for details). Ten of the 26 proteins were directly identified by peptide mass fingerprint (PMF-MS) with a sequence coverage ranging from 3% to 26% and MASCOT scores between 60 and 234 (reliable protein identification refers to Mascot score >56). Sixteen proteins were identified by MS/MS working on the lift mode after peptide fragmentation of the three monoisotopic peaks with higher intensity (Table 1 with additional information in Supplementary Table S3). Selected peptides had a median length of 11 (9–14) amino acids. Seven peptides presented a cysteine (C) carbamidomethylation and one peptide had a methionine (M) oxidation; both types of modifications were taken into account for the fragment mass analysis and MASCOT MS/MS ion search. Protein identification was based on the peptide with better performance after fragmentation and confirmed ($n = 9$ proteins) using results obtained from the additional selected peptides (Supplementary Table S4). Peptides 2 and 3 of seven proteins did not result in reliable protein identification and had to be discarded. MASCOT ion scores for the analyzed peptides were >50 (range: 54–102; Table 1), which was in line with a correct protein identification (MASCOT ion score threshold = 30 in MS/MS analysis).

Table 1. Mass spectrometry characteristics of identified proteins in urine of ADHF patients.

#	Protein name	Gene name	Swiss Prot number	Up/down regulation	Experimental pI	Molecular weight (KDa)	MS or MS/MS	MASCOT Score	Coverage
1	Lysosomal acid phosphatase	ACP2	P11117	↓	5.80	45.5	MS	63	7
2	Pancreatic α-amylase	AMY2A	P04746	↓	6.45	51.6	MS/MS	61	-
3	Annexin A10	ANXA10	Q9UJ72	↓	5.20	35.2	MS	60	19
4	Arylsulfatase A	ARSA	P15289	↑	5.50	49.6	MS	67	10
5	Zinc-α-2-glycoprotein	AZGP1	P25311	↑	4.8-5.1	41.6-43.5	MS	66	11
6	Complement C3	C3	P01024	↑	6.75	54.8	MS	62	3
7	Carbonic anhydrase 1	CA1	P00915	↑	6.70	30.1	MS/MS	71	-
8	Endosialin	CD248	Q9HCU0	↑	4.70	44.6-45.6	MS/MS	54	-
9	CD59 glycoprotein	CD59	P13987	↑	4.90	22.7	MS/MS	82	-
10	Cathepsin D	CTSD	P07339	↑	5.40	31.2	MS/MS	58	-
11	Fibrinogen β-chain	FGB	P02675	↓	4.90	18.7-19.8	MS/MS	55	-
12	Fibrinogen γ-chain	FGG	P02679	↑	5.30-5.35	48.0-48.2	MS/MS	55	-
13	Vitamin D binding protein	GC	P02774	↑	5.20	50.5	MS	94	17
14	Hemopexin	HPX	P02790	↑	5.30-5.35	55.4	MS/MS	70	-
15	Basement membrane-specific heparan sulfate proteoglycan core protein	HSPG2	P98160	↓	5.40	24.9	MS/MS	102	-
16	Inter-alpha-trypsin inhibitor heavy chain H4	ITIH4	Q14624	↓	4.9-5.1	36.6-37.2	MS	74	10
17	Kininogen-1	KNG1	P01042	↓	4.7-4.9	50.5-53.3	MS	63	8
18	Vesicular integral-membrane protein VIP36	LMAN2	Q12907	↓	5.20	35.2	MS/MS	60	-
19	Leucine-rich alpha-2-glycoprotein	LRG1	P02750	↑	4.60	47.4	MS/MS	79	-
20	Retinol binding protein	RBP4	P02753	↓	5.20	24.7-25.2	MS/MS	66	-
21	Alpha-1-antitrypsin	SERPINA1	P01009	↑	5.00-5.10	51.4-52.2	MS	130	19
22	Antithrombin III	SERPINC1	P01008	↑	5.20	52.6	MS/MS	78	-
23	Serotransferrin	TF	P02787	↑	6.00-6.40	56.5	MS	234	26
24	Trefoil factor 2	TFE2	Q03403	↓	5.20	11.1	MS/MS	83	-
25	Transthyretin	TTR	P02766	↑	5.30	15.9	MS/MS	61	-
26	Vitelline membrane outer layer protein 1 homolog	VMO1	Q7Z5L0	↓	4.65	21.2	MS/MS	87	-

#: 2DE—Gel ID number; pI: isoelectric point; MS: mass spectrometry. MS indicates MALDI-TOF while MS/MS refers to MALDI-TOF/TOF.

2.3. Changes in the ADHF Urine Protein Signature and Relation to Kidney and Heart Function

Table 2 shows the median (Q1–Q3) values of the spot(s) intensity (arbitrary units, AU) for the 26 proteins identified by PMF-MS and MS/MS with a median fold change >1.5-fold between the ADHF and HS groups. Differences in spot intensity between groups for all proteins except for the fibrinogen chain β (FGB) showed Q values (FDR correction) ≤0.06, indicating a maximal expected proportion of 6% false positives among all features.

Among 26 proteins, 13 (7 decreased and 6 increased levels) showed the strongest change (>3-fold vs. HS group) in patients within the lowest tertile for the glomerular filtration rate (median MDRD-4: 33.7 (31.1–41.2) mL/min/1.73 m²). In addition, four of these proteins showed major changes in association with a reduced LVEF (median lower tertile <40%) (Supplementary Figure S2).

2.4. Functional Characteristics and Pathway Analysis of the Differential Urine Protein Signature in ADHF

Tissue origin of the differential proteins in urine of ADHF patients was defined using the GeneCards database. Most of these proteins (65%) are produced in the liver, with three of them being also expressed in the kidney. Differential urinary proteins in ADHF were also expressed in the pancreas, brain, adipocytes, and lung in addition to the stomach, salivary

glands, and spleen. Of note, none of the ADHF differential proteins in urine had primary cardiac origin, according to the Genecards database (Figure 2A).

Table 2. Urinary spot volumes (AU) of the differential protein signature (2DE-MS) in urine of ADHF patients at hospital admission.

Protein ^a	Gene	HS (N=6)	ADHF (N=17)	p Value ^b	Q Value ^c
1	<i>ACP2</i>	0.89 [0.51–1.10]	0.37 [0.24–0.42]	0.049	0.046
2	<i>AMY2A</i>	1.07 [0.92–1.10]	0.47 [0.31–1.18]	0.089	0.060
3	<i>ANXA10</i>	0.55 [0.45–0.85]	0.33 [0.02–0.54]	0.077	0.056
4	<i>ARSA</i>	0.02 [0.001–0.04]	0.10 [0.06–0.20]	0.017	0.028
5	<i>AZGP1</i>	2.47 [1.61–2.81]	8.08 [4.92–12.94]	0.001	0.010
6	<i>C3</i>	0.24 [0.22–0.81]	0.89 [0.36–1.41]	0.083	0.058
7	<i>CA1</i>	0.002 [0.001–0.05]	0.27 [0.18–0.79]	0.010	0.027
8	<i>CD248</i>	0.18 [0.15–0.19]	1.12 [0.52–1.65]	0.003	0.013
9	<i>CD59</i>	0.47 [0.17–1.12]	1.68 [1.07–2.39]	0.027	0.038
10	<i>CTSD</i>	0.21 [0.16–0.33]	0.90 [0.21–1.36]	0.052	0.046
11	<i>FGB</i>	3.23 [2.60–3.87]	2.11 [1.57–2.78]	0.210	0.136
12	<i>FGG</i>	0.19 [0.02–0.28]	0.58 [0.15–1.75]	0.062	0.051
13	<i>GC</i>	0.77 [0.66–0.98]	1.71 [0.87–2.55]	0.042	0.044
14	<i>HPX</i>	1.00 [0.63–1.41]	2.05 [1.00–2.97]	0.048	0.046
15	<i>HSPG2</i>	3.96 [2.27–6.47]	1.13 [0.67–2.40]	0.015	0.028
16	<i>ITIH4</i>	10.66 [7.82–14.06]	4.25 [2.48–8.04]	0.006	0.021
17	<i>KNG1</i>	26.14 [18.40–35.01]	8.73 [3.82–16.11]	0.003	0.013
18	<i>LMAN2</i>	0.34 [0.28–0.48]	0.22 [0.07–0.35]	0.077	0.056
19	<i>LRG1</i>	0.09 [0.07–0.10]	0.87 [0.35–1.26]	0.014	0.028
20	<i>RBP4</i>	1.56 [1.41–1.68]	0.86 [0.71–1.16]	0.033	0.040
21	<i>SERPINA1</i>	1.58 [1.23–1.83]	4.53 [3.13–7.41]	0.013	0.028
22	<i>SERPINC1</i>	0.15 [0.11–0.19]	0.47 [0.20–0.63]	0.034	0.040
23	<i>TF</i>	1.22 [0.97–1.81]	7.31 [4.56–7.78]	0.001	0.010
24	<i>TFE2</i>	0.36 [0.002–0.41]	0.002 [0.001–0.06]	0.064	0.051
25	<i>TTR</i>	0.40 [0.39–0.67]	0.88 [0.66–1.45]	0.031	0.040
26	<i>VMO1</i>	4.03 [2.60–4.57]	1.74 [1.20–3.17]	0.023	0.035

^a 2DE—Gel ID number. Values are given as median [Q1–Q3]; ^b p values obtained by the Mann-Whitney test; ^c Q values obtained after FDR correction.

All 26 proteins differentially secreted in the urine of ADHF patients were subjected to the PANTHER database search for classification according to their molecular function and biological process based on Gene Ontology (GO) annotation terms. As shown in Supplementary Table S5, most of the identified proteins (85%) were involved in metabolic processes for lipids, carbohydrates, vitamins, and heme molecules (12 proteins) as well as in hemostasis (coagulation) and the complement pathway cascade (12 proteins). Other major biological processes were inflammatory and immune responses (9 proteins) and cell functions including differentiation, adhesion, and migration (6 proteins). The most common molecular functions for the differential protein pattern were protein binding (84% proteins), catalytic activity (38% proteins), and molecular transport (27%). Thirteen of the 26 proteins were related to two or more molecular functions while 11 proteins were related to several biological processes (Supplementary Table S5, Figure 2B).

Using the WebGestalt and Reactome platforms, four biological/molecular pathways were found to be overrepresented among the 26 urine proteins with a differential detection pattern in ADHF (Q-value < 0.05; Figure 3A). These referred to retinoid metabolism and transport (R-HSA-975634), platelet degranulation (R-HSA-114608), innate immune system (R-HSA-168249), and extracellular matrix organization (R-HSA-1484244). Within the first group, three different proteins were identified: retinol-binding protein 4 (*RBP4*), transthyretin (*TTR*), and heparan sulphate proteoglycan 2 (*HSPG2* or perlecan). Four proteins were related to platelet degranulation including fibrinogen β chain (*FGB*) and γ chain (*FGG*), serotransferrin (*TF*), and inter- α -trypsin inhibitor heavy chain H4 (*ITIH4*). Moreover, nine of the proteins differentially detected in the urine of ADHF patients were associated

to the innate immune system, wherein eight were increased (fibrinogen γ chains (*FGG*), α -1-antitrypsin (*A1AT*), CD59 glycoprotein (*CD59*), cathepsin D (*CTSD*), arylsulphatase A (*ARSA*), complement C3 (*C3*), transthyretin (*TTR*), and leucine-rich α -2-glycoprotein (*LRG1*) and only the fibrinogen β chain was decreased. The extracellular matrix organization pathway included five proteins, *FGG*, *TTR*, and *CTSD* with increased levels and *HSPG2* and *FGB* with decreased levels, in ADHF.

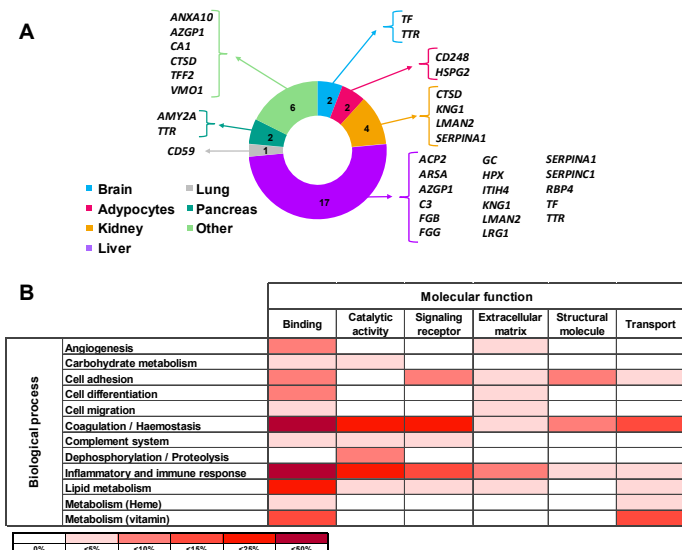


Figure 2. Main origin and function of the differential urinary proteins in ADHF. (A) Tissue origin of urinary proteins. Besides the listed organs, stomach, spleen, and salivary gland are included in the Others category. (B) Molecular function and biological process involving the urine differential proteins. Color intensity refers to the number of proteins involved, expressed as percentage of the total differential protein subset in urine ($n = 26$).

Network analysis (STRING search tool) revealed that 77% of the differential urinary proteins in ADHF are connected by direct or indirect interactions forming a single cluster, with a set of 14 proteins showing the highest number of interactions (>7 protein–protein interactions (PPI) each). From this cluster, 10 proteins participate in the top four pathways related to the differential urine signature, suggesting a close interplay between these biological processes in the physiopathology of ADHF. TTR and fibrinogen β and γ chains (*FGB* and *FGG*) were the most overrepresented proteins participating in three of the four identified pathways each (Figure 3B and Supplementary Figure S3). Both *FGG* and *TTR* showed >2 -fold changes when the urine of ADHF patients and healthy subjects was compared. Of these two proteins, TTR was selected for further quantitative validation studies, based on the involvement of this protein in pathophysiological processes associated with heart disease [16–18], kidney disorders [19], inflammation, and malnutrition [20,21], which refer to processes related with the pathophysiology and progression of heart failure.

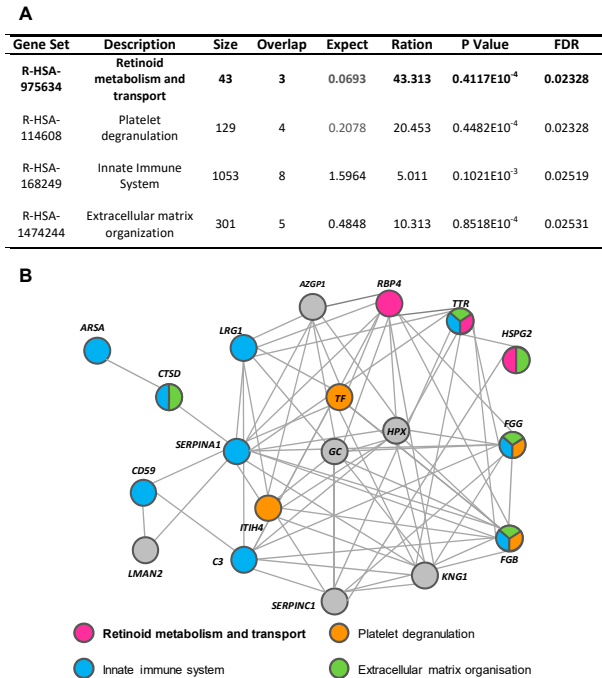


Figure 3. Pathways associated with identified urinary proteins. (A) Reactome pathways of urinary proteins of ADHF patients. (B) String network of urinary proteins identified in ADHF patients.

2.5. Urine and Plasma Transthyretin Levels in ADHF Patients

Transthyretin (TTR) was quantified by ELISA and its levels in urine were normalized by the total protein content in the sample. As shown in Figure 4A, ADHF patients ($n = 67$) showed significantly higher TTR urine levels than the healthy subject group (11.77 (3.65–64.27) vs. 6.62 (2.47–12.17) ng TTR/mg total protein, $p = 0.049$), validating the proteomic findings. Patients with renal dysfunction at hospital admission showed a trend to higher TTR levels (16.7 (6.4–70.9) TTR/mg total protein) compared to ADHF patients with normal renal function at hospital admission (5.2 (2.6–43.0) ng TTR/mg total protein, $p = 0.078$, Figure 4A).

Contrarily to urine, plasma median TTR level was significantly lower in the ADHF than in the healthy group (100.1 (71.3–123.7) vs. 136.6 (120.9–164.9) $\mu\text{g TTR/mL}$, $p < 0.001$). This difference was found regardless of the absence or presence of renal dysfunction (NRF and RD groups, $p < 0.001$ vs. HS group; Figure 4B). No differences were observed between ADHF patients with normal renal function and those with renal dysfunction at hospitalization (99.7 (66.9–115.8) $\mu\text{g TTR/mL}$ vs. 101.8 (74.3–127.1) $\mu\text{g TTR/mL}$, $p = 0.205$). No correlation between TTR levels in urine and plasma was observed ($\text{Rho} = 0.032$, $p = 0.813$, Figure 4C), suggesting that the decrease in TTR plasma levels is not only dependent on the urinary loss but rather on a balance between tissue expression/secretion and renal filtration. Interestingly, plasma TTR levels in ADHF patients at admission inversely correlated with plasma levels of C-reactive protein (CRP), the gold standard marker for systemic inflammation ($\text{Rho} = -0.303$, $p = 0.039$) that was significantly increased in ADHF patients

(Supplementary Figure S4). This correlation was maintained in ADHF patients with kidney dysfunction at admission (RD group; $Rho = -0.432$; $p = 0.043$) but not in the ADHF group with MDRD-4 levels in the physiological range (NRF group; $Rho = -0.228$; $p = 0.275$).

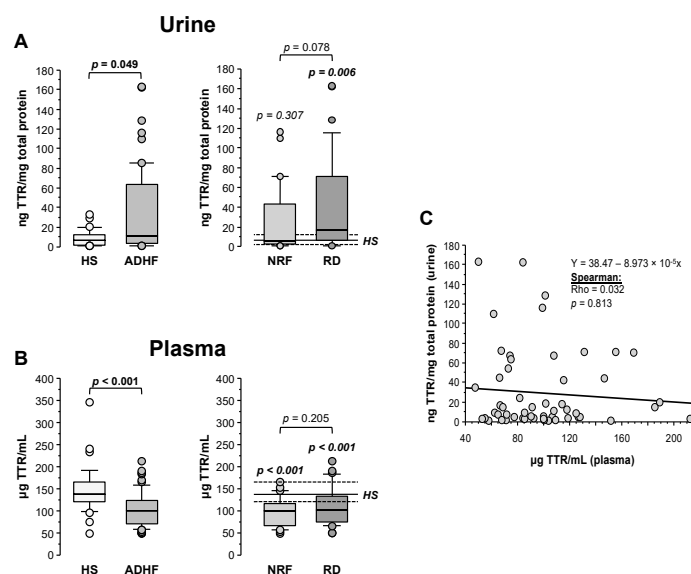


Figure 4. Urinary and plasma levels of transthyretin (TTR). (A) On the left, urinary levels of TTR obtained by immunoassay (ELISA) of healthy subjects and all ADHF patients ($n = 67$). On the right, urinary TTR of all ADHF patients with normal renal function at hospitalization (NRF, $n = 35$) and with renal dysfunction (RD, $n = 32$) at hospital admission. The p values in italics correspond to comparison with healthy subjects. Urine levels were normalized by total protein in urine. (B) TTR plasma levels of all ADHF patients and healthy subjects on the left. On the right, plasma levels of TTR of ADHF patients with normal renal function (NRF, $n = 35$) and with renal dysfunction (RD, $n = 32$) at hospital admission. The p values in italics correspond to the comparisons between each ADHF patient subgroup and healthy subjects. (C) Correlation between TTR plasma and urinary levels.

In the ADHF group, TTR levels in urine did not depend on age ($Rho = -0.002$; $p = 0.986$) and did not differ between sexes (men vs. women: 12.3 (3.7–67.1) vs. 9.4 (2.8–24.2) ng TTR/mg total protein; $p = 0.561$). TTR levels in the total ADHF patient group did not correlate with the LVEF ($Rho = -0.050$, $p = 0.706$). However, as shown in Supplementary Table S6, among ADHF patients with normal renal function (NRF group), those with reduced LVEF (<40%) had a TTR loss in urine >3-fold higher than patients with preserved LVEF (12.3 (3.3–64.1) vs. 4.1 (1.6–5.0) ng TTR/mg total protein; $p = 0.049$). This pattern was not observed in ADHF patients with renal dysfunction (RD group) at hospital admission, who presented high urine TTR loss regardless of the LVEF condition (reduced 12.0 (3.3–54.5) vs. preserved 15.1 (7.2–70.7) ng TTR/mg total protein, $p = 0.363$). In addition, urinary TTR levels did not differ between patients with and without a clinical history of ischemia and presence of cardiovascular risk factors and clinical characteristics such as atrial fibrillation and pulmonary hypertension, either in the total ADHF group or when the subgroups without and with renal dysfunction at admission were separately considered (see Supplementary Table S6).

2.6. Changes in Urine RBP4 Directly Correlate with TTR and Are Related to Renal Function

Retinol-binding protein 4 (RBP4), unlike results obtained by proteomics, showed 2-fold higher loss in urine for ADHF patients when compared with healthy subjects (HS), although differences did not achieve statistical significance (22.8 (3.8–60.9) vs. 11.9 (7.8–14.0) ng RBP4/mg total protein, $p = 0.244$, Figure 5A). Of note, ADHF patients with renal dysfunction (RD) at hospital admission had >4-fold higher RBP4 urine levels than those presenting normal renal function, who otherwise had urine values within the normal range (RD vs. NRF groups: 40.9 (9.5–248.7) vs. 9.7 (2.0–34.9) ng RBP4/mg total protein, $p = 0.002$, Figure 5B). A significant positive correlation was found between urinary levels of RBP4 and its transporter TTR in ADHF patients (Figure 5C).

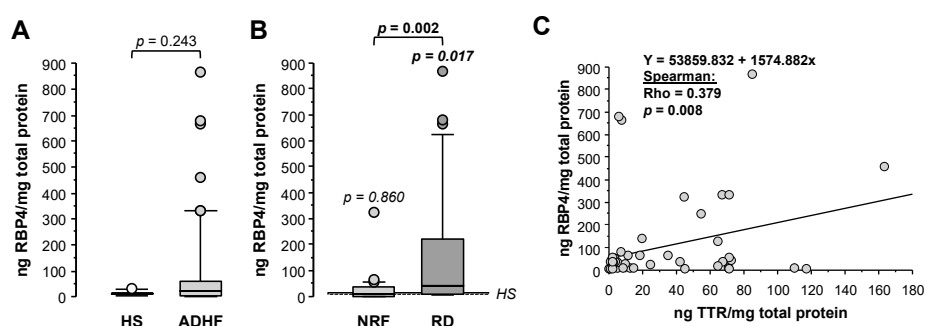


Figure 5. Urinary levels of retinol-binding protein 4 (RBP4). (A) Urinary levels of RBP4 obtained by immunoassay (ELISA) of all ADHF patients ($n = 67$) at hospital admission and healthy subjects. (B) Urinary levels of RBP4 of ADHF patients with normal renal function (NRF, $n = 35$) and with renal dysfunction (RD, $n = 32$) at hospital admission. The p values in italics correspond to comparison with healthy subjects. (C) Regression line of urinary RBP4 and TTR levels of ADHF patients at hospital admission.

2.7. RBP4 and TTR Levels in Urine at Hospital Admission Relate with Disease Evolution within 18-Month Follow-Up

Receiver operating characteristic (ROC) curve analysis evidenced that RBP4 urine levels significantly differentiate ADHF by their glomerular filtration rate (MDRD-4 values), with an AUC of 0.742 (95% CI (0.614–0.870), $p < 0.001$), with the cutoff value of 37.0 ng/mg total protein (57.1% sensitivity and 78.6% specificity) being the urine concentration that better discriminated patients with and without pathological glomerular filtration (MDRD-4 < 60 mL/min/1.73m²) at hospital admission. In addition, ROC analysis showed that combining RBP4 and TTR urine levels resulted in higher C-statistic values (AUC: 0.826 (0.705–0.947), $p < 0.001$) for discriminating ADHF patients according MDRD-4 levels (Figure 6A, Supplementary Table S7).

Within the 18-month follow-up after hospital discharge, 59% of the ADHF patients presented major clinical outcomes, which included rehospitalization (28 patients) due to heart and/or kidney decompensation, heart transplant (4 patients), and death (12 patients).

Kaplan–Meier analysis evidenced that values above a predicted probability of 0.346 (specificity 66.7%, sensitivity 91.3%) calculated from the AUC for combined urine levels of RBP4 and TTR at hospital admission associated with worse disease evolution and earlier presentation of major adverse events (cardiac and/or renal rehospitalization, heart transplant, or death, $p = 0.028$, Figure 6B) during the 18 months' evolution follow-up.

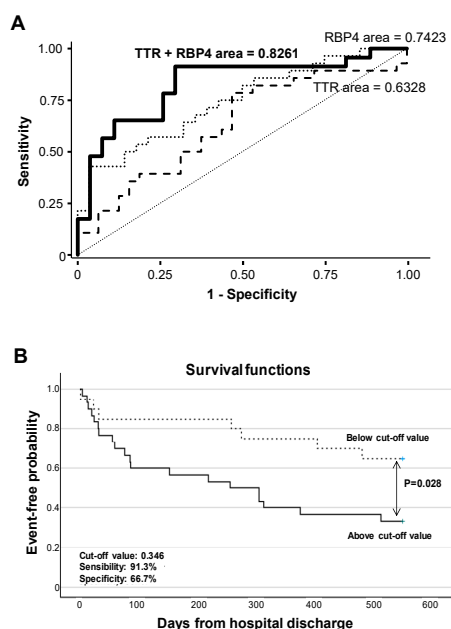


Figure 6. Discrimination and survival analyses of TTR and RBP4 levels. **(A)** ROC analysis of urinary TTR and RBP4 for the discrimination of ADHF by their glomerular filtration rate. **(B)** Kaplan–Meier curve analysis. Only the first major adverse clinical event during follow-up (28 rehospitalizations due to heart and/or kidney decompensation, 4 heart transplants, and 8 patient deaths) was considered for calculation of event-free probability.

3. Discussion

Acute decompensated heart failure (ADHF) is a complex clinical condition that may affect different organs and involve several pathophysiological mechanisms. Until now, the underlying biological processes have not been completely elucidated, emphasizing the need for a deeper understanding of the molecular functions and pathways associated to the ADHF pathophysiology. To address this problem, we carried out a discovery hypothesis-free study using 2DE coupled to MALDI-TOF/TOF mass spectrometry (2DE-MS) aimed to unravel a disease-specific differential proteomic profile in urine of ADHF patients at hospital admission and its potential link to pathophysiology.

In recent years, urine has become a promising biospecimen in clinical proteomics. Urine represents a combination of both blood ultrafiltrates and local secretion from kidney-specific cells and tubules, therefore reflecting systemic and renal diseases [22]. Moreover, in the absence of homeostatic regulation, the changes in urine proteins may detect small and early pathological changes [23]. Additionally, urine sampling has many advantages compared to blood including the availability of larger and more recurrent volumes without causing discomfort to the patient.

Here, by investigating the urine proteomic pattern of ADHF patients at hospital admission, we identified a protein signature of 26 unique proteins associated to the acute decompensation of heart failure that could characterize the pathophysiological changes in ADHF patients. Overall, the differential pattern refers to proteins acting through molecular

functions such as catalytic activity, signaling receptor binding and transport, and being involved in various biological processes including metabolism of lipids, vitamins, carbohydrates and heme-components, hemostatic and complement systems, and immune and inflammatory responses.

Of the 26 proteins with differential urine detection levels in ADHF, 17 were mainly of hepatic origin and, among them, 11 proteins showed the highest changes in the urine of ADHF patients with glomerular filtration below the pathological threshold (MDRD-4 <60 mL/min/1.73m²), which might relate to the concept of a pathological interaction among heart, kidney, and liver in heart failure patients leading to multi-organ deterioration and unfavorable disease evolution [24–26]. In this respect, Kawahira et al. [27] recently reported the prognostic value of impaired hepato-renal function in patients hospitalized for acute decompensated heart failure by combining the MELD-XI score, which includes data on bilirubin and creatinine reflecting liver and kidney function and the FIB-4 index that assesses liver fibrosis [28]. Indeed, cardiac dysfunction, especially in ADHF, can cause, in addition to elevated venous pressure, reduced liver blood flow and arterial flow, leading to hepatocyte atrophy, edema of the peripheral area, and liver stiffness [27,29]. Extending these clinical observations, in our study, leucine rich α -2-glycoprotein (*LRG1*) was near 100-fold higher in urine of ADHF patients. *LRG1* is a hepatic protein that is known to regulate endothelial TGF β signaling, a major factor in many progressive fibrotic diseases [30]. The potential relevance of *LRG1* in cardiac fibrosis has recently been suggested in a mice experimental model of chronic pressure overload-induced heart failure [31]. Additionally, zinc- α 2-glycoprotein (*AZGP1*), with 3–5-fold higher loss in urine of ADHF patients, might contribute to pathological tissue remodeling and disease progression. Thus, Sørensen-Zender et al. [32], using mice genetically deficient in *AZGP1*, described this protein to be involved in negative regulation of fibrosis through a TGF β -mediated mechanism.

In silico data analysis led to several other noteworthy observations that might contribute to gaining better understanding of the molecular events and pathological mechanisms participating in ADHF. Thus, an interesting insight that merged from using search tools such as WebGestalt, Reactome, and STRING was that the differential urinary protein subset fell into the top four categories of signal networks, including innate immune system and inflammation, platelet degranulation, extracellular matrix organization, and retinoid metabolism and transport. Furthermore, our study evidenced that 19 of the urine differential proteins participating in the four categories were interacting in a single network cluster, suggesting a close interplay among various biological pathways in association to the ADHF pathology. Cardiac decompensation accompanying acute heart failure (AHF) episodes has been related to systemic inflammatory responses, supported by elevated levels of high-sensitivity C-reactive protein (CRP), primarily reflecting innate immunity [33]. Additionally, interleukin-1 beta (IL-1 β), an end product resulting from the activation of the multimeric protein complex inflammasome, was associated with increased disease severity and risk of death in patients with acute decompensated heart failure [34].

Up to now, however, signaling pathways and molecules involved in this immune activation and systemic inflammatory response in ADHF were not known. Herein, extending the previous findings, we identified changes in urine levels of nine proteins linked to the innate immune system including fibrinogen, complement C3, glycoprotein CD59, α -1-antitrypsin (*SERPINA1*), cathepsin D (*CTSD*), arylsulphatase A (*ARSA*), leucine-rich α -2-glycoprotein (*LRG1*), and transthyretin (*TTR*). As such, cathepsin D, a major lysosomal protease involved in protein degradation and proteolytic activation of hormones and growth factors, is increasingly recognized for its involvement in inflammatory responses [35]. High serum levels of cathepsin D have been shown to associate with new-onset HF following ST segment elevation acute myocardial infarction [36]. Similarly, results from the BIOSTAT-CHF study (BIOlogy Study to Tailored Treatment in Chronic Heart Failure) evidenced that higher circulating cathepsin D levels correlate with more severe disease and higher rates of mortality and hospitalization in HF [37]. In addition, recent microarray gene expression data of peripheral blood mononuclear cells and single-cell

RNA sequencing data of cardiac macrophages have associated the upregulation of CTSD expression with a higher risk of developing a heart failure event within 6 months after suffering an acute myocardial infarction [38]. Results of a liquid chromatography (LC)-MS analysis of platelets in a dog model of acute congestive HF identified cathepsin D among 14 proteins with differential expression level related to the disease presentation [10]. Interestingly, platelet degranulation due to activation processes was among the four most represented biological functions related to the ADHF urine differential proteome in our study. Extrapolating from studies in ischemic heart disease [39], platelet activation has been suggested as a link between HF decompensation and troponin elevation, which otherwise accounts for higher rates of in-hospital mortality and post-discharge morbidity and mortality [40].

Reactome pathway analysis evidenced fibrinogen (beta and gamma chains) and transthyretin (TTR) as the best represented proteins, each one of them participating in three of the top four pathways and converging into key biological functions relevant for acute decompensated HF, such as inflammation and extracellular matrix (ECM) remodeling. Among them, only the fibrinogen gamma chain (FGG) and transthyretin showed >2-fold changes compared to healthy subjects. Both FGG and TTR are multifaceted proteins of hepatic origin, participating in mechanistic processes relevant in maintaining the organ homeostasis.

In the present study, as proof of concept, to validate the potential translational value of the differential proteomic signature identified by 2DE-MS in ADHF patients, we further analyzed levels of TTR and its binding ligand RBP4 using commercially available ELISA assays and compared with the clinical characteristics of the patients at hospital admission and disease progression within 18 months for follow-up after hospital discharge.

TTR triggers amyloid processes, and TTR amyloid cardiomyopathy is increasingly being recognized in the clinical setting as a possible heart failure origin [41]. Additionally, TTR, along with serotransferrin (TF), is involved in the acute inflammatory response in increased chronic inflammation [9]. More importantly, TTR is a crucial protein involved in the transport of retinol to peripheral tissues after forming a homotetramer complex with the retinol-specific carrier RBP4. At the molecular level, RBP4 promotes inflammatory damage to cardiac myocytes by Toll-like receptor 4 activation [42]. Until now, data on the role of RBP4 in patients with HF were scarce and with apparently controversial findings [43,44]. In addition, TTR is one of the main carriers of thyroxine (T4), a thyroid hormone associated with blood pressure and LVEF in ADHF during hospitalization [45]. Indeed, thyroid hormones have central regulatory actions in the cardiovascular system and patients with even mildly altered thyroid function have a worse prognosis in heart disease, particularly heart failure [46].

As identified by 2DE-MS, quantitative analysis with specific immunoassays evidenced higher loss of TTR in urine of ADHF patients, the difference being more evident in the group of patients with a deficient glomerular filtration according the MDRD-4 value. Interestingly, ADHF patients showed a lower median TTR level in plasma compared to the concentration range in healthy subjects, but this decrease was irrespective of the kidney function and did not correlate with the level of TTR in urine, suggesting that TTR values in plasma result from a dynamic balance between synthesis in the liver and secretion through the kidney. In agreement with the current findings, our group had previously evidenced significantly lower TTR levels in plasma of patients with an acute new-onset myocardial infarction (AMI) compared to healthy subjects [47]. Of note, plasma levels of the inflammatory marker CRP were significantly increased in ADHF patients at hospitalization and inversely correlated with plasma TTR. Similarly, the reported TTR decrease in AMI was especially evident in patients having CRP levels >3 mg/L at the moment of admission [47]. These results strongly suggest that the increased inflammatory background in ADHF patients might account for the decrease in TTR plasma levels in ADHF, beyond changes in glomerular filtration. Supporting this view, TTR plasma decrease in ADHF patients was found regardless of the kidney functional condition.

Inflammation is a major feature in heart failure [48], and the hepatic synthesis of transthyretin has been reported to be negatively regulated by inflammatory-related mechanisms and inflammatory cytokines such as interleukin 6 (IL-6) in a process dependent on the IL-6 nuclear factor or its homologous C/EBP nuclear factor [49]. Indeed, TTR is a negative acute-phase protein, and patients with severe sepsis often have very low TTR concentrations [50]. Recently, low plasma transthyretin concentration has been shown to associate with incident heart failure in the general population [51], and it is suggested that low plasma TTR levels could be a biomarker of transthyretin tetramer instability [52]. Increasing evidence supports the view that TTR tetramers, under unbalanced homeostatic conditions, dissociate in misfolded monomers that tend to aggregate and fibrillate and, after infiltrating the cardiac extracellular matrix, induce oxidative stress and mitochondrial damage and increase cardiac wall thickness and diastolic dysfunction [53]. Further studies are needed to better characterize the molecular mechanisms relating inflammation with TTR expression and/or its structural conformation in heart failure and the potential relevance of TTR monomers on the ADHF pathophysiology.

In the urine of ADHF patients, TTR was detected as a single spot of 15 kDa, which corresponds to its monomeric form. Due to the correlation between TTR and RBP4 levels in urine of ADHF patients, it is conceivable that the monomeric form was already abundantly present in the circulating blood since only TTR tetramers bind RBP4 and protect this low-molecular-weight transport protein (21 kDa) from being filtrated through the glomerulus [54]. We could not exclude, however, that TTR-non-related RBP4 forms also account for the increased urinary levels of this protein in ADHF. In this respect, Perduca et al. [55], by high-resolution, three-dimensional structure analysis of urine-purified RBP4, identified a second RBP4 form with high binding capacity to fatty acids but not to retinol and with low affinity for TTR. This complex RBP4 fatty acid form was only identified in urine in the presence of a glomerulopathy [55]. Accordingly, this RBP4 fatty acid complex form might account for the high increase in urinary RBP4 in ADHF patients with renal dysfunction compared with those with normal renal dysfunction at hospitalization and the healthy group. Further studies are needed to understand the pathophysiological relevance of these RBP4 fatty acid complex forms in ADHF.

To the best of our knowledge, the concomitant loss of TTR and RBP4 in urine during the early phase (hospital admission) of acute heart failure decompensation and their power when combined to identify patients with worse disease evolution and prognosis within an 18-month follow-up after hospital discharge have not been previously reported in the clinical setting of ADHF. Indeed, the Kaplan–Meier curve analysis revealed a potential implication of increased urinary loss of TTR and RBP4 in the disease progression and presentation of major adverse events.

4. Materials and Methods

4.1. Study Population and Study Design

This study included 67 patients (men and women over 18 years old; 71 (65–77) years old, 67% men) who were hospitalized due to ADHF between February 2017 and March 2020 at Hospital de la Santa Creu i Sant Pau (HSCSP) in Barcelona. Hospitalized ADHF patients were distributed into two different groups depending on their kidney function at admission. Renal function was given as MDRD-4 ($\text{mL}/\text{min}/1.73\text{m}^2$), which is a serum creatinine-based estimation obtained using the clinical data of the patients [56]. Levels below $60 \text{ mL}/\text{min}/1.73\text{m}^2$ were considered pathological. Two groups were formed: (1) ADHF patients with renal dysfunction at hospital admission (RD, $n = 32$) and (2) ADHF patients with normal renal function at hospital admission (NRF, $n = 35$) (Supplementary Table S1). After hospital discharge, ADHF patient were followed for 18 months and the adverse clinical outcomes (rehospitalization due to decompensation, heart transplant, and/or death) were registered. Twenty-eight patients required another hospitalization, 4 required heart transplants, and 12 patients died. A group of healthy subjects

(HS, $n = 35$, 50.5 (48.0–54.5) years) served to establish the normal range in the urine of the identified proteins.

The Ethics Committee of the Santa Creu i Sant Pau Hospital in Barcelona, Spain, approved this study, and it was performed according to principles of Helsinki's Declaration. All patients signed an informed consent prior to being included in the study. Patients undergoing chemotherapy, who were pregnant or had post-delivery ischemic heart syndrome in women, or had other causes of acute episode (myocardial infarction, myocarditis, or toxic etiology) were excluded from the study. Medications were not considered as exclusion criteria except those drugs required in oncological treatment (and patients who were already excluded).

4.2. Biological Samples

Urine and blood samples were collected at hospital admission. Urine samples were centrifuged to precipitate debris, aliquoted, and stored at $-80\text{ }^{\circ}\text{C}$ until further analysis. Urine samples for the HS reference group were collected in the morning, and samples were processed as described for the ADHF patients. Level of total protein in urine was analyzed in a Clima MC-15 analyzer using the specific Gernon kit (RAL S.A., Barcelona, Spain), as described by the providers.

Venous blood was drawn, after a 10–14-h fasting, from the cubital vein without tourniquet using a 20-gauge needle for all patients. All samples were processed identically within the first 2 h after extraction. Serum was aliquoted and stored at $-80\text{ }^{\circ}\text{C}$.

Blood creatinine (Jaffe reaction), NT-proBNP (electroquimioluminescence), urea (kinetic urease), and hemoglobin were analyzed by standard laboratory methods as part of the patients' routine analyses. Glomerular filtrate was calculated using the MDRD-4 algorithm that includes a patient's plasma creatinine levels, age, sex, and race [56].

4.3. Two-Dimensional Gel Electrophoresis and MALDI-TOF/TOF MS

Analysis of differential protein patterns was performed by two-dimensional gel electrophoresis (2DE) coupled to mass spectrometry, as previously described [47,57,58].

Urine samples (4 mL) of ADHF patients and healthy controls were concentrated and desalted by centrifugation (3220 g, 30 min, and $10\text{ }^{\circ}\text{C}$) using 3-kDa cutoff filter devices (Amicon Ultra-4, Millipore, Burlington, MA, USA) and 100 mM Tris-HCl, pH 7.6. A final volume of 1 mL was obtained and depleted of albumin and IgGs using the ProteoExtract Albumin/IgG Removal Kit (Calbiochem, San Diego, CA, USA), as reported by the providers. Thereafter, a sample buffer was exchanged to a urea-containing buffer (7M urea, 2M thiourea, 2% CHAPS) by centrifugation with the 3-kDa cutoff filter devices (3220 g, at room temperature) until a final volume of 400 μL was obtained. Protein concentration in urine extracts was measured with 2D-Quant Kit (GE Healthcare, Chicago, IL, USA).

Protein loads of 100 μg (analytical gels) and 300 μg (preparative gels) of the urea/thiourea/chaps urine extracts were applied to 17-cm dry strips (ReadyStrips IPG strips, pH 4–7 linear range; BioRad, San Diego, CA, USA) using the PROTEAN i12 IEF system (Bio-Rad, San Diego, CA, USA) for the first dimension, as previously described by our group [57,58]. The second dimension was resolved in 12% SDS-PAGE. Gels were fixed for 2 h (40% ethanol, 10% acetic acid) and developed with Flamingo (Bio-Rad, San Diego, CA, USA) for protein fluorescent staining using Typhoon 9500 with excitation wavelength at 512 nm, emission light wavelength of 535 nm, and an LPB filter. Protein spot quantification and analysis for differences between gels were performed using PDQuest analysis software (Bio-Rad, San Diego, CA, USA). Each spot was assigned a relative value (AU) that corresponded to the single spot volume compared to the volume of all spots in the gel, following background extraction and normalization between gels, as previously reported [57]. This software specifically analyzes differences in protein patterns, in which a master gel is created wherein all gels are included and used to compare with each individual sample.

Proteins were identified after in-gel tryptic digestion and extraction of peptides from the gel pieces by matrix-assisted laser desorption/ionization time of flight (MALDI-TOF)

using an AutoFlex III Smart beam MALDI-TOF/TOF (BrukerDaltonics, Billerica, MA, USA), as previously described [57]. Briefly, 1-mm² gel pieces were washed first with 25 mM ammonium bicarbonate for 20 min, with 25 mM ammonium bicarbonate/50% acetonitrile (3 times for 20 min), and finally dried with 100% acetonitrile. Then, gel pieces were rehydrated with 0.2 ng/ μ L of trypsin Gold (Promega) in 25 nM ammonium bicarbonate and incubated overnight at 30 °C. Trypsin activity was stopped by the addition of acetonitrile for 15 min at 37 °C, and peptides were extracted with 0.2% TFA after 30 min at room temperature. Peptides were concentrated using μ C18-Zip Tips (Merck-Millipore) according to manufacturer instructions. Samples and calibrants were mixed 1:1 with an alpha-Cyano-4-hydroxycinnamic acid (HCCA) matrix (0.7 mg/mL) and were applied to Anchor Chip plates (BrukerDaltonics, Billerica, MA, USA).

Spectra were acquired with flexControl on reflectron mode (mass range m/z 850–4000; reflectron 1, 21.06 kV; reflectron 2, 9.77 kV; ion source 1 voltage, 19 kV; ion source 2, 16.5 kV; detection gain, 2.37 \times) with an average of 3500 added shots at a frequency of 200 Hz. Samples were processed with flexAnalysis (version 3.0, Bruker Daltonics, Billerica, MA, USA) considering a signal-to-noise ratio >3, applying statistical calibration and eliminating background peaks. After processing, spectra were sent to the interface BioTools (version 3.2, Bruker Daltonics, Billerica, MA, USA), and MASCOT search on Swiss-Prot 57.15 database was performed (taxonomy, Homo sapiens; mass tolerance, 50 to 100; up to two trypsin missed cleavages; global modification: carbamidomethyl (C); variable modification: oxidation (M)). Identification was carried out by peptide mass fingerprinting (PMF) where a MASCOT score >56 and at least five matched peptides were accepted. Confirmation of the identified protein was performed by peptide fragmentation working on the LIFT mode (MS/MS) [57,58].

4.4. In Silico Analysis

The major bioinformatics tool GO was used to identify the function of genes and gene products of Homo sapiens. Through the WEB-based GENE SeT Analysis Toolkit (WebGestalt), the GO analysis was performed using the PANTHER (Protein ANALYSIS Through Evolutionary Relationships) classification database [59], and the pathway analysis was performed using Reactome [60].

STRING, an online, freely available software tool, was used to establish the PPI network [61], and all the cutoff points were combined to analyze the topology property of networks.

4.5. Enzyme-Linked Immunosorbent Assays

Identified proteins in urine and serum were quantified by enzyme-linked immunosorbent assay (ELISA) using the following kits. Transthyretin (TTR) levels in urine and plasma were analyzed using a Prealbumin (Transthyretin) ELISA kit (K6331, Immundiagnostik, Bensheim, Germany), with intra-assay precision of 3.4%, and 5.6% for inter-assay precision. Quantification was performed using only samples where TTR was detectable (90% of total). RBP4 urinary levels were analyzed using a Human Retinol Binding Protein 4 ELISA kit (ab196264, Abcam, Cambridge, UK), with intra-assay precision 5.1% and inter-assay precision of 8.9%. Concentrations of the urinary proteins (obtained by ELISA) were normalized with urine total protein content, measured in a Clima MC-15 analyzer using the specific Gernon kit to avoid any possible bias due to interindividual differences in protein secretion.

4.6. Statistical Analysis

Data are expressed as median and interquartile range (IQR). The n indicates the number of subjects tested. The normal distribution was determined via Kolmogorov–Smirnov test. Statistical differences between groups for non-normally distributed continuous variables were analyzed by non-parametric tests, including Mann–Whitney or Kruskal–Wallis tests. Frequencies of categorical variables were compared by Fisher exact and Chi-square analyses. Correlations between variables were determined using Spearman rank correlation

and pictured by single regression models. Due to the exploratory character of this proteomic study, determination of the sample size was based on past experience with similar studies [57]. The variability observed in the data (ADHF patients with and without renal dysfunction at hospital admission) from the proteomic studies served to guide the sample size in the quantitative analysis (ELISA method). Sample size was validated using the JavaScript-based method for simple power and sample size calculation when two independent groups are compared, which are provided in <http://www.stat.ubc.ca/~rollin/stats/ssize/n2.html> (accessed on 29 January 2022) [57]. Based on the mean urine TTR values of ADHF patients and HS and the pooled standard deviation of both groups (ADHF and HS), a sample size >32 gave a study power of >0.75 (type I error = 0.05, two-sided test).

Receiver operating characteristic (ROC) curve estimations and their corresponding C statistics (area under the curve (AUC) with their 95% CI) were calculated to determine the power to discriminate ADHF patients according to kidney function. Kaplan–Meier survival (free of adverse outcomes) analysis was performed after including the study variables in a logistic rank analysis to evaluate the value of the studied parameters for predicting disease progression (adverse outcome incidence) in ADHF patients.

Adjustments for multiple testing in the discovery proteomic study were performed by the false-discovery rate (FDR) using a two-stage, sharpened method described by Benjamini et al. [62]. The results of the calculated adjusted q values (FDR adjusted) indicated the probability of false positives for the identified proteins considered to be significant. Here, it refers to q values < 0.06, which represents more than 94% truly positive for differentially expressed urinary proteins.

Statistical analysis was performed using Stata v15 (SAS Institute, Cary, NC, USA) and SPSS v26 (IBM Corp, Armonk, NY). A *p* value ≤ 0.05 was considered statistically significant.

5. Conclusions

In the present study, by applying a proteomic approach based on 2D electrophoresis coupled with MALDI-TOF/TOF MS, we found a differential protein signature in the urine of patients presenting with acute decompensated heart failure at the moment of hospital admission. The 26-protein pattern highlights the complexity of ADHF pathophysiology with coordinated changes in proteins involved in molecular functions and biological processes related to the disease progression. Thus, we reported an increased urinary loss of proteins such as TTR and RBP4, which might have harmful impact on the disease evolution, resulting in higher risk for adverse outcomes after hospital discharge. Future studies are now warranted in larger populations to validate the relevance of the observed changes in TTR and RBP4 for the ADHF pathophysiology.

Supplementary Materials: The following are available online at <https://www.mdpi.com/article/10.3390/ijms23042344/s1>.

Author Contributions: Conceptualization, X.G.-M., L.B. and T.P.; methodology, T.P., M.G.-A. and E.D.-R.; software, M.G.-A. and E.D.-R.; validation, T.P., L.B., M.G.-A. and E.D.-R.; formal analysis, T.P., L.B., M.G.-A. and E.D.-R.; investigation, L.B., T.P. and M.G.-A.; data curation, T.P., L.B., M.G.-A. and E.D.-R.; writing—original draft preparation, M.G.-A., E.D.-R. and T.P.; writing—review and editing, T.P., L.B., X.G.-M., L.L., M.G.-A. and E.D.-R.; supervision, L.B. and T.P.; project administration, L.B. and T.P.; funding acquisition, L.B. and T.P. All authors have read and agreed to the published version of the manuscript.

Funding: This work was supported by the Fundació La Marató TV3 (Project number 20153110) to T.P., and the Spanish Agencia Estatal de Investigación (AEI)—Institute of Health Carlos III, ISCIII FIS PI19/01687 to T.P., Centro de Investigación Biomedica en Red Cardiovascular (CIBERCV-CB16/11/00411) to L.B., Red Terapia Celular TerCel RD16/0011/0018 to L.B., Spanish Ministry of Economy and Competitiveness of Science-PID2019-107160RB-I00 to L.B., and cofounded by FEDER Una Manera de Hacer Europa. Secretaria de Universitats i Recerca del Departament d'Empresa i Coneixement de Catalunya (2017 SGR 1480). We thank the Fundació Jesús Serra and Fundació de Investigació Cardiovascular, Barcelona, for their continuous support.

E.D.R. is a predoctoral fellow funded by the Fundació La Marató TV3 and the Cardiovascular Program-ICCC (IR-HSCSP).

Institutional Review Board Statement: The study was conducted according to the guidelines of the Declaration of Helsinki and approved by the Ethics Committee of the hospital de Santa Creu i Sant Pau (reference [16], 22 March 2016).

Informed Consent Statement: Informed consent was obtained from all subjects before inclusion in the study.

Data Availability Statement: The data presented in this study are available in supplementary material.

Acknowledgments: We gratefully acknowledge the valuable help and support of Montse Gómez-Pardo with the sample handling.

Conflicts of Interest: L.B. received institutional research grants from AstraZeneca; consultancy fees from Sanofi, Pfizer, and Novartis; and speaker fees from Lilly, Pfizer, and AstraZeneca. T.P. and L.B. are shareholders of the academic spin-off companies GlyCardial Diagnostics S.L. and Ivestatin Therapeutics S.L. All are unrelated to the present work. E.D.-R., M.G.-A., L.L. and X.G.-M. declare no conflict of interest.

References

- Emdin, M.; Vittorini, S.; Passino, C.; Clerico, A. Old and new biomarkers of heart failure. *Eur. J. Heart Fail.* **2009**, *11*, 331–335. [\[CrossRef\]](#)
- Nieminen, M.S.; Brutsaert, D.; Dickstein, K.; Drexler, H.; Follath, F.; Harjola, V.-P.; Hochadel, M.; Komajda, M.; Lassus, J.; Luis Lopez-Sendon, J.; et al. EuroHeart Failure Survey II (EHFS II): A survey on hospitalized acute heart failure patients: Description of population. *Eur. Heart J.* **2006**, *27*, 2725–2736. [\[CrossRef\]](#) [\[PubMed\]](#)
- Lala, A.; McNulty, S.E.; Mentz, R.J.; Dunlay, S.M.; Vader, J.M.; AbouEzzeddine, O.F.; DeVore, A.D.; Khazanie, P.; Redfield, M.M.; Goldsmith, S.R.; et al. Relief and recurrence of congestion during and after hospitalization for acute heart failure insights from diuretic optimization strategy evaluation in acute decompensated heart failure (DOSE-AHF) and cardiorenal rescue study in acute decompensated heart. *Circ. Heart Fail.* **2015**, *8*, 741–748. [\[CrossRef\]](#)
- Fonarow, G.C.; Adams, K.F.; Abraham, W.T.; Yancy, C.W.; Boscardin, W.J. Risk stratification for in-hospital mortality in acutely decompensated heart failure. *J. Am. Med. Assoc.* **2005**, *293*, 572–580. [\[CrossRef\]](#) [\[PubMed\]](#)
- Ronco, C.; Bellasi, A.; Di Lullo, L. Implication of Acute Kidney Injury in Heart Failure. *Heart Fail. Clin.* **2019**, *15*, 463–476. [\[CrossRef\]](#) [\[PubMed\]](#)
- Al-Naher, A.; Wright, D.; Devonald, M.A.J.; Pirmohamed, M. Renal function monitoring in heart failure – what is the optimal frequency? A narrative review. *Br. J. Clin. Pharmacol.* **2018**, *84*, 5–17. [\[CrossRef\]](#) [\[PubMed\]](#)
- Virzi, G.M.; Clementi, A.; Battaglia, G.G.; Ronco, C. Multi-Omics Approach: New Potential Key Mechanisms Implicated in Cardiorenal Syndromes. *Cardiorenal Med.* **2019**, *9*, 201–211. [\[CrossRef\]](#)
- Pedroza-Diaz, J.; Röthlisberger, S. Advances in urinary protein biomarkers for urogenital and non-urogenital pathologies. *Biochem. Med.* **2015**, *25*, 22–35. [\[CrossRef\]](#)
- Benabdelkamel, H.; Masood, A.; Ekhzaimy, A.A.; Alfadda, A.A. Proteomics profiling of the urine of patients with hyperthyroidism after anti-thyroid treatment. *Molecules* **2021**, *26*, 1991. [\[CrossRef\]](#)
- Levent, P.; Kocaturk, M.; Akgun, E.; Saril, A.; Cevik, O.; Baykal, A.T.; Tanaka, R.; Ceron, J.J.; Yilmaz, Z. Platelet proteome changes in dogs with congestive heart failure. *BMC Vet. Res.* **2020**, *16*, 1–13. [\[CrossRef\]](#)
- Petra, E.; He, T.; Lygirou, V.; Latosinska, A.; Mischak, H.; Vlahou, A.; Jankowski, J. Urine peptidome analysis in cardiorenal syndrome reflects molecular processes. *Sci. Rep.* **2021**, *11*, 1–11. [\[CrossRef\]](#) [\[PubMed\]](#)
- Ura, B.; Biffi, S.; Monasta, L.; Arrigoni, G.; Battisti, I.; Di Lorenzo, G.; Romano, F.; Aloisio, M.; Celsi, F.; Addobati, R.; et al. Two dimensional-difference in gel electrophoresis (2D-DIGE) proteomic approach for the identification of biomarkers in endometrial cancer serum. *Cancers* **2021**, *13*, 3639. [\[CrossRef\]](#) [\[PubMed\]](#)
- Cubedo, J.; Padró, T.; García-Moll, X.; Pintó, X.; Cinca, J.; Badimon, L. Serum proteome in acute myocardial infarction. *Clin. Investig. Arterioscler.* **2011**, *23*, 147–154. [\[CrossRef\]](#)
- Cubedo, J.; Padró, T.; Badimon, L. Coordinated proteomic signature changes in immune response and complement proteins in acute myocardial infarction: The implication of serum amyloid P-component. *Int. J. Cardiol.* **2013**, *168*, 5196–5204. [\[CrossRef\]](#) [\[PubMed\]](#)
- Chiva-Blanch, G.; Peña, E.; Cubedo, J.; García-Arguinzonis, M.; Pané, A.; Gil, P.A.; Perez, A.; Ortega, E.; Padró, T.; Badimon, L. Molecular mapping of platelet hyperreactivity in diabetes: The stress proteins complex HSPA8/Hsp90/CSK2 α and platelet aggregation in diabetic and normal platelets. *Transl. Res.* **2021**, *235*, 1–14. [\[CrossRef\]](#) [\[PubMed\]](#)
- Akashi, M.; Minami, Y.; Haruki, S.; Jujo, K.; Hagiwara, N. Prognostic implications of prealbumin level on admission in patients with acute heart failure referred to a cardiac intensive care unit. *J. Cardiol.* **2019**, *73*, 114–119. [\[CrossRef\]](#)

17. Franco, J.; Formiga, F.; Trullas, J.C.; Salamanca Bautista, P.; Conde, A.; Manzano, L.; Quirós, R.; Franco, Á.G.; Ezquerro, A.M.; Montero-Pérez-Barquero, M. Impact of prealbumin on mortality and hospital readmission in patients with acute heart failure. *Eur. J. Intern. Med.* **2017**, *43*, 36–41. [[CrossRef](#)]
18. Wang, W.; Wang, C.S.; Ren, D.; Li, T.; Yao, H.C.; Ma, S.J. Low serum prealbumin levels on admission can independently predict in-hospital adverse cardiac events in patients with acute coronary syndrome. *Medicine* **2018**, *97*, 1–5. [[CrossRef](#)]
19. Li, O.; Geng, X.; Ma, Q.; Wang, W.; Liu, R.; Yin, Z.; Wang, S.; Cai, G.; Chen, X.; Hong, Q. Gene Microarray Integrated with High-Throughput Proteomics for the Discovery of Transthyretin in Rhabdomyolysis-Induced Acute Kidney Injury. *Cell. Physiol. Biochem.* **2017**, *43*, 1673–1688. [[CrossRef](#)]
20. Bernstein, L.H.; Ingenbleek, Y. Transthyretin: Its response to malnutrition and stress injury. Clinical usefulness and economic implications. *Clin. Chem. Lab. Med.* **2002**, *40*, 1344–1348. [[CrossRef](#)]
21. Dellière, S.; Cynober, L. Is transthyretin a good marker of nutritional status? *Clin. Nutr.* **2017**, *36*, 364–370. [[CrossRef](#)] [[PubMed](#)]
22. Harpole, M.; Davis, J.; Espina, V. Current state of the art for enhancing urine biomarker discovery Current state of the art for enhancing urine biomarker discovery. *Expert Rev. Proteom.* **2016**, *9450*, 609–626. [[CrossRef](#)] [[PubMed](#)]
23. Wu, J.; Wang, W.; Chen, Z.; Xu, F.; Zheng, Y. Proteomics applications in biomarker discovery and pathogenesis for abdominal aortic aneurysm. *Expert Rev. Proteom.* **2021**, *18*, 305–314. [[CrossRef](#)] [[PubMed](#)]
24. Laribi, S.; Mebazaa, A. Cardiohepatic syndrome: Liver injury in decompensated heart failure. *Curr. Heart Fail. Rep.* **2014**, *11*, 236–240. [[CrossRef](#)] [[PubMed](#)]
25. McCullough, P.A.; Kellum, J.A.; Haase, M.; Müller, C.; Damman, K.; Murray, P.T.; Cruz, D.; House, A.A.; Schmidt-Ott, K.M.; Vescovo, G.; et al. Pathophysiology of the cardiorenal syndromes: Executive summary from the eleventh consensus conference of the acute dialysis quality initiative (ADQI). *Contrib. Nephrol.* **2013**, *182*, 82–98. [[CrossRef](#)]
26. Biegus, J.; Zymliński, R.; Sokolski, M.; Siwołowski, P.; Gajewski, P.; Nawrocka-Millward, S.; Poniewierka, E.; Jankowska, E.A.; Banasiak, W.; Ponikowski, P. Impaired hepato-renal function defined by the MELD XI score as prognosticator in acute heart failure. *Eur. J. Heart Fail.* **2016**, *18*, 1518–1521. [[CrossRef](#)] [[PubMed](#)]
27. Kawahira, M.; Tamaki, S.; Yamada, T.; Watanabe, T.; Morita, T.; Furukawa, Y.; Kawasaki, M.; Kikuchi, A.; Kawai, T.; Seo, M.; et al. Prognostic value of impaired hepato-renal function and liver fibrosis in patients admitted for acute heart failure. *ESC Heart Fail.* **2021**, *8*, 1274–1283. [[CrossRef](#)]
28. McPherson, S.; Hardy, T.; Dufour, J.F.; Petta, S.; Romero-Gomez, M.; Allison, M.; Oliveira, C.P.; Francque, S.; Van Gaal, L.; Schattenberg, J.M.; et al. Age as a Confounding Factor for the Accurate Non-Invasive Diagnosis of Advanced NAFLD Fibrosis. *Am. J. Gastroenterol.* **2017**, *112*, 740–751. [[CrossRef](#)]
29. Panchani, N.; Schulz, P.; Van Zyl, J.; Felius, J.; Baxter, R.; Yoon, E.T.; Baldawi, H.; Bindra, A.; Asrani, S.K. Liver stiffness and prediction of cardiac outcomes in patients with acute decompensated heart failure. *Clin. Transplant.* **2021**, e14545. [[CrossRef](#)]
30. Santander, C.; Brandan, E. Betaglycan induces TGF- β signaling in a ligand-independent manner, through activation of the p38 pathway. *Cell. Signal.* **2006**, *18*, 1482–1491. [[CrossRef](#)]
31. Liu, C.; Lim, S.T.; Teo, M.H.Y.; Tan, M.S.Y.; Kulkarni, M.D.; Qiu, B.; Li, A.; Lal, S.; Dos Remedios, C.G.; Tan, N.S.; et al. Collaborative Regulation of LRG1 by TGF- β 1 and PPAR- β / δ Modulates Chronic Pressure Overload-Induced Cardiac Fibrosis. *Circ. Heart Fail.* **2019**, *12*, 1–16. [[CrossRef](#)]
32. Sörensen-Zender, I.; Bhayana, S.; Susnik, N.; Rolli, V.; Batkai, S.; Baisantray, A.; Bahram, S.; Sen, P.; Teng, B.; Lindner, R.; et al. Zinc- α 2-Glycoprotein Exerts Antifibrotic Effects in Kidney and Heart. *J. Am. Soc. Nephrol.* **2015**, *26*, 2659–2668. [[CrossRef](#)] [[PubMed](#)]
33. Kalogeropoulos, A.P.; Tang, W.H.W.; Hsu, A.; Felker, G.M.; Hernandez, A.F.; Troughton, R.W.; Voors, A.A.; Anker, S.D.; Metra, M.; McMurray, J.J.V.; et al. High-sensitivity C-reactive protein in acute heart failure: Insights from the ASCEND-HF trial. *J. Card. Fail.* **2014**, *20*, 319–326. [[CrossRef](#)]
34. Pascual-Figal, D.A.; Bayes-Genis, A.; Asensio-Lopez, M.C.; Hernández-Vicente, A.; Garrido-Bravo, I.; Pastor-Perez, F.; Diez, J.; Ibáñez, B.; Lax, A. The Interleukin-1 Axis and Risk of Death in Patients With Acutely Decompensated Heart Failure. *J. Am. Coll. Cardiol.* **2019**, *73*, 1016–1025. [[CrossRef](#)] [[PubMed](#)]
35. Hausmann, M.; Obermeier, F.; Schreiter, K.; Spottl, T.; Falk, W.; Schölmerich, J.; Herfarth, H.; Saftig, P.; Rogler, G. Cathepsin D is up-regulated in inflammatory bowel disease macrophages. *Clin. Exp. Immunol.* **2004**, *136*, 157–167. [[CrossRef](#)] [[PubMed](#)]
36. Voors, A.A.; Anker, S.D.; Cleland, J.G.; Dickstein, K.; Filippatos, G.; van der Harst, P.; Hillege, H.L.; Lang, C.C.; ter Maaten, J.M.; Ng, L.; et al. A systems BIOlogy Study to Tailored Treatment in Chronic Heart Failure: Rationale, design, and baseline characteristics of BIOSTAT-CHF. *Eur. J. Heart Fail.* **2016**, *18*, 716–726. [[CrossRef](#)]
37. Hoes, M.F.; Tromp, J.; Ouwerkerk, W.; Bomer, N.; Oberdorf-Maass, S.U.; Samani, N.J.; Ng, L.L.; Lang, C.C.; van der Harst, P.; Hillege, H.; et al. The role of cathepsin D in the pathophysiology of heart failure and its potentially beneficial properties: A translational approach. *Eur. J. Heart Fail.* **2020**, *22*, 2102–2111. [[CrossRef](#)]
38. Chen, Q.; Yin, Q.; Song, J.; Liu, C.; Chen, H.; Li, S. Identification of monocyte-associated genes as predictive biomarkers of heart failure after acute myocardial infarction. *BMC Med. Genomics* **2021**, *14*, 1–13. [[CrossRef](#)]
39. Zhang, S.Z.; Jin, Y.P.; Qin, G.M.; Wang, J.H. Association of platelet-monocyte aggregates with platelet activation, systemic inflammation, and myocardial injury in patients with non-ST elevation acute coronary syndromes. *Clin. Cardiol.* **2007**, *30*, 26–31. [[CrossRef](#)]

40. Peacock, W.F.; De Marco, T.; Fonarow, G.C.; Diercks, D.; Wynne, J.; Apple, F.S.; Wu, A.H.B. Cardiac Troponin and Outcome in Acute Heart Failure. *N. Engl. J. Med.* **2008**, *358*, 2117–2126. [[CrossRef](#)]
41. Ruberg, F.L.; Grogan, M.; Hanna, M.; Kelly, J.W.; Maurer, M.S. Transthyretin amyloid cardiomyopathy: JACC State of the Art Review. *J. Am. Coll. Cardiol.* **2019**, *73*, 2872–2891. [[CrossRef](#)] [[PubMed](#)]
42. Gao, W.; Wang, H.; Zhang, L.; Cao, Y.; Bao, J.Z.; Liu, Z.X.; Wang, L.S.; Yang, Q.; Lu, X. Retinol-binding protein 4 induces cardiomyocyte hypertrophy by activating TLR4/MyD88 pathway. *Endocrinology* **2016**, *157*, 2282–2293. [[CrossRef](#)] [[PubMed](#)]
43. Majerczyk, M.; Choreza, P.; Mizia-Stec, K.; Bożentowicz-Wikarek, M.; Brzozowska, A.; Arabzada, H.; Owczarek, A.J.; Szybalska, A.; Grodzicki, T.; Więcek, A.; et al. Plasma Level of Retinol-Binding Protein 4, N-Terminal proBNP and Renal Function in Older Patients Hospitalized for Heart Failure. *Cardiorenal Med.* **2018**, *8*, 237–248. [[CrossRef](#)] [[PubMed](#)]
44. Bobbert, P.; Weithäuser, A.; Andres, J.; Bobbert, T.; Köhl, U.; Schultheiss, H.P.; Rauch, U.; Skurk, C. Increased plasma retinol binding protein 4 levels in patients with inflammatory cardiomyopathy. *Eur. J. Heart Fail.* **2009**, *11*, 1163–1168. [[CrossRef](#)]
45. Leite, A.R.; Neves, J.S.; Borges-Canha, M.; Vale, C.; Von Hafe, M.; Carvalho, D.; Leite-Moreira, A. Evaluation of thyroid function in patients hospitalized for acute heart failure. *Int. J. Endocrinol.* **2021**, *2021*, 6616681. [[CrossRef](#)]
46. Schmidt-Ott, U.M.; Ascheim, D.D. Thyroid Hormone and Heart Failure. *Curr. Heart Fail. Rep.* **2006**, *3*, 114–119. [[CrossRef](#)]
47. Cubedo, J.; Padró, T.; Alonso, R.; Cincá, J.; Mata, P.; Badimon, L. Differential proteomic distribution of TTR (pre-albumin) forms in serum and HDL of patients with high cardiovascular risk. *Atherosclerosis* **2012**, *222*, 263–269. [[CrossRef](#)]
48. Chaikijrajai, T. Wilson Reappraisal of Inflammatory Biomarkers in Heart Failure. *Curr Heart Fail Rep.* **2020**, *17*, 9–19. [[CrossRef](#)]
49. Johnson, A.M.; Merlini, G.; Sheldon, J.; Ichihara, K. Clinical indications for plasma protein assays: Transthyretin (prealbumin) in inflammation and malnutrition - International federation of clinical chemistry and laboratory medicine (IFCC): IFCC scientific division committee on plasma proteins (C-PP). *Clin. Chem. Lab. Med.* **2007**, *45*, 419–426. [[CrossRef](#)]
50. Clark, M.A.; Hentzen, B.T.H.; Plank, L.D.; Hill, G.L. Sequential changes in insulin-like growth factor 1, plasma proteins, and total body protein in severe sepsis and multiple injury. *J. Parenter. Enter. Nutr.* **1996**, *20*, 363–370. [[CrossRef](#)]
51. Greve, A.M.; Christoffersen, M.; Frikke-Schmidt, R.; Nordestgaard, B.G.; Tybjaerg-Hansen, A. Association of Low Plasma Transthyretin Concentration with Risk of Heart Failure in the General Population. *JAMA Cardiol.* **2021**, *6*, 258–266. [[CrossRef](#)]
52. Judge, D.P.; Heitner, S.B.; Falk, R.H.; Maurer, M.S.; Shah, S.J.; Wittles, R.M.; Grogan, M.; Selby, V.N.; Jacoby, D.; Hanna, M.; et al. Transthyretin Stabilization by AG10 in Symptomatic Transthyretin Amyloid Cardiomyopathy. *J. Am. Coll. Cardiol.* **2019**, *74*, 285–295. [[CrossRef](#)] [[PubMed](#)]
53. Porcari, A.; Merlo, M.; Rapezzi, C.; Sinagra, G. Transthyretin amyloid cardiomyopathy: An uncharted territory awaiting discovery. *Eur. J. Intern. Med.* **2020**, *82*, 7–15. [[CrossRef](#)] [[PubMed](#)]
54. Raghu, P.; Sivakumar, B. Interactions amongst plasma retinol-binding protein, transthyretin and their ligands: Implications in vitamin A homeostasis and transthyretin amyloidosis. *Biochim. Biophys. Acta Proteins Proteom.* **2004**, *1703*, 1–9. [[CrossRef](#)]
55. Perduca, M.; Nicolis, S.; Mannucci, B.; Galliano, M.; Monaco, H.L. Human plasma retinol-binding protein (RBP4) is also a fatty acid-binding protein. *Biochim. Biophys. Acta Mol. Cell Biol. Lipids* **2018**, *1863*, 458–466. [[CrossRef](#)] [[PubMed](#)]
56. Tarwater, K. Estimated glomerular filtration rate explained. *Mo. Med.* **2011**, *108*, 29–32. [[CrossRef](#)]
57. Cubedo, J.; Padró, T.; Alonso, R.; Mata, P.; Badimon, L. ApoL1 levels in high density lipoprotein and cardiovascular event presentation in patients with familial hypercholesterolemia. *J. Lipid Res.* **2016**, *57*, 1059–1073. [[CrossRef](#)]
58. García-Arguinzoniz, M.; Padró, T.; Lugano, R.; Llorente-Cortes, V.; Badimon, L. Low-density lipoproteins induce heat shock protein 27 dephosphorylation, oligomerization, and subcellular relocation in human vascular smooth muscle cells. *Arterioscler. Thromb. Vasc. Biol.* **2010**, *30*, 1212–1219. [[CrossRef](#)]
59. Mi, H.; Muruganujan, A.; Casagrande, J.T.; Thomas, P.D. Large-scale gene function analysis with PANTHER Classification System. *Nat. Protoc.* **2013**, *8*, 1551–1566. [[CrossRef](#)]
60. Jupe, S.; Fabregat, A.; Hermjakob, H. Expression data analysis with Reactome. *Curr. Protoc. Bioinform.* **2015**, *49*, 8.20.1–8.20.9. [[CrossRef](#)]
61. Szklarczyk, D.; Morris, J.H.; Cook, H.; Kuhn, M.; Wyder, S.; Simonovic, M.; Santos, A.; Doncheva, N.T.; Roth, A.; Bork, P.; et al. The STRING database in 2017: Quality-controlled protein-protein association networks, made broadly accessible. *Nucleic Acids Res.* **2017**, *45*, D362–D368. [[CrossRef](#)] [[PubMed](#)]
62. Benjamini, Y.; Krieger, A.M.; Yekutieli, D. Adaptive linear step-up procedures that control the false discovery rate. *Biometrika* **2006**, *93*, 491–507. [[CrossRef](#)]

Supplementary material

Urinary proteomic signature in acute decompensated heart failure: advances into molecular pathophysiology

Elisa Diaz-Riera^{1,2}; Maisa García-Arguinzonis¹, Laura López³, Xavier Garcia-Moll^{3,4},
Lina Badimon L^{1,4,5#}, Padro T^{1,4##}*

1 Cardiovascular-Program ICCG; Research Institute – Hospital Santa Creu i Sant Pau, IIB-Sant Pau, 08041 Barcelona, Spain; ediazr@santpau.cat (ED-R); mgarciaar@santpau.cat (MG-A); lbadimon@santpau.cat (LB); tpadro@santpau.cat (TP)

2 Faculty of Medicine, Universitat de Barcelona, 08036 Barcelona, Spain

3 Cardiology department, Hospital Santa Creu i Sant Pau, 08025 Barcelona, Spain; llopezl@santpau.cat (LL); xgarcia-moll@santpau.cat (XG-M)

4 Centro de Investigación Biomédica en Red Cardiovascular (CIBERCV) Instituto de Salud Carlos III, 28029 Madrid, Spain

5 Cardiovascular Research Chair, UAB, 08025 Barcelona, Spain

Equal contribution

***Correspondence:**

Dr Teresa Padro

tpadro@santpau.cat

Tel.: +34935565886;

Fax: +34-935565559

Supplementary Table S1: Clinical characteristics and risk factors of all patients.

	All patients N=67	NRF N=35	RD N=32	P-value
DEMOGRAPHIC CHARACTERISTICS				
Female/male, n	22/45	10/25	12/20	0.603
Age, years	71.0 [65.0-77.0]	69.0 [58.0-75.0]	74.0 [69.5-77.5]	0.008
Weight, kg	73.0 [61.6-86.8]	70 [61.2-86.6]	77.2 [62.0-88.6]	0.543
KIDNEY FUNCTION MARKERS				
Creatinine, $\mu\text{mol/L}$	105.0 [78.0-147.0]	78.0 [67.0-97.0]	147.0 [122.5-194.0]	<0.001
Glomerular filtration (MDRD-4) ^a	61.0 [40.9-83.3]	83.0 [68.9-99.0]	39.7 [31.3-45.0]	<0.001
Urea, mmol/L	10.2 [6.8-16.1]	7.0 [5.8-9.2]	16.5 [13.0-22.9]	<0.001
CARDIAC FUNCTION MARKERS				
NT-proBNP, ng/L	4.0 [2.3-8.6]	3.2 [1.9-6.4]	4.5 [2.8-14.7]	0.026
Left ventricular ejection fraction (LVEF), %	45.0 [33.0-58.0]	38.0 [33.0-57.0]	51.0 [35.5-59.5]	0.225
Preserved LVEF, N (%)	28 (42)	11 (31)	17 (53)	
Reduced LVEF, N (%)	27 (40)	18 (52)	9 (28)	0.125
Mid-range LVEF, N (%)	12 (18)	6 (17)	6 (19)	
Atrial fibrillation, N (%)	32 (48)	16 (47)	16 (50)	>0.999
Cardiovascular disease, N (%)	23 (34)	11 (31)	12 (38)	0.618
OTHER BIOCHEMICAL MARKERS				
Haemoglobin, g/L	122 [101-138]	128 [114-142]	110 [95-124]	0.004
RISK FACTORS; N (%)				
Active smoking	10 (15)	8 (23)	2 (6)	0.086
Hypertension	49 (74)	21 (62)	28 (88)	0.024
Pulmonary hypertension	16 (24)	8 (23)	8 (25)	>0.999
Diabetes mellitus type 2	30 (45)	11 (32)	19 (59)	0.047
Dyslipidaemia	46 (70)	20 (59)	26 (81)	0.063
BACKGROUND MEDICATION; N (%)				
Diuretics	49 (73)	21 (60)	28 (88)	0.014
Statins	43 (64)	18 (51)	25 (78)	0.040
Anticoagulants	27 (40)	14 (40)	13 (41)	>0.999
Antiplatelet agents	38 (57)	19 (54)	19 (59)	0.806
Beta-blockers	46 (69)	21 (60)	25 (78)	0.124
Antiarrhythmic agents	7 (10)	4 (11)	3 (9)	>0.999
Antidiabetics	27 (40)	8 (26)	19 (59)	0.003
Insulin	12 (18)	2 (6)	10 (31)	0.010
Oral antidiabetic agents	22 (33)	8 (23)	14 (44)	0.117
ACE inhibitor/ARB	43 (66)	26 (74)	17 (57)	0.189

^aMDRD-4 levels expressed in mL/min/1.73m²; Quantitative values were given in median [Q1-Q3]. P values of categorical variables were calculated with Fisher exact test, except for LVEF where χ^2 was used. P values of numerical data were calculated with Mann-Whitney, except for LVEF where Kruskal-Wallis was used. Diuretics: hydrochlorothiazide, furosemide, eplerenone, and spironolactone. Statins: atorvastatin, pravastatin, simvastatin, ezetimibe. Anticoagulants: warfarin, acenocumarol, bemparin, heparin, dabigatran, rivaroxaban, edoxaban, and apixaban. Antiplatelet agents: acetylsalicylic acid and clopidogrel. Beta-blockers: bisoprolol and carvedilol. Antiarrhythmic agents: amiodarone. Oral antidiabetic agents: metformin and repaglinide. Angiotensin-converting enzyme inhibitors (ACEI) include: captopril, enalapril, and ramipril. Angiotensin receptor blockers (ARB): losartan, olmesartan, and valsartan.

Supplementary Table S2: Clinical characteristics and risk factors of discovery phase patients.

	2DE-MS group N=17	All patients N=67	P value
DEMOGRAPHIC CHARACTERISTICS			
Female/male, n	3/14	22/45	0.565
Age, years	72 [69-76]	71 [65-77]	0.624
Weight, kg	76 [66-87]	73 [62-89]	0.583
KIDNEY FUNCTION MARKERS			
Creatinine, $\mu\text{mol/L}$	101 [73-131]	105.0 [78.0-147.0]	0.693
Glomerular filtration (MDRD-4) ^a	68 [43.2-81.7]	61.0 [40.9-83.3]	0.476
Urea, mmol/L	9.0 [5.8-13.1]	10.2 [6.8-16.1]	0.367
CARDIAC FUNCTION MARKERS			
NT-proBNP, $\mu\text{g/L}$	2.4 [1.7-4.6]	4.0 [2.3-8.6]	0.160
Left ventricular ejection fraction (LVEF), %	48 [33-56]	45 [33-58]	0.738
Preserved LVEF >50%, N (%)	8 (47)	28 (42)	
Mildly reduced LVEF 40-49%, N (%)	3 (18)	12 (18)	0.916
Reduced LVEF <40%, N (%)	6 (35)	27 (40)	
OTHER BIOCHEMICAL MARKERS			
Haemoglobin, g/L	122 [106-139]	122 [101-138]	0.889
MEDICAL HISTORY; N (%)			
Atrial fibrillation	12 (71)	32 (48)	0.283
Cardiovascular disease	4 (24)	23 (34)	0.563
Active smoking	3 (5)	10 (15)	0.721
Hypertension	12 (71)	49 (74)	>0.999
Pulmonary hypertension	6 (35)	16 (24)	0.364
Diabetes mellitus type 2	6 (35)	30 (45)	0.586
Dyslipidaemia	11 (65)	46 (70)	>0.999
BACKGROUND MEDICATION; N (%)			
Diuretics	11 (65)	49 (73)	0.253
Statins	9 (53)	43 (64)	0.415
Anticoagulants	10 (59)	27 (40)	0.415
Antiplatelet agents	7 (41)	38 (57)	0.286
Beta-blockers	11 (65)	46 (69)	0.777
Antiarrhythmic agents	0 (0)	7 (10)	0.335
Antidiabetics	3 (24)	27 (40)	0.265
ACE inhibitor/ARB	13 (76)	43 (66)	0.562

^aMDRD-4 levels expressed in mL/min/1.73m²; Quantitative values were given in median [Q1-Q3]; 2DE-MS group refers to a subgroup of patients used for discovery phase of 2D electrophoresis coupled with mass spectrometry. P values of categorical were calculated with Fisher exact test, except for LVEF where χ^2 was used. P values of numerical data were calculated with Mann-Whitney, except for LVEF where Kruskal-Wallis was used. Diuretics: hydrochlorothiazide, furosemide, eplerenone, and spironolactone. Statins: atorvastatin, pravastatin, simvastatin, ezetimibe. Anticoagulants: warfarin, acenocumarol, bempiparin, heparin, dabigatran, rivaroxaban, edoxaban, and apixaban. Antiplatelet agents: acetylsalicylic acid and clopidogrel. Beta-blockers: bisoprolol and carvedilol. Antiarrhythmic agents: amiodarone. Oral antidiabetic agents: metformin and repaglinide. Angiotensin-converting enzyme (ACE) inhibitors include: captopril, enalapril, and ramipril. Angiotensin receptor blockers (ARB): losartan, olmesartan, and valsartan.

Supplementary Table S3: Extended data from table 1 regarding mass spectrometry characteristics of identified proteins in urine

Gel-ID	Protein name	Gene name	Swiss Prot number	Theoretical pI	Experimental pI	Theoretical MW (KDa)	Experimental MW (KDa)	MS
1	Lysosomal acid phosphatase	<i>ACP2</i>	P11117	5.80	5.80	46.7	45.5	MS
2	Pancreatic α -amylase	<i>AMY2A</i>	P04746	6.45	6.45	57.7	51.6	MS
3	Annexin A10	<i>ANXA10</i>	Q9UJ72	5.13	5.20	37.3	35.2	MS
4	Arylsulphatase A	<i>ARSA</i>	P15289	5.57	5.50	53.6	49.6	MS
5	Zinc- α -2-glycoprotein	<i>AZGP1</i>	P25311	5.58	4.8-5.1	34.3	41.6-43.5	MS
6	Complement C3	<i>C3</i>	P01024	6.00	6.75	187.1	54.8	MS
7	Carbonic anhydrase 1	<i>CA1</i>	P00915	6.63	6.70	28.9	30.1	MS
8	Endosialin	<i>CD248</i>	Q9HCU0	5.14	4.70	80.9	44.6-45.6	MS
9	CD59 glycoprotein	<i>CD59</i>	P13987	5.18	4.90	14.2	22.7	MS
10	Cathepsin D	<i>CTSD</i>	P07339	5.60	5.40	44.6	31.2	MS
11	Fibrinogen β -chain	<i>FGB</i>	P02675	7.95	4.90	55.9	18.7-19.8	MS
12	Fibrinogen γ -chain	<i>FGG</i>	P02679	5.24	5.30-5.35	55.5	48.0-48.2	MS
13	Vitamin D binding protein	<i>GC</i>	P02774	5.22	5.20	52.9	50.5	MS
14	Hemopexin	<i>HPX</i>	P02790	6.43	5.30-5.35	51.7	55.4	MS
15	Basement membrane-specific heparan sulphate proteoglycan core protein	<i>HSPG2</i>	P98160	6.03	5.40	468.8	24.9	MS
16	Inter- α -trypsin inhibitor heavy chain H4	<i>ITIH4</i>	Q14624	6.00	4.9-5.1	103.4	36.6-37.2	MS
17	Kininogen-1	<i>KNG1</i>	P01042	6.23	4.7-4.9	72.0	50.5-53.3	MS
18	Vesicular integral-membrane protein VIP36	<i>LMAN2</i>	Q12907	6.06	5.20	40.2	35.2	MS
19	Leucine-rich α -2-glycoprotein	<i>LRG1</i>	P02750	5.66	4.60	38.2	47.4	MS
20	Retinol binding protein 4	<i>RBP4</i>	P02753	5.27	5.20	23.0	24.7-25.2	MS
21	α -1-antitrypsin	<i>SERPINA1</i>	P01009	5.37	5.00-5.10	46.7	51.4-52.2	MS
22	Antithrombin III	<i>SERPINC1</i>	P01008	5.95	5.20	52.6	52.6	MS
23	Serotransferrin	<i>TF</i>	P02787	6.70	6.00-6.40	77.1	56.5	MS
24	Trefoil factor 2	<i>TFF2</i>	Q03403	5.21	5.20	14.3	11.1	MS
25	Transthyretin	<i>TTR</i>	P02766	5.31	5.30	15.9	15.9	MS
26	Vitellogenesis factor 1 homolog	<i>VMO1</i>	Q7Z5L0	4.65	4.65	21.2	21.2	MS

pI: isoelectric point; MW: molecular weight; MS: mass spectrometry.

Supplementary Table S4: Selected peptide information of proteins identified by MS/MS in urine of ADHF patients.

Diaz-Riera et al. *Urinary proteomic signature in ADHF: advances into molecular pathophysiology*

Supplementary Table S4: Selected peptide information of proteins identified by MS/MS in

Gel-ID	Protein name	Gene name	Swiss Prot number	M/Z	Position	Sequence	Mod
2	Pancreatic α -amylase	AMY2A	P04746	1427.7	307-318	ALVFVDNHDNQR	
				1570.7	88-100	SGNEDEFRNMVTR	M
7	Carbonic anhydrase 1	CA1	P00915	985.4	82-90	GGPFSDSYR	
				970.6	161-169	VLDALQAIK	
8	Endosialin	CD248	Q9HCU0	1198.6	93-101	QCQLQRPLR	Cys
				1072.5	216-225	QPEGVGWWSR	
9	CD59 glycoprotein	CD59	P13987	1539.7	67-78	FEHCNFDVTTR	Cys
10	Cathepsin D	CTSD	P07339	1462.7	393-403	YYTVFDRDNNR	
11	Fibrinogen β -chain	FGB	P02675	1032.6	484-491	IRPFFPQQ	
12	Fibrinogen γ -chain	FGG	P02679	1034.5	293-301	VGPEADKYR	
				1194.5	32-40	DNCCILDER	Cys_C
				1545.8	418-432	LTIGEGQQHHLGGAK	
14	Hemopexin	HPX	P02790	1220.6	92-102	NFPSPVDAAFR	
				1268.7	209-219	FDPVRGEVPPR	
				1684.9	209-222	FDPVRGEVPPRYR	
				1666.8	4282-4295	LVSEDPINDGEWHR	
15	Basement membrane-specific heparan sulphate proteoglycan core protein	HSPG2	P98160	1601.9	4304-4318	RGSIQVDGEEVLVSGR	
				2413.2	4358-4379	NLVLHSARFGAPPQPLDLQ HR	
				1343.7	208-218	NRDHDTFHAVR	
18	Vesicular integral-membrane protein VIP36	LMAN2	Q12907	1073.5	210-218	DHDTFHAVR	
				989.55	251-260	VAAGAFQGLR	
19	Leucine-rich α -2-glycoprotein	LRG1	P02750	1152.6	165-175	ALGHLDLSGNR	
				1302.7	172-181	VKENFDKAR	
20	Retinol binding protein 4	RBP4	P02753	1106.5	29-37	QRQEELCLAR	Cys
				1675.8	185-198	LIVHNGYCDGRSER	Cys
				1302.7	172-181	QRQEELCLAR	
22	Antithrombin III	SERPINC1	P01008	1674.8	202-215	LQPLDFKENAEQSR	
24	Trefoil factor 2	TFF2	Q03403	1696.7	90-104	NCGYPGISPEECASR	Cys_C
25	Transthyretin	TTR	P02766	1394.7	56-68	AADDTWEPFASGK	
26	Vitelline membrane outer layer protein 1 homolog	VMO1	Q7Z5L0	1217.7	185-196	GLGDDTALNDAR	

M/Z: mass to charge ratio peaks, in bold those with highest MASCOT scores; position of amino acids corresponding to each peak and its sequence; variable modifications and methionine sulfoxide (MSO); miss-cleavage: up to two trypsin miss-cleavages accepted.

Supplementary Table S5: Biological processes and molecular functions of differential urinary proteins.

SwissProt number	Gene	Biological processes			Molecular functions		
		Cell function	Haemostatic & complement system	Inflammation & immune response	Metabolic processes	Binding	Catalytic activity
P11117	<i>ACP2</i>				•		•
P04746	<i>AMY2A</i>				•	•	•
Q9UJ72	<i>ANXA10</i>				•	•	
P15289	<i>ARSA</i>				•	•	
P25311	<i>AZGP1</i>	•	•				•
P01024	<i>C3</i>		•	•	•	•	
P00915	<i>CA1</i>		•			•	
Q9HCU0	<i>CD248</i>	•				•	
P13987	<i>CD59</i>		•			•	
P07339	<i>CTSD</i>				•		•
P02675	<i>FGB</i>	•	•	•		•	
P02679	<i>FGG</i>	•	•			•	
P02774	<i>GC</i>				•	•	•
P02790	<i>HPX</i>				•	•	•
P98160	<i>HSPG2</i>	•		•	•	•	
Q14624	<i>ITIH4</i>			•		•	
P01042	<i>KNG1</i>		•	•		•	
Q12907	<i>LMAN2</i>				•	•	•
P02750	<i>LRG1</i>	•		•		•	
P02753	<i>RBP4</i>		•		•	•	•
P01009	<i>SERPINA1</i>		•	•		•	
P01008	<i>SERPINC1</i>		•	•		•	
P02787	<i>TF</i>		•	•		•	•
Q03403	<i>TFF2</i>		•			•	
P02766	<i>TTR</i>				•	•	•
Q7Z5L0	<i>VMO1</i>					•	•

Cell function includes: angiogenesis, cell adhesion, differentiation, and migration.

Supplementary table S6: Urinary transthyretin levels in relation to patient clinical characteristics.

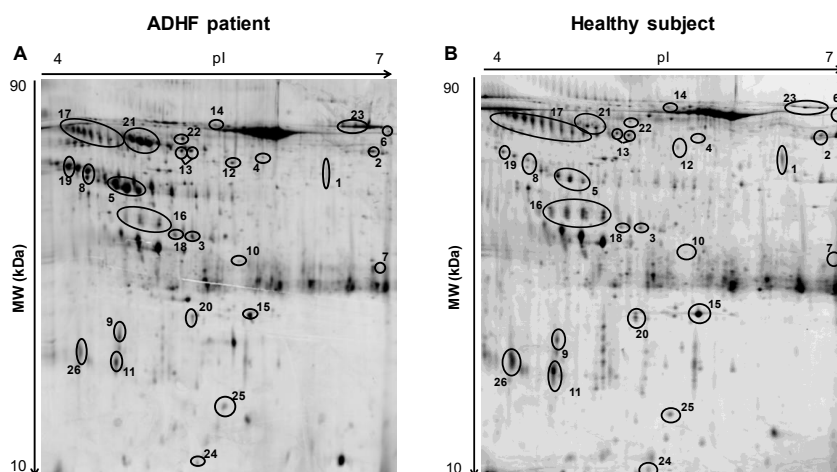
	ADHF patients		NRF		RD	
	N	Median [IQR]	N	Median [IQR]	N	Median [IQR]
LVEF						
Reduced (<40%)	27	12.3 [3.3-64.1]	18	12.3 [3.3-64.1] ^a	9	12.0 [3.3-54.5] ^b
Mildly reduced (40-49%)	12	15.0 [4.8-71.1]	6	9.7 [3.6-41.8]	6	19.6 [15.0-71.1]
Preserved (≥50%)	28	7.8 [3.7-64.4]	11	4.1 [1.6-5.0]	17	15.1 [7.2-70.7]
<i>P value</i>		0.653		0.126		0.428
Hypertension						
No	17	3.9 [2.8-64.1]	13	3.6 [2.4-64.1]	4	5.0 [3.3-70.7]
Yes	49	15.0 [5.0-64.4]	21	11.0 [4.2-43.0]	28	18.3 [7.6-71.1]
<i>P value</i>		0.144		0.433		0.353
Dyslipidaemia						
No	20	5.3 [3.3-54.5]	13	4.6 [3.0-40.5]	6	10.3 [5.0-54.5]
Yes	46	15.1 [4.3-67.1]	20	12.3 [2.2-44.2]	26	18.9 [7.6-72.3]
<i>P value</i>		0.205		0.685		0.263
Diabetes mellitus type II						
No	36	5.5 [3.3-44.2]	23	4.8 [3.3-41.8]	13	11.2 [5.0-54.5]
Yes	30	18.1 [7.6-71.1]	11	15.2 [1.6-45.0]	19	19.6 [7.6-85.2]
<i>P value</i>		0.098		0.767		0.160
Cardiovascular disease						
No	44	8.7 [3.4-43.4]	24	4.5 [2.4-35.1]	20	14.8 [5.0-64.4]
Yes	23	15.0 [5.3-97.3]	11	12.1 [2.8-64.1]	12	41.1 [7.2-128.3]
<i>P value</i>		0.145		0.416		0.270
Atrial fibrillation						
No	34	14.8 [4.8-64.4]	18	9.6 [3.3-64.1]	16	15.1 [7.2-64.4]
Yes	32	8.7 [3.3-54.5]	16	4.3 [2.2-41.8]	16	24.2 [3.7-84.8]
<i>P value</i>		0.701		0.439		0.800
Pulmonary hypertension						
No	51	11.2 [3.3-64.4]	27	5.2 [2.4-44.2]	24	18.3 [7.6-70.7]
Yes	16	12.3 [3.7-54.5]	8	8.2 [3.6-16.9]	8	15.0 [3.7-85.2]
<i>P value</i>		0.893		0.962		0.811

Urinary transthyretin levels in ng TTR/mg total protein. LVEF: left ventricular ejection fraction; NRF: ADHF patients with normal renal function at hospital admission; RD: ADHF patients with renal dysfunction at hospital admission; *P* values were calculated by Mann-Whitney test except for LVEF where Kruskal-Wallis test was used. Information of one patient was missing for hypertension, dyslipidaemia and diabetes mellitus type 2. ^{a,b}Comparison reduced vs preserved LVEF (Mann-Whitney), ^a*P*=0.049, ^b*P*=0.363.

Supplementary table S7: ROC (associated receiver operating characteristic) curve (AUC) analysis for determining power of urinary TTR and RBP4 levels in ADHF patients for GFR discrimination.

Protein	AUC Area	Lower limit	Upper limit	P-value
TTR	0.633	0.489	0.776	0.070
RBP4	0.742	0.614	0.870	<0.001
TTR + RBP4	0.826	0.705	0.947	<0.0001

TTR: transthyretin; RBP4: retinol binding protein 4, AUC: area under the curve.



Supplementary Figure S1. 2DE-PAGE gels of urinary samples from a representative ADHF patient (A) and a representative healthy subject (B) in a pI range of 4-7 and 12% SDS-PAGE gels.

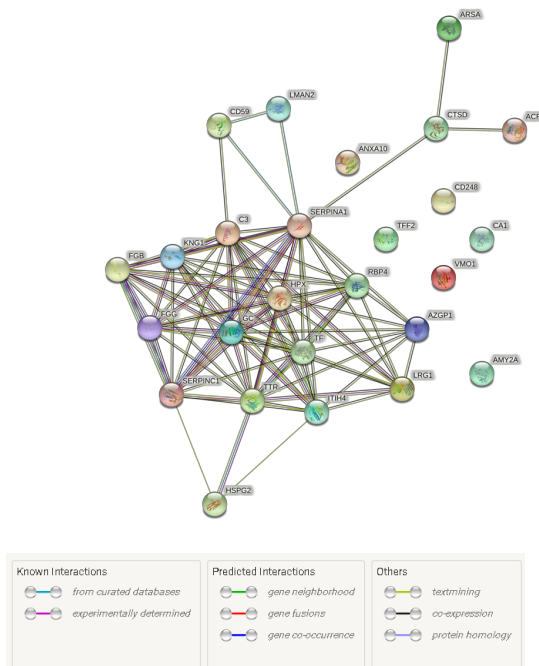
- | | | | |
|----|-------------------------------|----|---|
| 1 | Lysosomal acid phosphatase | 14 | Hemopexin |
| 2 | Pancreatic α -amylase | 15 | Basement membrane-specific heparan sulphate proteoglycan core protein |
| 3 | Annexin A10 | 16 | Inter- α -trypsin inhibitor heavy chain 4 |
| 4 | Zinc α -2-glycoprotein | 17 | Kininogen 1 |
| 5 | Arylsulphatase A | 18 | Vesicular integral-membrane protein VIP36 |
| 6 | Complement C3 | 19 | Leucine-rich α -2-glycoprotein |
| 7 | Carbonic anhydrase 1 | 20 | Retinol binding protein 4 |
| 8 | Endosialin | 21 | α -1-antitrypsin |
| 9 | CD59 glycoprotein | 22 | Antithrombin III |
| 10 | Cathepsin D | 23 | Serotransferrin |
| 11 | Fibrinogen β -chain | 24 | Trefoil factor 2 |
| 12 | Fibrinogen γ -chain | 25 | Transthyretin |
| 13 | Vitamin D binding protein | 26 | Vitelline membrane outer layer protein 1 homolog |

Protein	SwissProt number	Intensity change	MDRD-4			LVEF		
			T1	T2	T3	T1	T2	T3
<i>FGB</i>	P02675	down						
<i>LMAN2</i>	Q12907	down						
<i>ANXA10</i>	Q9UJ72	down						
<i>RBP4</i>	P02753	down						
<i>HPX</i>	P02790	up						
<i>TTR</i>	P02766	up						
<i>GC</i>	P02774	up						
<i>ACP2</i>	P11117	down						
<i>AMY2A</i>	P04746	down						
<i>VMO1</i>	Q7Z5L0	down						
<i>ITIH4</i>	Q14624	down						
<i>SERPINA1</i>	P01009	up						
<i>KNM1</i>	P01042	down						
<i>FGG</i>	P02679	up						
<i>SERPINC1</i>	P01008	up						
<i>AZGP1</i>	P25311	up						
<i>HSPG2</i>	P98160	down						
<i>CD59</i>	P13987	up						
<i>C3</i>	P01024	up						
<i>CTSD</i>	P07339	up						
<i>ARSA</i>	P15289	up						
<i>TF</i>	P02787	up						
<i>CD248</i>	Q9HCU0	up						
<i>LRG1</i>	P02750	up						
<i>TFF2</i>	Q03403	down						
<i>CA1</i>	P00915	up						

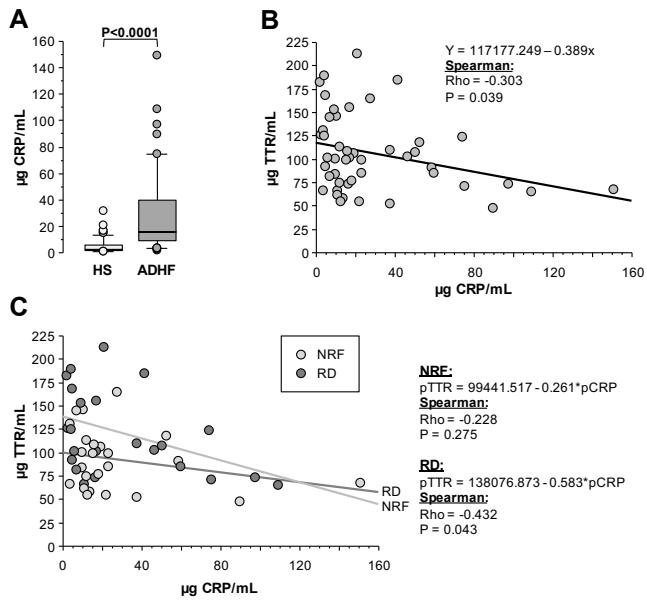
	Fold change
	1.5-2.0
	2.1-3.0
	3.1-5.0
	>5.1

	MDRD-4	LVEF
T1	33.7 [30.7-43.2]	33.0 [22.0-33.0]
T2	68.5 [62.5-71.7]	49.5 [47.0-55.0]
T3	97.8 [106.0-120.0]	60.0 [60.0-65.0]

Supplementary Figure S2. Fold change in urinary differential proteins according to renal function and left ventricular ejection fraction (LVEF) distributed by tertiles.



Supplementary Figure S3. Original STRING network showing the 26 differential proteins consistently detected in urine of ADHF patients and healthy subjects.



Supplementary Figure S4. Plasma C reactive protein (CRP) in ADHF patients at hospital admission. A) CRP levels of ADHF patients (N=67) and healthy subjects (HS), B) Significant correlation between CRP and TTR levels in ADHF patients. C) Regression lines of CRP and TTR correlations depending on kidney function, NRF in light grey and RD with dark grey.

5.2. Article 2

Association between Antithrombin III and Complement C3 in Acute Decompensated Heart Failure

Elisa Diaz-Riera; Maísa García Arguinzonis; Laura López; Xavier Garcia-Moll; Lina Badimon; Teresa Padro

Submitted: Journal of Thrombosis and Haemostasis

Objective: To study the relationship between coagulation and innate immune system in ADHF patients.

Highlights:

- Total antithrombin III (AT3), thrombin-antithrombin (TAT) and complement C3 (C3) are elevated in ADHF patients when compared to healthy subjects.
- AT3 associates with renal dysfunction and preserved/mildly reduced left ventricular ejection fraction beyond its activity as a haemostatic factor.
- In ADHF patients, AT3 positively correlates with plasma levels of the complement C3, independently of system inflammation defined by C-reactive protein.



Association between Antithrombin III and Complement C3 in Acute Decompensated Heart Failure

Journal:	<i>Thrombosis and Haemostasis</i>
Manuscript ID	TH-22-03-0162
Manuscript Type:	Original Article: Cellular Haemostasis and Platelets
Category:	Basic Science
Date Submitted by the Author:	31-Mar-2022
Complete List of Authors:	Diaz Riera, Elisa; Fundacio Institut de Recerca Hospital de la Santa Creu i Sant Pau, Cardiovascular Program-ICCC; Universitat de Barcelona Facultat de Medicina, Garcia-Arguinzonis, Maisa; Fundacio Institut de Recerca Hospital de la Santa Creu i Sant Pau, Cardiovascular Program-ICCC Lopez, Laura; Hospital de la Santa Creu i Sant Pau, Cardiology department Garcia-Moll, Xavier; Hospital de la Santa Creu i Sant Pau, Cardiology department; Centro de Investigación Biomédica en Red Enfermedades Cardiovasculares Badimon, Lina; Fundacio Institut de Recerca Hospital de la Santa Creu i Sant Pau, Cardiovascular Program-ICCC Padro, Teresa; Fundacio Institut de Recerca Hospital de la Santa Creu i Sant Pau, Cardiovascular Program-ICCC
Keywords:	Coagulation, Innate immune system, Acute decompensated heart failure, Complement system, Haemostasis
Abstract:	<p>Introduction: Activation of the coagulation and immune system has been documented in patients with acute decompensated heart failure (ADHF). By applying a proteomic approach, we detected changes in the coagulation component antithrombin III (AT3) and complement-C3 (C3), a component of innate immunity, in urine of ADHF patients. Here, we have investigated AT3 and C3 in urine and plasma of ADHF patients at hospital admission in relation to the disease pathophysiology and severity.</p> <p>Methods: ADHF patients admitted to the emergency room (N=67) were included in the study. ADHF comparison groups were defined by the glomerular filtration rate (pathological cut-off: MDRD-4 <60mL/min/1.73m²) and left ventricular ejection fraction (LVEF: cut-off value 40%). Healthy subjects (HS, N=60) were used to determine the normal range. Samples were collected at hospital admission and proteins quantitatively analysed by ELISA.</p> <p>Results: Total AT3, thrombin-AT3 (TAT) and C3 levels were elevated in ADHF patients when compared to HS. While plasma AT3 was increased in ADHF in the presence of renal dysfunction, TAT- and C3-levels did not follow the same pattern. Among the three variables, only AT3 was</p>

1
2
3
4
5
6
7
8
9
10
11
12
13
14
15
16
17
18
19
20
21
22
23
24
25
26
27
28
29
30
31
32
33
34
35
36
37
38
39
40
41
42
43
44
45
46
47
48
49
50
51
52
53
54
55
56
57
58
59
60

	<p>significantly increased in plasma of ADHF patients with LVEF>40%. ROC analysis confirmed AT3 capacity to discriminate ADHF patients according to LVEF. AT3 positively correlated with plasma C3, but no correlation was observed with C-reactive protein, gold standard of systemic inflammation.</p> <p>In conclusion, increased plasma AT3 levels associated to renal and heart function in ADHF, beyond its activity as thrombin inhibitor. Furthermore, AT3 directly related to C3-mediated innate immunity, independently of systemic inflammation.</p>
--	--

SCHOLARONE™
Manuscripts

1
2
3
4
5
6
7
8
9
10
11
12
13
14
15
16
17
18
19
20
21
22
23
24
25
26
27
28
29
30
31
32
33
34
35
36
37
38
39
40
41
42
43
44
45
46
47
48
49
50
51
52
53
54
55
56
57
58
59
60

1

2

Association between Antithrombin III and Complement C3 in

3

Acute Decompensated Heart Failure

4

5

Short title: Association of AT3 and C3 in ADHF

6

7

Elisa Diaz-Riera^{1,2}, Maïsa García-Arguinzonis¹, Laura López³, Xavier Garcia-Moll^{3,4}, Lina

8

Badimon^{1,4,5}, Teresa Padró^{1,4*}

9

10

¹Cardiovascular-Program ICCC; Research Institute – Hospital Santa Creu i Sant Pau, IIB-

11

Sant Pau, Barcelona, Spain; ²Faculty of Medicine, University of Barcelona (UB), Barcelona,

12

Spain; ³Cardiology Department, Hospital Santa Creu i Sant Pau, Barcelona, Spain; ⁴Centro

13

de Investigación Biomédica en Red Cardiovascular (CIBERCV) Instituto de Salud Carlos III,

14

Madrid, Spain; ⁵Cardiovascular Research Chair, UAB, Barcelona, Spain

15

16

Address for corresponding author (*):

17

Dr Teresa Padro

18

Cardiovascular-Program ICCC;

19

Research Institute Hospital Santa Creu i Sant Pau

20

Sant Antoni M^o Claret 167, 08025 Barcelona, Spain.

21

Phone: +34.935565886

22

Fax: +34.935565559

23

E-mail: tpadro@santpau.cat

24

25

Category of the manuscript: Original article

26

Manuscript word count: 4290 words

27

Abstract word count: 250 words

28

Total number of figures and tables: 1 table, 4 figures

29

Supplementary material online: 4 supplementary table, 3 supplementary figures

30

1
2
3
4
5
6
7
8
9
10
11
12
13
14
15
16
17
18
19
20
21
22
23
24
25
26
27
28
29
30
31
32
33
34
35
36
37
38
39
40
41
42
43
44
45
46
47
48
49
50
51
52
53
54
55
56
57
58
59
60

31

32 Abstract

33 **Introduction:** Activation of the coagulation and immune system has been documented in
34 patients with acute decompensated heart failure (ADHF). By applying a proteomic approach,
35 we detected changes in the coagulation component antithrombin III (AT3) and complement-
36 C3 (C3), a component of innate immunity, in urine of ADHF patients. Here, we have
37 investigated AT3 and C3 in urine and plasma of ADHF patients at hospital admission in
38 relation to the disease pathophysiology and severity.

39 **Methods:** ADHF patients admitted to the emergency room (N=67) were included in the
40 study. ADHF comparison groups were defined by the glomerular filtration rate (pathological
41 cut-off: MDRD-4 <60mL/min/1.73m²) and left ventricular ejection fraction (LVEF: cut-off value
42 40%). Healthy subjects (HS, N=60) were used to determine the normal range. Samples were
43 collected at hospital admission and proteins quantitatively analysed by ELISA.

44 **Results:** Total AT3, thrombin-AT3 (TAT) and C3 levels were elevated in ADHF patients
45 when compared to HS. While plasma AT3 was increased in ADHF in the presence of renal
46 dysfunction, TAT- and C3-levels did not follow the same pattern. Among the three variables,
47 only AT3 was significantly increased in plasma of ADHF patients with LVEF>40%. ROC
48 analysis confirmed AT3 capacity to discriminate ADHF patients according to LVEF. AT3
49 positively correlated with plasma C3, but no correlation was observed with C-reactive
50 protein, gold standard of systemic inflammation.

51 **In conclusion,** increased plasma AT3 levels associated to renal and heart function in ADHF,
52 beyond its activity as thrombin inhibitor. Furthermore, AT3 directly related to C3-mediated
53 innate immunity, independently of systemic inflammation.

54
55 **Keywords:** acute decompensated heart failure; coagulation; innate immune system;
56 complement system; haemostasis

57

1
2
3
4
5
6
7
8
9
10
11
12
13
14
15
16
17
18
19
20
21
22
23
24
25
26
27
28
29
30
31
32
33
34
35
36
37
38
39
40
41
42
43
44
45
46
47
48
49
50
51
52
53
54
55
56
57
58
59
60

58 **Abbreviations:** ADHF: acute decompensated heart failure; AT3: antithrombin III; AUC: area
59 under the curve; CRP: C reactive protein; C3: complement C3; GFR: glomerular filtration
60 rate; HF: heart failure; HS: healthy subjects; LVEF: left ventricular ejection fraction; MALDI-
61 ToF: matrix-assisted laser desorption /ionisation time-of-flight; NRF: normal renal function
62 patients at hospitalisation; RD: renal dysfunction patients at hospitalisation; ROC: receiver
63 operating characteristic; TAT: thrombin-antithrombin complex; TFPI: tissue factor pathway
64 inhibitor; 2DE-MS: 2 dimension electrophoresis – mass spectrometry

68 **What is know about the topic**

- 69 • Acute decompensated heart failure is associated with coagulation disorders deriving
70 in a hypercoagulable phenotype.
- 71 • Inflammation is a major pathophysiological contributor to heart failure
- 72 • increased levels of complement products derived from the activation of the C3
73 complement pathway have been reported in patients with clinical diagnostic of acute
74 heart failure

77 **What does this paper add**

- 78 • Total AT3 and thrombin-AT3 (TAT) levels are significantly increased in plasma of ADHF
79 patients at hospitalisation.
- 80 • AT3 associates with renal dysfunction and preserved / mildly reduced left ventricular
81 ejection fraction, probably with a role beyond its activity as a haemostatic factor.
- 82 • In ADHF patients, AT3 positively correlates with plasma levels of the complement C3, a
83 key component in innate immunity activity, independently of systemic inflammation
84 defined by C-reactive protein.

85

1
2
3
4
5
6
7
8
9
10
11
12
13
14
15
16
17
18
19
20
21
22
23
24
25
26
27
28
29
30
31
32
33
34
35
36
37
38
39
40
41
42
43
44
45
46
47
48
49
50
51
52
53
54
55
56
57
58
59
60

86 Introduction

87 The immune and haemostatic systems are tightly intertwined by the complement system and
88 the coagulation cascade¹. The innate immune cells can exert prothrombotic effects and
89 contribute to the so called *immunothrombosis*, firstly described in 2012.¹ Fibrin, the final
90 product of the coagulation cascade, has immune effects and can limit pathogen
91 dissemination, which suggests that coagulation is not only important in haemostasis, but also
92 in the host defence mechanisms.¹ The coagulation cascade can be activated by
93 inflammation as a response to pathogens through the interplay of platelets with innate
94 immunity cells.²

95 Coagulation, immune system activation and inflammation, with elevated pro-inflammatory
96 cytokines, are pivotal characteristics of the heart failure (HF).^{3,4} Antithrombin III (AT3) is a
97 coagulation inhibitor enzyme, along with vitamin K-dependent protein C and tissue factor
98 pathway inhibitor (TFPI).⁴ AT3, which is encoded by *SERPINC1* gene, is a serine protease
99 inhibitor, with a remarkable protease inhibition capacity when interacting with heparin-like
100 substances on the endothelial cell surface.⁵ AT3 inhibitory function mainly targets thrombin,
101 factor IXa, factor Xa, factor XI, and factor XII; function that is enhanced if a heparin-AT3
102 complex is formed (**Supplementary Figure I**). Moreover, AT3 seems to have some
103 pleiotropic actions favouring anti-inflammatory, anti-angiogenic, antiviral and antibacterial
104 functions.⁶

105 As a response to tissue injury from environmental (hemodynamic overloading or ischaemia)
106 or pathogenic origin, both innate and adaptive immune responses are activated in HF.^{7,8} The
107 complement system is an innate immune response panel that comprises more than 30
108 molecules⁹, with complement C3 having a central role in the three different complement
109 pathways⁸ (**Supplementary Figure I**). Ren *et al.*¹⁰ recently observed that explanted hearts
110 from patients with end-stage arrhythmogenic right ventricular cardiomyopathy had
111 upregulated levels of several complement system components, such as C3, C6, C7, C8, and
112 C9 in both ventricles. Inadequate complement activation can contribute to inflammatory and
113 immune related diseases.¹¹ A link between complement activation and adverse outcomes in
114 HF has also been reported.¹² Elevated anaphylatoxin C3a levels were able to predict
115 hospitalisation and mortality, and were associated with biomarkers of inflammation, cellular
116 stress response, acute phase reaction, endothelial cell activation, and oedematous
117 complications independently of disease severity in chronic HF patients.¹² Recently, high
118 levels of complement activation markers of the C3 pathway including C3bc and sC5b-9 have
119 been reported in patients with acute HF complications following ST-elevation myocardial
120 infarction (STEMI).¹³ Interestingly, a specific pattern of C3 system activation was identified in
121 a subgroup of STEMI patients with cardiogenic shock.¹³ In agreement, other components of

1
2
3 122 the activated C3 complement pathway, such as Factor B and C3bBbP, have been found
4 123 elevated in HF patients.¹⁴ Therefore, a dysregulated C3 pathway may play a key role in
5 124 cardiovascular pathological processes and directly associate with adverse cardiac
6 125 remodelling and mortality in HF patients.

7
8
9 126 By proteomic analysis our group identified changes in the complement system and the
10 127 intrinsic coagulation pathway in association with acute myocardial infarction in patients
11 128 treated according to guidelines.^{15,16} Using a similar proteomic approach, we have recently
12 129 described a specific urine protein signature in patients with ADHF that includes proteins of
13 130 the coagulation system and the complement cascade.¹⁷

14
15
16
17 131 In this study we have investigated the interplay between the coagulation inhibitor AT3 and
18 132 the complement component C3 in ADHF patients at hospital admission in relation to the
19 133 severity of the disease to gain a better understanding in the pathophysiology of heart failure
20 134 decompensation.
21
22
23
24 135

25 26 27 136 **Methods**

28
29 137 More detailed information is available in the Supplementary Materials
30
31

32 138 **Study population and study design**

33 139 This study population comprised a group of ADHF patients ($n=67$, 71.0 [65.0-77.0] years
34 140 old), with and without kidney dysfunction (RD- and NRF-groups) hospitalised at the Hospital
35 141 de la Santa Creu i Sant Pau (HSCSP), in Barcelona. A group of healthy subjects ($n=60$, 49.0
36 142 [44.5-53.5] years old) served to establish normal urine and plasma ranges for the studied
37 143 proteins.

38
39
40
41 144 Baseline demographic and clinical characteristics of the studied population are shown in
42 145 **Table 1**. At the time of hospitalisation, 48% of ADHF patients presented pathological GFR
43 146 levels, which was given as MDRD-4 (in mL/min/1.73m²) using the clinical data of the
44 147 patients.¹⁸ A MDRD-4 of 60 mL/min/1.73m² at hospital admission was considered as the
45 148 pathological cut-off point to differentiate patient groups. Patients with renal dysfunction
46 149 presented low GFR levels (RD group, MDRD-4: 39.7 [31.3-45.0] mL/min/1.73m², $p<0.001$)
47 150 compared to ADHF with normal renal function at hospitalisation (NRF group, MDRD-4: 83
48 151 [68.9-99.0] mL/min/1.73m²). RD patients had higher background comorbidities, mostly
49 152 hypertension, diabetes mellitus type 2 and dyslipidaemia. In addition, 34% of the ADHF
50 153 patients at admission had clinical evidence of prior cardiovascular disease, with no
51 154 differences between groups with and without renal dysfunction. ADHF patients had plasma
52 155 NT-proBNP values above the pathological cut-off defined by the European Society of
53
54
55
56
57
58
59
60

1
2
3 156 Cardiology's most recent Guidelines¹⁹, being levels in the RD group significantly higher than
4 157 those in the NRF group (4475 [2775-14656] ng/L vs 3079 [1562-6418] ng/L, $p=0.026$). Forty
5 158 per cent of ADHF patients had reduced left ventricular ejection fraction (LVEF $\leq 40\%$: 32 [21-
6 159 35]%), and 42% had a LVEF $\geq 50\%$ (60 [56-61]%) at admission. The remaining group of
7 160 patients (18%) presented mildly reduced LVEF, with values between 41-49% (45 [44-47]%),
8 161 as per the most recent Guidelines by the European Society of Cardiology.¹⁹ Mean
9 162 hospitalisation time was 10.8 ± 5.3 days for all patients. Background medication is shown in
10 163 **Supplementary Table I**.
11 164 The Ethics Committee of the Santa Creu i Sant Pau Hospital in Barcelona, Spain approved
12 165 this study, and it was performed according to principles of Helsinki's Declaration. All patients
13 166 signed an informed consent prior being included in the study. Patients under chemotherapy,
14 167 pregnancy or post-delivery ischemic heart syndrome in women, and other causes of acute
15 168 episode (myocardial infarction, myocarditis, or toxic aetiology) were excluded from the study.
16 169 Medication was not considered as exclusion criteria except those required in oncological
17 170 treatment (who were already excluded).

171 **Samples**

172 Urine and venous blood samples were collected at hospital admission. All samples were
173 processed identically within 30 minutes after obtention. Protease inhibitors (cOmplete Mini,
174 Roche, Basel, Switzerland) were added to urine samples at collection. Urine samples were
175 centrifuged (1200g, 10 min, room temperature) to precipitate debris, aliquoted and stored at
176 -80°C until further analysis. Level of total protein in urine were analysed in a Clima MC-15
177 analyser using the specific Gernon kit (RAL S.A., Barcelona, Spain), as described by
178 providers.
179 Plasma EDTA was obtained after centrifugation of blood samples at 1600g (20 min, room
180 temperature), aliquoted and stored at -80°C until analysed.
181 Blood creatinine (Jaffe reaction), NT-proBNP (electroquimioluminescence), urea (kinetic
182 urease), and haemoglobin were analysed by standard laboratory methods as part of the
183 patients' routine analyses. Glomerular filtrate was calculated using the MDRD-4 algorithm
184 that includes patient's plasma creatinine levels, age, sex, and race.¹⁸

185 **2DE electrophoresis and mass spectrometry**

186 Analysis of differential urine protein pattern was performed by two-dimensional
187 electrophoresis (2DE) followed by mass spectrometry for protein identification, as we have
188 recently described.¹⁷ Briefly, proteins in urine were separated and analysed by 2-DE. Protein
189 patterns were analysed for differences using PDQuest software. Proteins of interest were

60

1
2
3 190 excised for protein identification by matrix-assisted laser desorption/ionisation time-of-flight
4
5 191 (MALDI-TOF/TOF).¹⁷
6

7 192 **Western Blot and Immunoassays (ELISAs)**

9 193 Urinary protein extracts were resolved by 1-DE under reducing conditions and
10 194 electrotransferred to nitrocellulose membranes. AT3 detection was performed using a rabbit
11 195 monoclonal antibody (ab124808, Abcam, Cambridge, UK). Western Blot analysis of
12 196 thrombin-antithrombin complex was performed using a mouse monoclonal antibody
13 197 (ab191378, Abcam, Cambridge, UK). Complement C3 was detected by western blot by a
14 198 rabbit monoclonal antibody (ab200999, Abcam, Cambridge, UK). Band detection was
15 199 performed using chemiluminescent SuperSignal (FischerScientific, Waltham, MA, USA), a
16 200 molecular imager ChemiDoc XRS System, Universal Hood II (BioRad, San Diego, CA, USA)
17 201 and ChemiDoc MP (BioRad, San Diego, CA, USA) to visualise fluorescent antibodies.

23 202 Quantitative analysis of AT3 in urine samples was performed using the Human Antithrombin
24 203 III (AT3) AssayMax ELISA kit (AssayPro EA3301-1, St Charles, MO). Plasma EDTA samples
25 204 were analysed with an equivalent AssayMax kit for blood samples (AssayPro EA3303-1, St
26 205 Charles, MO, USA). Thrombin-antithrombin was measured in plasma EDTA samples using
27 206 Human TAT Complex ELISA Kit (AssayPro ET1020-1, St Charles, MO, USA). Analysis of
28 207 complement component C3 in urine was performed by Human Complement C3 AssayMax
29 208 ELISA Kit (AssayPro EC3201-7, St Charles, MO), while plasma EDTA samples were
30 209 analysed with human Complement C3 AssayMax ELISA Kit (AssayPro EC2101-1, St
31 210 Charles, MO). C reactive protein was quantified in plasma EDTA samples with Human CRP
32 211 AssayMax ELISA Kit (AssayPro EC1001-1, St Charles, MO). Concentrations of urinary
33 212 proteins (obtained by ELISA) were standardised to total protein content in the same samples
34 213 that were measured in a Clima MC-15 analyser using the specific Gernon kit. Each
35 214 immunoassay was performed according to providers' protocol.

45 215 **Statistical analysis**

46 216 Data are expressed as median and interquartile range (IQR). N indicates the number of
47 217 subjects tested. The normal distribution was assessed via the Kolmogorov-Smirnov test.
48 218 Differences between groups were determined by non-parametric tests, including Mann-
49 219 Whitney and Kruskal-Wallis tests. Frequencies of categorical variables were compared by
50 220 Fisher's exact test, except for LVEF where χ^2 was used. Correlations between variables
51 221 were determined using single regression models and Spearman rank correlation. Wilcoxon
52 222 Signed Rank test was used to compare patients' evolution. Sample size was validated using
53 223 the JavaScript based method for simple power and sample size calculation when two
54 224 independent groups are compared, that are provided in

1
2
3 225 <http://www.stat.ubc.ca/~rollin/stats/ssize/n2.html> (accessed March 5th 2022) [53]. Based on
4 226 the mean plasma values of ADHF patients and HS and the pooled standard deviation of both
5 227 groups (ADHF and HS) for AT3 and C3, a sample size >60 individuals in each group gave a
6 228 study power of >0.90 (type I error = 0.05, two-sided test).
7
8 229 Receiver operating characteristic (ROC) curve estimations and their corresponding C
9 230 statistics [area under the curve (AUC) with their 95% CI] were calculated to determine the
10 231 power to discriminate ADHF patients according to kidney function and left ventricular ejection
11 232 fraction, as well as disease severity and outcome. Statistical analysis was performed using
12 233 Stata (v15, StataCorp., College Station, TX, USA) and SPSS (v26, IBM Corp, Armonk NY,
13 234 USA). A P value ≤ 0.05 was considered statistically significant.

20 235 Results

23 236 Differential AT3 and C3 detection in urine of ADHF patients

24 237 In a proteomic study in urine of ADHF patients we identified antithrombin III (AT3, SwissProt
25 238 number P01008) and C3 (C3, SwissProt number P01024) among the proteins of the
26 239 coagulation and complement systems at hospital admission.¹⁷ In short, AT3 was detected in
27 240 human urine as a single spot by 2DE-MS with apparent molecular mass of 52.6 KDa and pI
28 241 5.20 and identified by MALDI-ToF spectrometry in modus MS/MS with a MASCOT score of
29 242 78. Complement C3 was also detected as a single spot of molecular mass 54.8 KDa and pI
30 243 6.7 by MALDI-ToF, with a MASCOT score of 62 and coverage value of 3%. Comparison of
31 244 2DE gels of healthy subjects (HS) and ADHF patients at admission showed a 3fold average
32 245 increase in AT3 intensity (median [IQR]: 3.0 [1.3-4.1 AU]; $p < 0.01$) and 2.8fold higher level in
33 246 C3 complement (2.8 [1.4-5.6] AU, $p = 0.04$).

34 247 The presence of both proteins in human urine was initially confirmed by western blot. As
35 248 shown in **Figure 1A**, AT3 was found as a major protein band of approximately 58 KDa. In
36 249 addition, a band of 75KDa corresponding to Thrombin-antithrombin (TAT) was detected, as
37 250 supported by using a second antibody specific for TAT complexes. Western blot analysis in
38 251 **Figure 1A** for urinary C3 evidenced different bands, which corresponded, according to the
39 252 molecular weight, to the whole C3 molecule (1, 185 KDa), and its activated proteolytic
40 253 fragments, C3 α -chain (2, 113 KDa), C3b α -chain (3, 104 KDa), C3c α -chain and C3dg (4
41 254 and 5, 39 KDa).

42 255 By quantitative ELISA, ADHF patients had significantly higher AT3 and C3 urine levels than
43 256 the HS group (AT3: 146.1 [33.0-283.2] vs 85.1 [30.7-142.4] ng AT3/mg total protein,
44 257 $p = 0.050$; C3: 34.7 [12.4-92.0] vs 11.2 [8.9-35.4] ng C3/mg total protein, $p = 0.043$; **Figure 1B**).
45 258 Urinary levels of AT3 and C3 significantly correlated in the ADHF group (Rho=0.523,
46 259 $p < 0.0001$, **Figure 1C**). To further test whether C3 and AT3 correlation was dependent on

1
2
3 260 age, the results were analysed separately according to median age of the ADHF population
4 261 (71 years old). AT3 and C3 had a correlation value of $Rho=0.509$ ($p=0.006$) in patients ≤ 71
5 262 years old, and those older than 71 years old had a correlation value of $Rho=0.571$ ($p=0.002$).
6
7 263 ADHF patients with renal dysfunction (RD group) showed higher AT3 levels than those with
8 264 normal renal function (RD vs NRF: 201.8 [57.4-409.5] vs 126.4 [30.3-176.7] ng AT3/mg total
9 265 protein, $p=0.014$). However, changes in C3 levels in urine of ADHF patients occurred
10 266 irrespectively of kidney function (RD vs NRF: 33.4 [11.9-144.3] vs 36.0 [12.9-85.7] ng C3/mg
11 267 total protein, $p=0.606$).
12
13
14
15
16 268

17 18 269 **Antithrombin III plasma levels in ADHF patients in relation with heart and** 19 20 270 **renal function**

21
22 271 Plasma AT3 (pAT3) levels in ADHF patients were significantly higher than those in HS
23 272 (367.4 [304.3-444.0] vs 280.8 [247.0-317.2] μg AT3/mL, $P<0.0001$, **Figure 2A**). With a
24 273 similar pattern as in the urine, ADHF patients with RD tended to have higher levels than the
25 274 NRF group (384.8 [342.3-468.2] vs 344.0 [293.5-407.5] μg AT3/mL, $p=0.070$), although the
26 275 differences between groups did not achieve statistical significance (**Figure 2A**).

27 276 Plasma levels at day three of hospitalisation remained significantly above the HS group
28 277 ($P<0.001$), without differing from the values at hospital admission ($p=0.113$ for paired
29 278 comparisons, **Figure 2B**), which seemed to detach the plasmatic increase in AT3 from an
30 279 acute phase reaction during the heart failure decompensation.

31 280 AT3 is the major serine protease inhibitor for thrombin in plasma and a key regulator of the
32 281 coagulation cascade. The levels of thrombin-antithrombin complex (TAT) were measured in
33 282 plasma samples of the study population and compared to total levels of AT3. Plasma TAT
34 283 (pTAT) concentration was in the range of ng/mL, representing a minor fraction of the AT3
35 284 detected in plasma (10^4 fold lower when compared in molar basis). Plasma levels of TAT
36 285 were significantly higher in ADHF than in HS (11.6 [9.2-15.8] vs 9.1 [8.1-11.0] ng TAT/mL,
37 286 $p=0.001$, **Figure 2C**), being the increased pTAT levels in ADHF unrelated to renal function of
38 287 the patients at hospitalisation (NRF- vs RD-group: 11.8 [9.3-16.0] vs 10.9 [9.2-14.4] ng
39 288 TAT/mL, $p=0.544$; **Figure 2C**).

40 289 Neither the levels of pAT3 nor those of pTAT were affected by age or sex. Moreover, pAT3
41 290 and pTAT were not dependent on the presence of common comorbidities, such as
42 291 hypertension, diabetes mellitus type 2 or dyslipidaemia, neither associated to presence /
43 292 absence of atrial fibrillation or prior cardiovascular disease (**Supplementary Table II**).
44 293 Interestingly, the highest plasma levels of AT3 levels were found in ADHF patients with LVEF
45 294 above 40% (preserved and mildly reduced LVEF) with median values of 383.8 [350.8-456.7]
46 295 μg AT3/mL compared with median values of 316.7 [280.9-395.3] in the group with reduced

1
2
3 296 LVEF ($\leq 40\%$, $p=0.034$). In line with this finding, ROC curve analysis showed that AT3
4 297 plasma levels discriminated ADHF patients below and above 40% LVEF with an AUC of
5 298 0.687 (95% CI [0.522-0.852], $p=0.026$; **Figure 2D**). The Youden index of this ROC
6 299 calculation indicated that 348.3 $\mu\text{g AT3/mL}$ was the most accurate value (77.4% sensitivity,
7 300 70.6% specificity) to discriminate both groups of patients. Differing from total AT3, pTAT
8 301 levels did not have power to discriminate ADHF patients by their LVEF (AUC: 0.511, 95% CI
9 302 [0.367-0.656], $p=0.879$, **Supplementary Table III**).
10 303 Forty percent of patients had background anticoagulation treatments. Levels of TAT and AT3
11 304 did not differ significantly between the groups with and without anticoagulation therapy at
12 305 hospital admission (**Supplementary Table IV**).
13
14 306 **Plasma AT3 levels correlated with complement C3 levels in ADHF**
15 307 **patients**
16 308 As shown in **Figure 3**, plasma levels of the complement C3 (pC3) were significantly higher in
17 309 ADHF than in HS (259.2 [238.7-282.4] vs 231.8 [213.8-254.6] $\mu\text{g C3/mL}$, $p<0.001$). No
18 310 differences were found between the NRF- and the RD- patients within ADHF groups (258.9
19 311 [226.5-275.3] vs 259.7 [240.9-282.4] $\mu\text{g C3/mL}$, $p=0.292$).
20 312 The pC3 levels were not associated to age nor to sex. ADHF patients with diabetes mellitus
21 313 (DM) type II (45% of the ADHF group) showed higher pC3 levels (with vs without DM: 268.1
22 314 [253.2-305.1] vs 247.6 [227.7-264.9] $\mu\text{g C3/mL}$, $p=0.015$). Other background comorbidities
23 315 including arterial hypertension, dyslipidaemia or pulmonary hypertension did not significantly
24 316 affect pC3 levels in ADHF (**Supplementary Table II**). Regarding cardiac function, pC3 levels
25 317 did not discriminate between ADHF patients with reduced LVEF ($\leq 40\%$) and those with
26 318 LVEF values $>40\%$ when ROC analysis was performed (**Supplementary Table III**).
27 319 In the study population (ADHF & HS), pAT3 significantly correlated with pC3 (Rho=0.537,
28 320 $p<0.001$), being the correlation maintained when ADHF populations and HS were separately
29 321 analysed (ADHF: Rho=0.477, $p=0.001$; HS: Rho=0.330, $p=0.010$, **Supplementary Figure**
30 322 **II**). Moreover, pC3 and pAT3 significantly correlated when separated according to reduced
31 323 LVEF ($\leq 40\%$, Rho=0.529, $p=0.029$) or LVEF $>40\%$ (Rho=0.411, $p=0.024$, **Supplementary**
32 324 **Figure III**). Unlike total pAT3, no correlation was found between plasma TAT and pC3 levels
33 325 in the total study population (Rho: 0.149, $p=0.127$, **Supplementary Figure II**) and neither
34 326 when the ADHF and HS groups were studied separately (ADHF: Rho=0.004, $p=0.978$; HS:
35 327 Rho: 0.064; $p=0.632$; **Figure 3B** and **Supplementary Figure II**).
36 328 Patients who required a heart transplant or died within the follow-up period presented lower
37 329 pC3 levels (240.9 [225.0-253.4] $\mu\text{g C3/mL}$) than patients with better outcome (262.3 [240.9-
38 330 287.3] $\mu\text{g C3/mL}$, $p=0.05$).
39 331

1
2
3
4
5
6
7
8
9
10
11
12
13
14
15
16
17
18
19
20
21
22
23
24
25
26
27
28
29
30
31
32
33
34
35
36
37
38
39
40
41
42
43
44
45
46
47
48
49
50
51
52
53
54
55
56
57
58
59
60

332 **Increased pAT3 levels in ADHF did not associate with systemic** 333 **inflammation**

334 Patients with ADHF had a high systemic inflammation at hospital admission, with plasma
335 values of C reactive protein in the interquartile range of 8.8 to 41.2 $\mu\text{g CRP/mL}$ (healthy
336 subjects' interquartile range: [1.4-5.5] $\mu\text{g CRP/mL}$, $P < 0.0001$).
337 ADHF patients did not differ significantly in AT3 and TAT levels when compared by CRP
338 plasma tertiles ($p = 0.241$ and $p = 0.892$, respectively, **Figure 4**), whereas significant
339 differences were found among the CRP tertile groups for C3 levels ($p = 0.002$; **Figure 4**).
340 Similarly, plasma AT3 did not correlate with pCRP levels ($Rho = 0.239$, $p = 0.106$) in ADHF
341 patients at hospital admission, whereas pCRP levels positively correlated with pC3 levels in
342 ADHF patients at hospital admission ($Rho = 0.492$, $p = 0.001$). These results strongly suggest
343 that pAT3 levels relate to the innate immunity response rather than to a systemic
344 inflammation in patients with ADHF.

345 **Discussion**

346 Acute heart failure is an important life-threatening condition regardless of therapeutic
347 advances, with a mortality rate ranging 4-7%.²⁰ Moreover, patients with heart failure present
348 recurrent re-hospitalisations²¹, which reflects, at least in part, our limited understanding of the
349 underlying pathologic mechanisms in acute heart failure decompensation.²² Identification and
350 characterisation of molecular targets behind acute heart failure events is crucial to better
351 stratify patients and to develop new therapeutic strategies.

352 Based on a 2DE-mass spectrometry proteomic approach, we have recently described a
353 differential protein signature that included proteins of innate immunity and the coagulation
354 system in urine of patients presenting ADHF.¹⁷ Here, we extend our previous finding and to
355 the best of our knowledge, we report for first time a significant increase in plasma AT3 in
356 ADHF patients compared to healthy individuals. Levels of AT3 in urine and plasma of ADHF
357 patients positively correlated with the key complement component C3, which also presented
358 urine and plasma levels significantly above the healthy range in ADHF patients, suggesting a
359 link between the increased presence of AT3, a major plasma glycoprotein of the serpin
360 superfamily, and activation of innate immunity processes. Interestingly, plasma AT3 did not
361 increase consensually with CRP, suggesting that changes in AT3 associate to specific
362 immune responses rather than a systemic inflammatory stimulus.

363 In agreement with our findings, other authors have reported increased levels of complement
364 products including sC5b-9, end-product of the C3 complement pathway, in patients with
365 clinical diagnostic of acute heart failure.²³ Until now, however, available results are
366 inconclusive and apparently controversial, being the potential pathophysiological role of

1
2
3 367 complement components in heart failure still emerging. In our study, in patients with acute
4 368 decompensation of chronic heart failure, the increase in plasma levels of the complement
5 369 component C3 was unrelated to the kidney function defined by the glomerular filtration rate.
6
7
8 370 Suffritti *et al.*²³ analysed the complement activation in patients with acute congestive heart
9
10 371 failure during hospitalisation and limited the changes in C3 to patients with preserved
11 372 ejection fraction.²³ We did not find such difference in our cohort of ADHF patients for C3
12 373 levels, and C3 did not discriminate ADHF patients by their LVEF. In contrast, AT3 values
13 374 were able to discriminate between ADHF patients with reduced LVEF ($\leq 40\%$ according to
14 375 ESC 2021 Guidelines¹⁹ within the ADHF cohort, but this was not observed with plasma TAT
15 376 levels. Yamamoto *et al.*²⁴ reported a significant correlation between LVEF and three
16 377 coagulation components: TAT, D-dimer and prothrombin in patients healed from myocardial
17 378 infarction. However, plasma TAT levels detected in our ADHF cohort did not correlate with
18 379 LVEF levels. These results suggest that additional pathological factors modulate the
19 380 association between coagulation variables and LVEF in cardiac pathologies.
20
21 381 Levels of complement components have been associated with adverse outcomes and
22 382 survival although with controversial findings.^{12,25} In this respect, Gombos *et al.*¹² reported that
23 383 elevated C3a levels were associated with higher re-hospitalisation rate and all-cause
24 384 mortality due to progression of heart failure. In contrast, in our ADHF study population
25 385 although C3 was significantly above the healthy range, the group of patients requiring heart
26 386 transplant or dying during the 18 months follow-up presented a median C3 plasma level
27 387 significantly lower than the group of patients with better outcome. In agreement with our
28 388 findings, Silva *et al.*²⁵ observed that low C3c levels were associated with higher risk of death
29 389 in acute heart failure patients. Similarly, Frey and colleagues⁸ observed that elevated C3c
30 390 levels associated with improved survival in heart failure patients with LVEF $< 40\%$.
31
32 391 Different studies have reported an association between the complement system components
33 392 and cardiac remodelling¹⁰, inflammation, and endothelial activation¹². We and others²⁵ have
34 393 found that levels of C3 components positively correlate with CRP suggesting an association
35 394 between systemic inflammation and activation of the C3 cascade.²⁶ Presence of systemic
36 395 inflammation in heart failure has been thoroughly studied; however the underlying
37 396 mechanisms remain unclear.²⁷ Nevertheless, elevated inflammatory markers have been
38 397 associated with poor prognosis.²⁸
39
40 398 The complement system is mainly activated through the three well recognised classical,
41 399 alternative and lectin pathways. However, it has been observed that kallikrein, another
42 400 coagulation cascade component, is also able to cleave C3 and activate the complement
43 401 system.²⁹ To notice, kallikrein is inhibited by AT3³⁰ (see supplementary Figure I). Therefore,
44 402 high AT3 plasma levels may contribute to higher levels of uncleaved C3.
45
46
47
48
49
50
51
52
53
54
55
56
57
58
59
60

1
2
3 403 Beyond its role as coagulation inhibitor, AT3 has been further associated with anti-
4 404 angiogenic and anti-inflammatory activities⁶, the latter being related to inhibition of platelet
5 and endothelial activation through a thrombin-mediated process.³¹ Therefore, we could not
6 405
7 406 exclude from our study that elevated AT3 acts as a compensation mechanism to reduce
8 inflammation in ADHF patients.
9 407
10
11 408 Angiogenesis associated with pathological hypertrophy is characterised by an inadequate
12 409 modification of cardiac microvasculature leading to cardiac underperfusion, which in turn
13 410 may cause cardiomyocyte death, hypoxia, and cardiac fibrosis, which are contributors to
14 411 heart failure development.³² Recent studies have related two latent isoforms of AT3 to its
15 412 anti-angiogenic activity.³³ Our current results do not differentiate these two AT3 isoforms, but
16 413 the high plasma levels of AT3 compared to those of TAT might result from the presence of
17 414 these latent forms. Further studies are warranted to better explain the mechanistic
18 415 involvement of AT3 in inflammatory and angiogenic processes related to cardiac remodelling
19 416 and heart failure progression.
20
21
22
23
24
25
26

27 417
28 418 In summary, this hypothesis-generating study, aimed to identify new molecular targets with
29 419 potential pathophysiologic relevance in ADHF, provides novel evidence on the association
30 420 between the protease inhibitor AT3 and the complement C3 in the setting of acute heart
31 421 failure decompensation. Thus, our results showed that ADHF patients present with high
32 422 levels of AT3 in urine and plasma at hospital admission. AT3 remained increased after 72h
33 423 of hospitalisation. Interestingly, only traces of AT3 were complexed with thrombin in plasma
34 424 of ADHF patients, suggesting an activity beyond anticoagulation. AT3 significantly correlated
35 425 with urea levels and, accordingly, AT3 levels were higher in patients with renal dysfunction
36 426 defined by glomerular filtration algorithm MDRD-4. Furthermore, plasma AT3 significantly
37 427 discriminated ADHF patients with LVEF \leq 40%. In addition, AT3 positively correlated with
38 428 plasma levels of the complement C3, a key component in innate immunity activity,
39 429 independently of systemic inflammation.
40
41
42
43
44
45
46
47

48

49 431 **Acknowledgments**

50 432 We gratefully acknowledge the valuable help and support of Montse Gómez-Pardo with the
51 433 sample handling.
52
53
54

55 434 **Funding**

56 435 This work was supported by the "Fundació La Marató TV3" (Project number 20153110) to
57 436 T.P., the Spanish Institute of Health Carlos III, ISCIII [FIS PI19/01687] to T.P.; Centro de
58
59
60

1
2
3 437 Investigación Biomédica en Red Cardiovascular (CIBERCV-CB16/11/00411) to L.B.; Spanish
4 438 Ministry of Economy and Competitiveness of Science "Agencia Estatal de Investigación
5 439 (AEI)" Proj Ref AEI / 10.13039/501100011033-[PID2019-107160RB-I00] to L.B.; and
6 440 cofounded by FEDER "Una Manera de Hacer Europa". Secretaria de Universitats i Recerca
7 441 del Departament d'Empresa i Coneixement de la Generalitat de Catalunya [2017 SGR
8 442 1480]. We thank Fundació Jesús Serra and Fundación de Investigación Cardiovascular,
9 443 Barcelona, for their continuous support. E.D.R. is a predoctoral fellow funded by the
10 444 "Fundació La Marató TV3" and the Cardiovascular Program-ICCC (IR-HSCSP).
11
12
13
14
15
16
17

18 446 **Supplementary Information**

19
20 447 **Additional File: Supplementary Table I:** ADHF patients' medication at hospital admission.
21
22 448 **Supplementary Table II:** Plasma levels of AT3, TAT, and C3 levels depending on patients'
23
24 449 risk factors. **Supplementary Table III:** ROC (associated receiver operating characteristic)
25
26 450 curve analysis for determining discriminatory power of plasma AT3 and C3 for LVEF
27
28 451 classification in ADHF patients at hospital admission. **Supplementary Table IV:** Plasma
29
30 452 levels of AT3, TAT, and C3 levels depending on patients medication. **Supplementary**
31
32 453 **Figure I:** Coagulation cascade and C3 pathway. **Supplementary Figure II:** Plasma C3
33
34 454 correlation with pAT3 and pTAT. **Supplementary Figure III:** Regression lines and Spearman
35
36 455 correlation between plasma C3 and AT3 depending on heart function.

37 456 **Ethics approval and consent to participate**

38
39 457 This study was reviewed and approved by the Ethical Committee for clinical research from
40
41 458 Hospital Santa Cruz y San Pablo in March 2016 (reference number 16/022). The patients
42
43 459 provided their written informed consent to participate in this study.

44 460 **Conflict of interests**

45
46
47
48 461 L.B. received institutional research grants from AstraZeneca, consultancy and speaker fees
49
50 462 from Sanofi, Pfizer, and Novartis. T.P, and L.B. are shareholders of the academic spin-off
51
52 463 companies GlyCardial Diagnostics S.L. and Ivestatin Therapeutics S.L. All unrelated to the
53
54 464 present work. EDR, MGA, LL, XGM declare no conflict of interest.

55 465

56
57
58
59
60

1
2
3
4
5
6
7
8
9
10
11
12
13
14
15
16
17
18
19
20
21
22
23
24
25
26
27
28
29
30
31
32
33
34
35
36
37
38
39
40
41
42
43
44
45
46
47
48
49
50
51
52
53
54
55
56
57
58
59
60**References**

- 466 **References**
- 467 1. Engelmann B, Massberg S. Thrombosis as an intravascular effector of innate
468 immunity. *Nat Rev Immunol.* 2013;13(1):34-45. doi:10.1038/nri3345
- 469 2. Stark K, Massberg S. Interplay between inflammation and thrombosis in
470 cardiovascular pathology. *Nat Rev Cardiol.* 2021;18(9):666-682. doi:10.1038/s41569-
471 021-00552-1
- 472 3. Perticone M, Zito R, Miceli S, et al. Immunity, Inflammation and Heart Failure: Their
473 Role on Cardiac Function and Iron Status. *Front Immunol.* 2019;10(2315).
474 doi:10.3389/fimmu.2019.02315
- 475 4. O'Donnell JS, O'Sullivan JM, Preston RJS. Advances in understanding the molecular
476 mechanisms that maintain normal haemostasis. *Br J Haematol.* 2019;186(1):24-36.
477 doi:10.1111/bjh.15872
- 478 5. Lu Z, Wang F, Liang M. SerpinC1/Antithrombin III in kidney-related diseases. *Clin Sci.*
479 2017;131(9):823-831. doi:10.1042/CS20160669
- 480 6. Rezaie AR, Giri H. Anticoagulant and signaling functions of antithrombin. *J Thromb*
481 *Haemost.* 2020;18(12):3142-3153. doi:10.1111/jth.15052
- 482 7. Mann DL. Innate immunity and the failing heart: The cytokine hypothesis revisited.
483 *Circ Res.* 2015;116(7):1254-1268. doi:10.1161/CIRCRESAHA.116.302317
- 484 8. Frey A, Ertl G, Angermann CE, Hofmann U, Störk S, Frantz S. Complement C3c as a
485 biomarker in heart failure. *Mediators Inflamm.* 2013;2013. doi:10.1155/2013/716902
- 486 9. Master Sankar Raj V, Gordillo R, Chand DH. Overview of C3 Glomerulopathy. *Front*
487 *Pediatr.* 2016;4(May):1-7. doi:10.3389/fped.2016.00045
- 488 10. Ren J, Tsilafakis K, Chen L, et al. Crosstalk between coagulation and complement
489 activation promotes cardiac dysfunction in arrhythmogenic right ventricular
490 cardiomyopathy. *Theranostics.* 2021;11(12):5939-5954. doi:10.7150/thno.58160
- 491 11. Morgan BP, Harris CL. Complement, a target for therapy in inflammatory and
492 degenerative diseases. *Nat Rev Drug Discov.* 2015;14(12):857-877.
493 doi:10.1038/nrd4657
- 494 12. Gombos T, Föhrhéc Z, Pozsonyi Z, et al. Complement anaphylatoxin C3a as a novel
495 independent prognostic marker in heart failure. *Clin Res Cardiol.* 2012;101(8):607-
496 615. doi:10.1007/s00392-012-0432-6
- 497 13. Thomas AM, Chaban V, Pischke SE, et al. Complement ratios C3bc/C3 and sC5b-
498 9/C5 do not increase the sensitivity of detecting acute complement activation
499 systemically. *Mol Immunol.* 2022;141:273-279. doi:10.1016/j.molimm.2021.11.016
- 500 14. Holt MF, Michelsen AE, Shahini N, et al. The Alternative Complement Pathway Is
501 Activated Without a Corresponding Terminal Pathway Activation in Patients With

- 1
2
3 502 Heart Failure. *Front Immunol.* 2021;12:800978. doi:10.3389/fimmu.2021.800978
4
5 503 15. Cubedo J, Padró T, Badimon L. Coordinated proteomic signature changes in immune
6 504 response and complement proteins in acute myocardial infarction: The implication of
7 505 serum amyloid P-component. *Int J Cardiol.* 2013;168(6):5196-5204.
8 506 doi:10.1016/j.ijcard.2013.07.181
9
10 507 16. Cubedo J, Ramaola I, Padró T, Martín-Yuste V, Sabate-Tenas M, Badimon L. High-
11 508 molecular-weight kininogen and the intrinsic coagulation pathway in patients with de
12 509 novo acute myocardial infarction. *Thromb Haemost.* 2013;110(6):1121-1134.
13 510 doi:10.1160/TH13-05-0381
14 511 17. Diaz-Riera E, García-Arguinzonis M, López L, Garcia-Moll X, Badimon L, Padro T.
15 512 Urinary Proteomic Signature in Acute Decompensated Heart Failure: Advances into
16 513 Molecular Pathophysiology. *Int J Mol Sci.* 2022;23:2344. doi:10.3390/ijms23042344
17 514 18. Tarwater K. Estimated glomerular filtration rate explained. *Mo Med.* 2011;108(1):29-
18 515 32. doi:10.1136/bmj.g264
19 516 19. McDonagh TA, Metra M, Adamo M, et al. 2021 ESC Guidelines for the diagnosis and
20 517 treatment of acute and chronic heart failure. *Eur Heart J.* 2021;42(36):3599-3726.
21 518 doi:10.1093/eurheartj/ehab368
22 519 20. Arrigo M, Jessup M, Mullens W, et al. Acute heart failure. *Nat Rev Dis Prim.*
23 520 2020;6(16). doi:10.1038/s41572-020-0151-7
24 521 21. Sinnenberg L, Givertz MM. Acute heart failure. *Trends Cardiovasc Med.*
25 522 2020;30(2):104-112. doi:10.1016/j.tcm.2019.03.007
26 523 22. Frangogiannis NG. Editor's Choice- Activation of the innate immune system in the
27 524 pathogenesis of acute heart failure. *Eur Hear journal Acute Cardiovasc care.*
28 525 2018;7(4):358-361. doi:10.1177/2048872617707456
29 526 23. Suffritti C, Tobaldini E, Schiavon R, et al. Complement and contact system activation
30 527 in acute congestive heart failure patients. *Clin Exp Immunol.* 2017;190(2):251-257.
31 528 doi:10.1111/cei.13011
32 529 24. Yamamoto K, Ikeda U, Fukazawa H, Mitsuhashi T, Sekiguchi H, Shimada K. Left
33 530 ventricular function and coagulation activity in healed myocardial infarction. *Am J*
34 531 *Cardiol.* 1998;81(7):920-923. doi:10.1016/S0002-9149(98)00014-9
35 532 25. Silva N, Martins S, Lourenço P, Bettencourt P, Guimarães JT. Complement C3c and
36 533 C4c as predictors of death in heart failure. *IJC Metab Endocr.* 2015;7:31-35.
37 534 doi:10.1016/J.IJCME.2015.02.001
38 535 26. Ricklin D, Lambris JD. Complement in immune and inflammatory disorders:
39 536 pathophysiological mechanisms. *J Immunol.* 2013;190(8):3831-3838.
40 537 doi:10.4049/jimmunol.1203487
41 538 27. Adamo L, Rocha-Resende C, Prabhu SD, Mann DL. Reappraising the role of

- 1
2
3 539 inflammation in heart failure. *Nat Rev Cardiol.* 2020;17(5):269-285.
4 540 doi:10.1038/S41569-019-0315-X
5
6 541 28. Shirazi LF, Bissett J, Romeo F, Mehta JL. Role of Inflammation in Heart Failure. *Curr*
7 542 *Atheroscler Rep.* 2017;19(6). doi:10.1007/s11883-017-0660-3
8
9 543 29. Irmischer S, Döring N, Halder LD, et al. Kallikrein Cleaves C3 and Activates
10 544 Complement. *J Innate Immun.* 2018;10(2):94-105. doi:10.1159/000484257
11
12 545 30. Hepner M, Karlaftis V. Antithrombin. In: Monagle P, ed. *Haemostasis: Methods and*
13 546 *Protocols.* Totowa, NJ: Humana Press; 2013:355-364. doi:10.1007/978-1-62703-339-
14 547 8_28
15
16 548 31. Levy JH, Sniecinski RM, Welsby IJ, Levi M. Antithrombin: Anti-inflammatory properties
17 549 and clinical applications. *Thromb Haemost.* 2016;115(4):712-728. doi:10.1160/TH15-
18 550 08-0687
19
20 551 32. Gogiraju R, Bochenek ML, Schäfer K. Angiogenic Endothelial Cell Signaling in
21 552 Cardiac Hypertrophy and Heart Failure. *Front Cardiovasc Med.* 2019;6(March).
22 553 doi:10.3389/fcvm.2019.00020
23
24 554 33. Broman LM. When antithrombin substitution strikes back. *Perfus (United Kingdom).*
25 555 2020;35(1_suppl):34-37. doi:10.1177/0267659120906770
26
27 556
28
29 557
30
31
32
33
34
35
36
37
38
39
40
41
42
43
44
45
46
47
48
49
50
51
52
53
54
55
56
57
58
59
60

1
2
3
4
5
6
7
8
9
10
11
12
13
14
15
16
17
18
19
20
21
22
23
24
25
26
27
28
29
30
31
32
33
34
35
36
37
38
39
40
41
42
43
44
45
46
47
48
49
50
51
52
53
54
55
56
57
58
59
60

558 **Legends to Figures**

559 **Figure 1: Urinary 2D electrophoresis (2DE) identification and western blot of** 560 **antithrombin III (AT3) and complement C3 (C3) at hospital admission. A)**

561 Representative 2DE spots of AT3 and C3 in urine samples of a representative ADHF patient
562 (ADHF) and a healthy subject (HS). Western blot of AT3, TAT and C3 of a urine sample of
563 an ADHF patient pool. C3 presents several bands corresponding to different C3 fragments:
564 1) whole C3; 2) C3 α -chain; 3) C3b α -chain; 4 and 5) C3c α_2 -chain and C3dg. **B)** Urinary
565 levels of ADHF patients of AT3 (left) and complement C3 (right) obtained by immunoassay
566 (ELISA). Urinary levels were normalised with total protein content in urine. **C)** Regression
567 line and correlation between AT3 and C3 urinary levels of ADHF patients at hospital
568 admission.

569
570 **Figure 2: Plasma levels of AT3 and TAT. A)** Plasma AT3 levels of ADHF patients and
571 healthy individuals (left), and plasma AT3 levels according to renal function in ADHF patients
572 (right). **B)** Plasma levels at hospital admission (day 0) and three days after hospital
573 admission (day 3) of ADHF patients. **C)** Plasma thrombin-antithrombin (TAT) levels of ADHF
574 patients and healthy individuals (left), and plasma TAT levels according to renal function in
575 ADHF patients (right). **D)** ROC curve of pAT3 and pTAT to discern between patients with
576 reduced ejection fraction ($\leq 40\%$, as per 2021 Guidelines by the European Society of
577 Cardiology) from the rest of the cohort.

578
579 **Figure 3: Plasma levels of complement C3 (C3) at hospital admission. A)** Plasma C3
580 levels of ADHF patients and healthy individuals (left), and plasma C3 levels according to
581 renal function in ADHF patients (right). **B)** Correlation of plasma C3 and AT3 levels in ADHF
582 patients at hospital admission. **C)** Correlation of C3 and TAT levels in ADHF patients at
583 hospital admission.

584
585 **Figure 4: Plasma levels of C reactive protein (CRP) at hospital admission.** Classification
586 of pAT3, pTAT and pC3 according to plasma CRP tertiles.

Table 1: Clinical characteristics of ADHF patients.

	All patients N=67	NRF N=35	RD N=32	P value
DEMOGRAPHIC CHARACTERISTICS				
Female/male, N	22/45	10/25	12/20	0.603
Age, years	71.0 [65.0-77.0]	69.0 [58.0-75.0]	74.0 [69.5-77.5]	0.008
KIDNEY FUNCTION MARKERS				
Creatinine, µmol/L	105.0 [78.0-147.0]	78.0 [67.0-97.0]	147.0 [122.5-194.0]	<0.001
Glomerular filtration (MDRD-4) ^a	61.0 [40.9-83.3]	83.0 [68.9-99.0]	39.7 [31.3-45.0]	<0.001
Urea, mmol/L	10.2 [6.8-16.1]	7.0 [5.8-9.2]	16.5 [13.0-22.9]	<0.001
CARDIAC FUNCTION MARKERS				
NT-proBNP, ng/L	3950 [2256-8584]	3079 [1562-6418]	4475 [2775-14656]	0.026
Left ventricular ejection fraction (LVEF), %	45.0 [33.0-58.0]	38.0 [33.0-57.0]	51.0 [35.5-59.5]	0.225
Reduced LVEF ≤40%, N (%)	29 (43)	19 (54)	10 (31)	
Mid-range LVEF 41-49%, N (%)	10 (15)	5 (14)	5 (16)	0.125
Preserved LVEF ≥50%, N (%)	28 (42)	11 (31)	17 (53)	
Atrial fibrillation, N (%)	32 (48)	16 (47)	16 (50)	>0.999
Cardiovascular disease, N (%)	23 (34)	11 (31)	12 (38)	0.618
OTHER BIOCHEMICAL MARKERS				
C reactive protein (CRP), µg/mL	16.0 [8.8-41.2]	15.4 [10.3-25.0]	16.4 [4.7-50.1]	0.882
Haemoglobin, g/L	122 [101-138]	128 [114-142]	110 [95-124]	0.004
RISK FACTORS; N (%)				
Active smoking	10 (15)	8 (23)	2 (6)	0.086
Hypertension	49 (74)	21 (62)	28 (88)	0.024
Pulmonary hypertension	16 (24)	8 (23)	8 (25)	>0.999
Diabetes mellitus type 2	30 (45)	11 (32)	19 (59)	0.047
Dyslipidaemia	46 (70)	20 (59)	26 (81)	0.063

^aMDRD-4 levels expressed in mL/min/1.73m². Quantitative values were given in median [Q1-Q3]. P values of categorical variables were calculated with Fisher exact test, except for LVEF where χ^2 was used. LVEF classification according to the 2021 Guidelines by the European Society of Cardiology. P values of numerical data were calculated with Mann-Whitney, except for LVEF where Kruskal-Wallis was used. L

1
2
3
4
5
6
7
8
9
10
11
12
13
14
15
16
17
18
19
20
21
22
23
24
25
26
27
28
29
30
31
32
33
34
35
36
37
38
39
40
41
42
43
44
45
46
47
48
49
50
51
52
53
54
55
56
57
58
59
60

Figure 1

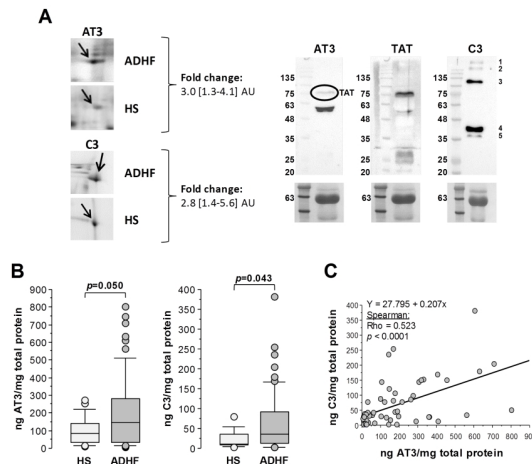


Figure 1: Urinary 2D electrophoresis (2DE) identification and western blot of antithrombin III (AT3) and complement C3 (C3) at hospital admission. A) Representative 2DE spots of AT3 and C3 in urine samples of a representative ADHF patient (ADHF) and a healthy subject (HS). Western blot of AT3, TAT and C3 of a urine sample of an ADHF patient pool. C3 presents several bands corresponding to different C3 fragments: 1) whole C3; 2) C3 α -chain; 3) C3b α -chain; 4 and 5) C3c α 2-chain and C3dg. B) Urinary levels of ADHF patients of AT3 (left) and complement C3 (right) obtained by immunoassay (ELISA). Urinary levels were normalised with total protein content in urine. C) Regression line and correlation between AT3 and C3 urinary levels of ADHF patients at hospital admission

190x274mm (284 x 284 DPI)

1
2
3
4
5
6
7
8
9
10
11
12
13
14
15
16
17
18
19
20
21
22
23
24
25
26
27
28
29
30
31
32
33
34
35
36
37
38
39
40
41
42
43
44
45
46
47
48
49
50
51
52
53
54
55
56
57
58
59
60

Figure 2

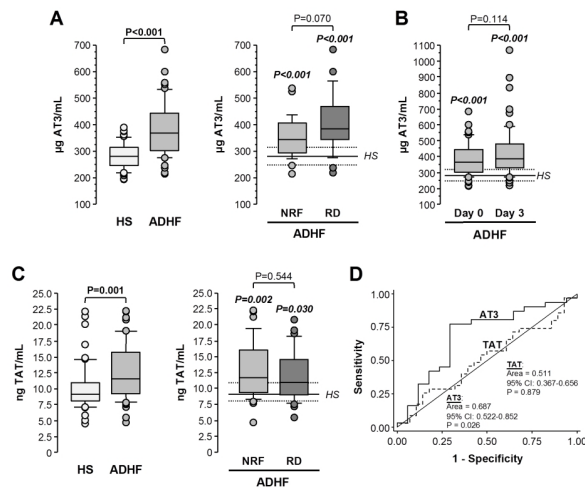


Figure 2: Plasma levels of AT3 and TAT. A) Plasma AT3 levels of ADHF patients and healthy individuals (left), and plasma AT3 levels according to renal function in ADHF patients (right). B) Plasma levels at hospital admission (day 0) and three days after hospital admission (day 3) of ADHF patients. C) Plasma thrombin-antithrombin (TAT) levels of ADHF patients and healthy individuals (left), and plasma TAT levels according to renal function in ADHF patients (right). D) ROC curve of pAT3 and pTAT to discern between patients with reduced ejection fraction ($\leq 40\%$, as per 2021 Guidelines by the European Society of Cardiology) from the rest of the cohort.

190x274mm (284 x 284 DPI)

1
2
3
4
5
6
7
8
9
10
11
12
13
14
15
16
17
18
19
20
21
22
23
24
25
26
27
28
29
30
31
32
33
34
35
36
37
38
39
40
41
42
43
44
45
46
47
48
49
50
51
52
53
54
55
56
57
58
59
60

Figure 3

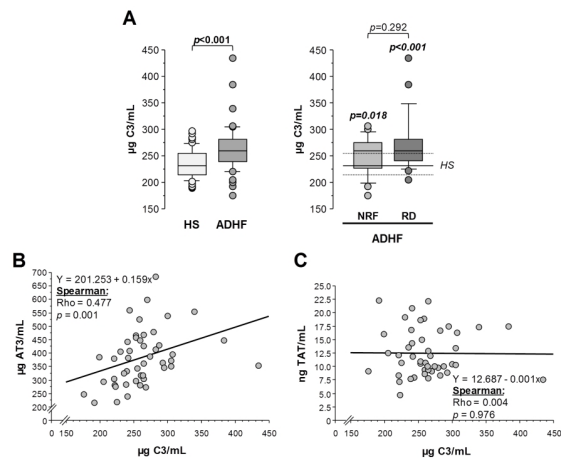


Figure 3: Plasma levels of complement C3 (C3) at hospital admission. A) Plasma C3 levels of ADHF patients and healthy individuals (left), and plasma C3 levels according to renal function in ADHF patients (right). B) Correlation of plasma C3 and AT3 levels in ADHF patients at hospital admission. C) Correlation of C3 and TAT levels in ADHF patients at hospital admission.

190x274mm (284 x 284 DPI)

1
2
3
4
5
6
7
8
9
10
11
12
13
14
15
16
17
18
19
20
21
22
23
24
25
26
27
28
29
30
31
32
33
34
35
36
37
38
39
40
41
42
43
44
45
46
47
48
49
50
51
52
53
54
55
56
57
58
59
60

Figura 4

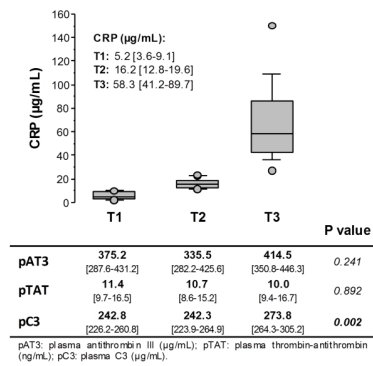


Figure 4: Plasma levels of C reactive protein (CRP) at hospital admission. Classification of pAT3, pTAT and pC3 according to plasma CRP tertiles.

190x274mm (284 x 284 DPI)

1
2
3
4
5
6
7
8
9
10
11
12
13
14
15
16
17
18
19
20
21
22
23
24
25
26
27
28
29
30
31
32
33
34
35
36
37
38
39
40
41
42
43
44
45
46
47
48
49
50
51
52
53
54
55
56
57
58
59
60

SUPPLEMENTARY MATERIAL

Association between Antithrombin III and Complement C3 in Acute Decompensated Heart Failure

Short title: Association of AT3 and C3 in ADHF

Elisa Diaz-Riera^{1,2}, Maísa García-Arguinzonis¹, Laura López³, Xavier Garcia-Moll^{3,4},
Lina Badimon^{1,4,5}, Teresa Padro^{1,4*}

¹Cardiovascular-Program ICCG; Research Institute – Hospital Santa Creu i Sant Pau, IIB-Sant Pau, Barcelona, Spain; ² Faculty of Medicine, University of Barcelona (UB), Barcelona, Spain; ³Cardiology Department, Hospital Santa Creu i Sant Pau, Barcelona, Spain; ⁴Centro de Investigación Biomédica en Red Cardiovascular (CIBERCV) Instituto de Salud Carlos III, Madrid, Spain; ⁵Cardiovascular Research Chair, UAB, Barcelona, Spain

Address for corresponding author (*):

Dr Teresa Padro
Cardiovascular-Program ICCG;
Research Institute Hospital Santa Creu i Sant Pau
Sant Antoni M^a Claret 167, 08025 Barcelona, Spain.
Phone: +34.935565886.
Fax: +34.935565559.
E-mail: tpadro@santpau.cat

Supplementary Table I: ADHF patients' medication at hospital admission.

	All patients N=67	NRF N=35	RD N=32	P value
BACKGROUND MEDICATION; N (%)				
Diuretics	49 (73)	21 (60)	28 (88)	0.014
Statins	43 (64)	18 (51)	25 (78)	0.040
Anticoagulants	27 (40)	14 (40)	13 (41)	>0.999
Antiplatelet agents	38 (57)	19 (54)	19 (59)	0.806
β-blockers	46 (69)	21 (60)	25 (78)	0.124
Antiarrhythmic agents	7 (10)	4 (11)	3 (9)	>0.999
Antidiabetics	27 (40)	8 (26)	19 (59)	0.003
Insulin	12 (18)	2 (6)	10 (31)	0.010
Oral antidiabetic agents	22 (33)	8 (23)	14 (44)	0.117
ACE inhibitor/ARB	43 (66)	26 (74)	17 (57)	0.189

P values of categorical variables were calculated with Fisher exact test. Diuretics: hydrochlorothiazide, furosemide, eplerenone, and spironolactone. Statins: atorvastatin, pravastatin, simvastatin, ezetimibe. Anticoagulants: warfarin, acenocumarol, bempiparin, heparin, dabigatran, rivaroxaban, edoxaban, and apixaban. Antiplatelet agents: acetylsalicylic acid and clopidogrel. Beta-blockers: bisoprolol and carvedilol. Antiarrhythmic agents: amiodarone. Oral antidiabetic agents: metformin and repaglinide. Angiotensin-converting enzyme inhibitors (ACEI) include: captopril, enalapril, and ramipril. Angiotensin receptor blockers (ARB): losartan, olmesartan, and valsartan.

Supplementary Table II: Plasma levels of AT3, TAT, and C3 levels depending on patients' risk factors.

	All ADHF patients			
	N	pAT3 Median [IQR]	pTAT Median [IQR]	pC3 Median [IQR]
Sex				
Male	45	354.6 [305.0-466.9]	10.7 [8.6-15.0]	259.5 [239.1-278.8]
Female	22	382.2 [303.6-414.5]	12.4 [10.3-16.2]	253.2 [238.7-282.4]
<i>P value</i>		0.957	0.171	0.868
LVEF				
Reduced ($\leq 40\%$)	29	316.7 [280.9-395.3] ^a	11.0 [9.2-15.2] ^b	259.2 [235.1-268.1] ^c
Mildly reduced (41-49%)	10	397.1 [360.8-514.9]	9.3 [7.9-12.4]	273.6 [241.2-293.8]
Preserved ($\geq 50\%$)	28	383.8 [333.9-446.8]	12.4 [10.0-17.3]	256.0 [239.1-287.3]
<i>P value</i>		0.078	0.122	0.657
Cardiovascular disease				
No	44	382.2 [305.0-465.7]	12.1 [10.0-16.0]	254.8 [235.1-273.8]
Yes	23	354.6 [283.5-409.3]	10.2 [8.4-12.7]	266.0 [241.2-299.2]
<i>P value</i>		0.347	0.074	0.278
Atrial fibrillation				
No	34	353.1 [294.2-446.3]	12.2 [8.5-15.9]	249.2 [230.3-278.8]
Yes	32	375.2 [310.9-444.1]	11.2 [10.0-15.8]	262.6 [241.4-290.1]
<i>P value</i>		0.865	0.789	0.281
Arterial hypertension				
No	17	379.6 [333.9-395.3]	12.0 [9.3-16.1]	243.7 [238.7-263.9]
Yes	49	364.0 [294.2-456.7]	11.5 [7.3-15.5]	262.0 [240.9-282.4]
<i>P value</i>		0.899	0.847	0.307
Dyslipidaemia				
No	20	345.8 [316.6-405.6]	11.9 [8.8-16.8]	241.9 [238.9-254.8]
Yes	46	379.6 [303.6-466.9]	11.6 [9.3-15.8]	264.5 [240.9-282.4]
<i>P value</i>		0.291	0.663	0.096
Diabetes mellitus type II				
No	36	362.4 [310.1-410.1]	12.0 [9.4-16.2]	247.6 [227.7-264.9]
Yes	30	390.1 [300.2-472.9]	10.6 [8.5-14.8]	268.1 [253.1-305.1]
<i>P value</i>		0.296	0.351	0.015
Pulmonary hypertension				
No	51	362.4 [295.3-428.4]	11.3 [9.1-15.8]	260.2 [240.9-282.4]
Yes	16	392.6 [316.6-456.7]	12.4 [14.5-15.5]	247.1 [230.3-263.9]
<i>P value</i>		0.594	0.399	0.194

Plasma levels of AT3 and C3 in $\mu\text{g/mL}$, plasma levels of TAT in ng/mL . LVEF: left ventricular ejection fraction. P values were calculated by Mann-Whitney test except for LVEF where Kruskal-Wallis test was used. Information of one patient was missing for hypertension, dyslipidaemia, and diabetes mellitus type 2. ^{a,b,c} Comparison reduced vs preserved LVEF (Mann-Whitney), ^a P=0.082, ^b P=0.336, ^c P=0.734.

Supplementary Table III: ROC (associated receiver operating characteristic) curve analysis for determining discriminatory power of plasma AT3 and C3 for LVEF classification in ADHF patients at hospital admission.

LVEF \leq 40% vs >40%	
pAT3	
Area	0.687
95% CI	0.522-0.852
<i>P value</i>	0.026
pTAT	
Area	0.511
95% CI	0.367-0.656
<i>P value</i>	0.879
pC3	
Area	0.559
95% CI	0.391-0.727
<i>P value</i>	0.493

pAT3: plasma antithrombin III; pTAT: plasma thrombin-antithrombin complex; pC3: plasma complement C3; CI: confidence interval

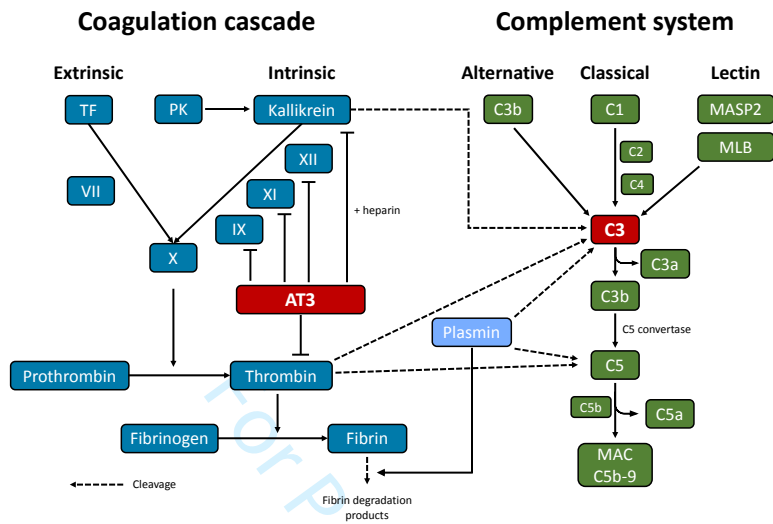
pAT3: plasma antithrombin III; pC3: plasma complement C3; CI: confidence interval

Supplementary Table IV: Plasma levels of AT3, TAT, and C3 levels depending on patients medication.

All ADHF patients	pAT3		pTAT	pC3
	N	Median [IQR]	Median [IQR]	Median [IQR]
Diuretics				
No	18	379.6 [325.2-414.5]	10.2 [8.4-13.6]	264.7 [235.1-287.3]
Yes	49	354.6 [303.6-446.3]	12.1 [9.8-16.0]	256.7 [240.9-269.7]
<i>P value</i>		0.754	0.121	0.568
Statins				
No	24	351.5 [294.3-416.5]	12.4 [9.3-15.5]	248.4 [236.9-264.8]
Yes	43	375.2 [310.1-451.5]	10.9 [9.2-15.8]	260.2 [240.9-287.3]
<i>P value</i>		0.406	0.686	0.281
Anticoagulants				
No	40	375.2 [310.8-451.5]	11.5 [8.9-15.0]	259.2 [235.1-282.4]
Yes	27	362.4 [284.9-435.1]	11.9 [9.4-16.0]	259.2 [240.9-271.7]
<i>P value</i>		0.462	0.565	0.779
Antiplatelet agents				
No	29	380.9 [300.2-435.1]	12.4 [10.0-16.8]	253.3 [234.5-267.4]
Yes	38	359.3 [310.1-451.5]	10.8 [8.6-12.9]	264.3 [243.6-292.9]
<i>P value</i>		0.869	0.078	0.160
Beta-blockers				
No	21	342.2 [274.4-405.6]	11.8 [9.7-15.9]	238.7 [221.3-273.8]
Yes	46	370.8 [325.2-446.3]	10.9 [8.9-15.8]	264.1 [243.7-282.4]
<i>P value</i>		0.165	0.637	0.065
Antiarrhythmic agents				
No	60	354.6 [295.3-428.4]	11.9 [9.4-15.8]	254.1 [235.1-278.8]
Yes	7	446.3 [364.0-538.9]	9.4 [8.8-15.8]	269.7 [265.1-292.9]
<i>P value</i>		0.076	0.512	0.091
Antidiabetic agents				
No	40	345.8 [283.5-405.6]	11.9 [9.4-16.2]	253.2 [225.0-265.1]
Yes	27	428.4 [353.0-478.8]	10.5 [8.4-14.2]	280.6 [253.3-305.3]
<i>P value</i>		0.018	0.273	0.005
ACE inhibitor/ARB				
No	22	380.9 [345.8-446.3]	12.4 [9.4-16.7]	254.8 [238.7-292.9]
Yes	43	342.3 [288.1-435.1]	11.4 [9.2-14.9]	258.9 [237.1-268.9]
<i>P value</i>		0.251	0.606	0.468

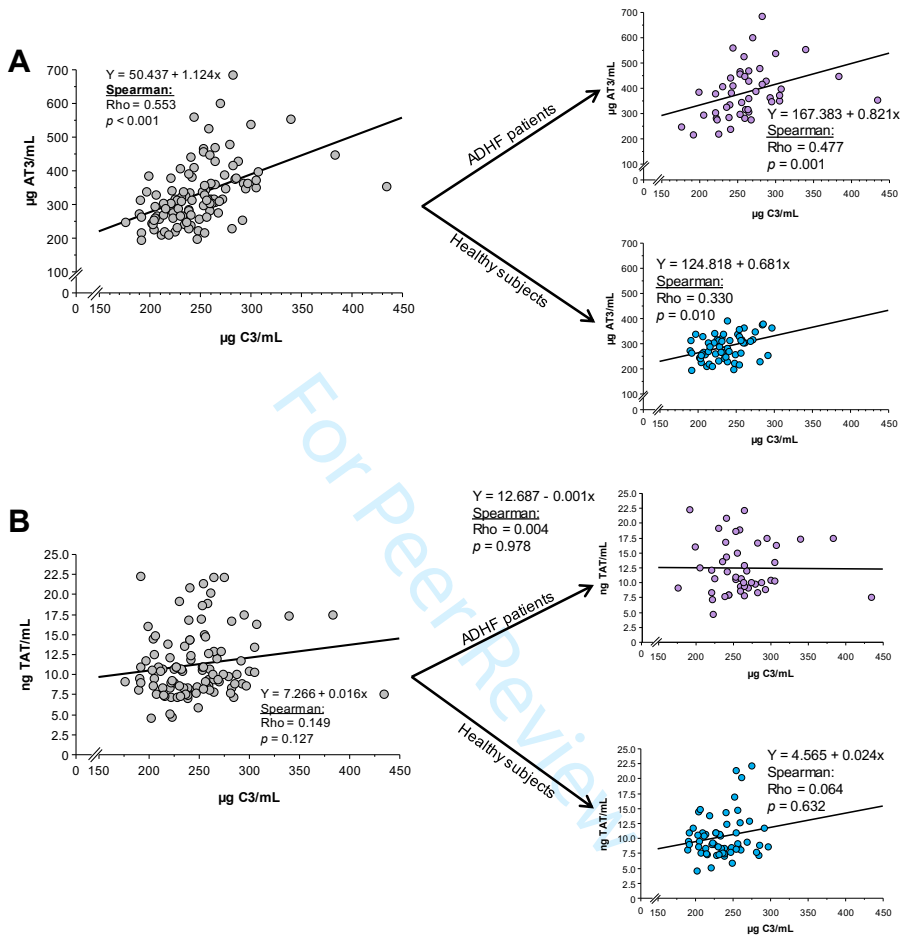
Plasma levels of AT3 and C3 in $\mu\text{g/mL}$, plasma levels of TAT in ng/mL . P values were calculated by Mann-Whitney. Diuretics: hydrochlorothiazide, furosemide, eplerenone, and spironolactone. Statins: atorvastatin, pravastatin, simvastatin, ezetimibe. Anticoagulants: warfarin, acenocumarol, bempiparin, heparin, dabigatran, rivaroxaban, edoxaban, and apixaban. Antiplatelet agents: acetylsalicylic acid and clopidogrel. Beta-blockers: bisoprolol and carvedilol. Antiarrhythmic agents: amiodarone. Oral antidiabetic agents: metformin and repaglinide. Angiotensin-converting enzyme inhibitors (ACEI) include: captopril, enalapril, and ramipril. Angiotensin receptor blockers (ARB): losartan, olmesartan, and valsartan.

1
2
3
4
5
6
7
8
9
10
11
12
13
14
15
16
17
18
19
20
21
22
23
24
25
26
27
28
29
30
31
32
33
34
35
36
37
38
39
40
41
42
43
44
45
46
47
48
49
50
51
52
53
54
55
56
57
58
59
60



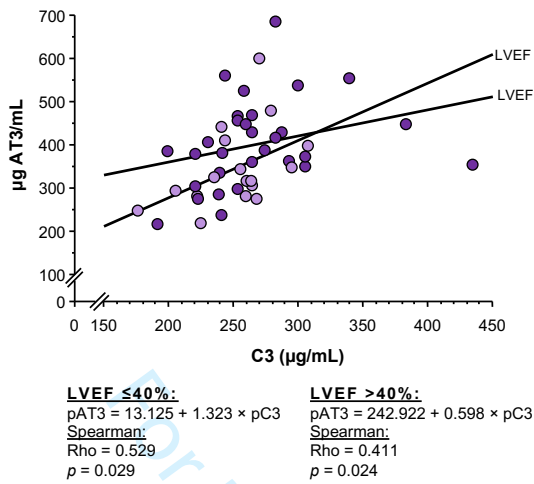
Supplementary Figure I: Coagulation cascade and C3 pathway.

1
2
3
4
5
6
7
8
9
10
11
12
13
14
15
16
17
18
19
20
21
22
23
24
25
26
27
28
29
30
31
32
33
34
35
36
37
38
39
40
41
42
43
44
45
46
47
48
49
50
51
52
53
54
55
56
57
58
59
60



Supplementary Figure II: Plasma C3 correlation with pAT3 and pTAT. A) Correlation between plasma C3 and plasma AT3 levels of the entire cohort (ADHF and HS) on the left, and separately on the right. **B)** Correlation between plasma C3 and plasma TAT levels of the entire cohort (ADHF and HS) on the left, and separately on the right.

1
2
3
4
5
6
7
8
9
10
11
12
13
14
15
16
17
18
19
20
21
22
23
24
25
26
27
28
29
30
31
32
33
34
35
36
37
38
39
40
41
42
43
44
45
46
47
48
49
50
51
52
53
54
55
56
57
58
59
60



Supplementary Figure III: Regression lines and Spearman correlation between plasma C3 and AT3 depending on heart function.

5.3. Article 3

VITAMIN D BINDING PROTEIN AND RENAL INJURY IN ACUTE DECOMPENSATED HEART FAILURE

Elisa Diaz-Riera; Maisa García Arguinzonis; Laura López; Xavier Garcia-Moll; Lina Badimon; Teresa Padro

Accepted: Frontiers in Cardiovascular Medicine

Front. Cardiovasc. Med. DOI: 10.3389/fcvm.2022.829490

Objective: To evaluate urinary levels of Vitamin D binding protein (VDBP) and its association with renal function and its potential use as a biomarker in kidney function deterioration in ADHF patients.

Highlights:

- VDBP was found elevated in urine of ADHF at hospital admission by 2DE-MS.
- When analysed by immunoassay, ADHF patients also presented high VDBP levels in urine.
- Urinary levels remained high in patients who developed kidney function deterioration, whereas they dropped to the healthy range in patients who maintained healthy renal function.
- The combination of urinary levels of VDBP, cystatin C and KIM-1 provided a significant ability to detect patients at high risk of developing kidney function deterioration.

30/4/22 18:51

Correu - EDiazR@santpau.cat

Frontiers: Your manuscript is accepted - 829490

cardiovascularmedicine.editorial.office@frontiersin.org

dc. 27/4/2022 16:37

Per a: Elisa Diaz Riera <EDiazR@santpau.cat>;

Dear Dr Diaz-Riera,

Frontiers in Cardiovascular Medicine has sent you a message. Please click 'Reply' to send a direct response

I am pleased to inform you that your manuscript "Vitamin D Binding Protein and renal injury in acute decompensated heart failure" has been approved for production and accepted for publication in Frontiers in Cardiovascular Medicine, section Heart Failure and Transplantation.

Proofs are being prepared for you to verify before publication. We will also perform final checks to ensure your manuscript meets our criteria for publication (<https://www.frontiersin.org/about/review-system#ManuscriptQualityStandards>).

The title, abstract and author(s) list you provided during submission is currently online and will be replaced with the final version when your article is published. Please do not communicate any changes until you receive your proofs.

Any questions? Please visit our Production Help Center page for more information: <https://zendesk.frontiersin.org/hc/en-us/categories/200397292-Article-Production->

You can click here to access the final review reports and manuscript: <http://www.frontiersin.org/Review/EnterReviewForum.aspx?activationno=f27b0c96-1314-4557-aeaf-afef1fa6e7cf>

As an author, it is important that you keep your Frontiers research network (Loop) profile up to date, so that you and your publications are more discoverable. You can update your profile pages (profile picture, short bio, list of publications) using this link: <https://loop.frontiersin.org/people/>

Best regards,

Your Frontiers in Cardiovascular Medicine team

Frontiers | Editorial Office - Collaborative Peer Review Team
www.frontiersin.org
35 New Broad Street
London - EC2M 1NH
Office T 41 21 510 1725

For technical issues, please contact our IT Helpdesk (support@frontiersin.org) or visit our Frontiers Help Center (zendesk.frontiersin.org/hc/en-us)

We want to hear about your experience with Frontiers.

We are constantly striving to improve our peer review process, please complete our short 3-minute survey to tell us about your experience, your opinion is important and will guide future development.

https://frontiersin.qualtrics.com/jfe/form/SV_aW5zUzZO1ZbOKO6?survey=authorapproved&ArticleId=829490&UserId=1579570&FinalDecision=Accepted

Thank you very much for taking the time to share your thoughts.

Manuscript title: Vitamin D Binding Protein and renal injury in acute decompensated heart failure
Journal: Frontiers in Cardiovascular Medicine, section Heart Failure and Transplantation
Article type: Original Research
Authors: Elisa Diaz-Riera, Maisa García-Arguinzonis, Laura Lopez, Xavier Garcia-Moll, Lina Badimon, Teresa Padro
Manuscript ID: 829490
Edited by: Ernesto Martinez-Martinez

<https://correuhsp.santpau.cat/owa/#path=/mail/inbox>

1/1

Vitamin D Binding Protein and renal injury in acute decompensated heart failure

Elisa Diaz-Riera^{1, 2}, Maisa García-Arguinzonis¹, Laura Lopez³, Xavier Garcia-Moll^{3, 4}, Lina Badimon^{1, 4, 5}, Teresa Padro^{1, 4*}

¹Cardiovascular Program-ICCC, Institut de Recerca de l'Hospital de la Santa Creu i Sant Pau, Spain, ²Facultat de Medicina, University of Barcelona, Spain, ³Servicio de Cardiología, Hospital de la Santa Creu i Sant Pau, Spain, ⁴Centro de Investigación Biomédica en Red en Enfermedades Cardiovasculares (CIBERCV), Spain, ⁵Cardiovascular Research Chair, Universitat Autònoma de Barcelona, Spain

Submitted to Journal:
Frontiers in Cardiovascular Medicine

Specialty Section:
Heart Failure and Transplantation

Article type:
Original Research Article

Manuscript ID:
829490

Received on:
05 Dec 2021

Revised on:
22 Apr 2022

Journal website link:
www.frontiersin.org

Conflict of interest statement

The authors declare that the research was conducted in the absence of any commercial or financial relationships that could be construed as a potential conflict of interest

Author contribution statement

XGM, LB and TP: study concept and design. LL, XGM: patient inclusion, data and sample acquisition. ED-R, MG-A, TP: methodology, formal analysis. ED-R, LB, TP: statistical analysis and result interpretation. ED-R, LB, TP: writing—original draft preparation. ED-R, MG-A, LL, XGM, LB, TP: review and editing. LB and TP: funding acquisition. All authors have read and agreed to the published version of the manuscript.

Keywords

renal dysfunction, Vitamin D binding protein (Gc), Urine sample analysis, Heart Failure, Proteomics, two dimension electrophoresis - MS/MS

Abstract

Word count: 308

Background: Renal function in acute decompensated heart failure (ADHF) is strong predictor of disease evolution and poor outcome. Current biomarkers for early diagnostic of renal injury in the setting of ADHF are still controversial and their association to early pathological changes needs to be established. By applying a proteomic approach, we aimed to identify early changes in the differential urine protein signature associated with development of renal injury in patients hospitalised due to ADHF.

Material and methods: Patients (71 [64-77] years old) admitted at the emergency room with ADHF and hospitalised were investigated (N=64). Samples (urine/serum) were collected at hospital admission (day 0) and 72 hours later (day 3). Differential serum proteome was analysed by two-dimensional electrophoresis and MALDI-ToF/ToF. Validation studies were performed by ELISA. **Results:** Proteomic analysis depicted urinary vitamin D binding protein (uVDBP) as a two spots protein with increased intensity in ADHF and significant differences depending on the glomerular filtration rate (GFR). Urinary VDBP in ADHF patients at hospitalisation was >3fold higher than in healthy subjects, with the highest levels in those ADHF patients already presenting renal dysfunction. At day 3, urine VDBP levels in patients maintaining normal renal function dropped to normal values (P=0.03 vs day 0). In contrast, urine VDBP levels remained elevated in the group developing renal injury, with values 2fold above the normal range (P<0.05), while serum creatinine and GF levels were within the physiological range in this group. Urinary VDBP in ADHF positively correlated with markers of renal injury such as cystatin C and KIM-1 (Kidney Injury Molecule 1). By ROC-analysis, urinary VDBP, when added to cystatin C and KIM-1, improved the prediction of renal injury in ADHF patients.

Conclusions: We showed increased urine VDBP in ADHF patients at hospital admission and a differential uVDBP evolution pattern at early stage of renal dysfunction, before pathological worsening of GFR is evidenced.

Contribution to the field

Worsening renal function in the treatment of acute decompensated heart failure (ADHF) associates with adverse outcomes and longer hospital stays. There is a growing consensus about the poor effectiveness of serum creatinine measurement to detect initial stages of renal damage and the urgent need of more reliable biological variables for early detection of acute kidney injury in ADHF patients during hospitalisation. • By a mass spectrometry-based protein discovery study, we identify an elevated urinary loss of Vitamin D Binding Protein (VDBP), the main carrier of vitamin D, in the urine of patients hospitalised with acute decompensated heart failure (ADHF). • High levels of urinary VDBP loss at 72 hours hospitalisation associate with early stages of renal injury at the time that plasma creatinine and glomerular filtration rate are still found within the normal physiological range. • As indicated by the C-statistics, the logistic regression model obtained by adding urinary VDBP to Cystatin C and KIM-1 levels improves discrimination of ADHF patients at high risk of presenting renal injury before hospital discharge.

Funding statement

This work was supported by the “Fundació La Marató TV3” (Project number 20153110) to T.P., and the Spanish “Agencia Estatal de Investigación (AEI)” - Institute of Health Carlos III, ISCIII [FIS PI19/01687 to T.P, Centro de Investigación Biomedica en Red Cardiovascular (CIBERCV-CB16/11/00411) to LB, Red Terapia Celular TerCel- RD16/0011/0018 to LB, CIBERCV to LB; Spanish Ministry of Economy and Competitiveness of Science- PID2019-107160RB-I00 to LB]; and cofounded by FEDER “Una Manera de Hacer Europa”. Secretaria de Universitats i Recerca del Departament d'Empresa i Coneixement de la Generalitat de Catalunya [2017 SGR 1480]. We thank Fundación Jesús Serra and Fundación de Investigación Cardiovascular, Barcelona, for their continuous support.

Ethics statements***Studies involving animal subjects***

Generated Statement: No animal studies are presented in this manuscript.

Studies involving human subjects

Generated Statement: The studies involving human participants were reviewed and approved by Accepted by the Ethical Committee for clinical research from Hospital Santa Cruz y San Pablo in March 2016 (ref number 16/022). The patients/participants provided their written informed consent to participate in this study.

Inclusion of identifiable human data

Generated Statement: No potentially identifiable human images or data is presented in this study.

Data availability statement

Generated Statement: The raw data supporting the conclusions of this article will be made available by the authors, without undue reservation.

In review



Vitamin D Binding Protein and renal injury in acute decompensated heart failure

1 **Elisa Diaz-Riera**^{1,2}; **Maisa García-Arguinzonis**¹, **Laura López**³, **Xavier Garcia-Moll**^{3,4}, **Lina**
2 **Badimon L**^{1,4,5}, **Padró, T**^{1,4*}

3 ¹Cardiovascular-Program ICCC; Research Institute – Hospital Santa Creu i Sant Pau, IIB-Sant Pau,
4 Barcelona, Spain

5 ²Faculty of Medicine, University of Barcelona (UB), 08036 Barcelona, Spain

6 ³Cardiology Department, Hospital Santa Creu i Sant Pau, Barcelona, Spain

7 ⁴Centro de Investigación Biomédica en Red Cardiovascular (CIBERCV) Instituto de Salud Carlos
8 III, Madrid, Spain; ⁵Cardiovascular Research Chair, UAB, Barcelona, Spain

9

10 * **Correspondence:** Dr Teresa Padro; email: tpadro@santpau.cat; Cardiovascular Program-ICCC,
11 Research Institute Hospital Santa Creu i Sant Pau, Sant Antoni M^a Claret 167, 08025 Barcelona,
12 Spain, Phone: +34 935565886, Fax: +34 935565559.

13

14 **Keywords:** Acute decompensated heart failure; renal dysfunction; proteomics; VDBP; kidney injury
15 associated proteins

16

17

18 **Abstract**

19 **Background:** Renal function in acute decompensated heart failure (ADHF) is strong predictor of
20 disease evolution and poor outcome. Current biomarkers for early diagnostic of renal injury in the
21 setting of ADHF are still controversial and their association to early pathological changes needs to be
22 established. By applying a proteomic approach, we aimed to identify early changes in the differential
23 urine protein signature associated with development of renal injury in patients hospitalised due to
24 ADHF.

25 **Material and methods:** Patients (71 [64-77] years old) admitted at the emergency room with ADHF
26 and hospitalised were investigated (N=64). Samples (urine/serum) were collected at hospital
27 admission (day 0) and 72 hours later (day 3). Differential serum proteome was analysed by two-
28 dimensional electrophoresis and MALDI-ToF/ToF. Validation studies were performed by ELISA.

29 **Results:** Proteomic analysis depicted urinary vitamin D binding protein (uVDBP) as a two spots
30 protein with increased intensity in ADHF and significant differences depending on the glomerular
31 filtration rate (GFR). Urinary VDBP in ADHF patients at hospitalisation was >3fold higher than in

VDBP and Acute Heart Failure

32 healthy subjects, with the highest levels in those ADHF patients already presenting renal dysfunction.
33 At day 3, urine VDBP levels in patients maintaining normal renal function dropped to normal values
34 ($P=0.03$ vs day 0). In contrast, urine VDBP levels remained elevated in the group developing renal
35 injury, with values 2fold above the normal range ($P<0.05$), while serum creatinine and GF levels
36 were within the physiological range in this group. Urinary VDBP in ADHF positively correlated with
37 markers of renal injury such as cystatin C and KIM-1 (Kidney Injury Molecule 1). By ROC-analysis,
38 urinary VDBP, when added to cystatin C and KIM-1, improved the prediction of renal injury in
39 ADHF patients.

40 **Conclusions:** We showed increased urine VDBP in ADHF patients at hospital admission and a
41 differential uVDBP evolution pattern at early stage of renal dysfunction, before pathological
42 worsening of GFR is evidenced.

43

44

45 1 Introduction

46 Renal insufficiency is present as comorbidity in nearly a quarter of patients hospitalised due to acute
47 decompensated heart failure (ADHF) (1,2) and the evolution of renal function has prognostic
48 relevance in these patients (2). Indeed, ADHF is frequently complicated by acute kidney injury
49 during hospitalisation (2,3), which is associated with adverse outcomes and longer hospital stays
50 (2,4,5). In this respect, a recent meta-analysis indicated that all-cause mortality increased
51 significantly in ADHF patients with compared to those without acute kidney injury (5). The complex
52 relationship between heart failure and renal dysfunction may result of a combination of hormonal,
53 hemodynamic, inflammatory factors (6) and aggressive decongestive treatment (7). In turn, kidneys
54 are responsible for sodium homeostasis playing a key role to control intravascular and interstitial
55 fluid accumulation (congestion) in heart failure (8). Until now, however, the mechanisms
56 participating in the cardiorenal axis pathology need to be better understood, and the early differential
57 protein pattern associated to these processes remains to be identified.

58 Deterioration of kidney function is frequently recognised by the rise of serum creatinine levels, or by
59 the decline of glomerular filtration rate (GFR). However, creatinine levels can also be influenced by
60 several factors such as advanced age, sex, excessive protein intake, muscle mass, medication, or
61 intense exercise (9). Nowadays, early changes in other molecular components have been suggested
62 including kidney injury molecule 1 (KIM-1), Cystatin C (CysC) or neutrophil gelatinase-associated
63 lipocalin (NGAL) (10–13), but their usefulness for detecting early pathological changes is
64 controversial and their value has not been consistently proven (14,15). Therefore, identification of
65 molecular components that accurately facilitate early detection of renal injury and may contribute to
66 a better stratification of patients with ADHF and enhance their management remains a medical
67 challenge.

68 Over the last decade, urinary proteome has become a potential source of novel disease molecular
69 patterns and urinary proteomic analysis in heart failure has been used to identify the differential
70 expression profile associated to earlier diagnosis of the disease (16–18) and to establish diagnostic
71 classifiers in heart failure patients with specific disease conditions (19).

72 In this study we applied a mass spectrometry-based protein discovery approach (20,21) aimed to
73 identify urinary proteins associated to renal dysfunction in hospitalised ADHF patients. By

VDBP and Acute Heart Failure

74 proteomics, we have identified significant changes in Vitamin D Binding Protein (VDBP), a member
75 of the albumin superfamily of binding proteins that is produced in the liver, filtered through the
76 glomerulus as a complex with vitamin D3 (25[OH]D3) and actively reabsorbed in the proximal
77 tubule cells (22,23).

78 Anomalous urinary loss of VDBP, due to impaired proximal tubular reabsorption, has been reported
79 in the setting of renal damage in preclinical studies and metabolic-disease related nephropathies in
80 humans (24,25). In this hypothesis-generating study, we analysed urinary VDBP levels in association
81 with renal function in ADHF patients during the first 72 hour hospitalisation after an acute event to
82 investigate the value of VDBP to provide accurate pathophysiologic information on **kidney function**
83 **deterioration** in ADHF before creatinine levels rise.

84

85 2 Materials and Methods

86 2.1 Study population and study design

87 This study refers to patients with acute decompensated heart failure that were hospitalised in Hospital
88 de la Santa Creu i Sant Pau (HSCSP), in Barcelona, between February 2017 and March 2020.
89 Hospitalised ADHF patients were distributed in two different groups depending on their kidney
90 function at admission. Renal function was shown as MDRD-4 ($\text{mL}/\text{min}/1.73\text{m}^2$), a serum creatinine-
91 based estimation obtained using clinical data of the patients. Levels below $60\text{mL}/\text{min}/1.73\text{m}^2$ were
92 considered pathological. Two groups were formed: I) ADHF patients with renal dysfunction at
93 hospital admission (RD) and II) ADHF patients with normal renal function at hospital admission
94 (NRF). From this latter NRF group, two further subgroups were made based on the evolution of the
95 renal function during hospitalisation. Patients who developed **renal function deterioration to**
96 **pathological levels (RI-Group; $\text{MDRD-4} < 60\text{mL}/\text{min}/1.73\text{m}^2$)** and those who maintained normal
97 renal function (noRI). A group of healthy subjects (HS, N=13, 50 [37-63] years) was used to
98 establish the normal range in urine of the identified proteins (**Figure 1**).

99 The Ethics Committee of the Santa Creu i Sant Pau Hospital in Barcelona, Spain approved this study
100 and it was performed according to principles of Helsinki's Declaration. All patients signed an
101 informed consent prior being included in the study. Patients under chemotherapy, pregnancy or post-
102 delivery ischemic heart syndrome in women, and other causes of acute episode (myocardial
103 infarction, myocarditis, or toxic aetiology) were excluded from the study. Medication was not
104 considered as exclusion criteria except those required in oncological treatment (who were already
105 excluded).

106 2.2 Biological samples

107 Urine and blood samples were collected at hospital admission and at day 3 of hospitalisation, **when**
108 **patients no longer showed signs of dehydration due to the acute event. Samples at hospital**
109 **admission were collected as soon as possible after hospitalisation.** Urine obtained at 72h refers to
110 the first urine in the morning and blood extraction. Blood extraction at day 3 was performed at the
111 same time of urine collection. All samples were processed identically and within 30 minutes after
112 obtention. Protease inhibitors (cOmplete Mini, Roche, Basel, Switzerland) were added to urine
113 samples at collection. Urine samples were centrifuged (1200g, 10 min, room temperature) to
114 precipitate debris, aliquoted and stored at -80°C until further analysis. Level of total protein in urine

VDBP and Acute Heart Failure

115 were analysed in a Clima MC-15 analyser using the specific Gernon kit (RAL S.A., Barcelona,
116 Spain), as described by the providers.

117 Serum was obtained after maintaining blood samples 30 min at 37°C followed by 30 min at 4°C.
118 Thereafter, samples were centrifuged at 1800g (30 min, 4°C), aliquoted and stored at -80°C until
119 analysed.

120 Blood creatinine (Jaffe reaction), NT-proBNP (electroquimioluminescence), urea (kinetic urease),
121 and haemoglobin were analysed by standard laboratory methods as part of the patients' routine
122 analyses. Glomerular filtrate was calculated using the MDRD-4 algorithm that includes patient's
123 plasma creatinine levels, age, sex, and race (26). Total protein and creatinine in urine were analysed
124 in a Clima MC-15 analyser using Gernon kits for creatinine and total protein (RAL S.A., Barcelona,
125 Spain).

126 Urine samples for the HS reference group were collected in the morning and samples were processed
127 as described for the ADHF patients.

128 2.3 2DE electrophoresis and mass spectrometry

129 Analysis of differential protein patterns was performed by a proteomic approach using two-
130 dimensional electrophoresis (2DE) followed by mass-spectrometry for protein identification, as
131 previously described (27).

132 Urine samples (4mL) of ADHF patients and healthy controls were concentrated and desalted by
133 centrifugation (3220g, 30 min, and 10°C) using 3kDa cut-off filter devices (Amicon Ultra-4,
134 Millipore, Burlington, MA, USA) and 100mM Tris-HCl, pH 7.6. A final volume of 1mL was
135 obtained and depleted of albumin and IgGs using the ProteoExtract Albumin/IgG Removal Kit
136 (Calbiochem, San Diego, CA, USA), as reported by the providers. Thereafter, sample buffer was
137 exchanged to a urea-containing buffer (7M urea, 2M thiourea, 2% CHAPS), by centrifugation with
138 the 3 kDa cut-off filter devices (3220g, at room temperature) until a final volume of 400 µl was
139 obtained. Protein concentration in urine extracts was measured with 2D-Quant Kit (GE Healthcare,
140 Chicago, IL, USA) and 100 µg total protein aliquots were prepared.

141 A 100 µg aliquot was used to perform the individual 2DE analytical gels and 300 µg for the
142 preparative gels (pool from five representative samples), which refer to, approximately, 1 mL and
143 3ml, respectively, of original urine samples. Each aliquot of the urea/thiourea/chaps urine extracts
144 was applied to 17 cm dry strips (ReadyStrips IPG strips, pH 4–7 linear range; BioRad, San Diego,
145 CA, USA), using the PROTEAN i12 IEF system (Bio-Rad, San Diego, CA, USA) for the first
146 dimension, as previously described in our group (28,29). The second dimension was resolved in 12%
147 SDS-PAGE. Gels were fixed for two hours (40% ethanol, 10% acetic acid), developed with
148 Flamingo (Bio-Rad, San Diego, CA, USA) for protein fluorescent staining. Protein spot
149 quantification and analysis for differences between gels was performed using PDQuest analysis
150 software (Bio-Rad, San Diego, CA, USA). Each spot was assigned a relative value (AU) that
151 corresponds to the single spot volume compared to the volume of all spots in the gel, following
152 background extraction and normalisation between gels, as previously reported (28). This software
153 specifically analyses differences in protein patterns, in which a master gel is created wherein all gels
154 are included and used to compare with each individual sample.

155 Proteins were identified after in-gel tryptic digestion and extraction of peptides from the gel pieces by
156 matrix-assisted laser desorption/ionisation time-of-flight (MALDI-TOF) using an AutoFlex III Smart

VDBP and Acute Heart Failure

157 beam MALDI-TOF/TOF (BrukerDaltonics, Billerica, MA, USA), as previously described (28).
158 Samples and calibrants were mixed 1:1 with alpha-Cyano-4-hydroxycinnamic acid (HCCA) matrix
159 (0.7mg/mL) and were applied to Anchor Chip plates (BrukerDaltonics, Billerica, MA, USA).

160 Spectra were acquired with flexControl on reflectron mode, (mass range m/z 850–4,000; reflectron 1,
161 21.06 kV; reflectron 2, 9.77 kV; ion source 1 voltage, 19 kV; ion source 2, 16.5kV; detection gain,
162 $2.37\times$) with an average of 3,500 added shots at a frequency of 200 Hz. Samples processed with
163 flexAnalysis (version 3.0, Bruker Daltonics, Billerica, MA, USA) considering a signal-to-noise ratio
164 >3 , applying statistical calibration, and eliminating background peaks. After processing, spectra were
165 sent to the interface BioTools (version 3.2, Bruker Daltonics, Billerica, MA, USA), and MASCOT
166 search on Swiss-Prot 57.15 database was done [taxonomy, Homo sapiens; mass tolerance, 50 to 100;
167 up to two trypsin miss cleavages; global modification: carbamidomethyl (C); variable modification:
168 oxidation (M)]. Identification was carried out by peptide mass fingerprinting (PMF) where a
169 MASCOT scores >56 and at least five matched peptides was accepted. Confirmation of identified
170 protein was performed by peptide fragmentation working on the LIFT mode (MS/MS) (27,28).

171 2.4 Western Blot

172 Urinary protein extracts were resolved by 1-DE under reducing conditions and electrotransferred to
173 nitrocellulose membranes. Urinary VDBP detection was performed using a rabbit monoclonal
174 antibody (ab81307, 1:5000 in 5% NFDN-TBST, Abcam, Cambridge, UK). Band detection was
175 performed using chemiluminescent SuperSignal (FischerScientific, Waltham, MA, USA) and a
176 molecular imager ChemiDoc XRS System, Universal Hood II (BioRad, San Diego, CA, USA).

177 2.5 Immunoassays

178 VDBP was analysed in urine and serum samples using Human Vitamin D BP Quantikine ELISA kit
179 (DVDBP0B, R&D Systems, Minneapolis, MN, USA) with a sensitivity of 0.338 ng/mL, and with
180 intra-assay variability $<2.5\%$ and variability $<7\%$ in inter-assay trials. Urinary Cystatin C (uCysC)
181 levels were analysed using Human Cystatin C ELISA kit from Biovendo (RD191009100,
182 Biovendo, Brno, Czech Republic), with a sensitivity of 0.25 ng/mL, intra-assay variability $<4\%$, and
183 with inter-assay variability $<11\%$. Urinary KIM-1 levels were analysed using Human KIM1 ELISA
184 Kit (ab235081, Abcam, Cambridge, UK) with a sensitivity of 1.28pg/mL, and with intra-assay
185 variability $<3\%$ and inter-assay variability $<7\%$. Each immunoassay was performed according to the
186 providers' protocol. **Concentrations of the proteins in urine were expressed per total protein
187 content in the same sample to correct for difference in total protein concentration.**

188 2.6 Statistical analysis

189 Data are expressed as median \pm interquartile range (IQR). N indicates the number of subjects tested.
190 The normal distribution was determined via Kolmogorov-Smirnov test. Statistic differences between
191 groups for non-normally distributed continuous variables were analysed by non-parametric tests,
192 including Mann-Whitney or Kruskal-Wallis tests. Frequencies of categorical variables were
193 compared by Chi-square analyses. Correlations between variables were determined using single
194 regression models and Spearman rank correlation. Wilcoxon Signed Rank test was used to compare
195 each patient evolution. Due to the exploratory character of this proteomic study, determination of the
196 sample size was based on past experience with similar studies (28). Data of ADHF patients at
197 hospital admission obtained from the proteomic studies served to check sample size in the validation
198 quantitative analysis (ELISA method). Minimal required sample size was calculated and validated
199 using the JavaScript based method for simple power and sample size calculation when two

VDBP and Acute Heart Failure

200 independent groups are compared, provided in <http://www.stat.ubc.ca/~rollin/stats/ssize/n2.html> (28).
201 Based on the median value of ADHF patients at hospitalisation the pooled interquartile range of the
202 studied population, our sample size gave a study power of >0.75 (type I error = 0.05, two-sided test).
203 Receiver operating characteristic (ROC) curve analyses was used to calculate the area under the
204 curve for each variable along with its 95% CI and to determine the power to discriminate renal
205 function deterioration. Statistical analysis was performed using Stata v15 and SPSS v26. A P value
206 ≤0.05 was considered statistically significant.

207

208 3 Results

209 3.1 Clinical characteristics of the ADHF patient population

210 Baseline demographic, clinical characteristics and background medication of the studied population
211 are given in **Table 1**. Briefly, this refers to 64 ADHF patients with median age of 71 [64-77] years
212 and with 68% males, who were hospitalised at Hospital de la Santa Creu i Sant Pau (HSCSP), in
213 Barcelona. At the time of hospitalisation, 47% of ADHF patients presented pathological GFR levels
214 (RD group; MDRD-4: 41.1 [30.7-45.3] mL/min/1.73m², P<0.001,) while the other 53% of ADHF
215 (NRF group) presented GFR levels within the normal range with MDRD-4 >60 mL/min/1.73m²
216 (82.3 [69.0-98.3] mL/min/1.73m²). Thirty-eight per cent of ADHF patients within the NRF group
217 (normal kidney function at hospital admission) **showed renal function deterioration with GFR**
218 **values below the pathological cut-off (60ml/min/1.73m²), which referred to a mean increase of**
219 **45% of serum creatinine, after day 5 of hospitalisation (Group RI; see Figure 1).**

220 All ADHF patients had plasma NT-proBNP values above the pathological cut-off (1.8 µg/L), being
221 levels in the RD group significantly higher than those in the NRF group (5.2 [3.0-14.7] µg/L vs 3.4
222 [1.9-6.4] ng/L, P=0.022). Forty-two per cent of ADHF patients had reduced left ventricular ejection
223 fraction (LVEF; 32 [21-35]%), and 42% had a LVEF above 50% (60 [56-61]%) at admission. The
224 remaining group of patients (16%) presented mid-range LVEF, with values between 40-49% (46 [44-
225 47]%). Mean hospitalisation time was 10.8±5.3 days for all patients, however a longer trend was
226 observed in the subgroup of patients developing RI compared with those who maintained normal
227 renal function (12 [9-17] days; 9 [7-11] days, respectively, P=0.075).

228 **Regarding medication, 73% of our study group were already under diuretic treatment before**
229 **hospital admission. Upon hospitalisation due to ADHF, patients are given intravenous**
230 **furosemide (dosage depending on their clinical condition, prior diuretic dosage and renal**
231 **function) until stabilisation for decongestion. Afterwards, patients were administered**
232 **furosemide orally, and complemented with other diuretics if needed, and the dose was**
233 **dependent on the patients' condition and response to avoid increases in serum creatinine.**

234 A representative subgroup of 17 ADHF patients (76% male, 72 [69-76] years old), with renal
235 dysfunction (RD, N=5) and with normal renal function (NRF, N=12) at hospitalisation was used for
236 proteomic studies in an initial discovery phase. Demographic and clinical characteristics of this
237 subgroup are given in (**Supplementary Table I**).

238

239 3.2 Urine differential proteomic profile in ADHF patients

This is a provisional file, not the final typeset article

VDBP and Acute Heart Failure

240 The urinary proteome of ADHF patients at hospital admission was compared to a healthy control
 241 group in the discovery phase. A total of 23 differential proteins were detected, with varying functions
 242 (cell signalling, cell metabolism, coagulation, acute phase response), as shown in **Supplementary**
 243 **Figure I**. Three differential proteins were associated to vitamin metabolism and identified as
 244 transthyretin (TTR, Swiss-Prot P02766, Mascot-score 61), retinol binding protein 4 (RBP4, Swiss-
 245 Prot P02753, Mascot-score 66), and Vitamin D Binding Protein (VDBP, Swiss-Prot P21614, Mascot-
 246 score 72) (**Supplementary Table II**)

247 VDBP in urine was identified by 2DE-MS/MS as two spots with pI within 5.25-5.30 and a molecular
 248 weight of 50.3 KDa (**Figure 2A**; and **Supplementary Figure II**). By Western Blot analysis, VDBP
 249 was found as a single band in urine samples of ADHF patients (**Figure 2B**). Comparing to healthy
 250 subjects, ADHF patients at hospital admission showed a 2fold higher urinary levels (ADHF, n=17,
 251 1.71 [0.87-2.55] AU vs 0.77 [0.66-0.98] AU of HS, n=6, P=0.042, **Figure 2C**). Within ADHF
 252 patients at hospitalisation, the RD group (n=5, 2.98 [1.71-4.66] AU) presented the highest values,
 253 these being 2fold higher than those of the NRF group (n=12, 1.58 [0.76-2.12] AU, P=0.058) (**Figure**
 254 **2D**).

255 While no differences were observed between patients depending on presence of atrial fibrillation
 256 (P=0.228), prior cardiovascular disease (P=0.428), hypertension (P=0.113), dyslipidaemia (P=0.833),
 257 or diabetes mellitus (DM2, P=0.228).

258

259 3.3 Increased levels of urinary VDBP in ADHF patients at hospital admission

260 In validation studies (N=64), ADHF patients presented significantly higher VDBP levels in urine
 261 (48.2 [13.0-100.8] ng/mg total protein) than those in the defined healthy range (12.6 [11.2-22.0]
 262 ng/mg total protein, P<0.01) when quantified by specific ELISA (**Figure 3A**). More specifically, the
 263 RD and NRF groups had median uVDBP levels (85.5 [17.7-171.7] ng/mg total protein and 38.8
 264 [10.2-76.0] ng/mg total protein, respectively) 6fold (P=0.001) and 3fold (P=0.072), respectively,
 265 above the median value of the defined healthy range. In addition, ADHF patients with pathological
 266 GFR levels at hospital admission (RD group) had higher VDBP loss in urine than those in the NRF
 267 group (P=0.012) (**Figure 3B**).

268 Urinary levels of VDBP (uVDBP) in ADHF patients at hospital admission (day 0) significantly
 269 correlated with NT-proBNP (Rho=0.337, P=0.019) and GFR (Rho=-0.379, P=0.005) in ADHF
 270 patients. In contrast, uVDBP did not associate with LVEF (Rho=0.013, P=0.924) and no differences
 271 were found in uVDBP levels between patients with reduced LVEF (<40%) and preserved LVEF
 272 (>50%, P=0.885). Moreover, the uVDBP levels did not differ significantly between patients with and
 273 without atrial fibrillation (P=0.337) or previous cardiovascular disease (P=0.437). To notice, levels of
 274 uVDBP were not affected by age (Rho=0.106, P=0.437) or sex (P=0.563) nor by common
 275 comorbidities such as hypertension (75%, P=0.0851), dyslipidaemia (70%, P=0.212, **Supplementary**
 276 **Table III**).

277 **VDBP has been previously studied within diabetic nephropathy. The 44% of the patients in the**
 278 **ADHF study population had diabetes, with a trend towards higher frequency of diabetes in the**
 279 **RD- compared to the NRF-group (P=0.079; Table 1).** However, uVDBP levels did not
 280 significantly differ between diabetic and non-diabetic patients (P=0.635), neither in the NRF-group
 281 (P=0.572) nor in the RD-group (P=0.594, see **Supplementary Table III**). **Furthermore, as shown**
 282 **in Supplementary Figure IV, diabetic patients were homogeneously distributed when the**

VDBP and Acute Heart Failure

283 population was divided in VDBP-tertiles. A similar pattern was observed when the groups with
284 normal- and reduced- renal function at hospital admission were separately considered (NRF-
285 group vs RD-group; χ^2 : P=0.789 for differences in the pattern distribution of diabetic patients).
286 Moreover, as summarised in **Supplementary Table IV**, urinary VDBP levels did not depend on
287 background medication, including statins, anticoagulant and antiplatelets, betablockers and ACE
288 inhibitors (P>0.05 between treated and non-treated patients for all medications)

289

290 3.4 VDBP levels at day 3 hospitalisation

291 The 38.2% of patients in the NRF group presented a worsening of renal function to pathological
292 values between day 5 hospitalisation and hospital discharge (RI group; N=13), whereas renal
293 function was not significantly affected in the remaining 61.8% of the patients in the NRF group
294 (noRI group; N=21), with GFR >60 mL/min/1.73m² (see **Figure 1**).

295 At day 3, as shown in **Figure 3B**, patients who did not develop renal injury (noRI group) during the
296 hospitalisation period showed a significant drop of uVDBP to values within the HS range (noRI-
297 group: 11.1 [5.7-21.2] ng/mg total protein at day 3; P=0.030 in comparison with values at day 0). In
298 contrast, uVDBP levels remained high and did not significantly differ from values at admission
299 (P=0.530) in those patients who were going to develop renal injury (RI group) before hospital
300 discharge. It is to notice, however, that patients in the RI-group still presented GFR levels within the
301 normal physiological range (68.1 [61.5-77.8] mL/min/1.73m²) at day 3 hospitalisation.

302 Patients in the RD group (GFR: 42.3 [31.6-52.4] mL/min/1.73m²) maintained elevated levels of
303 uVDBP (85.7 [22.0-173.9] ng/mg total protein) at day 3 with a median value >6fold higher than in
304 the noRI group (P=0.007; **Figure 3C**).

305 Analysis of sera samples obtained at day 3 hospitalisation did not show significant differences in
306 VDBP levels between noRI and RI groups (**Figure 4A**; P=0.603). Additionally, RD group did not
307 present different levels with noRI patients (P=0.660, **Figure 4A**) nor with RI patients (P=0.874,
308 **Figure 4A**). No correlation was found between urine and serum VDBP levels in ADHF patients
309 (Rho=0.020; P=0.879; **Figure 4B**). In addition, at day 3, no correlation was shown between GFR and
310 serum VDBP levels (Rho=0.060, P=0.657) in ADHF, whereas GFR significantly correlated with
311 VDBP levels in urine (Rho=-0.472, P=0.001) (**Supplementary Figure III**).

312

313 3.5 Urinary VDBP levels added to cystatin C and KIM-1 improved discrimination of ADHF 314 patients with renal deterioration during hospitalisation

315 Cystatin C and KIM-1 have been proposed to change during early renal injury (10,11,30). Cystatin C
316 in urine of ADHF patients negatively correlated with GFR at admission (Rho=-0.363; P=0.007) and
317 values were 2fold higher than those in the HS group (6.07 [2.34-11044] vs 3.90 [3.12-5.72] μ g/mg
318 total protein), although differences did not achieve statistical significance (P=0.189). At day 3
319 hospitalisation, urinary cystatin C (uCysC) did not differ between ADHF groups, although an
320 increasing trend was observed in RD patients when compared with those maintaining normal renal
321 function (noRI) during the hospitalisation period (P=0.072) (**Figure 5A**). Similarly, the highest KIM-
322 1 levels in urine (uKIM-1) at day 3 were found in the RD group with significant differences when

VDBP and Acute Heart Failure

323 compared with the RI and noRI groups (**Figure 5B**). **However, no differences were observed**
324 **between noRI and RI groups at three days of hospitalisation (Figure 5B).**

325 Levels of uVDBP negatively correlated with GFR and a significant positive correlation was found
326 with uCysC and uKIM-1 in ADHF patients at day 3 hospitalisation (**Supplementary Table V**).
327 Stronger positive correlations levels were found when only ADHF patients with GFR above 60
328 mL/min/1.73m² were considered (noRI and RI groups; **Figures 5C and 5D**).

329 We tested whether each one of the proteins (uVDBP, uCysC, uKIM-1) had the potential to
330 discriminate renal injury in ADHF patients by ROC curve analysis (**Supplementary table VI-A**).
331 None of the 3 proteins presented a significant discriminating ability when taken individually, with
332 urinary levels of VDBP presenting the largest area under the curve (AUC=0.579) compared to those
333 of KIM-1 (AUC=0.487) and cystatin C (AUC=0.476), **although differences among them did not**
334 **achieve statistical significance (Supplementary table VI-B)**. The combination of cystatin C and
335 KIM-1 showed a greater area under the curve, but still not statistically significant (AUC=0.604,
336 P=0.312). However, the addition of VDBP levels to this combination significantly increased the
337 discriminating value for **renal function deterioration** in ADHF patients (AUC=0.711, P=0.018,
338 **Figure 5F**), whereas the combination of VDBP with either cystatin C or KIM-1 alone was not
339 significant (P=0.428 and P=0.089, respectively).

340 **Due to the impact of age in renal dysfunction, the combination of aggregating VDBP, CysC**
341 **and KIM-1 for an early discrimination of ADHF patients with subclinical renal function**
342 **deterioration during hospitalisation was further reanalysed in an age-adjusted subgroup of**
343 **patients (age; RI- vs noRI-subgroups: 74 [69-77] vs 69 [63-72] years, P= 0.304; N=13/group).**
344 **As shown in Supplementary Figure V, in this age-adjusted cohort the discrimination power of**
345 **combining VDBP, CysC and KIM-1 remained statistic significantly (AUC: 0.711 [0.536-0.885],**
346 **P=0.018). Adding age to the 3-variable cluster did not significantly modify the AUC to early**
347 **discriminate patients with and without deterioration of kidney function during hospitalisation.**

348

349 4 Discussion

350 Heart and kidneys are closely interconnected through complex bidirectional mechanistic interactions
351 in their underlying pathophysiology (31), which is collectively known as cardiorenal syndrome (6)
352 and often referred to as type-1 cardiorenal syndrome when having a primary and acute cardiac
353 condition, such as ADHF, that triggers acute kidney injury (4). In hospitalised ADHF patients,
354 occurrence of acute kidney injury during the treatment frequently affects key therapeutic decisions,
355 resulting in incomplete decongestion of the patients (5).

356 There is a growing consensus about the poor effectiveness of serum creatinine measurement to detect
357 initial stages of cardiorenal syndrome type 1 (32) and the urgent need of more reliable biological
358 variables for early detection of **kidney function deterioration** in ADHF patients (2,4–6) in order to
359 better stratify their risk during the first days hospitalisation. **NGAL (33), KIM-1 (34), and cystatin**
360 **C (35) had provided promising results at detecting severe renal damage in ADHF patients and**
361 **other cardiac syndromes; however, negative studies (15,32,36–38) have also been reported.**
362 **There is certainly controversy regarding their relative diagnostic power.**

363 Therefore, we performed an exploratory proteomic study aimed to identify urinary protein associated
364 with early changes of renal function impairment in patients hospitalised with diagnostic of ADHF.

VDBP and Acute Heart Failure

365 Urinary proteins have been extensively studied in acute heart failure as they may be more sensitive to
366 renal injury and structural damage than serum creatinine. Until now, however, there is insufficient
367 evidence to translate the usefulness of measuring these proteins as clinical diagnostic tool.

368 **Our hypothesis-generating study is based on an untargeted mass-spectrometry approach.** We
369 identified a differential pattern of proteins involved in Vitamin A and D homeostasis in prospectively
370 collected spot-urine samples of ADHF patients when arriving to the emergency room. More
371 specifically, we have found that urinary VDBP levels are markedly elevated in ADHF patients, being
372 changes more evident in those patients with reduced GFR, suggesting an association between low
373 GFR and high VDBP levels. Unfortunately, we cannot discern if low GFR levels in the RD patients
374 evidenced a chronic renal dysfunction or were a result of the acute decompensated event. Our
375 findings are consistent with previous reports on urinary VDBP in the setting of pathologies
376 associated to nephropathies in humans. In systemic lupus erythematosus, urinary VDBP was
377 significantly elevated in patients with lupus nephritis and associated with disease severity (39). In
378 addition, VDBP has been studied in diabetic nephropathy and has shown to correlate with
379 microalbuminuria suggesting a diagnostic value in this pathology (40). Interestingly, it was
380 previously reported that urinary VDBP was strongly and consistently elevated in rats with induced
381 nephropathy very early in the course of the disease (25). VDBP has also been associated with major
382 contrast induced nephropathy events 90 days after exposure to contrast media in patients undergoing
383 coronary angioplasty (24). To our knowledge, however, it was not shown so far that the changes in
384 urinary VDBP levels are detected before renal injury is evidenced in hospitalised ADHF patients.

385 It is to notice that urinary VDBP significantly correlated with plasma NT-proBNP and the level of
386 GFR, suggesting VDBP as a protein associated with cardiorenal syndrome. This finding is in line
387 with a previous study using NT-proBNP and cystatin C, as a marker of renal function, to identify the
388 cardiorenal status in patients with refractory heart failure on cardiac resynchronisation therapy (41).
389 The fact that no relationship between VDBP and ejection fraction was found might result from the
390 heterogeneity of our study population. Indeed, heart failure patients with reduced and preserved
391 ejection fraction are frequently considered as two different phenotype entities with differences in
392 pathophysiological pathways deriving in the cardiorenal syndrome (42,43).

393 As suggested before, high urinary VDBP in ADHF patients at hospital admission may partially
394 reflect a temporary **kidney function deterioration** event due to impaired renal perfusion as
395 consequence of low cardiac output and systemic venous congestion (8,44). However, the maintained
396 urinary VDBP loss in ADHF patients with GFR below 60mL/min/1.73m² after 3 days of
397 hospitalisation suggest that high VDBP levels in urine associate to a renal structural damage in these
398 patients, **that might derive into cardiorenal syndrome type 1.**

399 Indeed, among ADHF patients with normal renal function at hospital admission (NRF group),
400 urinary VDBP remains high at day 3 in those patients presenting worsening of the renal function at a
401 later stage of the hospitalisation period, while patients who maintained normal renal function
402 presented a decrease of urinary VDBP into the healthy range. Interestingly, these changes at day 3
403 were observed before any apparent pathological change in plasma creatinine levels and the GFR, that
404 when occurred it was detected after 4-5 days hospitalisation. This finding suggests that urinary
405 VDBP is sensitive to early pathological changes occurring in kidney **and identifying those patients**
406 **with subclinical kidney function deterioration.**

407 High urinary VDBP levels in ADHF patients may result from renal tubular injury or reflect
408 hemodynamic or functional changes in GFR (24,25). Our results showed no association between

VDBP and Acute Heart Failure

409 urinary VDBP loss and serum levels of VDBP supporting a tubular damage leading to diminished
410 reabsorption and consequently higher urinary excretion as the most possible process accounting for
411 the high VDBP levels in urine of ADHF patients. **In this respect, Chaykovska et al (24) also**
412 **proposed, the increase of VDBP levels could be associated with the severity of renal damage.**

413 **Although the underlying mechanisms remain unclear, we could speculate that elevated levels of**
414 **VDBP in urine could regulate tubular cell function after endocytosis via megalin, since megalin**
415 **is involved in the active uptake of VDBP complexed to 25-hydroxy vitamin D3 in the proximal**
416 **tubules (45). A reduced uptake of VDBP, as in kidney disease conditions, could lead to**
417 **intrarenal losses of VDBP and vitamin D metabolites (45). Further studies are needed to**
418 **evidence whether VDBP is a relevant cardiorenal connector protein transmitting heart-to-**
419 **kidney signals.**

420 Other proteins in urine including KIM-1 and cystatin C have been related to renal failure and more
421 specifically to tubular damage (14,15). Supporting this finding, at day 3 of hospitalisation, KIM-1
422 levels were significantly elevated only in those patients with a pathological GFR. Also, a trend to
423 higher values was observed in the levels of urinary cystatin C although it did not achieve statistical
424 significance. In contrast, ADHF patients with $GFR > 60 \text{ mL/min/1.73m}^2$ at day 3 hospitalisation had
425 KIM-1 and cystatin C levels that did not differ from the normal healthy range regardless of the
426 subsequent evolution of the kidney function. Different pattern of VDBP and cystatin C and KIM-1 in
427 urine of ADHF patients at day 3 could be due to differences in the time-response of the cellular
428 processes occurring at the proximal tubular cells after injury. Thus, KIM-1 is a protein expressed in
429 proximal tubular cells after injury, but barely found in normal kidney (46), whereas the presence of
430 cystatin C and VDBP in urine result of a deficient endocytic receptor-mediated uptake, catabolism
431 and degradation of this protein by the tubular cells (47,48). Further studies are guaranteed to better
432 understand whether differences in the endocytic process and/or cell catabolism account for the VDBP
433 and cystatin C patterns in urine of ADHF patients.

434 The positive correlation of urinary VDBP with cystatin C and KIM-1 and day 3 of hospitalisation
435 strongly suggest that renal tubular insult accounts for acute **kidney function deterioration** in
436 patients with ADHF. Differences with two previous studies suggesting a lack of association between
437 worsening of renal function and tubular injury in ADHF, might be explained by the fact that these
438 studies just focused on the expression / secretion of proteins related to tubular cell injury such as
439 KIM-1 and NGAL (49,50), without considering other molecules reflecting a dysfunctional cell
440 phenotype.

441 Subsequently, ROC analysis was carried out to study the value of VDBP compared to cystatin C and
442 KIM-1 in association with incident **kidney function deterioration** in hospitalised ADHF patients. In
443 our study population, none of the three proteins showed enough discriminative power when
444 considered separately, nor did it when considering the joint detection of cystatin C and KIM-1.
445 However, when VDBP was added the AUC achieved statistical significance, suggesting that urine
446 VDBP combined with urine values of cystatin C and KIM-1 might serve as new diagnostic tool to
447 discriminate ADHF patients regarding their risk of developing renal function deterioration during
448 hospitalisation.

449 **Age is an important factor of kidney injury risk and development (51). In this respect, we want**
450 **to highlight as a study limitation the age difference between ADHF patients with and without**
451 **renal dysfunction at admission. However, VDBP levels did not correlate with age in our study**
452 **population, suggesting the independence of both variables. In addition, it is interesting to notice**

VDBP and Acute Heart Failure

453 that the discriminating power of VDBP, clustered with cystatin C and KIM-1 for kidney
454 function deterioration in hospitalized ADHF patients is maintained when age-adjusted ADHF
455 groups were compared. Thus, to the best of our knowledge, this is the first study reporting an
456 association between urinary VDBP and renal worsening in ADHF during hospitalisation. Still,
457 the limited sample size and high heterogeneity of the study population in their characteristics,
458 etiopathology and disease background need to be recognized. Therefore, further studies in
459 larger groups are needed to confirm our findings and validate the impact of urinary VDBP in
460 ADHF and incident kidney disease.

461 VDBP is forming a complex with the 25-(OH) vitamin D3 when present in the urine. Tubular
462 reabsorption of this complex is a critical process into the conversion of vitamin D into its active
463 metabolite that is secreted into the circulation (52). Damage to proximal tubules in ADHF leading to
464 a deficient reabsorption of VDBP-25-(OH) vitamin D3 complex, could result in diminished amounts
465 of vitamin D active metabolite, also known as 1,25-dihydroxycholecalciferol and calcitriol. In this
466 respect, Vitamin D deficiency has been previously associated to several diseases concerning renal
467 failure (53,54), cardiovascular health (55), certain types of cancer, type 2 diabetes, metabolic
468 syndrome, inflammatory bowel disease, and several others (56,57). Vitamin D has been studied
469 within chronic heart failure (58), however, to our knowledge there are no publications associating
470 ADHF with vitamin D.

471 In summary, VDBP has been consistently detected by 2DE-MS/MS as two spots in urine of ADHF
472 patients at hospital admission in this exploratory study, wherein the ADHF patients presented higher
473 urinary levels than healthy subjects. Additionally, ADHF patients presenting kidney dysfunction at
474 hospitalisation showed the highest urinary loss of VDBP. A significant drop in urinary VDBP is
475 observed within 3 days in patients with normal renal function during the hospitalisation period. On
476 the contrary, those patients who developed renal function deterioration maintained high levels of
477 VDBP loss in urine, while their GFR levels were within normal physiological range at that time.
478 When performing ROC analysis, the addition of urinary VDBP to renal injury markers such as
479 urinary cystatin C and KIM-1 gave statistical power to anticipate renal damage. Therefore, a daily
480 follow-up of VDBP urinary secretion could help to determine whether patients' kidneys are prone to
481 failure and prevent it using more appropriate and personalised therapeutic techniques.

482

483 5 Abbreviations

484 ADHF: acute decompensated heart failure; CysC: cystatin C; GFR: glomerular filtration rate; KIM-1:
485 kidney injury molecule 1; LVEF: left ventricular ejection fraction; NGAL: neutrophil gelatinase-
486 associated lipocalin; RD: renal dysfunction patients art hospitalisation; noRI: patients who did not
487 develop renal injury; NRF: normal renal function patients at hospitalisation; RI: patients who
488 developed renal injury; VDBP: vitamin D binding protein; 2DE: two-dimension electrophoresis

489

VDBP and Acute Heart Failure

490 **6 Acknowledgements**

491 We gratefully acknowledge the valuable help and support of Montse Gómez-Pardo with the sample
492 handling.

493

494 **7 Authors contribution**

495 XGM, LB and TP: study concept and design. LL, XGM: patient inclusion, clinical data and sample
496 acquisition. ED-R, MG-A, TP: methodology, formal analysis. ED-R, LB, TP: statistical analysis and
497 result interpretation. ED-R, LB, TP: writing—original draft preparation. ED-R, MG-A, LL, XGM,
498 LB, TP: manuscript review and editing. LB and TP: funding acquisition. All authors have read and
499 agreed to the submitted version of the manuscript.

500

501 **8 Sources of Funding**

502 This work was supported by the “Fundació La Marató TV3” (Project number 20153110) to T.P.; the
503 H2020-JTI-IMI2-2017-13-two-stage Project 821283 –TransBioLine to L.B. & T.P.; the Spanish
504 “Agencia Estatal de Investigación (AEI)” - Institute of Health Carlos III, ISCIII [FIS PI19/01687 to
505 T.P; Centro de Investigación Biomedica en Red Cardiovascular (CIBERCV-CB16/11/00411) to LB;
506 Spanish Ministry of Economy and Competitiveness of Science-PID2019-107160RB-I00 to LB; and
507 cofounded by FEDER "Una Manera de Hacer Europa". Secretaria de Universitats i Recerca del
508 Departament d'Empresa i Coneixement de la Generalitat de Catalunya [2017 SGR 1480]. We thank
509 Fundació Jesús Serra and Fundació de Investigació Cardiovascular (Barcelona) for their
510 continuous support. EDR is a predoctoral fellow funded by the “Fundació La Marató TV3” and the
511 Cardiovascular Program-ICCC (IR-HSCSP).

512

513 **9 Conflicts of interest**

514 L.B. received institutional research grants from AstraZeneca; consultancy fees from Sanofi, Pfizer
515 and Novartis; speaker fees from Lilly, Pfizer, and AstraZeneca. T.P., and L.B. are shareholders of the
516 academic spin-off companies GlyCardial Diagnostics S.L. and Ivestatin Therapeutics S.L. All
517 unrelated to the present work. EDR, MGA, LL, XGM declare no conflict of interest.

518

519 **10 Contribution to the field**

520 Worsening renal function in the treatment of acute decompensated heart failure (ADHF) associates
521 with adverse outcomes and longer hospital stays. There is a growing consensus about the poor
522 effectiveness of serum creatinine measurement to detect initial stages of renal damage and the urgent
523 need of more reliable biological variables for early detection of acute kidney injury in ADHF patients
524 during hospitalisation.

VDBP and Acute Heart Failure

- 525 • By a mass spectrometry-based protein discovery study, we identify an elevated urinary loss of
526 Vitamin D Binding Protein (VDBP), the main carrier of vitamin D, in the urine of patients
527 hospitalised with acute decompensated heart failure (ADHF).
- 528 • High levels of urinary VDBP loss at 72 hours hospitalisation associate with early stages of
529 renal function deterioration at the time that plasma creatinine and glomerular filtration rate are
530 still found within the normal physiological range.
- 531 • As indicated by the C-statistics, the logistic regression model obtained by adding urinary
532 VDBP to Cystatin C and KIM-1 levels improves discrimination of ADHF patients at high risk
533 of presenting renal injury before hospital discharge.

534

535

536 **11 References**

- 537 1. Grande D, Gioia MI, Terlizze P, Iacoviello M. Heart failure and kidney disease. *Adv Exp*
538 *Med Biol.* 2018;1067:219–38.
- 539 2. Metra M, Nodari S, Parrinello G, Bordonali T, Bugatti S, Danesi R, et al. Worsening renal
540 function in patients hospitalised for acute heart failure: Clinical implications and prognostic
541 significance. *Eur J Heart Fail.* 2008;10(2):188–95.
- 542 3. Aronson D. Cardiorenal syndrome in acute decompensated heart failure: A new approach.
543 *Expert Rev Cardiovasc Ther.* 2012;177–89.
- 544 4. Ronco C, McCullough P, Anker SD, Anand I, Aspromonte N, Bagshaw SM, et al. Cardio-
545 renal syndromes: Report from the consensus conference of the acute dialysis quality initiative.
546 *Eur Heart J.* 2010;31(6):703–11.
- 547 5. Damman K, Valente MAE, Voors AA, O'Connor CM, Van Veldhuisen DJ, Hillege HL. Renal
548 impairment, worsening renal function, and outcome in patients with heart failure: An updated
549 meta-analysis. *Eur Heart J.* 2014;35(7):455–69.
- 550 6. Ronco C, Haapio M, House AA, Anavekar N, Bellomo R. Cardiorenal Syndrome. *J Am Coll*
551 *Cardiol.* 2008;52(19):1527–39.
- 552 7. Palazzuoli A, Ruocco G. Heart–Kidney Interactions in Cardiorenal Syndrome Type 1. *Adv*
553 *Chronic Kidney Dis.* 2018;25(5):408–17.
- 554 8. Verbrugge FH. Utility of Urine Biomarkers and Electrolytes for the Management of Heart
555 Failure. *Curr Heart Fail Rep.* 2019;16(6):240–9.
- 556 9. Manguba AS, Vela Parada X, Coca SG, Lala A. Synthesizing Markers of Kidney Injury in
557 Acute Decompensated Heart Failure: Should We Even Keep Looking? *Curr Heart Fail Rep.*
558 2019;16(6):257–73.
- 559 10. Sokolski M, Zymliński R, Biegus J, Siwołowski P, Nawrocka-Millward S, Todd J, et al.
560 Urinary levels of novel kidney biomarkers and risk of true worsening renal function and

VDBP and Acute Heart Failure

- 561 mortality in patients with acute heart failure. *Eur J Heart Fail.* 2017 Jun;19(6):760–7.
- 562 11. Hu Y, Liu H, Du L, Wan J, Li X. Serum cystatin C predicts AKI and the prognosis of patients
563 in coronary care unit: A prospective, observational study. *Kidney Blood Press Res.*
564 2017;42(6):961–73.
- 565 12. Katagiri D, Doi K, Honda K, Negishi K, Fujita T, Hisagi M, et al. Combination of Two
566 Urinary Biomarkers Predicts Acute Kidney Injury After Adult Cardiac Surgery. *Ann Thorac*
567 *Surg.* 2012;93(2):577–83.
- 568 13. Devarajan P. Neutrophil gelatinase-associated lipocalin: A promising biomarker for human
569 acute kidney injury. *Biomark Med.* 2010;4(2):265–80.
- 570 14. Urbschat A, Gauer S, Paulus P, Reissig M, Weipert C, Ramos-Lopez E, et al. Serum and
571 urinary NGAL but not KIM-1 raises in human postrenal AKI. *Eur J Clin Invest.*
572 2014;44(7):652–9.
- 573 15. Breidthardt T, Sabti Z, Ziller R, Rassouli F, Twerenbold R, Kozuharov N, et al. Diagnostic
574 and prognostic value of cystatin C in acute heart failure. *Clin Biochem.* 2017;50(18):1007–13.
- 575 16. Kuznetsova T, Mischak H, Mullen W, Staessen JA. Urinary proteome analysis in hypertensive
576 patients with left ventricular diastolic dysfunction. *Eur Heart J.* 2012;33(18):2342–50.
- 577 17. Campbell RT, Jasilek A, Mischak H, Nkuipou-Kenfack E, Latosinska A, Welsh PI, et al. The
578 novel urinary proteomic classifier HF1 has similar diagnostic and prognostic utility to BNP in
579 heart failure. *ESC Hear Fail.* 2020;7(4):1595–604.
- 580 18. He T, Mischak M, Clark AL, Campbell RT, Delles C, Díez J, et al. Urinary peptides in heart
581 failure: a link to molecular pathophysiology. *Eur J Heart Fail.* 2021;2.
- 582 19. Farmakis D, Koeck T, Mullen W, Parissis J, Gogas BD, Nikolaou M, et al. Urine proteome
583 analysis in heart failure with reduced ejection fraction complicated by chronic kidney disease:
584 feasibility, and clinical and pathogenetic correlates. *Eur J Heart Fail.* 2016;18(7):822–9.
- 585 20. Cubedo J, Padró T, Garcia-Moll X, Pintó X, Cinca J, Badimon L. Serum proteome in acute
586 myocardial infarction. *Clin e Investig en Arterioscler.* 2011;23(4):147–54.
- 587 21. Ramaiola I, Padró T, Peña E, Juan-Babot O, Cubedo J, Martin-Yuste V, et al. Changes in
588 thrombus composition and profilin-1 release in acute myocardial infarction. *Eur Heart J.*
589 2015;36(16):965–75.
- 590 22. Eshbach ML, Weisz OA. Receptor-Mediated Endocytosis in the Proximal Tubule. *Annu Rev*
591 *Physiol.* 2017;79:425–48.
- 592 23. Leheste JR, Rolinski B, Vorum H, Hilpert J, Nykjaer A, Jacobsen C, et al. Megalin knockout
593 mice as an animal model of low molecular weight proteinuria. *Am J Pathol.*
594 1999;155(4):1361–70.
- 595 24. Chaykovska L, Heunisch F, Von Einem G, Alter ML, Hocher CF, Tsuprykov O, et al. Urinary
596 Vitamin D binding protein and KIM-1 are potent new biomarkers of major adverse renal

VDBP and Acute Heart Failure

- 597 events in patients undergoing coronary angiography. *PLoS One*. 2016;11(1):1–11.
- 598 25. Mirković K, Doorenbos CRC, Dam WA, Lambers Heerspink HJ, Slagman MCJ, Nauta FL, et
599 al. Urinary Vitamin D Binding Protein: A Potential Novel Marker of Renal Interstitial
600 Inflammation and Fibrosis. *PLoS One*. 2013;8(2):1–9.
- 601 26. Tarwater K. Estimated glomerular filtration rate explained. *Mo Med*. 2011;108(1):29–32.
- 602 27. Cubedo J, Padró T, Garcia-Moll X, Pintó X, Cinca J, Badimon L. Proteomic signature of
603 apolipoprotein J in the early phase of new-onset myocardial infarction. *J Proteome Res*.
604 2011;10(1):211–20.
- 605 28. Cubedo J, Padró T, Alonso R, Mata P, Badimon L. ApoL1 levels in high density lipoprotein
606 and cardiovascular event presentation in patients with familial hypercholesterolemia. *J Lipid*
607 *Res*. 2016;57(6):1059–73.
- 608 29. García-Arguinzonis M, Padró T, Lugano R, Llorente-Cortes V, Badimon L. Low-density
609 lipoproteins induce heat shock protein 27 dephosphorylation, oligomerization, and subcellular
610 relocalization in human vascular smooth muscle cells. *Arterioscler Thromb Vasc Biol*.
611 2010;30(6):1212–9.
- 612 30. Han X, Zhang S, Chen Z, Adhikari BK, Zhang Y, Zhang J, et al. Cardiac biomarkers of heart
613 failure in chronic kidney disease. *Clin Chim Acta*. 2020;510(May):298–310.
- 614 31. Kumar U, Garimella P, Wettersten N. Cardiorenal syndrome-Pathophysiology. *Cardiol Clin*.
615 2019;37(3):251–65.
- 616 32. Atici A, Emet S, Cakmak R, Yuruyen G, Alibeyoglu A, Akarsu M, et al. Type I cardiorenal
617 syndrome in patients with acutely decompensated heart failure: the importance of new renal
618 biomarkers. *Eur Rev Med Pharmacol Sci*. 2018;22(11):3534–43.
- 619 33. Angeletti S, Fogolari M, Morolla D, Capone F, Costantino S, Spoto S, et al. Role of neutrophil
620 gelatinase-associated lipocalin in the diagnosis and early treatment of acute kidney injury in a
621 case series of patients with acute decompensated heart failure: A case series. *Cardiol Res*
622 *Pract*. 2016;2016:3708210.
- 623 34. Huang Y, Don-Wauchope AC. The clinical utility of kidney injury molecule 1 in the
624 prediction, diagnosis and prognosis of acute kidney injury: A systematic review. *Inflamm*
625 *Allergy - Drug Targets*. 2011;10(4):260–71.
- 626 35. Zhang Z, Lu B, Sheng X, Jin N. Cystatin C in prediction of acute kidney injury: A systemic
627 review and meta-analysis. *Am J Kidney Dis*. 2011;58(3):356–65.
- 628 36. Breidhardt T, Socrates T, Drexler B, Noveanu M, Heinisch C, Arenja N, et al. Plasma
629 neutrophil gelatinase-associated lipocalin for the prediction of acute kidney injury in acute
630 heart failure. *Crit Care*. 2012;16(1):R2.
- 631 37. Verbrugge FH, Dupont M, Shao Z, Shrestha K, Singh D, Finucan M, et al. Novel Urinary
632 Biomarkers in Detecting Acute Kidney Injury, Persistent Renal Impairment and All-cause
633 Mortality following Decongestive Therapy in Acute Decompensated Heart Failure Frederik. *J*

VDBP and Acute Heart Failure

- 634 Card Fail. 2013;19(9):621–8.
- 635 38. Legrand M, de Berardinis B, Gaggin HK, Magrini L, Belcher A, Zanca B, et al. Evidence of
636 uncoupling between renal dysfunction and injury in cardiorenal syndrome: Insights from the
637 BIONICS study. *PLoS One*. 2014;9(11):1–8.
- 638 39. Go D, Lee JY, Kang MJ, Lee EY, Lee EB, Yi EC, et al. Urinary vitamin D-binding protein, a
639 novel biomarker for lupus nephritis, predicts the development of proteinuric flare. *Lupus*.
640 2018;27(10):1600–15.
- 641 40. Bai X, Luo Q, Tan K, Guo L. Diagnostic value of VDBP and miR-155-5p in diabetic
642 nephropathy and the correlation with urinary microalbumin. *Exp Ther Med*. 2020;20(5):1–1.
- 643 41. Truong QA, Szymonifka J, Januzzi JL, Contractor JH, Deaño RC, Chatterjee NA, et al.
644 Cardiorenal Status using Amino Terminal Pro Brain Natriuretic Peptide and Cystatin C on
645 Cardiac Resynchronization Therapy Outcomes: From the BIOCRT Study Quynh. *Hear*
646 *Rhythm*. 2019;16(6):928–35.
- 647 42. Yamagishi T, Matsushita K, Minamishima T, Goda A, Sakata K, Satoh T, et al. Comparison of
648 risk factors for acute worsening renal function in heart failure patients with and without
649 preserved ejection fraction. *Eur J Intern Med*. 2015;26(8):599–602.
- 650 43. Agrawal A, Naranjo M, Kanjanahattakij N, Rangaswami J, Gupta S. Cardiorenal syndrome in
651 heart failure with preserved ejection fraction—an under-recognized clinical entity. *Heart Fail*
652 *Rev*. 2019;24(4):421–37.
- 653 44. Schefold JC, Filippatos G, Hasenfuss G, Anker SD, Von Haehling S. Heart failure and kidney
654 dysfunction: Epidemiology, mechanisms and management. *Nat Rev Nephrol*.
655 2016;12(10):610–23.
- 656 45. Fowlkes JL, Bunn RC, Cockrell GE, Clark LM, Wahl EC, Lumpkin CK, et al. Dysregulation
657 of the intrarenal vitamin D endocytic pathway in a nephropathy-prone mouse model of type 1
658 diabetes. *Exp Diabetes Res*. 2011;2011:269378.
- 659 46. van Timmeren M, van den Heuvel M, Bailly V, Bakker S, van Goor H, Stegeman C. Tubular
660 kidney injury molecule-1 (KIM-1) in human renal disease. *J Pathol*. 2007;212:209–17.
- 661 47. Jensen D, Kierulf-Lassen C, Kristensen MLV, Nørregaard R, Weyer K, Nielsen R, et al.
662 Megalin dependent urinary cystatin C excretion in ischemic kidney injury in rats. *PLoS One*.
663 2017;12(6):1–13.
- 664 48. Bennett MR, Pordal A, Haffner C, Pleasant L, Ma Q, Devarajan P. Urinary vitamin D-binding
665 protein as a biomarker of steroid-resistant nephrotic syndrome. *Biomark Insights*. 2016;11:1–
666 6.
- 667 49. Dupont M, Shrestha K, Singh D, Awad A, Kovach C, Scarpino M, et al. Lack of significant
668 renal tubular injury despite acute kidney injury in acute decompensated heart failure. *Eur J*
669 *Heart Fail*. 2012;14(6):597–604.
- 670 50. Ahmad T, Jackson K, Rao VS, Tang WHW, Brisco-Bacik MA, Chen HH, et al. Worsening

VDBP and Acute Heart Failure

- 671 renal function in patients with acute heart failure undergoing aggressive diuresis is not
672 associated with tubular injury. *Circulation*. 2018;137(19):2016–28.
- 673 51. Coca SG. Acute Kidney Injury in Elderly Persons. *Am J Kidney Dis* [Internet].
674 2010;56(1):122–31. Available from: <http://dx.doi.org/10.1053/j.ajkd.2009.12.034>
- 675 52. Nykjaer A, Dragun D, Walther D, Vorum H, Jacobsen C, Herz J, et al. An endocytic pathway
676 essential for renal uptake and activation of the steroid 25-(OH) vitamin D3. *Cell*.
677 1999;96(4):507–15.
- 678 53. Teng M, Wolf M, Ofsthun MN, Lazarus JM, Hernán MA, Camargo CA, et al. Activated
679 injectable vitamin D and hemodialysis survival: A historical cohort study. *J Am Soc Nephrol*.
680 2005;16(4):1115–25.
- 681 54. Wolf M, Shah A, Gutierrez O, Ankers E, Monroy M, Tamez H, et al. Vitamin D levels and
682 early mortality among incident hemodialysis patients. *Kidney Int*. 2007;72(8):1004–13.
- 683 55. Anderson JL, May HT, Horne BD, Bair TL, Hall NL, Carlquist JF, et al. Relation of vitamin D
684 deficiency to cardiovascular risk factors, disease status, and incident events in a general
685 healthcare population. *Am J Cardiol*. 2010;106(7):963–8.
- 686 56. Bouillon R, Carmeliet G. Vitamin D insufficiency: Definition, diagnosis and management.
687 *Best Pract Res Clin Endocrinol Metab*. 2018;32:669–84.
- 688 57. Battistini C, Ballan R, Herkenhoff ME, Saad SMI, Sun J. Vitamin d modulates intestinal
689 microbiota in inflammatory bowel diseases. *Int J Mol Sci*. 2021;22(1):1–22.
- 690 58. Witte KK, Byrom R, Gierula J, Paton MF, Jamil HA, Lowry JE, et al. Effects of Vitamin D on
691 Cardiac Function in Patients With Chronic HF: The VINDICATE Study. *J Am Coll Cardiol*.
692 2016;67(22):2593–603.
- 693
- 694
- 695

VDBP and Acute Heart Failure

696 12 Legends to Figures

697 **Figure 1. Study design.** ADHF patients were divided in two groups at hospital admission depending
698 on their glomerular filtration rate. RD group included patients with glomerular filtration rate <60
699 ml/min/1.73m², while NRF presented glomerular filtration rate above this cut-off. At day 3, NRF
700 patients were divided in two groups depending on their kidney function evolution. RI patients
701 developed renal function deterioration defined by glomerular filtration rate <60 ml/min/1.73m²,
702 while noRI patients maintained normal glomerular filtration rate. Urine and blood samples were
703 obtained at hospital admission and at day 3 of hospitalisation. Protein extracts from urine were
704 prepared and samples analysed by two-dimensional (2DE)-electrophoresis and mass-spectrometry for
705 identification of differential protein patterns. Validation studies were performed by ELISA. Sample
706 size is given in Figure.

707 **Figure 2. Proteomic analysis of urine samples (A)** Representative 2-DE image of human urine
708 samples in a pI range of 4–7 and 12% SDS-PAGE gels. Vitamin D binding protein (VDBP) was
709 identified as 2 spots (pI: 5.25-5.30; Mw:50.3 KDa) in ADHF patients (N=17) and healthy subjects
710 (n=6). **(B)** Western blot analysis showed one single band for VDBP in urine samples. **(C and D)** Box
711 plot diagrams [median (IQR)] of the intensity of both VDBP spots at hospital admission. In **(C)**
712 Comparison between ADHF patients and healthy subjects (HS). **(D)** Differences in VDBP intensity
713 between ADHF patient with (N=12) and without (N=5) renal dysfunction (RD and NRF for GFR
714 values below and above 60 ml/min/1.73m², respectively). Mann-Whitney test was used for
715 comparison between groups in C and D. Statistical significance for P <0.05.

716 **Figure 3. Urinary VDBP in ADHF patients during hospitalisation: Validation studies.** Box plot
717 diagrams [median (IQR)] refer to levels of urinary VDBP quantified by ELISA. VDBP in urine was
718 normalised by the total protein content in each sample and expressed as ng VDBP/mg total protein.
719 Mann-Whitney test was performed for comparison between groups at: **(A)** hospital admission, **(I)**
720 ADHF patients (N=64) vs healthy subjects (HS, N=13), **(II)** ADHF patients with glomerular filtration
721 rate (GFR) below (N=34) and above 60 ml/min/1.73m² at hospital admission (N=30); **(B)** 3 days of
722 hospitalisation, **(I)** comparison between day-0 (D0) and day-3 (D3) for ADHF patients maintaining
723 normal renal function (noRI: N=21) and presenting with renal function deterioration (RI: N=13) after
724 3 days hospitalisation, and in patients with present renal dysfunction at hospitalisation (RD, N=30);
725 and **(II)** Comparison between ADHF subgroups (Mann Whitney was performed after Kruskal-Wallis
726 test for multiple group comparison showed P-value <0.05).

727 **Figure 4. Serum VDBP in ADHF patients at day 3 hospitalisation. (A)** Box plot diagrams
728 [median (IQR)] of VDBP levels quantified by ELISA in serum of ADHF patients already presenting
729 renal dysfunction at hospital admission (RD), developing renal function deterioration during
730 hospitalisation (RI) and maintaining normal renal function (noRI). Groups comparisons were made by
731 Kruskal-Wallis and Mann Whitney. **(B)** Spearman correlation (Rho) between VDBP levels in serum
732 and urine in ADHF patients at day 3 hospitalisation.

733 **Figure 5. Markers of tubular damage (urinary CysC and KIM-1) in ADHF patients at day 3**
734 **hospitalisation.** Box plot diagrams [median (IQR)] refer to **(A)** cystatin C (CysC) and **(B)** KIM-1
735 (Kidney-Injury-Molecule-1) in the subgroups of ADHF patients as described in Figure 4A. **(C and**
736 **D)** Spearman correlation (Rho) between urinary VDBP levels and CysC and KIM-1, respectively, in
737 all ADHF patients. **(E)** ROC curve analyses (C-Statistics) for the prediction of renal function
738 deterioration presentation in ADHF patients (N=34). AUC indicates area under the curve.

739

VDBP and Acute Heart Failure

740 Table 1: Patient baseline characteristics.

	All patients N=64	NRF N=34	RD N=30	P-value
DEMOGRAPHIC CHARACTERISTICS; median [IQR]				
Female/male, N	20/44	9/25	11/19	0.146
Age, years	71.0 [64.0-77.0]	59.0 [58.0-75.0]	74.5 [69.0-78.0]	0.010
Weight, kg	72.6 [61.2-86.6]	70.0 [59.8-86.8]	75.8 [62.0-84.0]	0.591
KIDNEY FUNCTION MARKERS				
Creatinine, $\mu\text{mol/L}$	104.5 [78.0-146.3]	78.5 [67.8-96.8]	147.0 [120.8-195.5]	<0.001
Glomerular filtration (MDRD-4)	61.3 [41.8-83.1]	82.3 [69.0-98.2]	41.1 [31.0-45.3]	<0.001
Urea, mmol/L	10.1 [7.0-15.6]	7.1 [5.8-9.2]	16.5 [12.9-23.0]	<0.001
CARDIAC FUNCTION MARKERS				
NT-proBNP, $\mu\text{g/L}$	4.14 [2.5-8.9]	3.4 [1.9-6.4]	5.2 [3.0-14.7]	0.022
Left ventricular ejection fraction (LVEF), %	45.5 [33.0-57.5]	37.5 [33.0-57.0]	51.0 [33.0-58.0]	0.297
Preserved LVEF, N (%)	27 (42)	11 (32)	16 (53)	
Reduced LVEF, N (%)	27 (42)	18 (53)	9 (30)	0.158
Mid-range LVEF, N (%)	10 (16)	5 (15)	5 (17)	
Atrial fibrillation, N (%)	31 (48)	16 (47)	15 (50)	>0.999
Cardiovascular disease, N (%)	20 (31)	10 (29)	10 (33)	0.791
OTHER BIOCHEMICAL MARKERS				
Haemoglobin, g/L	122 [104-138]	129 [114-141]	113 [96-125]	0.008
RISK FACTORS; N (%)				
Active smoking	10 (16)	8 (24)	2 (7)	0.088
Hypertension	47 (73)	21 (62)	26 (87)	0.046
Pulmonary hypertension	16 (25)	8 (24)	8 (27)	0.781
Diabetes mellitus type 2	28 (44)	11 (32)	17 (57)	0.079
Dyslipidaemia	44 (69)	20 (59)	24 (80)	0.108
BACKGROUND MEDICATION; N (%)				
Diuretics	47 (73)	21 (59)	27 (90)	0.011
Statins	41 (64)	18 (53)	23 (77)	0.068
Anticoagulants	26 (41)	14 (41)	12 (40)	>0.999
Antiplatelet agents	36 (56)	19 (56)	17 (57)	>0.999
Beta-blockers	44 (69)	21 (62)	23 (77)	0.281
Antiarrhythmic agents	6 (9)	4 (12)	2 (7)	0.676
Antidiabetics	24 (38)	8 (21)	17 (57)	0.010
Insulin	11 (17)	2 (6)	9 (30)	0.018
Oral antidiabetic agents	21 (33)	8 (24)	13 (43)	0.114
ACE inhibitor/ARB	43 (67)	26 (76)	17 (57)	0.114

P values compare NRF and RD patients, and it is calculated using Fisher exact test, except for LVEF where χ^2 was used. Diuretics: hydrochlorothiazide, furosemide, eplerenone, and spironolactone. Statins: atorvastatin, pravastatin, simvastatin, ezetimibe. Anticoagulants: warfarin, acenocumarol, bempiparin, heparin, dabigatran, rivaroxaban, edoxaban, and apixaban. Antiplatelet agents: acetylsalicylic acid and clopidogrel. Beta-blockers: bisoprolol and carvedilol. Antiarrhythmic agents: amiodarone. Oral antidiabetic agents: metformin and repaglinide. Angiotensin-converting enzyme inhibitors (ACEI) include: captopril, enalapril, and ramipril. Angiotensin receptor blockers (ARB): losartan, olmesartan, and valsartan.

741

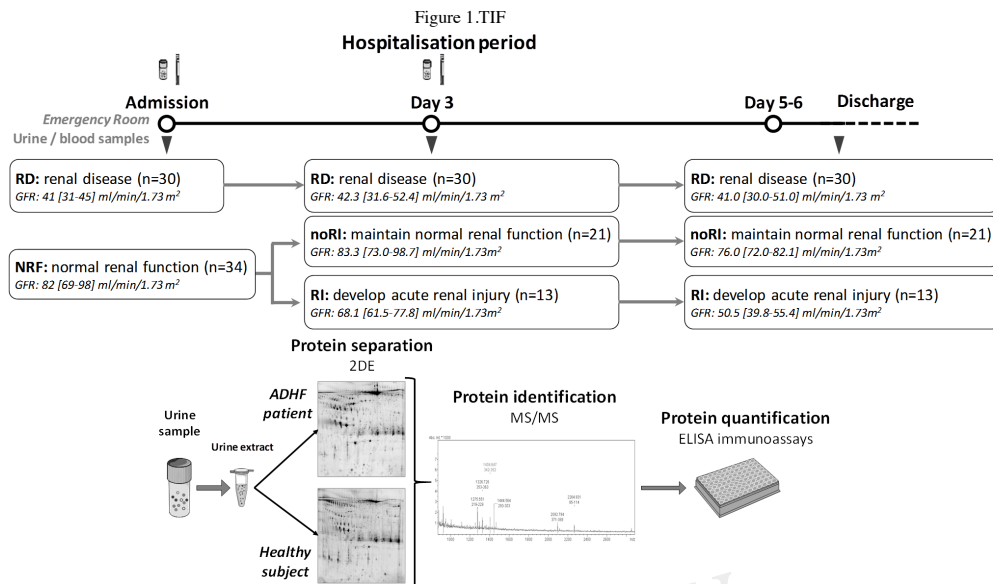


Figure 1: Study design. ADHF patients were divided in two groups at hospital admission depending on their glomerular filtration rate. RD group included patients with glomerular filtration rate <60 ml/min/1.73m², while NRF presented glomerular filtration rate above this cut-off. At day 3, NRF patients were divided in two groups depending on their kidney function evolution. RI patients developed renal injury defined by glomerular filtration rate <60 ml/min/1.73m², while noRI patients maintained normal glomerular filtration rate. Urine and blood samples were obtained at hospital admission and at day 3 oh hospitalisation. Protein extracts from urine were prepared and samples analysed by two-dimensional (2DE)-electrophoresis and mass-spectrometry for identification of differential protein patterns. Validation studies were performed by ELISA. Sample size is given in Figure.

Figure 2.TIF

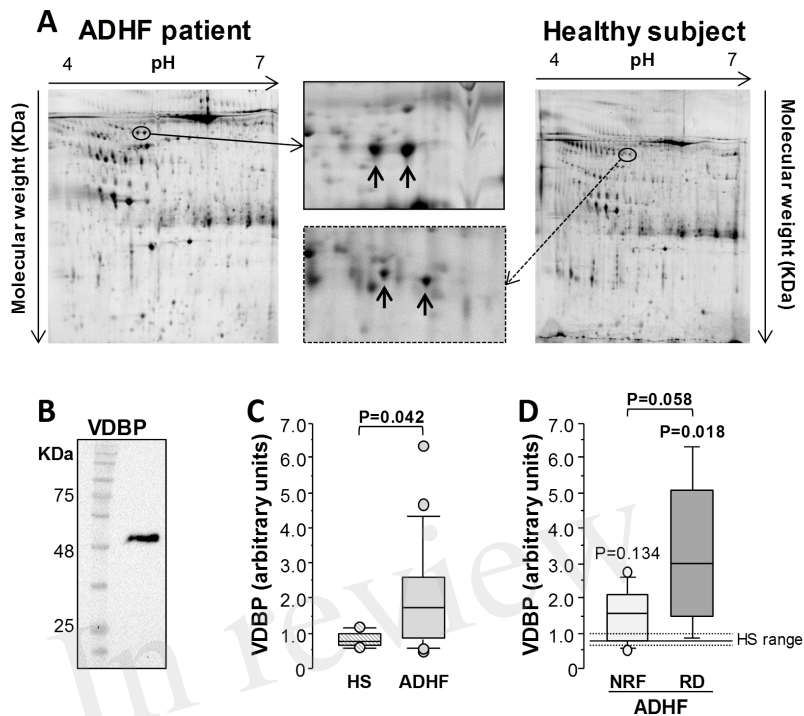


Figure 2. Proteomic analysis of urine samples (A) Representative 2-DE image of human urine samples in a pI range of 4–7 and 12% SDS-PAGE gels. Vitamin D binding protein (VDBP) was identified as 2 spots (pI: 5.25-5.30; Mw:50.3 kDa) in ADHF patients (N=17) and healthy subjects (n=6). **(B)** Western blot analysis showed one single band for VDBP in urine samples. **(C and D)** Box plot diagrams [median (IQR)] of the intensity of both VDBP spots at hospital admission. In **(C)** Comparison between ADHF patients and healthy subjects (HS). **(D)** Differences in VDBP intensity between ADHF patient with (N=12) and without (N=5) renal dysfunction (RD and NRF for GFR values below and above 60 ml/min/1.73m², respectively). Mann-Whitney test was used for comparison between groups in C and D. Statistical significance for P < 0.05.

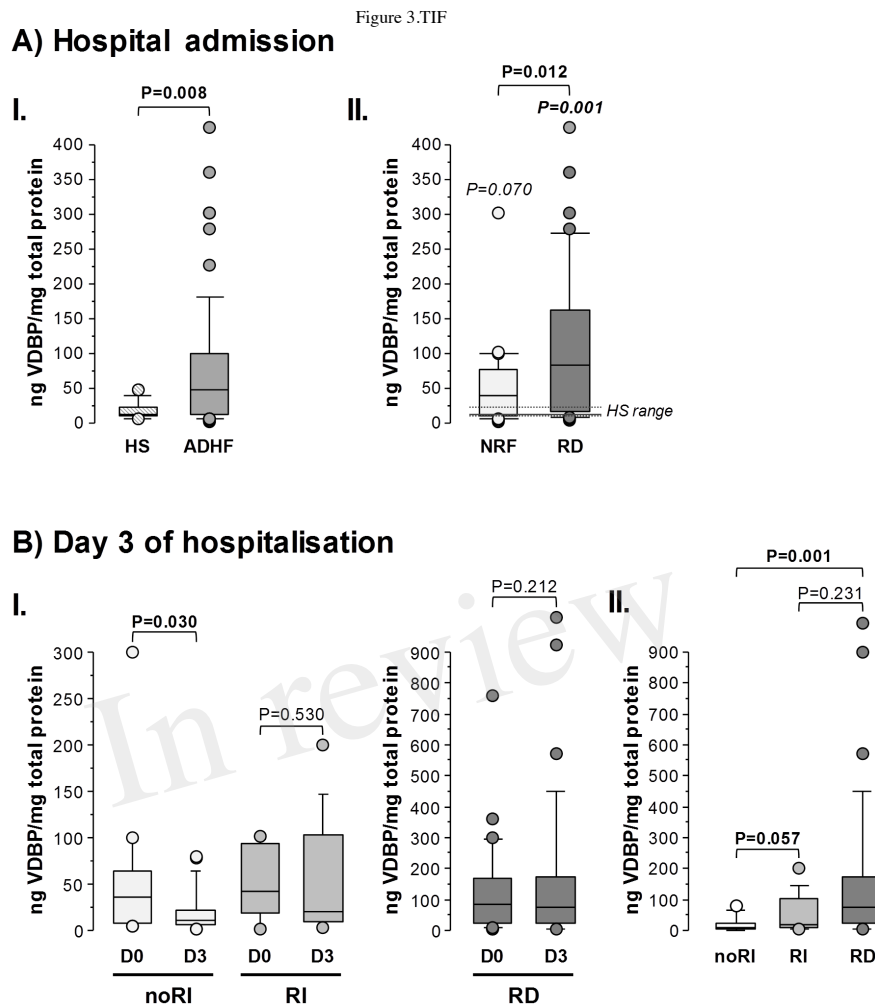


Figure 3. Urinary VDBP in ADHF patients during hospitalisation: Validation studies. Box plot diagrams [median (IQR)] refer to levels of urinary VDBP quantified by ELISA. VDBP in urine was normalised by the total protein content in each sample and expressed as ng VDBP/mg total protein. Mann-Whitney test was performed for comparison between groups at: **(A)** hospital admission, (I) ADHF patients (N=64) vs healthy subjects (HS, N=13), (II) ADHF patients with glomerular filtration rate (GFR) below (N=34) and above 60 ml/min/1.73m² at hospital admission (N=30); **(B)** 3 days of hospitalisation, (I) comparison between day-0 (D0) and day-3 (D3) for ADFH patients maintaining normal renal function (noRI: N=21) and presenting with kidney injury (RI: N=13) after 3 days hospitalisation, and in patients with established renal dysfunction (RD, N=30); and (II) Comparison between ADHF subgroups (Mann Whitney was performed after Kruskal-Wallis test for multiple group comparison showed P-value <0.05).

Figure 4.TIF

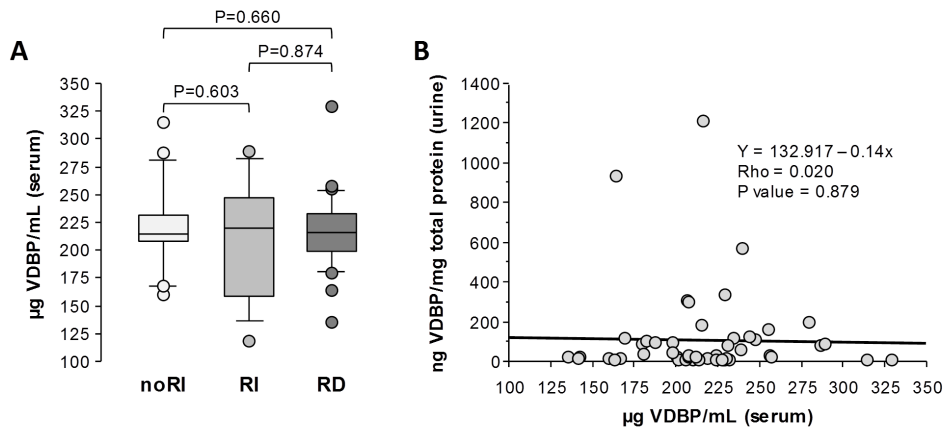


Figure 4: Serum VDBP in ADHF patients at day 3 hospitalisation. (A) Box plot diagrams [median (IQR)] of VDBP levels quantified by ELISA in serum of ADHF patients already presenting renal dysfunction at hospital admission (RD), developing kidney injury during hospitalisation (RI) and maintaining normal renal function (noRI). Groups comparisons we made by Kruskal-Wallis and Mann Whitney. (B) Spearman correlation (Rho) between VDBP levels in serum and urine in ADHF patients at day 3 hospitalisation.

Figure 5.TIF

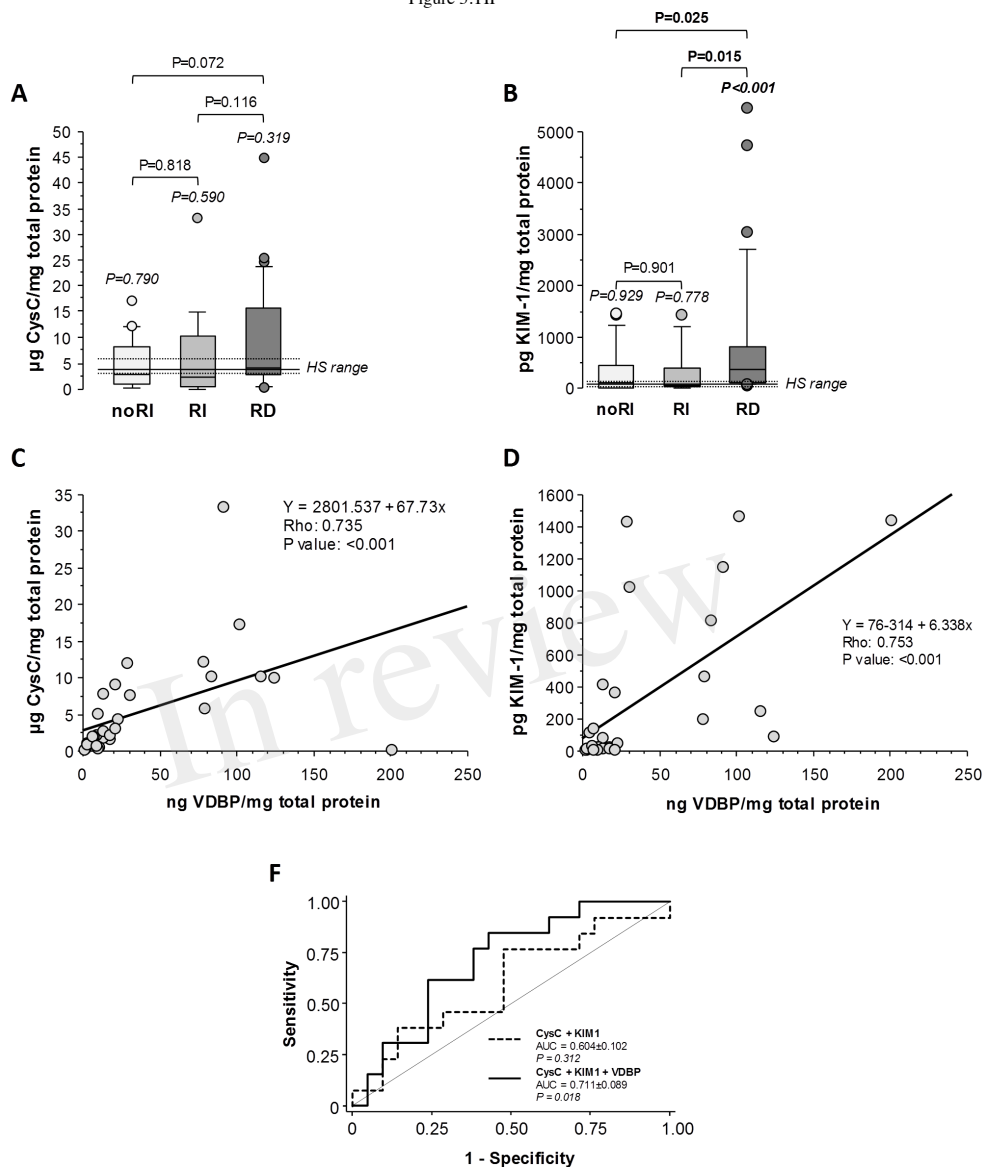


Figure 5. Markers of tubular damage (urinary CysC and KIM-1) in ADHF patients at day 3 hospitalisation. Box plot diagrams [median (IQR)] refer to (A) cystatin C (CysC) and (B) KIM-1 (Kidney Injury Molecule 1) in the subgroups of ADHF patients as described in Figure 4A. (C and D) Spearman correlation (Rho) between urinary VDBP levels and CysC and KIM-1, respectively. (E) ROC curve analyses (C-Statistics) for the prediction of kidney injury presentation in ADHF patients (N=34). AUC indicates area under the curve.



Supplementary material

Vitamin D Binding Protein and renal injury in acute decompensated heart failure

Elisa Diaz-Riera^{1,2}; Maïsa García-Arguinzonis¹, Laura López³, Xavier Garcia-Moll^{3,4}, Lina Badimon L^{1,4,5}, Padró, T^{1,4*}

¹Cardiovascular-Program ICCC; Research Institute – Hospital Santa Creu i Sant Pau, IIB-Sant Pau, Barcelona, Spain

²Faculty of Medicine, University of Barcelona (UB), 08036 Barcelona, Spain

³Cardiology Department, Hospital Santa Creu i Sant Pau, Barcelona, Spain

⁴Centro de Investigación Biomédica en Red Cardiovascular (CIBERCV) Instituto de Salud Carlos III, Madrid, Spain; ⁵Cardiovascular Research Chair, UAB, Barcelona, Spain

***Correspondence:**

Dr Teresa Padro

tpadro@santpau.cat

Supplementary Table I: ADHF patients' characteristics in the discovery phase at hospital admission by 2 dimension electrophoresis

	All patients N=17	ADHF-NRF n=12	ADHF-RD n=5	P-value
DEMOGRAPHIC CHARACTERISTICS; median [IQR]				
Female/male, N	3/14	2/10	1/4	
Age, years	72.0 [69.0-76.0]	71.0 [63.5-76.5]	74.0 [71.0-75.0]	0.561
Weight, kg	75.8 [65.8-86.6]	82.1 [65.8-93.0]	73.0 [61.3-78.7]	0.322
KIDNEY FUNCTION MARKERS				
Creatinine, µmol/L	101 [73-131]	86 [66.5-103]	191 [147-197]	0.002
Glomerular filtration (MDRD-4)	68 [43.2-81.7]	73.6 [65.3-109.5]	32.2 [30.7-35.2]	0.002
Urea, mmol/L	9.0 [5.8-13.1]	6.5 [5.3-9.1]	23.1 [22.1-25.5]	0.002
CARDIAC FUNCTION MARKERS				
NT-proBNP, ng/L	2424 [1734-4570]	2094 [1346-4293]	2591 [2256-19677]	0.157
Left ventricular ejection fraction (LVEF), %	48.0 [33.0-56.0]	47.5 [34.0-58.0]	51.0 [33.0-55.0]	0.832
Preserved LVEF, N (%)	8 (47)	5 (42)	3 (60)	
Reduced LVEF, N (%)	6 (35)	4 (33)	2 (40)	0.462
Mid-range LVEF, N (%)	3 (18)	3 (25)	0 (0)	
Atrial fibrillation, N (%)	11 (65)	7 (58)	4 (80)	0.600
Cardiovascular disease, N (%)	4 (24)	2 (17)	2 (40)	0.538
OTHER BIOCHEMICAL MARKERS				
Haemoglobin, g/L	122 [106-139]	126 [114-141.5]	106 [104-121]	0.225
RISK FACTORS; N (%)				
Active smoking	3 (18)	3 (25)	0 (0)	>0.999
Hypertension	13 (77)	9 (75)	4 (80)	>0.999
Pulmonary hypertension	6 (35)	4 (33)	2 (40)	>0.999
Diabetes mellitus type 2	6 (35)	3 (25)	3 (60)	0.280
Dyslipidaemia	12 (71)	9 (67)	3 (60)	0.600
BACKGROUND MEDICATION; N (%)				
Diuretics	10 (59)	5 (42)	5 (100)	0.044
Statins	9 (53)	6 (35)	3 (60)	>0.999
Anticoagulants	9 (53)	5 (42)	4 (80)	0.294
Antiplatelet agents	7 (41)	5 (42)	2 (40)	>0.999
Beta-blockers	11 (65)	6 (50)	5 (100)	0.102
Antiarrhythmic agents	0 (0)	0 (0)	0 (0)	>0.999
Antidiabetics	4 (24)	1 (8)	3 (60)	0.053
Insulin	3 (18)	0 (0)	3 (60)	0.015
Oral antidiabetic agents	3 (18)	1 (8)	2 (40)	0.191
ACE inhibitor/ARB	13 (76)	9 (75)	4 (80)	>0.999

P values calculated with Fisher exact test, except for LVEF where χ^2 was used. Diuretics: hydrochlorothiazide, furosemide, eplerenone, and spironolactone. Statins: atorvastatin, pravastatin, simvastatin, ezetimibe, fenofibrates. Anticoagulants: warfarin, acenocumarol, bemiparin, heparin, tinzaparin, dabigatran, rivaroxaban, edoxaban, and apixaban. Antiplatelet agents: acetylsalicylic acid and clopidogrel. Beta-blockers: bisoprolol and carvedilol. Antiarrhythmic agents: amiodarone. Oral antidiabetic agents: metformin and repaglinide. Angiotensin-converting enzyme inhibitors (ACEI) include: captopril, enalapril, and ramipril. Angiotensin receptor blockers (ARB): losartan, olmesartan, and valsartan.

Supplementary Table II: Proteins associated to vitamin metabolism presenting a differential detection pattern in urine of ADFH at hospital admission.

Protein name	Gene name	Swiss Prot number	Theoretical pI	Molar weight (KDa)	MASCOT Score	Function
Retinol-binding protein 4	<i>RBP4</i>	P02753	5.27	23.0	66*	Vitamin A
Transthyretin	<i>TTR</i>	P02766	5.31	15.9	61*	
Vitamin D-binding protein	<i>GC</i>	P02774	5.22	21.5	72*	Vitamin D

Proteins identified by 2DE-MS/MS. MASCOT score refers to detection by MS/MS.

Supplementary Table III: Urine VDBP levels obtained by immunoassay according to patients' characteristics and risk factors at hospital admission.

	ADHF patients		ADHF-NRF		ADHF-RD	
	N	Median [IQR]	N	Median [IQR]	N	Median [IQR]
Sex						
Male	44	49.2 [12.3-125.7]	25	35.4 [12.0-78.0]	19	125.7 [32.6-227.5]
Female	20	47.2 [13.6-85.5]	9	41.6 [8.0-76.0]	11	54.5 [17.7-118.4]
<i>P value</i>		0.563		0.823		0.209
LVEF						
Reduced (<40%)	27	40.0 [20.5-97.3]	18	38.8 [20.8-71.6]	9	125.7 [12.0-161.2]
Mid-range (40-49%)	10	63.4 [26.9-141.3]	5	43.7 [23.4-74.0]	5	130.8 [46.7-270.6]
Preserved (>50%)	27	64.7 [10.3-108.4]	11	10.3[5.3-78.0]	16	76.6 [42.2-163.3]
<i>P value</i>		0.815		0.598		0.773
Atrial fibrillation						
No	32	43.6 [10.3-98.3]	17	30.2 [8.6-45.8]	15	91.7 [32.6-161.2]
Yes	31	71.6 [17.7-102.2]	16	71.6 [12.0-95.1]	15	73.6 [17.7-171.7]
<i>P value</i>		0.337		0.123		0.961
Cardiovascular disease						
No	44	46.4 [11.1-110.3]	24	30.2 [8.1-71.6]	20	91.7 [17.7-163.3]
Yes	20	55.5 [30.0-94.6]	10	45.4 [33.1-86.0]	10	64.7 [22.3-236.6]
<i>P value</i>		0.538		0.205		0.915
Arterial hypertension						
No	16	33.1 [10.3-57.1]	12	33.1 [8.6-45.7]	4	52.7 [12.8-120.7]
Yes	47	69.6 [20.2-125.7]	21	12.0 [41.6-94.0]	26	85.5 [32.6-180.5]
<i>P value</i>		0.085		0.383		0.375
Dyslipidaemia						
No	19	30.2 [8.6-91.7]	13	28.8 [8.6-45.8]	6	91.7 [13.6-279.1]
Yes	44	61.8 [20.2-118.4]	20	41.6 [12.0-94.0]	24	83.3 [32.6-163.3]
<i>P value</i>		0.212		0.313		0.852
Diabetes mellitus type II						
No	35	48.1 [12.0-99.4]	22	35.7 [8.3-67.6]	13	118.4 [47.1-161.2]
Yes	28	61.8 [20.2-171.7]	11	38.8 [20.8-76.0]	17	64.7 [12.3-180.5]
<i>P value</i>		0.635		0.572		0.594
Pulmonary hypertension						
No	48	49.2 [17.7-118.4]	26	40.0 [12.0-94.0]	22	85.5 [32.6-163.3]
Yes	16	45.8 [8.6-76.0]	8	27.4 [5.4-71.6]	8	76.7 [12.0-227.5]
<i>P value</i>		0.388		0.359		0.816

LVEF: left ventricular ejection fraction. Values given in ng VDBP/mg total protein.

Supplementary Table IV: Effect of background medication on urine VDBP levels in ADHF patients at hospital admission

	ADHF patients		ADHF-NRF		ADHF-RD	
	N	Median [IQR]	N	Median [IQR]	N	Median [IQR]
Diuretics						
No	16	41.6 [8.6-81.1]	13	30.2 [8.1-78.0]	3	220.9 [83.1-360.7]
Yes	48	49.2 [13.6-118.4]	21	40.0 [12.0-76.0]	27	85.5 [17.7-163.3]
<i>P value</i>		0.567		0.822		0.309
Statins						
No	23	38.0 [10.3-81.1]	16	25.2 [8.3-64.4]	7	96.4 [17.7-171.7]
Yes	41	55.5 [20.8-125.7]	18	41.1 [20.8-94.0]	23	85.5 [32.6-163.3]
<i>P value</i>		0.213		0.288		0.907
Anticoagulants						
No	38	45.7 [11.3-95.0]	20	34.5 [9.5-64.4]	18	74.4 [22.4-143.3]
Yes	26	62.6 [15.7-156.5]	14	41.1 [12.0-94.0]	12	149.7 [17.7-279.1]
<i>P value</i>		0.354		0.630		0.236
Antiplatelet agents						
No	28	44.7 [11.1-120.7]	15	11.1 [6.0-64.4]	13	88.6 [29.9-162.2]
Yes	36	55.5 [24.1-100.8]	19	41.6 [27.4-94.0]	17	81.1 [12.3-180.5]
<i>P value</i>		0.477		0.121		0.961
Beta-blockers						
No	20	47.1 [10.3-102.2]	13	12.0 [5.4-76.0]	7	122.0 [47.1-161.2]
Yes	44	49.2 [17.7-99.4]	21	41.3 [20.8-78.0]	23	81.1 [13.6-180.5]
<i>P value</i>		0.527		0.281		0.683
Antiarrhythmic agents						
No	58	44.4 [12.0-102.2]	30	30.2 [8.6-71.6]	28	85.5 [32.6-171.7]
Yes	6	62.6 [31.9-78.0]	4	62.6 [40.6-77.0]	2	83.7 [17.7-149.7]
<i>P value</i>		0.791		0.255		0.781
Antidiabetic agents						
No	39	46.5 [11.1-98.9]	26	30.2 [8.1-78.0]	13	118.4 [47.1-161.2]
Yes	25	64.7 [26.4-176.1]	8	55.2 [31.9-76.0]	17	64.7 [12.3-180.5]
<i>P value</i>		0.330		0.236		0.594
ACE inhibitor/ARB						
No	21	61.8 [13.6-161.2]	8	45.6 [8.6-78.0]	13	96.7 [29.9-176.1]
Yes	43	45.8 [12.3-95.1]	26	35.4 [12.0-76.0]	17	85.5 [12.3-163.3]
<i>P value</i>		0.452		>0.999		0.626

P values calculated using Mann-Whitney. Median values given in ng VDBP/mg total protein. Diuretics: hydrochlorothiazide, furosemide, eplerenone, and spironolactone. Statins: atorvastatin, pravastatin, simvastatin, ezetimibe, fenofibrates. Anticoagulants: warfarin, acenocumarol, bempiparin, heparin, tinzaparin, dabigatran, rivaroxaban, edoxaban, and apixaban. Antiplatelet agents: acetylsalicylic acid and clopidogrel. Beta-blockers: bisoprolol and carvedilol. Antiarrhythmic agents: amiodarone. Oral antidiabetic agents: metformin and repaglinide. Angiotensin-converting enzyme inhibitors (ACEI) include: captopril, enalapril, and ramipril. Angiotensin receptor blockers (ARB): losartan, olmesartan, and valsartan.

Supplementary Table V: Correlation values between VDBP and markers of renal function (GFR, Cystatin C) and kidney damage (KIM-1) in ADHF patients (N=64) at day 3 of hospitalisation.

VDBP				
	Correlation	Lower limit	Upper limit	P value
GFR	-0.396	-0.602	-0.141	0.003
Cystatin C	0.596	0.389	0.746	<0.001
KIM-1	0.477	0.237	0.662	<0.001

VDBP: Vitamin D Binding Protein; GFR: glomerular filtration rate; KIM-1: Kidney Injury Molecule 1

Supplementary Table VI: ROC (associated receiver operating characteristic) curve (AUC) analysis for determining discriminatory power of urine VDBP for incident AKI in ADHF patients at day 3 of hospitalisation.

A. ROC curves of urinary levels of VDBP, cystatin C, KIM-1, and the combination of all three proteins.

Protein	AUC Area	Error deviation	Lower limit	Upper limit	P-value
VDBP	0.579	0.105	0.374	0.783	<i>0.446</i>
CysC	0.476	0.105	0.270	0.682	<i>0.818</i>
KIM-1	0.487	0.103	0.284	0.690	<i>0.901</i>
CysC + KIM-1 + VDBP	0.711	0.089	0.536	0.885	<i>0.018</i>

VDBP: Vitamin D Binding Protein; CysC: Cystatin C; KIM1: Kidney Injury Molecule 1.

B. P values of the comparison of AUC for all three proteins and their combination.

	VDBP	CysC	KIM-1	CysC + KIM-1 + VDBP
VDBP		0.479	0.532	0.338
CysC	0.479		0.940	0.088
KIM-1	0.532	0.940		0.100
CysC + KIM-1 + VDBP	0.338	0.088	0.100	

VDBP: Vitamin D Binding Protein; CysC: Cystatin C; KIM1: Kidney Injury Molecule 1.

Supplementary Table VII: Urine Cystatin C levels according to patients' characteristics and risk factors at hospital admission.

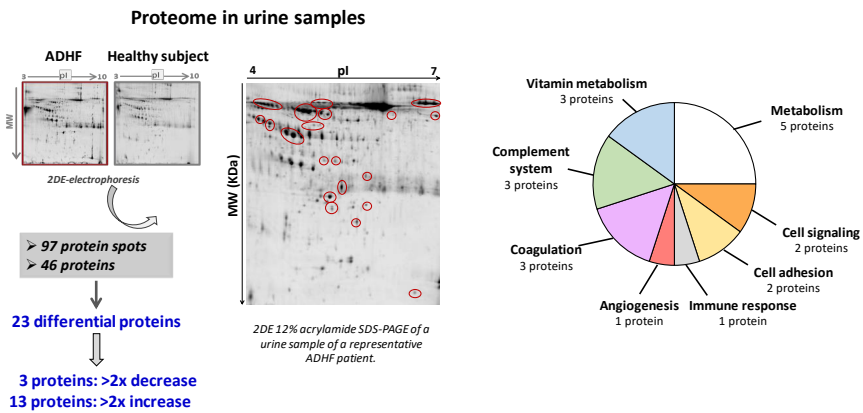
	ADHF patients		ADHF-NRF		ADHF-RD	
	N	Median [IQR]	N	Median [IQR]	N	Median [IQR]
Sex						
Male	44	3.97 [2.10-11.44]	25	3.12 [2.02-8.77]	19	9.03 [2.39-14.41]
Female	20	6.32 [2.74-9.84]	9	4.97 [2.08-8.86]	11	9.21 [4.85-20.75]
<i>P value</i>		0.438		0.760		0.763
LVEF						
Reduced (<40%)	27	5.86 [2.37-10.02]	18	3.97 [2.34-9.29]	9	9.03 [2.39-13.24]
Mid-range (40-49%)	10	4.33 [2.43-11.64]	5	2.43 [0.79-6.12]	5	9.79 [4.33-22.23]
Preserved (>50%)	27	5.52 [2.04-13.16]	11	3.38 [2.00-6.06]	16	9.21 [2.31-20.75]
<i>P value</i>		0.958		0.327		0.862
Atrial fibrillation						
No	32	4.33 [2.10-11.44]	17	2.73 [2.02-8.24]	15	9.03 [3.02-14.88]
Yes	31	4.97 [2.31-10.09]	16	3.97 [2.11-8.77]	15	9.21 [2.31-20.75]
<i>P value</i>		0.973		0.629		0.771
Cardiovascular disease						
No	44	4.75 [2.09-9.44]	24	2.73 [2.00-4.97]	20	9.03 [3.49-14.88]
Yes	20	9.56 [2.62-17.35]	10	9.69 [5.86-12.59]	10	6.43 [2.9-27.65]
<i>P value</i>		0.099		0.003		>0.999
Arterial hypertension						
No	16	5.46 [2.02-9.29]	12	4.73 [2.02-8.77]	4	7.40 [3.32-10.69]
Yes	47	5.07 [2.22-13.24]	21	2.85 [2.08-8.86]	26	9.03 [2.39-21.12]
<i>P value</i>		0.532		0.819		0.539
Dyslipidaemia						
No	19	8.24 [2.11-13.24]	13	7.15 [2.02-9.29]	6	11.44 [4.85-13.24]
Yes	44	4.66 [2.22-9.95]	20	2.85 [2.08-7.74]	24	8.81 [2.39-20.75]
<i>P value</i>		0.535		0.409		0.618
Diabetes mellitus type II						
No	35	7.74 [2.22-9.95]	22	3.06 [1.93-8.81]	13	9.95 [6.32-14.88]
Yes	28	3.97 [2.10-13.26]	11	3.97 [2.73-4.97]	17	4.09 [1.79-20.75]
<i>P value</i>		0.696		0.540		0.207
Pulmonary hypertension						
No	48	6.32 [2.22-13.26]	26	3.41 [2.02-8.86]	22	9.03 [3.49-21.12]
Yes	16	3.39 [2.11-9.29]	8	3.39 [2.11-6.06]	8	6.07 [1.79-11.44]
<i>P value</i>		0.233		0.760		0.180

LVEF: left ventricular ejection fraction. Median values given in µg CysC/mg total protein.

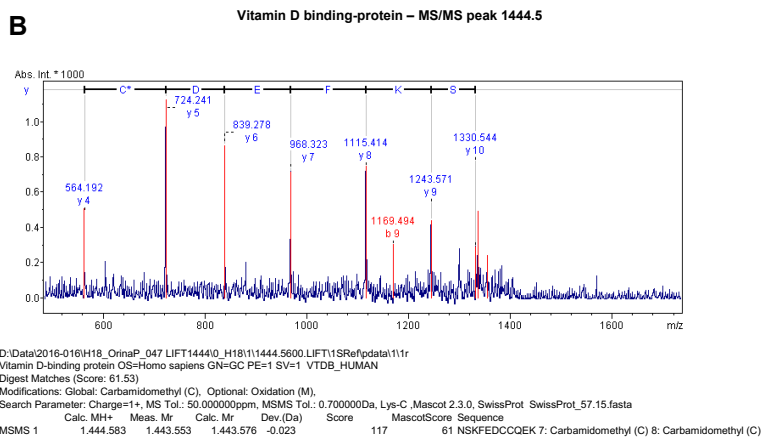
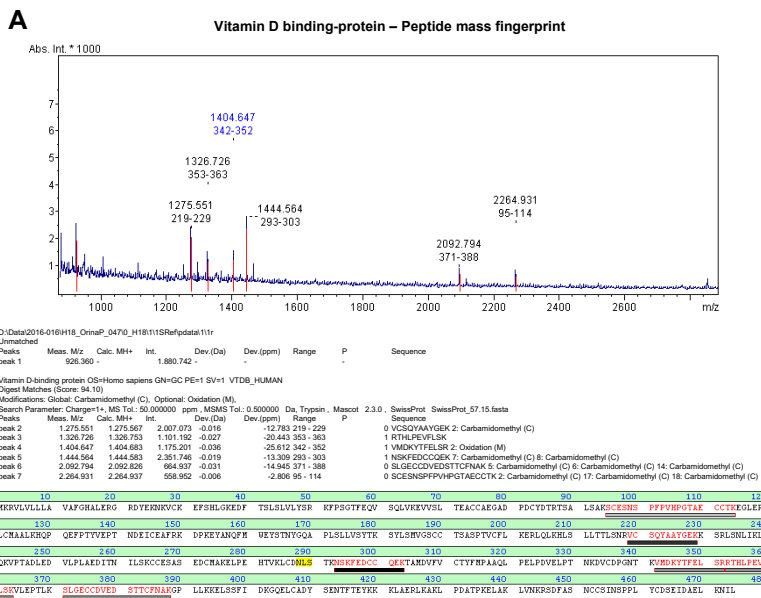
Supplementary Table VIII: Urine KIM-1 levels according to patients' characteristics and risk factors at day 3 of hospitalisation.

	ADHF patients		ADHF-NRF		ADHF-RD	
	N	Median [IQR]	N	Median [IQR]	N	Median [IQR]
Sex						
Male	44	181.0 [23.5-462.6]	25	53.6 [11.3-366.7]	19	383.5 [169.4-862.6]
Female	20	260.1 [41.3-897.2]	9	203.0 [17.4-1022.7]	11	352.4 [81.6-803.4]
<i>P</i> value		0.806		0.598		0.509
LVEF						
Reduced (<40%)	27	203.0 [29.4-803.4]	18	89.2 [11.3-366.7]	9	359.8 [121.8-803.4]
Mid-range (40-49%)	10	233.5 [81.6-467.2]	5	467.2 [21.3-1149.9]	5	232.7 [99.5-234.2]
Preserved (>50%)	27	216.9 [20.7-745.6]	11	20.7 [4.9-145.2]	16	568.7 [216.9-907.3]
<i>P</i> value		0.932		0.334		0.364
Atrial fibrillation						
No	32	259.4 [84.3-816.6]	17	203.0 [7.4-815.3]	15	408.8 [177.3-862.6]
Yes	31	114.0 [21.3-438.8]	16	39.1 [18.2-195.9]	15	352.4 [82.9-745.6]
<i>P</i> value		0.260		0.589		0.343
Cardiovascular disease						
No	44	133.5 [19.8-727.8]	24	23.0 [7.2-341.9]	20	328.0 [110.7-810.6]
Yes	20	322.2 [86.3-657.1]	10	224.8 [53.6-420.7]	10	438.8 [91.0-907.4]
<i>P</i> value		0.253		0.174		0.710
Arterial hypertension						
No	16	129.6 [9.3-416.9]	12	71.7 [7.2-291.7]	4	560.7 [186.3-1935.7]
Yes	47	234.2 [53.1-803.4]	21	53.6 [18.9-815.3]	26	359.8 [99.5-803.4]
<i>P</i> value		0.352		0.653		0.724
Dyslipidaemia						
No	19	81.6 [4.4-366.7]	13	18.9 [4.4-216.7]	6	294.0 [81.6-407.3]
Yes	44	240.4 [76.1-1006.8]	20	89.2 [21.0-1045.3]	24	438.8 [121.8-907.4]
<i>P</i> value		0.009		0.060		0.250
Diabetes mellitus type II						
No	35	246.6 [18.9-817.8]	22	87.3 [7.4-815.3]	13	407.3 [99.5-817.8]
Yes	28	169.4 [75.4-448.3]	11	53.6 [17.4-114.0]	17	356.1 [121.8-745.6]
<i>P</i> value		0.945		0.516		0.810
Pulmonary hypertension						
No	48	265.56 [68.27-903.1]	26	118.3 [21.3-815.3]	22	438.8 [232.7-990.9]
Yes	16	75.4 [5.7-312.1]	8	12.3 [4.2-66.4]	8	154.2 [75.4-576.4]
<i>P</i> value		0.016		0.026		0.071

LVEF: left ventricular ejection fraction. Median values given in pg KIM-1/mg total protein.



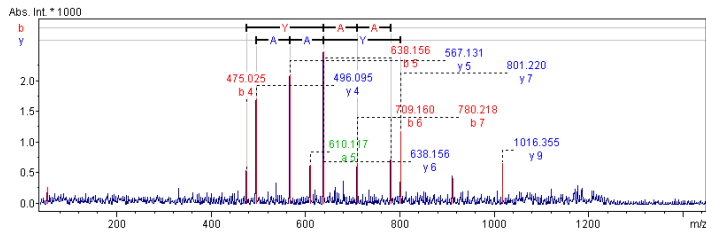
Supplementary Figure I: Distribution of differential proteins detected in 2-dimension electrophoresis gels (left), and on the right are the differential proteins distributed according to their different functions.



Supplementary Figure II: A) Peptide mass fingerprint of a representative VDBPspot. B) MS/MS analysis of peak 1444.5 of a representative VDBP spot.

C

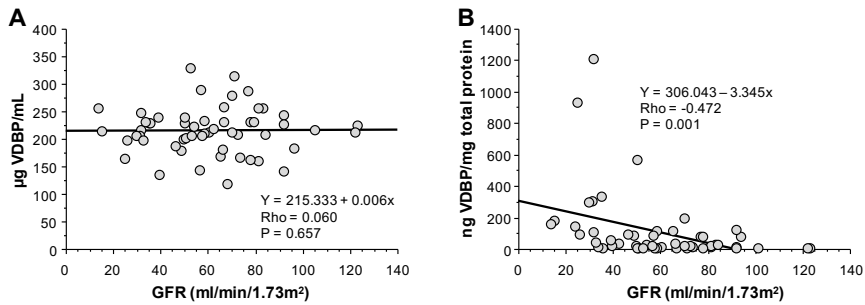
Vitamin D binding-protein – MS/MS peak 1275.5



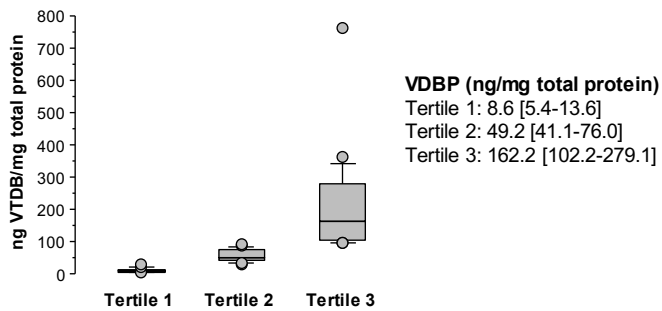
D:\Data\2016-016\H18_OrinaP_047 LIFT1275\0_H18\1\1275.5500.LIFT\1SRef\data\1\1r
 Vitamin D-binding protein OS=Homo sapiens OX=9606 GN=GC PE=1 SV=2 VTDB_HUMAN
 Digest Matches (Score: 41.86)
 Search Parameter: Charge=1+, MS Tol.:50.000000 ppm, MSMS Tol.:0.500000 Da, Trypsin, Mascot 2.7.0.7, SwissProt SwissProt_2021_02.fasta
 Modifications: Global: Carbamidomethyl (C), Optional: Oxidation (M),

MSMS	1	Calc. MH+	Meas. Mr	Calc. Mr	Dev.(Da)	Score	MascotScore	Sequence
		1,275.567	1,274.543	1,274.560	-0.017	24	41	VCSQYAA YG E K: Carbamidomethyl (C)

Supplementary Figure II (continued): C) MS/MS analysis of peak 1275.5 of a representative VDBP spot.

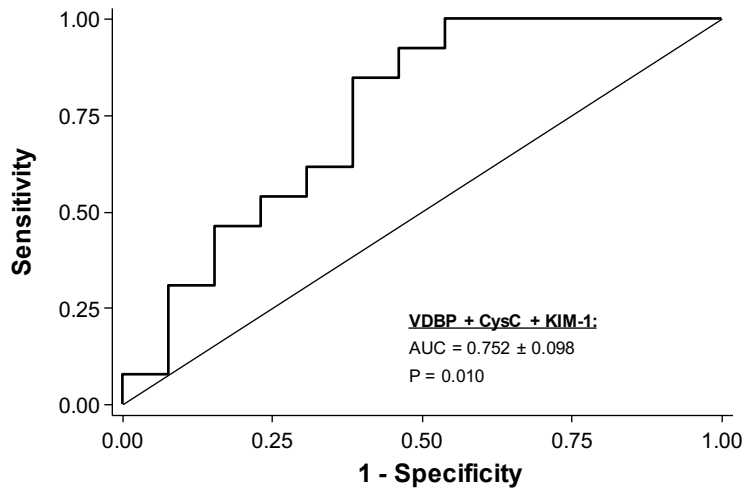


Supplementary Figure III: A) Serum VDBP levels did not correlate with GFR at day 3 of hospitalisation, however, urinary VDBP levels presented a statistically significant correlation with GFR at the same time point.



Diabetes patient distribution				
Total ADHF population (N=23)	7	9	7	} P value 0.789
NFR (N=9)	3	4	2	
RD (N=14)	4	5	5	

Supplementary Figure IV: diabetes distribution according VDBP tertiles in the ADHF population. Values at hospital admission for the total ADHF population and the groups of normal renal function (NRF) and renal dysfunction (RD) patients.



Protein	AUC Area	Error deviation	Lower limit	Upper limit	P-value
VDBP	0.579	0.105	0.374	0.783	0.446
CysC	0.476	0.105	0.270	0.682	0.818
KIM-1	0.487	0.103	0.284	0.690	0.901
CysC + KIM-1 + VDBP	0.711	0.089	0.536	0.885	0.018
Age	0.618	0.116	0.391	0.846	0.308
Age + CysC + KIM-1 + VDBP	0.728	0.109	0.515	0.941	0.036

VDBP: Vitamin D Binding Protein; CysC: Cystatin C; KIM1: Kidney Injury Molecule 1.

Supplementary Figure V: ROC characteristics of the VDBP, CysC and KIM-1 cluster for early discrimination of patients with renal deterioration compared to age.

5.4. Article 4

Alternative C3 Complement System: Lipids and Atherosclerosis

Maisa García-Arguinzonis; **Elisa Diaz-Riera**; Esther Peña; Rafael Escate; Oriol Juan-Babot; Pedro Mata; Lina Badimon; Teresa Padró

Published: International Journal of Molecular Sciences

Int. J. Mol. Sci. 2021, 22, 5122. <https://doi.org/10.3390/ijms22105122>

Objective: To investigate the role of complement C3 in association with lipoprotein levels in atherosclerosis progression and C3 effects on function and phenotype of vascular smooth muscle cells.

Highlights:

- Extracellular matrix of human atherosclerotic lesions presents a differential profile of the complement C3 cascade, with increased levels of C3 activation products.
- Activation products of C3 modulate adhesion and migration of vascular smooth muscle cells exposed to atherogenic conditions.



Article

Alternative C3 Complement System: Lipids and Atherosclerosis

Maisa Garcia-Arguinzonis ¹, Elisa Diaz-Riera ¹, Esther Peña ^{1,2}, Rafael Escate ^{1,2}, Oriol Juan-Babot ¹, Pedro Mata ³, Lina Badimon ^{1,2,4,†} and Teresa Padro ^{1,2,*,†}

¹ Cardiovascular Program-ICCC, Research Institute-Hospital Santa Creu i Sant Pau, IIB-Sant Pau, 08025 Barcelona, Spain; mgarciaar@santpau.cat (M.G.-A.); ediazr@santpau.cat (E.D.-R.); epena@santpau.cat (E.P.); rescate@santpau.cat (R.E.); ojuan@santpau.cat (O.J.-B.); lbadimon@santpau.cat (L.B.)

² Centro de Investigación Biomédica en Red Cardiovascular (CIBERCV), Instituto de Salud Carlos III, 28029 Madrid, Spain

³ Fundación Hipercolesterolemia Familiar, 28010 Madrid, Spain; pmata@colesterolfamiliar.org

⁴ Cardiovascular Research Chair, UAB, 08025 Barcelona, Spain

* Correspondence: tpadro@santpau.cat; Tel.: +34-935-565-886; Fax: +34-935-565-559

† Both authors contributed equally.



Citation: Garcia-Arguinzonis, M.; Diaz-Riera, E.; Peña, E.; Escate, R.; Juan-Babot, O.; Mata, P.; Badimon, L.; Padro, T. Alternative C3 Complement System: Lipids and Atherosclerosis. *Int. J. Mol. Sci.* **2021**, *22*, 5122. <https://doi.org/10.3390/ijms22105122>

Academic Editors: Maria I. Dorobantu and Maya Simionescu

Received: 17 April 2021

Accepted: 6 May 2021

Published: 12 May 2021

Publisher's Note: MDPI stays neutral with regard to jurisdictional claims in published maps and institutional affiliations.



Copyright: © 2021 by the authors. Licensee MDPI, Basel, Switzerland. This article is an open access article distributed under the terms and conditions of the Creative Commons Attribution (CC BY) license (<https://creativecommons.org/licenses/by/4.0/>).

Abstract: Familial hypercholesterolemia (FH) is increasingly associated with inflammation, a phenotype that persists despite treatment with lipid lowering therapies. The alternative C3 complement system (C3), as a key inflammatory mediator, seems to be involved in the atherosclerotic process; however, the relationship between C3 and lipids during plaque progression remains unknown. The aim of the study was to investigate by a systems biology approach the role of C3 in relation to lipoprotein levels during atherosclerosis (AT) progression and to gain a better understanding on the effects of C3 products on the phenotype and function of human lipid-loaded vascular smooth muscle cells (VSMCs). By mass spectrometry and differential proteomics, we found the extracellular matrix (ECM) of human aortas to be enriched in active components of the C3 complement system, with a significantly different proteomic signature in AT segments. Thus, C3 products were more abundant in AT-ECM than in macroscopically normal segments. Furthermore, circulating C3 levels were significantly elevated in FH patients with subclinical coronary AT, evidenced by computed tomographic angiography. However, no correlation was identified between circulating C3 levels and the increase in plaque burden, indicating a local regulation of the C3 in AT arteries. In cell culture studies of human VSMCs, we evidenced the expression of C3, C3aR (anaphylatoxin receptor) and the integrin $\alpha_M\beta_2$ receptor for C3b/iC3b (RT-PCR and Western blot). C3mRNA was up-regulated in lipid-loaded human VSMCs, and C3 protein significantly increased in cell culture supernatants, indicating that the C3 products in the AT-ECM have a local vessel-wall niche. Interestingly, C3a and iC3b (C3 active fragments) have functional effects on VSMCs, significantly reversing the inhibition of VSMC migration induced by aggregated LDL and stimulating cell spreading, organization of F-actin stress fibers and attachment during the adhesion of lipid-loaded human VSMCs. This study, by using a systems biology approach, identified molecular processes involving the C3 complement system in vascular remodeling and in the progression of advanced human atherosclerotic lesions.

Keywords: atherosclerosis; cardiovascular disease; complement system; proteomics; mass spectrometry

1. Introduction

Familial hypercholesterolemia (FH), an autosomal-dominant disorder mainly caused by the loss-of-function mutations in the low-density lipoprotein (LDL) receptor, is associated with an increased risk of atherosclerosis and ultimately premature cardiovascular event presentation, resulting in lifelong exposure to high-LDL cholesterol levels [1–5]. Increasing evidence suggests that FH patients recurrently present an inflammatory phenotype that is maintained despite treatment with lipid lowering therapies according to

guidelines [6–9]. We and others have demonstrated that adult FH patients have higher levels of extracellular microvesicles originating from inflammatory cells in plasma [6] as well as circulating mononuclear cells and monocyte-derived macrophages with inflammatory phenotypes [7,10].

The complement system is an important component of the innate immunity and plays a key role in the regulation of inflammation. Particularly relevant is the activation of the alternative C3 system, in which the different pathways of the complement system converge, leading to the formation of active C3 proteolytic products, C5 convertases and eventually the activation of the terminal complement proteins C5 to C9 and the formation of the membrane attack complex (MAC) [11,12]. The C3 system is tightly regulated by a cascade of components, including activators (Factor B), inhibitors (Factor H) and cell surface proteins acting as receptors (CR1, C3aR and $\alpha_M\beta_2$ integrin).

Atherosclerosis is widely recognized as a lipid-induced chronic inflammatory disease of the arterial wall with the activation of resident cells and recruitment of circulating leukocytes [13]. The complement system has been repeatedly associated with vascular remodeling [14] and atherosclerosis [15]. Results from experimental animal models and human samples suggest that complement activation may exert dual atheroprotective and proatherogenic effects mainly associated with the initial and terminal stages of the complement cascade, respectively [16,17]. However, the impact of the C3 complement system in atherogenesis is not fully understood.

C3 complement products and their cell receptors have been detected by immunohistochemistry in areas with atherosclerotic lesions of different severity in human arteries [18,19], which has led to the hypothesis that local activation of the alternative-complement system is involved in atherosclerotic plaque progression and complication [15]. In contrast, prior studies in mice models of atherosclerosis (*Ldlr*^{-/-} or *ApoE*^{-/-} *Ldlr*^{-/-} background) and knock-out C3 expression (*C3*^{-/-}) evidenced that atherosclerotic lesions developed in the absence of C3 have a lower content of vascular smooth muscle cells (VSMCs) and collagen, hallmark of vulnerable plaques, and are of a larger size than those plaques developed in animals with a sufficient content of C3 [20,21]. A potential effect of C3 on the proliferation of VSMCs during atherogenesis was suggested by a recent study, in *ApoE*^{-/-} mice fed a high-fat Western diet, in which dedifferentiated clonally expanding vascular SMC showed an up-regulated C3 expression [22] and also by prior results linking C3a with the increasing proliferation of mouse VSMCs [23].

Results from two recent studies evidenced a noticeable increase in arterial wall inflammation, assessed by fluorodeoxyglucose positron emission tomography imaging, in FH patients with high LDL levels with healthy controls [24,25]. The up-regulation of components of the complement cascade, including C3-derived products, have been reported in two studies in FH patients with no clinical evidence of coronary artery disease [23,26]. To date, however, we do not know whether circulating C3 levels relate to the intensity and profile of atherosclerotic plaque burden. Moreover, little is known regarding the interplay among LDL, C3 complement products and VSMCs, although VSMCs are the key cellular components in the development and complication of atherosclerotic lesions.

Therefore, the present study was conducted to investigate the relationship between circulating C3 complement, lipids and atherosclerotic plaque burden in FH patients with subclinical atherosclerosis. In addition, using a mass spectrometry-based proteomic approach, combined with transcriptomic analysis and in vitro functional assays, we analyzed the pattern of the C3 complement components in the extracellular matrix (ECM) of human atherosclerotic plaques and investigated C3 complement expression and effects on migration kinetics of lipid-loaded VSMCs.

2. Results

2.1. Characteristics of the FH Patient Population

FH patients from the SAFEHEART cohort were included ($N = 49$; 31 men and 18 women). The mean age was 44.7 ± 10.5 years (men: 45.4 ± 11.4 years; women

43.7 ± 9.2 years). The baseline demographic and clinical characteristics of the studied FH-population are shown in Table 1. All subjects were on lipid-lowering treatment (LLT) and treated with statins as per the guidelines for > 1 year (mean treated years before inclusion in the study were 14.9 ± 6.7 years). The mean LDL-cholesterol (LDL-C) in the FH group was 136.3 ± 36.0 mg/dL.

Table 1. Demographic, biochemical and clinical variables: Familial hypercholesterolemia and healthy subject groups.

	Familial Hypercholesterolemia n = 49	Healthy Subjects n = 28
Demographic Characteristics; mean ± SD		
Female/male, n	18/31	16/12
Age, years	38.6 ± 11.3	24.5 ± 4.6
Risk Factors; n (%)		
Smokers	14 (29)	12 (43)
Hypertension	1 (2)	0 (0)
Diabetes mellitus	0 (0)	0 (0)
Dyslipidaemia	48 (98)	0 (0)
Biochemical Data, Mean ± SD		
Total cholesterol, mg/dL	282 ± 72	170 ± 20
Triglycerides, mg/dL	104 ± 67	77 ± 35
HDL cholesterol, mg/dL	47 ± 11	56 ± 15
LDL cholesterol, mg/dL	221 ± 78	99 ± 15
Apo A1, mg/dL	135 ± 20	139 ± 29
Apo B, mg/dL	134 ± 41	61 ± 10
Lipoprotein(a), mg/dL	42 ± 35	18 ± 21
Glucose, mg/dL	89 ± 9	78 ± 9
C-reactive protein	1.86 ± 2.6	0.73 ± 0.2
Subclinical Atherosclerotic Disease; (%)		
Plaque burden, %	23.5 ± 6.3	-
Calcium burden, %	2.2 ± 2.5	-
Non-calcium burden	21.3 ± 5.3	-
Background Medication; n (%)		
Angiotensin-converting-enzyme inhibitors	0 (0)	0 (0)
Angiotensin II receptor blockers	1 (2)	0 (0)
Beta-blockers	0 (0)	0 (0)
Diuretics	2 (4)	0 (0)
Statins *	39 (80)	0 (0)

SD: standard deviation * Includes: rosuvastatin, ezetimibe, atorvastatin, simvastatin, lovastatin, pravastatin, Fluvastatin, pitavastatin, resins, and fibrates. Healthy subject population was used to establish the C3 range in a healthy group.

None of the FH patients had a clinical history of cardiovascular disease (CVD). Less than 5% of patients with FH presented hypertension or Type-2 diabetes. Eleven FH patients (22%) were active tobacco smokers. The mean value for 5- and 10-year CVD risk in the FH patients, according to the SAFEHEART-risk score (SAFEHEART-RS), was 1.00 ± 0.76 % and 2.13 ± 1.6 %, respectively.

All FH subjects included in the study presented subclinical atherosclerosis, assessed by computed tomographic angiography (CTA) and quantified by SAPC software [27]. The mean value for the total plaque burden was 23.5 ± 6.3% and, specifically, the median calcified plaque burden was 2.2 ± 2.5%, and that of non-calcified-plaque burden was 21.3 ± 5.3%. FH patients with plaque burden above the median values (high plaque burden) had a significantly higher estimated cardiovascular risk based on SAFEHEART-RS, both at 5 (0.77 ± 0.76% vs. 1.24 ± 0.15%; $p = 0.03$) and 10 years (1.65 ± 1.59% vs. 2.60 ± 0.15%; $p = 0.03$).

2.2. C3 Complement in Patients with Hypercholesterolemia and Subclinical Atherosclerosis

Circulating levels of C3 complement were significantly elevated ($p < 0.001$) in subjects with a genetic diagnosis of FH and subclinical coronary atherosclerosis, when compared to the plasma levels of C3 in young healthy subjects at low atherosclerotic risk (subjects without CV risk factors and age between 18 and 35 years) (Figure 1A). Plasma C3 complement levels were significantly correlated with LDL-C levels (Spearman correlation: Rho value = 0.412, $p < 0.001$), ApoB levels (Spearman correlation: Rho = 0.562, $p < 0.001$) and

Lp(a) (Spearman correlation: $Rho = 0.244$, $p = 0.034$) when the whole study population was considered (healthy subjects and FH patients) (Figure 1B). No significant correlation was found with other lipid variables, including triglycerides (Spearman correlation: $=0.021$, $p = 0.856$) and HDL-cholesterol (Spearman correlation: $Rho = -0.144$, $p = 0.213$). Levels of circulating C3 in FH patients did not significantly vary in relation to the severity of total-plaque burden (Figure 1C). Circulating levels of C-reactive protein (CRP) in FH patients were below 1mg/L in all subjects (median [IQR] mg/L: 0.035[0.020–0.258]).

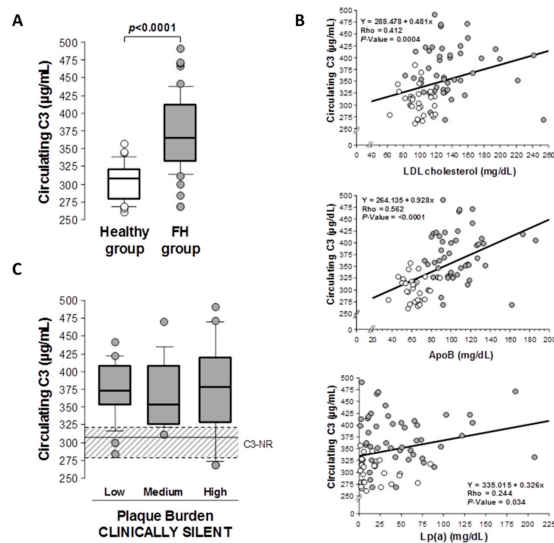


Figure 1. Circulating C3 complement in patients with hypercholesterolemia and subclinical atherosclerosis. (A) Plasma circulating C3 complement ($\mu\text{g/mL}$) in subjects with genetic diagnosis of FH and subclinical atherosclerosis ($n = 49$) compared to levels in a young healthy population ($n = 28$). (B) Correlation between plasma C3 levels and LDL-C, ApoB and Lp(a) levels in the study population (FH patients with subclinical atherosclerosis and healthy population). (C) Circulating C3 complement by plaque burden tertiles in FH patients. Dashed box (C3-NR) indicates the normal range of C3 levels in a healthy population ($n = 28$). Results are shown as median \pm SE. $p < 0.05$ was considered statistically significant (Mann-Whitney and Kruskal-Wallis tests).

2.3. C3 Alternative System Components in Human Advanced Atherosclerotic Lesions

Human atherosclerotic aortas were obtained from the Eulalia Study Biobank (ICCC) [28]. The extracellular matrix (ECM) of human aortas was enriched in active components of the C3 system with a significantly different proteomic signature in atherosclerotic areas when compared to lesion-free segments. Specifically, by two-dimensional electrophoresis (2DE) and MS/MS (MALDI-ToF/ToF), the complement-protein C3 was consistently identified as two independent spots (s1 and s2) in the ECM of atherosclerotic lesions (Figure 2A and Figure S1), whereas only weaker or non-consistent signals for s1 and s2 were identified in the ECM of aortic segments without macroscopic evidence of atherosclerotic lesions. When analyzed by Western blot (Figure 2B), protein extracts from aortic ECM showed three different C3-positive bands corresponding, based on their molecular size, to the full-length molecule (185 kDa), the C3 α -chain (113 kDa, obtained after proteolytic loss of a four-arginine peptide) and the final proteolytic product C3c-fragment

(39.5 kDa, α -chain). ECM extracts from atherosclerotic (AT) segments had >3-fold higher intensity in the C3-positive bands than protein extracts from non-lesion (nL) segments (AT vs. nL: $p < 0.05$ for intensity differences for each protein band).

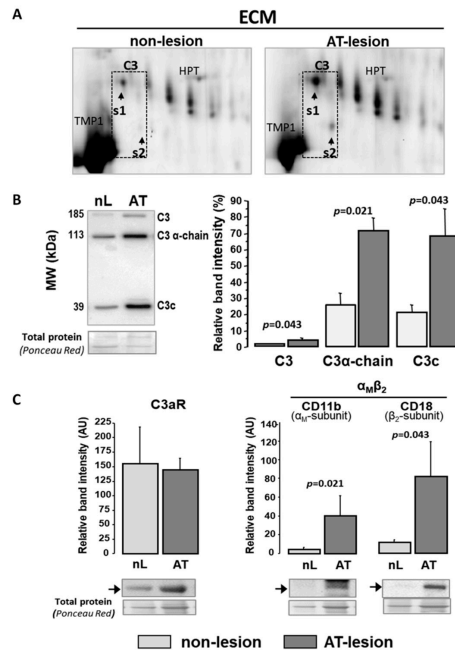


Figure 2. C3 complement components in human atherosclerotic lesions. (A) Representative 2D-gel images for protein extracts from normal and atherosclerotic ECM of human aortas ($n = 3$ independent with nL and AT segments). Arrow heads indicate position of spots identified as C3 by MALDI-ToF/ToF (Mascot score = 82). Tropomyosin-1 (TMP1) and Haptoglobin (HPT) are indicated as landmarks. (B,C) Western Blot analysis for C3 and C3 receptors in total extracts from non-lesion (nL) and atherosclerotic (AT) segments of human aortas ($n = 4$ independent arteries with nL and AT segments). (B) denotes C3 activation products, and C refers to receptors C3aR and $\alpha_M\beta_2$ for C3a and iC3b/C3b (C3 activation products). Band relative intensity was normalized against total protein, visualized with Ponceau Red staining and expressed as mean \pm SEM. The antibody against C3 recognizes complete full-length C3 (C3), C3 α -chain (C3 α -chain) and C3 α -chain-fragment 2 from C3c (C3c), product of degradation of iC3b. $p < 0.05$ was considered statistically significant (Mann–Whitney test).

Moreover, C3-activated fragment receptors were consistently detected in the cell-protein fraction (SDS fraction) of aortic extracts, both from control and atherosclerotic areas (Figure 2C). Western blot analysis showed significantly higher levels of the α_M and β_2 subunits (CD11b and CD18, respectively) of the integrin $\alpha_M\beta_2$ (iC3b/C3b receptor) in atherosclerotic segments, whereas the expression level of the anaphylatoxin C3a receptor (C3aR) did not significantly differ between non-lesion and atherosclerotic aortic segments (Figure 2C).

2DE-MS/MS analysis of human aortic ECM also evidenced the presence of C3 system regulatory components (Figure 3A), including the complement factor H (CFH) and CFH-related proteins CFHR1 and CFHR5. CFHR1 and CFHR5 were identified as two independent clusters of 7 and 4 spots (MW of 37–40 and 55 kDa), respectively. CFHR1 and CFHR5 clusters showed 2.5- and 3.8-fold (average of cluster spots) higher labeling signals in the ECM samples from atherosclerotic segments than those from normal aortic tissue (Table 2) and a different spot pattern distribution in normal and atherosclerotic segments of the aortic vessel wall (see Figure 3A). In addition, the complement component C5 (detected as α -chain) and its proteolytic products were consistently found in the aortic vessel wall, regardless of the presence of atherosclerotic lesions (Figure 3C). It is worth noting that the relative abundance of C5 fragmentation products (C5 α 1 and C5 α 1-1) was lower in atherosclerotic than in apparently normal segments.

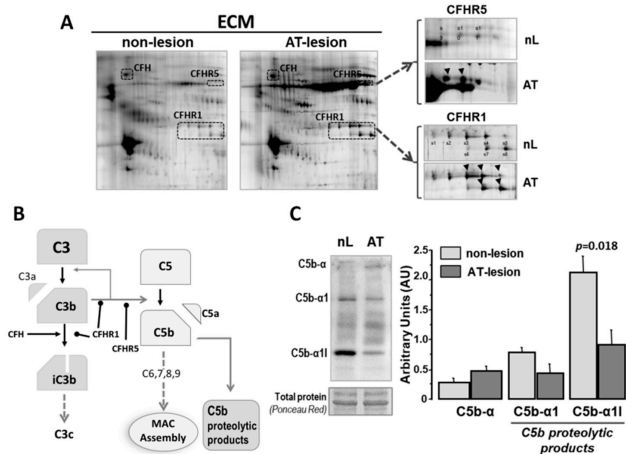


Figure 3. C3 complement regulatory components in human atherosclerotic lesions. (A) Representative 2D-gel images ($n = 3$ independent with nL- and AT segments) of the proteomic pattern corresponding to CFH, CFHR1 (s1 to s8) and CFHR5 (s9 to s11). Arrows indicate spots with significantly increased expression in AT-lesion samples (See Table 2). (B) Scheme of the proteolytic C3 cascade indicating steps regulated by CFHRs. (C) Western blot analysis of C5 α chain proteolysis products in total extracts from non-lesion (nL) and atherosclerotic (AT) segments of human aortas ($n = 4$ independent arteries with nL and AT segments). Bars refer to arbitrary units of volume intensity in the Western blot bands (Mean \pm SEM). Significance ($p < 0.05$, Mann–Whitney test) is indicated.

Table 2. C3 complement-system proteins identified on advanced atherosclerotic-lesion human aortas.

Fraction	Protein	UniProt-Code	Gene-Code	MS-Score *	Seq/Int Cov. (%) *	MW (kDa)	pI-Value	Fold-Change
sb-ECM	Complement Factor H	P08603	CFH	102	9.9/78.4	143.7	6.20	\approx (1.2)
Sb-ECM	Complement Factor H-related protein 1	Q03591	CFHR1	120	28.2/95.3	38.8	8.70	\uparrow (2.4)
Sb-ECM	Complement Factor H-related protein 5 **	Q9BXR6	CFHR5	28	–	66.4	7.00	\uparrow (3.9)
Lb-ECM	Complement C3	P01024	C3	83	9.4/76.7	188.6	6.00	\uparrow (2.9)

Proteins were identified by peptide mass fingerprint and confirmed by MS/MS by MALDI ToF/ToF. * Mascot Score, sequence and intensity coverage are expressed as representative values. ** Only identified by MS/MS.

2.4. C3 Alternative Pathway Components Expression in Vascular Wall Resident Cells

Complement factor C3 was consistently transcribed by human VSMCs (hVSMCs), and C3mRNA levels were up-regulated (1.7-fold, $p < 0.05$; Figure 4A) in lipid-loaded hVSMCs (24 h exposure to 100 $\mu\text{g}/\text{mL}$ aggregated LDL agLDL). The significant protein expression of C3, receptor C3aR (anaphylatoxin receptor) and integrin $\alpha_M\beta_2$ (CD11b/CD18) receptor for C3b/iC3b was also observed in hVSMCs (Figure 4B). In contrast, agLDL did not significantly affect the protein expression levels of the cell membrane receptors C3aR and integrin $\alpha_M\beta_2$ (Figure 4C). Interestingly, the protein levels of C3 (C3 α -chain) were significantly increased in cell culture supernatants when hVSMCs were incubated in the presence of agLDL (Figure 4B). All together, these results indicate that there is a local synthesis of C3 components that were released to the ECM of atherosclerotic plaques.

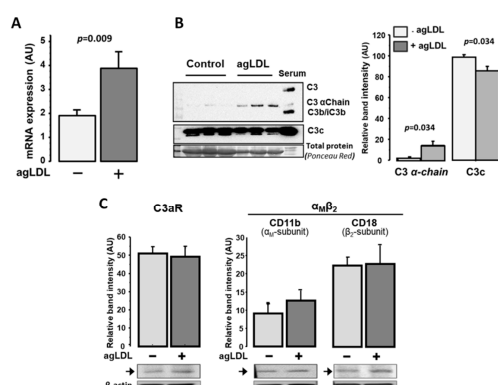


Figure 4. C3 alternative pathway components expression in human VSMCs. (A) mRNA quantification by real-time PCR using specific primers for human C3 in human VSMCs treated with or without agLDL (100 $\mu\text{g}/\text{mL}$). (B) Protein levels of C3 and C3-derived products in the supernatant of hVSMCs treated with or without agLDL (100 $\mu\text{g}/\text{mL}$). Human serum (Serum) was used as a positive control for C3 ($n = 3$ independent experiments). (C) Western blot analysis for C3a receptor (C3aR) and $\alpha_M\beta_2$ (C11b/CD18) integrin (receptor for C3b/iC3b) in lysates of hVSMCs incubated with or without agLDL (100 $\mu\text{g}/\text{mL}$). Band intensity is given in arbitrary units as mean \pm SEM and statistical significance ($p < 0.05$, Mann–Whitney test) is indicated ($n = 4$ independent experiments).

2.5. Exogenous C3 Proteolytic Products, AgLDL and VSMC Function

Lipid-loaded VSMCs have an impaired migration rate and cell attachment dynamics [29–31]. As shown in Figure 5, exogenously added C3 proteolytic products (10 nM C3a or 100 nM iC3b) partially reversed the impairment of the human VSMC (hVSMC) repair function induced by aggregated LDL (agLDL) to levels that did not differ significantly from the wound repairing capacity of hVSMC control cells. C3a induced a significant increase in the migrating capacity of lipid-loaded hVSMCs into the wound area. A similar trend, although non-significant, was observed with iC3b. C3 proteolytic products did not affect the wound-repairing capacity of control VSMCs (not exposed to agLDL).

Moreover, the addition of iC3b (100nM) to hVSMCs in adhesion experiments induced a significant increase in the attachment capacity of the cells, both in the absence and presence of agLDL. The effect was more evident (higher percentage of increase) and more prolonged in time (up to 2 h after seeding) in the lipid-loaded hVSMCs compared to cells not exposed to agLDL (Table 3). In addition, exogenously added iC3b enhanced the organization of the F-actin cytoskeleton during cell adhesion. This was especially evident in hVSMCs exposed

to agLDL that otherwise did not show any organized net of actin fibers (F-actin positive), 60 min after seeding (Figure 6).

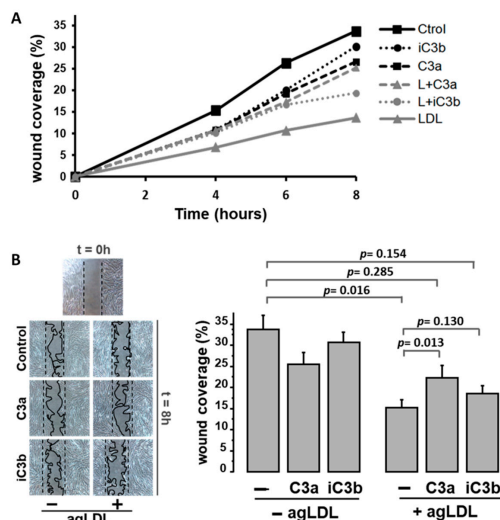


Figure 5. Effects of exogenous C3 proteolytic products on migration of human lipid-loaded hVSMCs. Results for wound coverage (%) in an in vitro model of wound repairing of FCS-stimulated hVSMCs treated with/without agLDL (100 µg/mL) in the presence or absence of C3a (10 nM) or iC3b (100 nM), (*n* = 6 independent experiments in duplicates). (A) Time-course for wound coverage by hVSMCs. *Control* and *LDL*: cells incubated in the absence of C3 products, without or with agLDL, respectively. *iC3b* and *L+iC3b*: cells incubated with iC3b without or with agLDL. *C3a* and *L+C3a*: cells incubated with C3a without or with agLDL. (B) Representative microphotographs of wound-repairing model by hVSMCs taken at 0 and 8 h after inducing double-side injury. Bar diagrams refer to quantitative values for the % of wound covered area after 8 h injury. Band intensity is given in arbitrary units as mean ± SEM (*n* = 6 independent experiments in duplicates). *p* < 0.05 was considered statistically significant (Mann–Whitney and Kruskal–Wallis tests).

Table 3. Effect of iC3b on cell adhesion capacity in the absence and presence of agLDL.

	Control		+iC3b		
			30 min	60 min	120 min
-agLDL	100.0 ± 0.0		93.9 ± 4.4	115.9 ± 4.8 *	93.7 ± 14.0
+agLDL	100.0 ± 0.0		65.4 ± 1.8	122.0 ± 2.6	177.1 ± 42.3 *

Results refer to the number of attached cells from a total of 1×10^5 seeded cells, expressed as percentage of attached cells in the groups non-receiving iC3b (controls). Cell viability was in all cases >95% as determined by trypan blue staining. Results are given as mean ± SD of three independent experiments in duplicates. * *p*-values for comparison (Mann–Whitney test) between cells with/without agLDL -/+ addition of exogenous iC3b at 3 different time points. * *p* < 0.05.

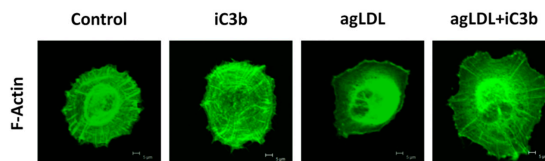


Figure 6. iC3b induces actin fiber polymerization and cytoskeleton rearrangement in hVSMCs exposed to agLDL. Confocal microscopy images of attached hVSMCs, 60 min after seeding. Representative photomicrographs of control cells and agLDL treated cells, in the presence/absence of exogenous iC3b (100 nM). Cells were labelled for F-actin with Alexa Cy3 488-phalloidin.

3. Discussion

The C3 complement system is an important mediator of innate immunity responses and a key component of the complement system. Accumulating evidence indicates that high levels of C3 account for an increased risk of cardiovascular disease in humans [19,22,32] especially in patients with metabolic pathologies [33]. To date, however, most of the studies addressed to investigate the involvement of the complement system in the atherosclerotic process have focused on the C5b-derived terminal pathway of the complement system (reviewed in [14,15]).

Previous studies primarily employed immunohistochemistry to localize C3 components in the human atherosclerotic vessel wall [18,19]. Here, using mass spectrometry-based proteomics, we identified a differential protein signature of the alternative C3 complement system in the intima layer of atherosclerotic lesions compared to macroscopically apparent normal segments of human aortas. It is important to note that the sequential protein extraction method used in this study made it possible to separately investigate proteins located in the extracellular matrix (ECM) and those in the cellular fraction of the intima. Using this approach, we revealed an enrichment of the C3 complement proteolytic products and regulators of the C3 cascade, such as the factor H/CFHR family in the matrisome (subset of non-structural regulatory proteins) of the human atherosclerotic ECM.

In addition to being a structural support to provide cell anchorage, the components of the ECM interact with vascular resident and infiltrated cells, regulating their phenotype and function [34]. Thus, our results strongly suggest that the C3 complement components present in the atherosclerotic ECM are key players in the outside-in signaling that occurs in key vascular cells involved in atherosclerosis progression. In agreement, we and others [35,36] have consistently identified anaphylatoxin receptors in human atherosclerotic arteries. In addition, this study evidenced increased levels of $\alpha_M\beta_2$ integrin in the cell fraction of atherosclerotic lesions, supporting the relevance of the iC3b/C3b-mediated signaling in the atherosclerotic process.

An unresolved question, with apparently controversial findings to date, refers to the origin of the vascular components of the alternative complement system since the C3 complement is mainly synthesized in the liver [37,38]. In the present study, we evidenced elevated levels of circulating C3 in clinically asymptomatic patients with genetic diagnosis of FH and subclinical atherosclerosis (assessed by CTA) when compared with plasma levels in young healthy subjects, suggesting a maintained activation of the innate immune response in FH, although all patients were long-term treated with LLT as per the guidelines [27]. Interestingly, these results extend our own previous findings reporting on higher levels of cMVs derived from inflammatory cells, specifically monocyte- and lymphocyte-derived cMVs, in FH patients under long-term LLT [6]. In this respect, monocyte/macrophage has been described to express complement proteins in response to several pro-atherogenic conditions, including high levels of cholesterol [39]. It is worth noting, however, that all FH patients in our study had circulating levels of CRP below 1mg/L, showing very low systemic inflammation which might be related to the fact that all patients were treated according to the guidelines with the highest LLT for more than one

year, and they had a well-compensated lipid profile. Further studies might help to gain a better understanding of the association between immune cell activation and inflammatory markers in heterozygous FH patients and their relevance for disease progression.

Plasmatic C3 was positively correlated with levels of LDL-C and Apo-B in the whole population under study (healthy subjects and FH patients), whereas no correlation was found with other lipid components, such as triglycerides and HDL-C. In agreement, a previous study based on two-dimensional electrophoresis analysis of serum samples from four FH patients and four healthy subjects identified a protein spot as C3 in the serum of FH patients and reported a positive correlation between levels of the C3a product and total plasma cholesterol [23]. From our results in FH patients, we could not exclude that the higher content of C3 in the atherosclerotic ECM results from the LDL flux into the intimal arterial wall and the retention of ApoB-rich lipoprotein particles in the intimal ECM space by binding to proteoglycans, which in turn favors their modification to form aggregates (agLDL) [40,41]. However, in the present study, although we found a local C3 accumulation in the atherosclerotic ECM of human aortas, the levels of C3 in the systemic circulation do not seem to be a sensitive measure of the plaque burden severity measured by CTA imaging in FH patients with subclinical coronary atherosclerosis. This finding prompts us to hypothesize that vascular resident cells may represent a main source of C3 in human atherosclerotic plaques.

Supporting our view, experimental studies on hyperlipidemic Apolipoprotein-E knockout (ApoE-KO) mice fed a high-fat diet evidenced C3mRNA up-regulation in aortic tissue, even before atherosclerotic plaque formation [23]. Interestingly, clonally expanding SMC, recently linked to neointimal formation and atherosclerotic plaque pathogenesis [42,43], overexpressed C3 complement factor in *ApoE*^{-/-} mice fed a high-fat Western diet [22]. Due to the post-mortem condition of the aortic samples, we could not analyze mRNA expression in the human atherosclerotic lesions in the present study, but we evidenced that cultured human VSMCs express C3mRNA and that C3 complement is consistently over-expressed when cells are exposed to atherogenic agLDL for 24 h periods. In agreement with this, supernatants of lipid-loaded cells were enriched in the C3 α chain, a C3 form that was not present in the agLDL, but significantly increased in the atherosclerotic ECM of human aortas, supporting the relevance of VSMCs as a source of C3 complement active forms in the lesions. In contrast, the C3c fragments detected in the atherosclerotic intimal ECM seem mainly to have a systemic origin, entering the arterial intima through the LDL. Indeed, the serum showed a strong signal for C3c fragments, the final proteolysis product derived from C3 complement activation, when analyzed by Western blot, and a similar fragment was also found in purified agLDL (Figure S2). C3c has been described as a biomarker of heart failure [44], periodontitis [45] or amyotrophic lateral sclerosis [46], but its role and function needs to be further investigated.

As shown by Wang et al., C3 expressed by the clonal SMC induced proatherogenic effects, including the paracrine regulation of macrophage inflammation and autocrine-induced SMC proliferation [22]. Among the C3 proteolytic fragments resulting from the C3 cascade activation, C3a and iC3b/C3b are widely recognized as highly bioactive molecules directly involved in the regulation of cell phenotype and function [47]. In particular, C3a has been described to act as a chemoattractant for neural crest cells [48] and, through its receptor C3aR, to control leukocyte recruitment and endothelial activation in cerebral microvessel inflammation [49].

We previously described that agLDL, resembling the LDL retained and aggregated in the ECM of the intimal layer in areas with atherosclerosis [40,50,51], is internalized by human VSMCs, inducing changes in their phenotype and impairing cell functions, such as adhesion and migration, mainly mediated by effects on actin-cytoskeleton dynamics and organization [31,52,53]. In the present study, we demonstrate that the inhibitory effect of agLDL on VSMC migration is ameliorated by the presence of exogenous C3a to a level that did not significantly differ from the migration capacity of the control group (non-exposed to agLDL) in an in vitro wound healing assay. Interestingly, C3a did not

show a similar enhancing effect of cell migration in the control hVSMCs. Similarly, we found that exogenously added- iC3b promoted attachment during the cell adhesion and reorganization of the F-actin cytoskeleton network. This effect was more evident and maintained in lipid-loaded cells that otherwise would not present any organized actin cytoskeleton shortly after seeding.

In summary, our results demonstrated for the first time the presence and differential abundance of active products of the C3 system in the ECM of human atherosclerotic lesions. In addition, we provided evidence of the capacity of C3-derived products, beyond their well-known role in inflammation and immunity, to modulate the migratory and repair function of VSMCs that is impaired by LDL. These results suggest the C3 complement pathway is a novel player in vascular remodeling and in the progression of advanced human atherosclerotic lesions.

4. Materials and Methods

4.1. Human Samples

4.1.1. Subjects with Familial Hypercholesterolemia and Healthy Volunteers

The present study included 49 subjects with a genetic diagnosis of heterozygous familial hypercholesterolemia (FH) and thus lifelong exposure to high LDL plasma levels and high risk of premature atherosclerosis from the SAFEHEART cohort. A group of young healthy volunteers (non-FH subjects, $N = 28$) from the same cohort was used as reference group to establish the normal plasma range of C3 levels in a healthy population, at very low risk of presenting subclinical atherosclerosis. Demographic and clinical data of the FH patients and the healthy volunteers are provided in Table 1 and Table S1. Neither the FH nor the healthy group included pregnant subjects. Cases of sepsis or infections and with history of cancer or suspected clinical cardiovascular events were excluded. This part of the study was approved by the Local Ethics Committee for Clinical Investigation in the Fundación Jiménez Díaz (CEIC-FJD; Madrid, Spain) (protocol number: 01/09) and was conducted according to the Declaration of Helsinki (2013), and written informed consent was obtained from all participants [54].

Coronary atherosclerotic plaque characterization was performed by computed tomographic angiography (CTA), as previously described [27]. Coronary atherosclerotic-plaque burden was characterized and quantified using the SAPC (QAngio CT (Research Edition V2.1.16.1; Medis Specials, Leiden, The Netherlands) software. SAPC measurements were performed by a blinded operator, unaware of any clinical or biochemical data. [27].

4.1.2. Aortas and Coronary Arteries

Abdominal aortic tissue was obtained from the Biobank of the Eulalia Study on out-of-hospital sudden death [28]. Autopsy was performed within 18 h after death (age 34–79 years old) following the established forensic protocol [55,56], and the study was approved by the Institutional Ethical Committee for Clinical Investigation (Hospital Santa Creu i Sant Pau; Barcelona, Spain). The samples were processed immediately. After the removal of connective tissue and adherent blood, the specimens were divided into grossly homogeneous parts. Aortic wall segments were classified by their macroscopic appearance according to the presence and severity of atherosclerotic lesions. In this study, we compared macroscopically normal-appearing areas with atherosclerotic plaques (raised white or yellow-white plaques) obtained from the same artery ($N = 4$ individual aortas). From all segments, the intima layer was dissected from the media, snap-frozen in liquid N_2 and stored at $-80\text{ }^{\circ}\text{C}$.

To confirm the validity of the macroscopic classification, representative samples of each type of segment were examined histologically. To this aim, segments from each aortic tissue were embedded with paraffin, and $5\mu\text{M}$ sections were stained with Masson's trichrome to identify cellular areas (Figure S3). The images were captured with an Olympus microscope Vanox AHB3 (Hamburg, Germany) coupled with a Sony 3CCD color video camera and processed using Visilog (Sony ESPAC, San Jose, CA, USA) software (version 4.1.5).

4.1.3. VSMC Culture and LDL Preparation

Primary human VSMCs (Cell Application, Inc., San Diego, CA, USA) were cultured in M199 medium containing 20% FBS and used between passage four and seven, as previously described [30]. Unless otherwise indicated, experiments were performed in subconfluent monolayers after incubation without or with aggregated LDL (agLDL; 100 µg/mL) for 16 h.

Human LDLs (density 1.019–1.063 g/mL) were purified by ultracentrifugation from pooled sera of normocholesterolemic volunteers, and agLDLs were generated by vortexing LDL (1 mg/mL), according to the initial method described by Guyton et al. [57] and as previously performed in our group [58]. This method has been shown to produce similar LDL aggregation as LDL versican incubation [59].

LDL protein concentration was determined using the bicinchoninic acid (BCA)-method (ThermoFisher, Rockford, IL, USA) and LDL purity assessed by agarose gel electrophoresis (SAS-MX Lipo-kit, Helena Biosciences, Gateheads, UK). LDL preparations were tested to exclude the presence of endotoxin (Limulus amoebocyte lysate test, BioWhittaker, Walkersville, MD, USA) and potential bacterial contamination that could derive in confounding results, and this proved to be negative in all cases. LDLs used in the experiments were less than 48 h old. LDL oxidation in all LDL preparations was excluded by assessing thiobarbituric-acid-reactive substance (TBARS) formation, according to Ohkawa et al. [60] with slight modifications [61].

4.2. Tissue Processing and Extraction of ECM Proteins

Aortic ECM proteins were extracted according to Didangelos et al. [62]. Briefly, 300 mg segments of aortic tissue (intima layer) were diced in 8–10 pieces (approximately $2 \times 2 \text{ mm}^2$ size) and washed 5 times with PBS containing 25 mM EDTA. ECM-soluble proteins were obtained by incubating the aortic samples for 4 h at room temperature (RT) under mild agitation at 800 rpm, with 0.5 M NaCl, 10 mM Tris (pH 7.5), supplemented with 25 mM EDTA (10:1 buffer volume to tissue weight). Tissue pieces were left to drop. Then, the supernatant was collected, cleaned up with desalting Zeba-Spin columns (ThermoFisher, Rockford, IL, USA) and precipitated overnight with 5 volumes of chilled 100% acetone at -20°C . Proteins were re-dissolved in deglycosylation buffer (NaCl 150 mM; sodium acetate 50 mM; EDTA 10 mM, supplemented with 0.05 units of Heparinasell; Chondroitinase ABC and Endo- β -Galactosidase). Then, tissue samples were incubated with 0.08% SDS (10:1 buffer volume to tissue weight) and 25 mM EDTA for a further 4 h (RT, mild agitation at 800 rpm). SDS supernatant was collected. Thereafter, tissue pieces were incubated for 48 h in guanidine-HCl buffer (4 M guanidine-HCl, 50 mM sodium acetate, pH 5.8 supplemented with 25 mM EDTA). After removing the guanidine with 100% ethanol, samples were centrifuged at $16,000 \times g$ (10 min) and stored at -80°C . All buffers contained protease inhibitors (1 tablet/50 mL, Complete-EDTA free Roche) and phosphatase inhibitors (1%). Reagents were obtained from Sigma-Aldrich ((Merck KGaA, Darmstadt, Germany). The purity of each fraction was confirmed by Western blot with specific antibodies against β -actin (ab8228, Abcam, 1/1000); ColI (ab6308, Abcam, 1/1000) and AEBP1 (#250461, Antibodies Online, 1/500; Aachen, Germany), that specifically partitioned in the NaCl-, SDS- and guanidin-HCl-fractions (Figure S4).

4.3. 2D Electrophoresis/Mass Spectrometry Analysis

Proteins (150 µg) were identified by matrix-assisted laser desorption/ionization time of flight (MALDI-ToF/ToF) mass spectrometry (Bruker Daltonics Autoflex III Smartbeam; Bruker Daltonik GmbH, Leipzig, Germany) after separation by two-dimensional electrophoresis (2-DE) [63]. Differential protein pattern analysis by 2DE was performed with arterial segments (apparently normal and atherosclerotic) obtained from 3 independent aortas. To guarantee the highest homogeneity and ensure better comparability, protein extracts from all arterial segments ($N = 6$) were run simultaneously in an Ettan-Dalt-6 Device (GE-Healthcare, Uppsala, Sweden), and analysis was performed in duplicate. Protein spots

in the gels were labeled by fluorescence (Flamingo labeling, Bio-Rad), scanned (Typhoon, GE-Healthcare, Uppsala, Sweden) and analyzed for differences in the protein pattern between groups with PD-Quest 8.0.1 software (Bio-Rad, Hercules, CA, USA). Quantification of the protein spot volume was performed with the PD-Quest 8.0.1 software (Bio-Rad, Hercules, CA, USA) as previously described [29,63]. Briefly, the software created a single master that included all gels included in the analysis. A relative value that corresponds to the single spot volume compared to the total volume of the spots in each gel was assigned to each spot in the gels. Afterwards, this value was subjected to background extraction, and the final intensity value was then normalized by the local regression model (LOESS) method included in the software [29,63]. For protein identification, mass spectrometry (MS) spectra were submitted to a MASCOT (Matrix Science Ltd, London, UK) search on Swiss-Prot 57.15 database using the following parameters: taxonomy *Homo sapiens*, mass tolerance 50–100, up to 2 missed cleavages; carbamidomethyl (C) as global modification and oxidation (M) as variable modification. Identification was accepted with a score higher than 56 for peptide mass fingerprint and 20 for MS/MS.

4.4. Western Blot and ELISA Assays

Protein antigen levels in total lysates, obtained with RIPA buffer (50 mM Tris HCl pH 8.0, 150 mM NaCl, 0.5% triton X-100, 0.5% Sodium deoxyclodate, 0.1% SDS) as we previously described [30], and from ECM extracts (see above), were analyzed by Western blot, as described previously [52] using the following primary antibodies: C3 (ab200199, dilution 1/2000, Abcam, Cambridge, UK); C5 (Abcam ab11876, dilution 1/500); C3aR (Abcam ab126250, dilution 1/1000); CD11b (Abcam ab133357, dilution 1/1000); CD18 (Abcam ab119830, dilution 1/500); Human β -actin (Abcam ab8226, dilution 1/5000) and total protein (Ponceau staining) were used as loading controls. Western blot bands were visualized by chemiluminescence using a peroxidase enzymatic reaction (Supersignal, ThermoFisher, Rockford, IL, USA) and quantified with a ChemiDoc™ XRS system using Image Lab software (Bio-Rad, Hercules, CA, USA).

Quantitative plasma analysis of C3 was performed by a commercial double antibody sandwich enzyme-linked immunosorbent assay (AssayPro EC2101-1, St Charles MO, USA) with a lower limit of detection of 83 ng/mL calculated by 2SD from the mean of a zero standard. The intra-assay and inter-assay precision were CV < 5.2 and < 8.9%, respectively.

4.5. RNA Extraction and Real-Time PCR Analysis

Total RNA was extracted from areas with migrating VSMCs (wound border) or non-migrating cells after 6 h of wounding (Figure S3) or from growth-arrested cells (maintained 18 h in M199 without FBS supplementation) using an RNeasy Mini Kit (Qiagen, ref. 74104), according to the manufacturer's instructions. RNA concentration was determined with a NanoDrop ND-1000 spectrophotometer (NanoDrop Technologies), and purity was checked with the A260/A280 ratio.

mRNA levels were analyzed by real-time PCR [59] using an RT² Profiler PCR targeted array for human cell motility (Qiagen; Cat. no. 330231 PAHS-128ZA) to compare gene expression profiles between migrating and non-migrating hVSMCs and with TaqMan fluorescent real-time PCR probes (ThermoFischer, Rockford, IL, USA) to quantify C3 (Hs00163811-m1). Human GAPDH (4326317E) was used as an endogenous control. Samples were analyzed in duplicate, and only mRNAs with expression levels below 32 cycles were accepted.

4.6. Cell Adhesion and Wound-Healing Assays

Migration studies were performed with human VSMCs seeded in a culture insert (ibidi 2-well culture insert, ibidi GmbH, Martinsried, Germany) and left in M-199 with 10% FCS with or without 100 μ g/mL agLDL until cell confluence was achieved. When indicated, C3a (10 nM) or iC3b (100 nM) were added to the culture medium 1 h before stimulation with agLDL and maintained during the assay. After removing the culture

inserts, cells were washed with PBS and maintained in M199 migration medium (10% FCS) with its corresponding treatment for a total of 8 h. Migration on the cell-depleted area was controlled using an inverted microscope (Leica DMIRE2, Wetzlar, Germany) with a 10× lens magnification. Images were taken at 2 h intervals. During migration, cells were maintained at 37 °C in a humidified atmosphere of 5% CO₂. The cell-free area of each field was quantitatively determined using ImageJ software. Changes in the viability of the cells due to agLDL had been previously excluded [64].

Cell attachment studies were performed as previously described [53]. Briefly, subconfluent cultures of VSMCs were incubated with or without iC3b (100 nM), in the presence/absence of agLDL (100 µg/mL) for 16 h. Cells were then harvested with trypsin, suspended in 5% FBS-containing medium and seeded (1×10^5 cells) on FBS-coated glass bottom dishes in the presence or absence of iC3b (100 nM) and/or agLDL (100 µg/mL). At different time periods (30 min, 1 h and 3 h), attached cells were released by trypsination, stained with trypan blue for determination of cell viability and counted in a Neubauer chamber. Alternatively, at these time periods, cells were fixed with 4% paraformaldehyde for immunolabeling and confocal microscopy.

4.7. Confocal Focal Microscopy

Cells fixed with 4% paraformaldehyde were permeabilized (0.5% Tween-PBS), blocked with 1% bovine serum albumin (BSA), immunolabeled for F-actin and analyzed by confocal microscopy as previously described [30,31,52] using Alexa Fluor 633 or 488 phalloidin (Molecular Probes) on a Leica TCS SP2-AOBS inverted fluorescence microscope (Leica Microsystems Heidelberg GmbH, Mannheim, Germany). Fluorescent images were acquired in a scan format of 1024 × 1024 pixels at intervals of 0.1 mm (20 slides) and processed with the TCS-AOBS software (Leica). Maximal intensity projection values were calculated using the LASAF Leica Software and given as AU/mm².

4.8. Statistical Analysis

Results are presented as the mean ± SEM (standard error of the mean), except when indicated. Outlier expressions were excluded by Chauvenet's criterion. Sample distribution was verified by the Shapiro–Wilk test. Statistical differences between groups were analyzed by non-parametric tests (Kruskal–Wallis or Mann–Whitney), as indicated. StatView software (Abacus Concepts) and SPSS Statistics Version 21.0.0 (SPSS, Chicago, IL, USA) were used for statistical analysis, and a *p*-value < 0.05 was considered statistically significant.

Supplementary Materials: The following are available online at <https://www.mdpi.com/article/10.3390/ijms22105122/s1>.

Author Contributions: Conceptualization, T.P. and L.B.; methodology, M.G.-A. and E.P.; validation, M.G.-A., E.D.-R. and T.P.; formal analysis, T.P., L.B., M.G.-A., E.D.-R. and R.E.; investigation, M.G.-A., E.D.-R., E.P., R.E., P.M., O.J.-B. and T.P.; resources, L.B. and T.P.; writing—original draft preparation, M.G.-A., T.P. and L.B.; writing—review and editing, M.G.-A., E.D.-R., E.P., R.E., O.J.-B., P.M., L.B., T.P.; visualization, M.G.-A., L.B., T.P.; supervision, T.P. and L.B.; project administration, T.P. and L.B.; funding acquisition, T.P. and L.B. All authors have read and agreed to the published version of the manuscript.

Funding: This work was supported by the Institute of Health Carlos III, ISCIII [FIS PI19/01687, to T.P.; Red Terapia Celular TerCel-RD16/0011/0018 to L.B.; CIBERCV to L.B.; Spanish Ministry of Economy and Competitiveness of Science-PID2019-107160RB-I00 to L.B.; and cofounded by FEDER “Una Manera de Hacer Europa”. Secretaria d’Universitats i Recerca del Departament d’Empresa i Coneixement de la Generalitat de Catalunya [2017 SGR 1480]. We thank Fundació Jesus Serra and Fundació de Investigació Cardiovascular, Barcelona, for their continuous support.

Institutional Review Board Statement: The study in humans (SAFEHEART Cohort) was approved by the Local Ethics Committee of the Investigación Clínica Fundación Jimenez Diaz (CEIC-FJD; Madrid, Spain) (protocol number: 01/09) and was conducted according to the Declaration of Helsinki (2013). Post-mortem studies in autopsy material were performed following an established forensic

protocol [56,57], and the study was approved by the Institutional Ethical Committee for Clinical Investigation of the Hospital Santa Creu i Sant Pau (Barcelona, Spain).

Informed Consent Statement: Written informed consent was obtained from all subjects involved in the study.

Data Availability Statement: Not Applicable.

Acknowledgments: Authors are indebted to Roberta Lugano, Montse Gomez-Pardo and Esther Gerbolès for their technical support. R.E. is a CIBERCV investigator. E.D.R. is a recipient of a predoctoral research fellowship from the Cardiovascular Program-ICCC (IR-HSCSP).

Conflicts of Interest: The authors declare no conflict of interest.

References

- Ridker, P.M. LDL cholesterol: Controversies and future therapeutic directions. *Lancet* **2014**, *384*, 607–617. [CrossRef]
- Vogt, A. The genetics of familial hypercholesterolemia and emerging therapies. *Appl. Clin. Genet.* **2015**, *8*, 27–36. [CrossRef]
- Brown, M.S.; Goldstein, J.L. Familial hypercholesterolemia: Defective binding of lipoproteins to cultured fibroblasts associated with impaired regulation of 3-hydroxy-3-methylglutaryl coenzyme a reductase activity. *Proc. Natl. Acad. Sci. USA* **1974**, *71*, 788–792. [CrossRef]
- De Isla, L.P.; Alonso, R.; Watts, G.F.; Mata, N.; Cerezo, A.S.; Muñoz, O.; Fuentes, F.; Diaz-Diaz, J.L.; de Andrés, R.; Zambón, D.; et al. Attainment of LDL-Cholesterol treatment goals in patients with familial hypercholesterolemia. *J. Am. Coll. Cardiol.* **2016**, *67*, 1278–1285. [CrossRef]
- Neeffjes, L.A.; Kate, G.-J.R.T.; Alexia, R.; Nieman, K.; Galema-Boers, A.J.; Langendonk, J.G.; Weustink, A.C.; Mollet, N.R.; Sijbrands, E.J.; Krestin, G.P.; et al. Accelerated subclinical coronary atherosclerosis in patients with familial hypercholesterolemia. *Atherosclerosis* **2011**, *219*, 721–727. [CrossRef]
- Suades, R.; Padro, T.; Alonso, R.; López-Miranda, J.; Mata, P.; Badimon, L. Circulating CD45+/CD3+ lymphocyte-derived microparticles map lipid-rich atherosclerotic plaques in familial hypercholesterolaemia patients. *Thromb. Haemost.* **2014**, *111*, 111–121. [CrossRef]
- Escate, R.; Mata, P.; Cepeda, J.M.; Padreó, T.; Badimon, L. miR-505-3p controls chemokine receptor up-regulation in macrophages: Role in familial hypercholesterolemia. *FASEB J.* **2017**, *32*, 601–612. [CrossRef]
- Bahrami, A.; Liberale, L.; Reiner, Ž. Inflammatory biomarkers for cardiovascular risk stratification in familial hypercholesterolemia. *Rev. Physiol. Biochem. Pharmacol.* **2020**, *177*, 25–52.
- Holven, K.B.; Narverud, I.; Lindvig, H.W.; Halvorsen, B.; Langslet, G.; Nenseter, M.S.; Ulven, S.M.; Ose, L.; Aukrust, P.; Retterstøl, K. Subjects with familial hypercholesterolemia are characterized by an inflammatory phenotype despite long-term intensive cholesterol lowering treatment. *Atherosclerosis* **2014**, *233*, 561–567. [CrossRef]
- Real, J.T.; Martínez-Hervas, S.; García-García, A.-B.; Civera, M.; Pallardo, F.V.; Ascaso, J.F.; Vina, J.R.; Chaves, E.J.; Carmena, R.; García-García, A.-B. Circulating mononuclear cells nuclear factor-kappa B activity, plasma xanthine oxidase, and low grade inflammatory markers in adult patients with familial hypercholesterolaemia. *Eur. J. Clin. Investig.* **2010**, *40*, 89–94. [CrossRef] [PubMed]
- Merle, N.S.; Church, S.E.; Fremeaux-Bacchi, V.; Roumenina, L.T. Complement system Part I—Molecular mechanisms of activation and regulation. *Front. Immunol.* **2015**, *6*, 262. [CrossRef]
- Merle, N.S.; Noe, R.; Halbwachs-Mecarelli, L.; Fremeaux-Bacchi, V.; Roumenina, L.T. Complement system part II: Role in immunity. *Front. Immunol.* **2015**, *6*, 257. [CrossRef]
- Poston, R.N. Atherosclerosis: Integration of its pathogenesis as a self-perpetuating propagating inflammation: A review. *Cardiovasc. Endocrinol. Metab.* **2019**, *8*, 51–61. [CrossRef]
- Martin-Ventura, J.L.; Martínez-Lopez, D.; Roldan-Montero, R.; Gomez-Guerrero, C.; Blanco-Colio, L.M. Role of complement system in pathological remodeling of the vascular wall. *Mol. Immunol.* **2019**, *114*, 207–215. [CrossRef] [PubMed]
- Vlaicu, S.I.; Tatomir, A.; Rus, V.; Mekala, A.P.; Mircea, P.A.; Niculescu, F.; Rus, H. The role of complement activation in atherogenesis: The first 40 years. *Immunol. Res.* **2016**, *64*, 1–13. [CrossRef] [PubMed]
- Speidl, W.S.; Kastl, S.P.; Huber, K.; Wojta, J. Complement in atherosclerosis: Friend or foe? *J. Thromb. Haemost.* **2010**, *9*, 428–440. [CrossRef] [PubMed]
- Wezel, A.; De Vries, M.R.; Lagrauw, H.M.; Foks, A.C.; Kuiper, J.; Quax, P.H.; Bot, I. Complement factor C5a induces atherosclerotic plaque disruptions. *J. Cell. Mol. Med.* **2014**, *18*, 2020–2030. [CrossRef] [PubMed]
- Hansson, G.K.; Holm, J.; Kral, J.G. Accumulation of IgG and complement factor C3 in human arterial endothelium and atherosclerotic lesions. *Acta Pathol. Microbiol. Scand. Ser. A Pathol.* **1984**, *92*, 429–435. [CrossRef]
- Ge, X.; Xu, C.; Liu, Y.; Zhu, K.; Zeng, H.; Su, J.; Huang, J.; Ji, Y.; Tan, Y.; Hou, Y. Complement activation in the arteries of patients with severe atherosclerosis. *Int. J. Clin. Exp. Pathol.* **2018**, *11*, 1–9.
- Buono, C.; Come, C.E.; Witztum, J.L.; Maguire, G.F.; Connelly, P.W.; Carroll, M.; Lichtman, A.H. Influence of C3 deficiency on atherosclerosis. *Circulation* **2002**, *105*, 3025–3031. [CrossRef] [PubMed]

21. Persson, L.; Borén, J.; Robertson, A.-K.L.; Wallenius, V.; Hansson, G.K.; Pekna, M. Lack of complement factor C3, but not factor B, increases hyperlipidemia and atherosclerosis in apolipoprotein E-/- low-density lipoprotein receptor-/- mice. *Arter. Thromb. Vasc. Biol.* **2004**, *24*, 1062–1067. [[CrossRef](#)] [[PubMed](#)]
22. Wang, Y.; Nanda, V.; DiRenzo, D.; Ye, J.; Xiao, S.; Kojima, Y.; Howe, K.L.; Jarr, K.-U.; Flores, A.M.; Tsantilas, P.; et al. Clonally expanding smooth muscle cells promote atherosclerosis by escaping efferocytosis and activating the complement cascade. *Proc. Natl. Acad. Sci. USA* **2020**, *117*, 15818–15826. [[CrossRef](#)] [[PubMed](#)]
23. Verdeguer, F.; Kubicek, M.; Pla, D.; Vila-Caballer, M.; Civeira, F.; Castro, C.; Vinué, Á.; Pocoví, M.; Calvete, J.J.; Andrés, V. Complement regulation in murine and human hypercholesterolemia and role in the control of macrophage and smooth muscle cell proliferation. *Cardiovasc. Res.* **2007**, *76*, 340–350. [[CrossRef](#)]
24. Van Wijk, D.F.; Sjouke, B.; Figueroa, A.; Emami, H.; van der Valk, F.M.; MacNabb, M.H.; Hemphill, L.C.; Schulte, D.M.; Koopman, M.G.; Lobatto, M.E.; et al. Nonpharmacological lipoprotein apheresis reduces arterial inflammation in familial hypercholesterolemia. *J. Am. Coll. Cardiol.* **2014**, *64*, 1418–1426. [[CrossRef](#)] [[PubMed](#)]
25. Toutouzias, K.; Skoumas, J.; Koutagiari, I.; Benetos, G.; Pianou, N.; Georgakopoulos, A.; Galanakis, S.; Antonopoulos, A.; Drakopoulou, M.; Oikonomou, E.K.; et al. Vascular inflammation and metabolic activity in hematopoietic organs and liver in familial combined hyperlipidemia and heterozygous familial hypercholesterolemia. *J. Clin. Lipidol.* **2018**, *12*, 33–43. [[CrossRef](#)]
26. Sampietro, T.; Bigazzi, F.; Rossi, G.; Pino, B.D.; Puntoni, M.R.; Sbrana, F.; Chella, E.; Bionda, A. Upregulation of the immune system in primary hypercholesterolaemia: Effect of atorvastatin therapy. *J. Intern. Med.* **2005**, *257*, 523–530. [[CrossRef](#)] [[PubMed](#)]
27. De Isla, L.P.; Alonso, R.; De Diego, J.J.G.; Muñoz-Grijalvo, O.; Diaz-Diaz, J.L.; Zambón, D.; Miramontes, J.P.; Fuentes, F.; De Andrés, R.; Werenitzky, J.; et al. Coronary plaque burden, plaque characterization and their prognostic implications in familial hypercholesterolemia: A computed tomographic angiography study. *Atherosclerosis* **2021**, *317*, 52–58. [[CrossRef](#)]
28. Subirana, M.T.; Juan-Babot, J.O.; Puig, T.; Lucena, J.; Rico, A.; Salguero, M.; Borondo, J.C.; Ordóñez, J.; Arimany, J.; Vázquez, R.; et al. Specific characteristics of sudden death in a mediterranean spanish population. *Am. J. Cardiol.* **2011**, *107*, 622–627. [[CrossRef](#)] [[PubMed](#)]
29. Garcia-Arguinzonis, M.; Padró, T.; Lugano, R.; Llorente-Cortes, V.; Badimon, L. Low-Density lipoproteins induce heat shock protein 27 dephosphorylation, oligomerization, and subcellular relocalization in human vascular smooth muscle cells. *Arter. Thromb. Vasc. Biol.* **2010**, *30*, 1212–1219. [[CrossRef](#)]
30. Lugano, R.; Peña, E.; Casani, L.; Badimon, L.; Padró, T. UPA promotes lipid-loaded vascular smooth muscle cell migration through LRP-1. *Cardiovasc. Res.* **2013**, *100*, 262–271. [[CrossRef](#)]
31. Padró, T.; Peña, E.; Garcia-Arguinzonis, M.; Llorente-Cortes, V.; Badimon, L. Low-density lipoproteins impair migration of human coronary vascular smooth muscle cells and induce changes in the proteomic profile of myosin light chain. *Cardiovasc. Res.* **2007**, *77*, 211–220. [[CrossRef](#)]
32. Engström, G.; Hedblad, B.; Janzon, L.; Lindgärde, F. Complement C3 and C4 in plasma and incidence of myocardial infarction and stroke: A population-based cohort study. *Eur. J. Cardiovasc. Prev. Rehabil.* **2007**, *14*, 392–397. [[CrossRef](#)]
33. Van Greevenbroek, M.M.; Arts, I.C.; Van Der Kallen, C.J.; Geijselaers, S.L.; Feskens, E.J.; Jansen, E.H.; Schalkwijk, C.G.; Stehouwer, C.D.; Hertle, E. Distinct associations of complement C3a and its precursor C3 with atherosclerosis and cardiovascular disease. *Thromb. Haemost.* **2014**, *111*, 1102–1111. [[CrossRef](#)]
34. Imanaka-Yoshida, K. Extracellular Matrix Remodeling in Vascular Development and Disease. In *Etiology and Morphogenesis of Congenital Heart Disease*; Nakanishi, T., Markwald, R.R., Baldwin, H.S., Keller, B.B., Srivastava, D., Yamagishi, H., Eds.; Springer: Tokyo, Japan, 2016; Chapter 29.
35. Oksjoki, R.; Kovanen, P.T.; Pentikäinen, M.O. Role of complement activation in atherosclerosis. *Curr. Opin. Lipidol.* **2003**, *14*, 477–482. [[CrossRef](#)] [[PubMed](#)]
36. Vijayan, S.; Asare, Y.; Grommes, J.; Soehnlein, O.; Lutgens, E.; Shagdarsuren, G.; Togtokh, A.; Jacobs, M.J.; Fischer, J.W.; Bernhagen, J.; et al. High expression of C5L2 correlates with high proinflammatory cytokine expression in advanced human atherosclerotic plaques. *Am. J. Pathol.* **2014**, *184*, 2123–2133. [[CrossRef](#)]
37. Hertle, E.; Van Greevenbroek, M.; Arts, I.; Van Der Kallen, C.; Feskens, E.; Schalkwijk, C.; Stehouwer, C. Complement activation products C5a and sC5b-9 are associated with low-grade inflammation and endothelial dysfunction, but not with atherosclerosis in a cross-sectional analysis: The CODAM study. *Int. J. Cardiol.* **2014**, *174*, 400–403. [[CrossRef](#)] [[PubMed](#)]
38. Martínez-López, D.; Roldan-Montero, R.; García-Marqués, F.; Nuñez, E.; Jorge, I.; Camafeita, E.; Minguez, P.; de Cordoba, S.R.; López-Melgar, B.; Lara-Pezzi, E.; et al. Complement C5 protein as a marker of subclinical atherosclerosis. *J. Am. Coll. Cardiol.* **2020**, *75*, 1926–1941. [[CrossRef](#)] [[PubMed](#)]
39. Suzuki, M.; Becker, L.; Pritchard, D.K.; Gharib, S.A.; Wijsman, E.M.; Bammler, T.K.; Beyer, R.P.; Vaisar, T.; Oram, J.F.; Heinecke, J.W. Cholesterol accumulation regulates expression of macrophage proteins implicated in proteolysis and complement activation. *Arter. Thromb. Vasc. Biol.* **2012**, *32*, 2910–2918. [[CrossRef](#)] [[PubMed](#)]
40. Camejo, G.; Hurt-Camejo, E.; Wiklund, O.; Bondjers, G. Association of apo B lipoproteins with arterial proteoglycans: Pathological significance and molecular basis. *Atherosclerosis* **1998**, *139*, 205–222. [[CrossRef](#)]
41. Williams, K.J. Arterial wall chondroitin sulfate proteoglycans: Diverse molecules with distinct roles in lipoprotein retention and atherogenesis. *Curr. Opin. Lipidol.* **2001**, *12*, 477–487. [[CrossRef](#)]

42. Shankman, L.S.; Gomez, D.; Cherepanova, O.A.; Salmon, M.; Alencar, G.F.; Haskins, R.M.; Swiatlowska, P.; Newman, A.A.C.; Greene, E.S.; Straub, A.C. KLF4-dependent phenotypic modulation of smooth muscle cells has a key role in atherosclerotic plaque pathogenesis. *Nat. Med.* **2015**, *21*, 628–637. [[CrossRef](#)] [[PubMed](#)]
43. Chappell, J.; Harman, J.L.; Narasimhan, V.M.; Yu, H.; Foote, K.; Simons, B.D.; Bennett, M.R.; Jorgensen, H.F. Extensive proliferation of a subset of differentiated, yet plastic, medial vascular smooth muscle cells contributes to neointimal formation in mouse injury and atherosclerosis models. *Circ. Res.* **2016**, *119*, 1313–1323. [[CrossRef](#)]
44. Frey, A.; Ertl, G.; Angermann, C.E.; Hofmann, U.; Störk, S.; Frantz, S. Complement C3c as a biomarker in heart failure. *Mediat. Inflamm.* **2013**, *2013*, 1–7. [[CrossRef](#)] [[PubMed](#)]
45. Grande, M.A.; Belstrom, D.; Damgaard, C.; Holmstrup, P.; Thangaraj, S.S.; Nielsen, C.H.; Palarasah, Y. Complement split product C3c in saliva as biomarker for periodontitis and response to periodontal treatment. *J. Periodontol. Res.* **2021**, *56*, 27–33. [[CrossRef](#)]
46. Goldknopf, I.L.; Sheta, E.A.; Bryson, J.; Folsom, B.; Wilson, C.; Duty, J.; Yen, A.A.; Appel, S.H. Complement C3c and related protein biomarkers in amyotrophic lateral sclerosis and Parkinson's disease. *Biochem. Biophys. Res. Commun.* **2006**, *342*, 1034–1039. [[CrossRef](#)]
47. Pagano, M.B.; Zhou, H.-F.; Ennis, T.L.; Wu, X.; Lambris, J.D.; Atkinson, J.P.; Thompson, R.W.; Hourcade, D.E.; Pham, C.T. Complement-dependent neutrophil recruitment is critical for the development of elastase-induced abdominal aortic aneurysm. *Circulation* **2009**, *119*, 1805–1813. [[CrossRef](#)]
48. Carmona-Fontaine, C.; Theveneau, E.; Tzekou, A.; Tada, M.; Woods, M.; Page, K.M.; Parsons, M.; Lambris, J.D.; Mayor, R. Complement Fragment C3a Controls Mutual Cell Attraction during Collective Cell Migration. *Dev. Cell* **2011**, *21*, 1026–1037. [[CrossRef](#)]
49. Wu, F.; Zou, Q.; Ding, X.; Shi, D.; Zhu, X.; Hu, W.; Liu, L.; Zhou, H. Complement component C3a plays a critical role in endothelial activation and leukocyte recruitment into the brain. *J. Neuroinflamm.* **2016**, *13*, 1–14. [[CrossRef](#)]
50. Öörni, K.; Pentikäinen, M.O.; Ala-Korpela, M.; Kovanen, P.T. Aggregation, fusion, and vesicle formation of modified low density lipoprotein particles: Molecular mechanisms and effects on matrix interactions. *J. Lipid Res.* **2000**, *41*, 1703–1714. [[CrossRef](#)]
51. Badimon, L.; Martínez-González, J.; Llorente-Cortés, V.; Rodríguez, C.; Padro, T. Cell biology and lipoproteins in atherosclerosis. *Curr. Mol. Med.* **2006**, *6*, 439–456. [[CrossRef](#)]
52. Padró, T.; Lugano, R.; García-Arguinzonis, M.; Badimon, L. LDL-Induced impairment of human vascular smooth muscle cells repair function is reversed by HMG-CoA reductase inhibition. *PLoS ONE* **2012**, *7*, e38935. [[CrossRef](#)] [[PubMed](#)]
53. Lugano, R.; Pena, E.; Badimon, L.; Padro, T. Aggregated low-density lipoprotein induce impairment of the cytoskeleton dynamics through urokinase-type plasminogen activator/urokinase-type plasminogen activator receptor in human vascular smooth muscle cell. *J. Thromb. Haemost.* **2012**, *10*, 2158–2167. [[CrossRef](#)]
54. Mata, N.; Alonso, R.; Badimon, L.; Padró, T.; Fuentes, F.; Muñoz, O.; Perez-Jiménez, F.; López-Miranda, J.; Díaz, J.L.; Vidal, J.L.; et al. Clinical characteristics and evaluation of LDL-cholesterol treatment of the Spanish Familial Hypercholesterolemia Longitudinal Cohort Study (SAFEHEART). *Lipids Health Dis.* **2011**, *10*, 94. [[CrossRef](#)] [[PubMed](#)]
55. Brinkmann, B. Harmonisation of Medico-Legal Autopsy Rules. *Int. J. Leg. Med.* **1999**, *113*, 1–14. [[CrossRef](#)] [[PubMed](#)]
56. Basso, C.; Burke, M.; Fornes, P.; Gallagher, P.J.; De Gouveia, R.H.; Sheppard, M.; Thiene, G.; Van Der Wal, A.; On Behalf of the Association for European Cardiovascular Pathology. Guidelines for autopsy investigation of sudden cardiac death. *Virchows Archiv* **2007**, *452*, 11–18. [[CrossRef](#)] [[PubMed](#)]
57. Guyton, J.R.; Klemp, K.F.; Mims, M.P. Altered ultrastructural morphology of self-aggregated low density lipoproteins: Coalescence of lipid domains forming droplets and vesicles. *J. Lipid. Res.* **1991**, *32*, 953–962. [[CrossRef](#)]
58. Llorente-Cortés, V.; Martínez-González, J.; Badimon, L. Esterified cholesterol accumulation induced by aggregated LDL uptake in human vascular smooth muscle cells is reduced by HMG-CoA reductase inhibitors. *Arter. Thromb. Vasc. Biol.* **1998**, *18*, 738–746. [[CrossRef](#)]
59. Llorente-Cortés, V.; Otero-Viñas, M.; Badimon, L. Differential role of heparan sulfate proteoglycans on aggregated LDL uptake in human vascular smooth muscle cells and mouse embryonic fibroblasts. *Arter. Thromb. Vasc. Biol.* **2002**, *22*, 1905–1911. [[CrossRef](#)]
60. Ohkawa, H.; Ohishi, N.; Yagi, K. Assay for lipid peroxides in animal tissues by thiobarbituric acid reaction. *Anal. Biochem.* **1979**, *95*, 351–358. [[CrossRef](#)]
61. Escate, R.; Padro, T.; Badimon, L. LDL accelerates monocyte to macrophage differentiation: Effects on adhesion and anoikis. *Atherosclerosis* **2016**, *246*, 177–186. [[CrossRef](#)]
62. Didangelos, A.; Yin, X.; Mandal, K.; Saje, A.; Smith, A.; Xu, Q.; Jahangiri, M.; Mayr, M. Extracellular matrix composition and remodeling in human abdominal aortic aneurysms: A proteomics approach. *Mol. Cell. Proteom.* **2011**, *10*. [[CrossRef](#)] [[PubMed](#)]
63. Cubedo, J.; Padró, T.; García-Arguinzonis, M.; Vilahur, G.; Miñambres, I.; Pou, J.M.; Ybarra, J.; Badimon, L. A novel truncated form of apolipoprotein A-I transported by dense LDL is increased in diabetic patients. *J. Lipid Res.* **2015**, *56*, 1762–1773. [[CrossRef](#)] [[PubMed](#)]
64. Llorente-Cortés, V.; Otero-Viñas, M.; Camino-López, S.; Llampayas, O.; Badimon, L. Aggregated low-density lipoprotein uptake induces membrane tissue factor procoagulant activity and microparticle release in human vascular smooth muscle Cells. *Circulation* **2004**, *110*, 452–459. [[CrossRef](#)] [[PubMed](#)]

Supplementary Information

Alternative C3-complement system: lipids and atherosclerosis

Maisa Garcia-Arguinzonis¹, Elisa Diaz-Riera¹, Esther Peña^{1,2}, Rafael Escate^{1,2}, Oriol Juan-Babot¹, Pedro Mata³, Lina Badimon^{1,2,4#}, Teresa Padro^{1,2#*}

Both authors contributed equally

¹Cardiovascular Program-ICCC, Research Institute- Hospital Santa Creu i Sant Pau, IIB-Sant Pau, Barcelona.Spain

²Centro de Investigación Biomédica en Red cardiovascular (CIBERCV) Instituto de Salud Carlos III, Madrid, Spain.

³Fundación Hipercolesterolemia Familiar, Madrid, Spain

⁴Cardiovascular Research Chair, UAB, Barcelona, Spain

Address for corresponding author (*):

Dr Teresa Padro

Cardiovascular Program-ICCC

Research Institute Hospital Santa Creu i Sant Pau

Sant Antoni M^a Claret 167, 08025 Barcelona, Spain

Phone: +34 935565886

Fax: +34 935565559

E-mail: tpadro@santpau.cat

Table S1: Demographic, biochemical and clinical variables: Familial hypercholesterolemia and healthy subject groups

	FH population n=49	Reference group n=28
Female/male, n	18/31	16/12
Age, years	44.69±10.5	24.5±4.6
BMI	25.7±3	22.4±2.9
RISK FACTORS; n (%)		
Active smoking	11 (22)	12 (43)
Hypertension	2 (4)	0 (0)
Type 2 diabetes	1 (2)	0 (0)
SAFEHEART risk 5 years, %	1.00±0.76	-
SAFEHEART risk 10 years, %	2.13±1.6	-
BIOCHEMICAL DATA; MEAN ± SD		
Total cholesterol, mg/dL	206.7±38	169.7±21
Triglycerides, mg/dL	90.6±49	76.8±35
HDL cholesterol, mg/dL	52.1±13	55.7±16
Non-HDL cholesterol, mg/dL	154.6±40	114.0±16.7
LDL cholesterol, mg/dL	136.3±36	98.6±15
Apo A1, mg/dL	126.5±17	139.5±29
Apo B, mg/dL	106.6±24	61.5±10
Lipoprotein a, mg/dL	48.8±46	18.5±21
Glucose, mg/dL	91.0±9	78.3±9
SUBCLINICAL ATHEROSCLEROTIC DISEASE; (%)		
Plaque burden, %	23.5±6.3	-
Calcium burden, %	2.2±2.5	-
Non-calcium burden, %	21.3±5.3	-
BACKGROUND MEDICATION; n (%)		
Angiotensin-converting-enzyme inhibitors	0 (0)	0 (0)
Angiotensin II receptor blockers	1 (2)	0 (0)
Beta-blockers	0 (0)	0 (0)
Diuretics	2 (4)	0 (0)
Statins*	49 (100)	0 (0)
Lipid-lowering treatment, years	14.8±6.7	

SD: standard deviation. *Includes: rosuvastatin, ezetimibe, atorvastatin, simvastatin, lovastatin, pravastatin, fluvastatin, pitavastatin, resins, and fibrates.

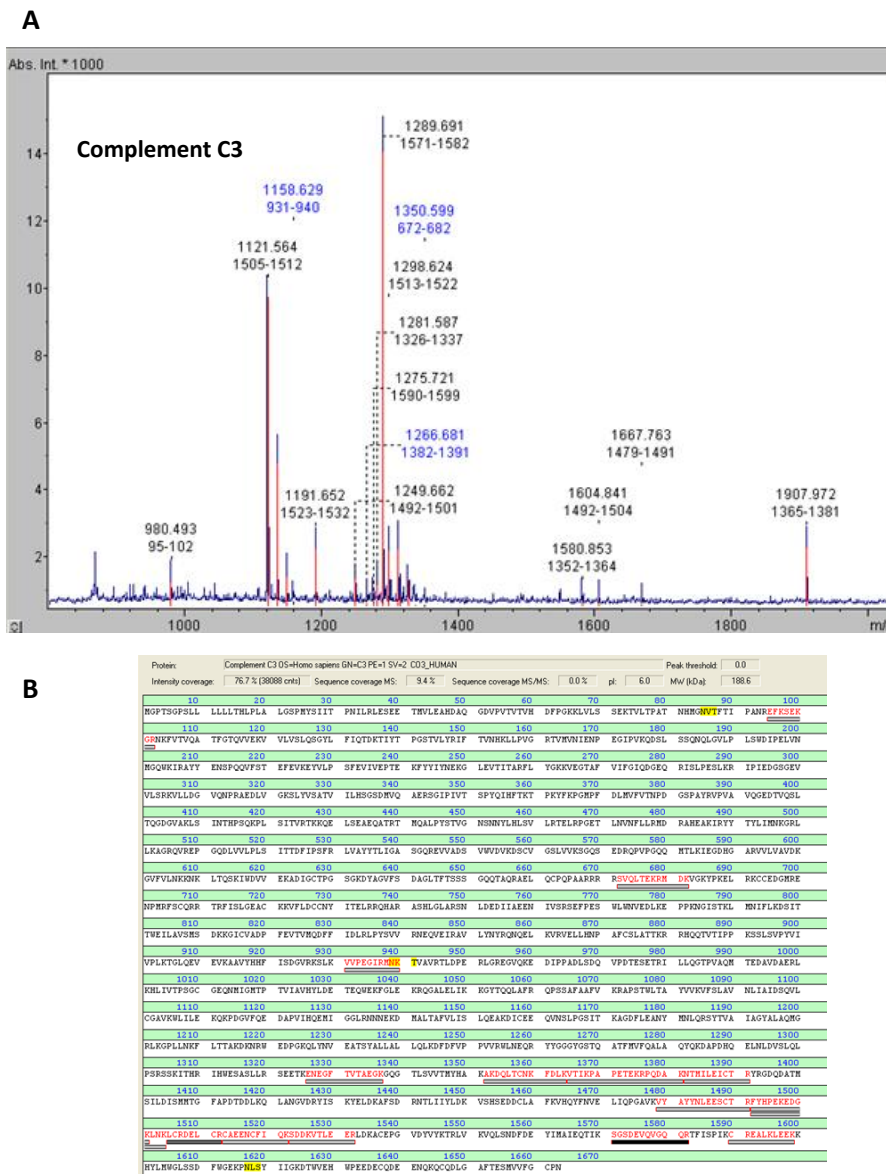


Figure S1: Mass Spectrometry Analysis. Identification by MALDI ToF/ToF of Complement C3 on 2D-PAGE from soluble fraction of ECM from human aortas, identified by a MASCOT search on Swiss-Prot 57.15 database with a Score of 82, a sequence coverage of 9.4% and intensity coverage of 76.7%. To identify the following parameters were used: taxonomy *Homo sapiens*, mass tolerance 50–100, up to 2 miss cleavage; global modification: carbamidomethyl (C); variable modification: oxidation (M). Identification was accepted with a score higher than 56. Spectrum(A) and sequence Coverage (B) obtained with a Smartbeam AutoFlex III and visualized with BioTools Software (version 3.02, Bruker)

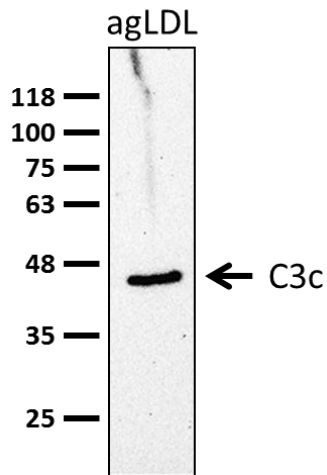


Figure S2: Western Blot analysis for C3 in agLDL. 250 μ l of agLDL (1 μ g/mL) was precipitated with ice cold acetone O.N. and resuspended in 25 μ l of 50mM Tris-HCl pH 8.0 and analyzed by western blot using C3 primary antibody (Abcam ab200199, dilution 1/2000) and visualized by chemiluminescence using a peroxidase enzymatic reaction (Supersignal, Pierce) and quantified with a ChemiDoc™ XRS system using using Image Lab software (Bio-Rad).

HUMAN AORTAS

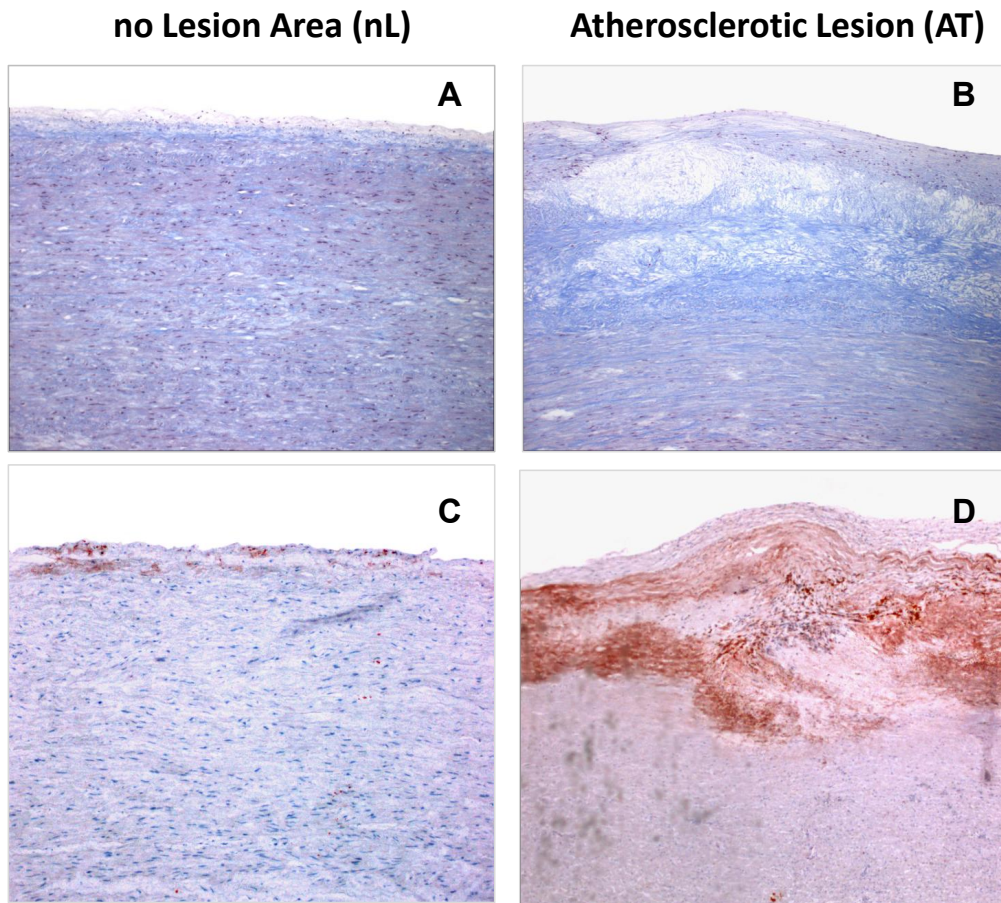


Figure S3: Histological analysis of human aorta. **A** and **C** Macroscopically normal-appearing areas (nL: no lesion areas) or **B** and **D** Areas with atherosclerotic plaques (AT segment). Aortic segments were embedded with paraffin and 5 μ M sections were stained with Masson's trichromic to identify cellular areas. **C** and **D** Representative of atherosclerotic plaque segment stained for lipids with Oil Red O. The images were captured with an Olympus microscope Vanox AHBT3 coupled with a Sony 3CCD color video camera and processed using Visilog (Sony ESPAC) software (version 4.1.5). Magnification x60

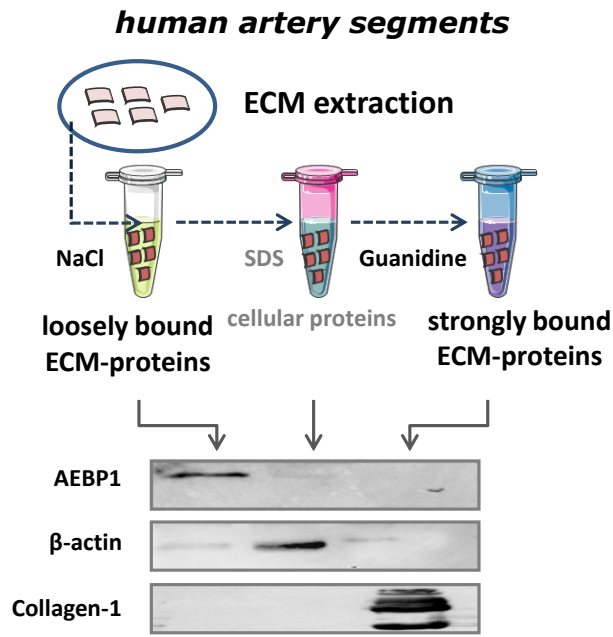


Figure S4: Schematic diagram representing tissue extraction of human aorta. Segments of human aorta with or with advanced atherosclerotic lesions and without atherosclerosis obtained from sudden death cases were sequentially extracted to obtain the ECM protein fraction as described in the Material and Methods section. Extraction purity was confirmed by western blot using specific antibodies for each fraction: AEBP1 (Adipocyte enhancer-binding protein 1) for the loosely bound ECM protein fraction; β-actin for the intracellular proteins fraction and Collagen-1 the for strongly bound ECM-protein fraction.

CHAPTER VI: DISCUSSION

6. Discussion

Acute decompensated heart failure (ADHF) is a complex clinical condition that affects several organs and involves many pathophysiological mechanisms (47,265). It is known that several pathways play a role in adverse heart remodelling and disease progression, such as RAAS, complement system, haemostasis, inflammation, among others. However, their exact role and the long-term consequences stemming from their dysregulation have not been completely elucidated, emphasising the need for a deeper understanding of the molecular functions and pathways associated to the ADHF pathophysiology (45). To address this problem, we carried out a discovery hypothesis-free study using 2DE coupled to MALDI/ToF-ToF mass-spectrometry (2DE-MS) aimed to unravel a disease-specific differential proteomic profile of ADHF patients at hospital admission and its potential link to pathophysiology.

To address this problem, we carried out as the main goal a discovery hypothesis-free study based on a top-down proteomic approach aimed to unravel a disease-specific differential protein pattern in ADHF patients at hospital admission and its potential link to pathophysiology.

In recent years, urine has become a promising biospecimen in clinical proteomics (207). Urine represents a combination of both blood ultrafiltrates and local secretion from kidney specific cells and tubules, therefore reflecting systemic and renal diseases. Moreover, in the absence of homeostatic regulation the changes in urine proteins may detect small and early pathological changes (206). Besides, urine sampling has many advantages compared to blood including the availability of larger and more recurrent volumes without causing discomfort to the patient (266).

The identified ADHF differential pattern refers to proteins acting through molecular functions such as catalytic activity, signalling receptor binding and transport, and being involved in various biological processes including metabolism of lipids, vitamins, carbohydrates and heme components, haemostatic and complement systems, and immune and inflammatory responses. Furthermore, 17 of the 26 proteins were of hepatic origin, with 11 proteins showing the highest changes of urinary levels in ADHF patients with GFR below the pathological threshold (MDRD-4 <60 mL/min/1.73m²). This effect could be related to a pathological interaction between heart, kidney and liver in heart failure patients that can lead to multi-organ deterioration and unfavourable disease evolution (268–270) (267–269).

Within identified proteins, several of them had been previously studied within different heart disorders. For example, leucine rich α -2-glycoprotein (*LRG1*) and zinc- α -2-glycoprotein (*AZGP1*) have been studied in cardiac fibrosis (270,271); α -1-antitrypsin (*SERPINA1*) was recently studied in chronic heart failure (272); complement C3 and several other complement components have also been associated with heart diseases (88,273,274). Retinol binding protein (RBP4), encoded by *RBP4* gene, could be associated with cardiomyocyte hypertrophy (275) and inflammatory cardiomyopathy (276), and ischaemia (277). To notice, RBP4 has also been studied within kidney disease (278).

Among the identified proteins, transthyretin (TTR), which is encoded by TTR gene, has also been increasingly studied in the setting of heart failure due to its involvement in cardiac amyloidosis (112,279–281). Furthermore, TTR is a pivotal protein involved in the transport of RBP4, which simultaneously carries retinol, and also is one of the main transporters of thyroxine (T4) (282), a thyroid hormone that has been previously associated to blood pressure and LVEF in ADHF during hospitalisation (283). It has been observed that hormones have central

regulatory actions in the cardiovascular system and patients with even mildly altered thyroid function have a worse prognosis in heart disease, particularly in heart failure (284).

In line with results of other studies concerning coronary artery disease (285), acute coronary syndrome (286), and those of our group in myocardial infarction (287), TTR levels in ADHF patients at hospitalisation, independently of kidney function, were significantly lower to those of healthy individuals. This thesis' results, along with literature information strongly suggest that there is an increased inflammatory background in ADHF patients that could lead to decreased TTR levels, beyond glomerular filtration status, which is also depicted by the significant correlation between plasma TTR and CRP levels at hospitalisation. High urinary levels of RBP4 were observed in ADHF patients at hospitalisation, and significantly higher in patients with renal dysfunction at admission. Urinary TTR and RBP4 loss significantly correlated, and it is conceivable that the monomeric form was already circulating abundantly in blood, and since only TTR tetramers bind RBP4 and protect it from being filtered in the glomerulus, more RBP4 was filtered and lost (288). This might have a pathological relevance in ADHF patients since increasing evidence suggest that TTR-tetramers, under unbalanced homeostatic conditions, dissociate in misfolded monomers that tend to aggregate and fibrillate. After infiltrating the cardiac extracellular matrix TTR induces oxidative stress and mitochondrial damage, increases cardiac wall thickness, and diastolic dysfunction (289). Supporting this view, low plasma transthyretin concentration has been shown to associate with incident heart failure in the general population (290) and suggested that low plasma TTR levels could be a biomarker of transthyretin tetramer instability (291).

Two other proteins with a differential pattern in the urine of ADHF patients were antithrombin III (AT3), a relevant protease inhibitor in the

coagulation cascade, and C3, a key component of the complement system, one of the fastest acting mechanisms associated to innate immunity and to production of proinflammatory molecules (292).

Although the complement system is mainly activated through three main pathways: classical, lectin, and alternative, several components of the coagulation cascade also activate the complement system (293). On the one hand, the components of the complement system interact with the coagulation cascade (293). Thus, MASP1 and MASP2, activators of the C3-complement pathway, are able to promote coagulation by the cleavage of fibrinogen and factor XIII, and to generate thrombin from prothrombin, respectively (294,295).

In addition, Huber-Lang *et al.* (90) observed that thrombin might substitute C3-dependent C5 convertase in the setting of genetic C3 absence. Later Amara *et al.* (296) speculated that several coagulation cascade components were able to generate the activated C3 (C3a) and C5 (C5a), among which factors IX-XI, thrombin and plasmin are mentioned. Irmischer *et al.* (297) recently reported that kallikrein, another coagulation cascade molecule, activate the complement system by cleaving C3. Within the coagulation cascade, AT3 is able to inhibit several components, mainly thrombin, but also kallikrein, factors IX, XI and XII, especially if bound to heparin (298).

In this thesis, it was observed that ADHF patients presented elevated AT3 levels in both urine and plasma, being the higher AT3 plasma levels found in ADHF patients with preserved or mildly reduced LVEF and in those patients kidney dysfunction. AT3 main function is to inhibit thrombin by the formation of the complex thrombin-antithrombin (TAT). Although TAT was also significantly increased in ADHF patients, no association was found with heart or kidney function. TAT levels in plasma were several orders of magnitude lower than AT3 (0-1 nM TAT

vs 1000-10000 nM AT3). All these findings suggest a function for plasma AT3 in ADHF beyond its main role in coagulation as thrombin inhibitor.

As seen for AT3, complement C3 levels are elevated in urine and plasma of ADHF patients compared to healthy individuals. Interestingly, AT3 plasma and urine levels significantly correlate with those of C3 in ADHF patients at hospitalisation, whereas no correlation was observed between AT3 and CRP, suggesting a link between AT3 and activation of innate immunity processes beyond a systemic inflammation.

In previous studies the complement system was associated with adverse outcomes and survival in cardiovascular pathologies, with controversial findings (88,94,95,299). Thus, Suffriti *et al.* (299) and Frey *et al.* (88) reported that elevated complement activation products were associated with better outcomes, whereas Gombos *et al.* (94) reported the relevance of high C3a levels in the prediction of higher rehospitalisation rate, cardiovascular events, and mortality. In agreement with the two former publications, our results indicated that low C3 levels were associated with worse outcome and prognosis.

Dysregulated activation of the complement system and inflammatory response might lead to left ventricular dysfunction and remodelling, which are hallmark characteristics of HF (300) and associated with its progression (301). In this thesis, as proof of concept to validate the relevance of C3 in tissue remodelling, we performed studies in human atherosclerotic arteries and in vitro cell culture studies with human vascular smooth muscle cells, in which the effects of C3-activation products such as C3a and C3b on cell function were investigated.

To notice, active products of the C3-system are significantly increased in the pathological extracellular matrix (ECM) in human atherosclerotic vessels. Moreover, C3 and its cell receptor are expressed by human VSMC, a key cell component for vessel wall remodelling during atherosclerosis. Furthermore, our results provided evidence of the

capacity of C3-derived products, beyond its well-known role in inflammation and immunity, to modulate the migratory and repair function of VSMC when exposed to pathological conditions. These results of this proof-of concept study suggest the C3-complement pathway as a novel player in pathologic tissue remodelling, playing a role in the interaction between ECM and non-immune tissue resident cells.

The ECM is vital for the proper structure and functionality for many organs (109), including the heart. It is dynamically remodelled, however, disruptions and dysregulations in its composition and/or structure can be pathological (302), leading to tissue damage. Future studies are needed to proof if in the heart ECM such C3-associated processes result in an adverse remodelling of the myocardium ending in heart failure.

Among the several molecules studied within atherosclerosis and heart failure is vitamin D (303), which may inhibit cardiomyocyte hypertrophy, as it was observed in neonatal rats (304) Vitamin D is also suggested to play a role in ECM remodelling since mice lacking vitamin D receptor (VDR) presented elevated levels of matrix metalloproteinases and fibrosis, and reduced tissue inhibitors of metalloproteinases (305). In agreement, deficient levels of vitamin D have been associated with risk of ventricle remodelling, heart failure, and adverse clinical outcome (306).

Vitamin D binding protein (VDBP) is the main carrier for vitamin D in plasma (307). Interestingly, the results of this thesis evidenced an exacerbated loss of VDBP in the urine of ADHF patients at hospital admission, being the urinary VDBP levels especially in those patients with kidney disfunction.

The increased urinary VDBP is maintained after 72 hours hospitalisation in those patients suffering from acute kidney function deterioration during hospitalisation. Importantly, this pattern in VDBP is observed

before patients show a pathologic glomerular filtration rate, suggesting a potential value of VDBP as marker of subclinical kidney dysfunction in ADHF patients. Due to these changes or lack thereof, urinary VDBP levels were studied as a possible kidney function deterioration biomarker. Even though cystatin C and kidney injury molecule 1 (KIM-1) have had promising results as biomarkers of AKI (184,308), although with controversial results (173,185,186). None of these protein alone, that is VDBP, cystatin C or KIM-1, was able to predict AKI in our ADHF population. However, the combination of these levels and the urinary levels of current potential biomarkers of renal injury CysC and KIM-1 could be used as new diagnostic tool to stratify ADHF patients regarding the risk of developing renal injury during hospitalisation.

In urine, VDBP is forming a complex with 25-(OH) vitamin D3. In normal conditions setting, this complex is reabsorbed in the proximal tubule back into circulation, which is a crucial step for vitamin D conversion into its active metabolite (309). Damage to proximal tubules, and consequent VDBP urinary loss, could imply deficient amounts of vitamin D reabsorbed into circulation and increased loss through urine. In this respect, vitamin D deficiency has been previously related to cardiovascular disease (310), kidney disease (311,312), and heart failure (306), therefore, low vitamin D levels could aggravate heart dysfunction in ADHF patients, further worsening their prognosis.

In summary, ADHF patients present 26 differentially excreted proteins that are associated with inflammation, immune system, and transport. Their levels have been associated with ADHF pathophysiology and adverse outcomes in line with previous publications. Nevertheless, novel information regarding TTR, AT3, C3, and VDBP roles in heart failure has been presented.

CHAPTER VII: CONCLUSIONS

7. Conclusions

The conclusions of this thesis are the following:

1. Acute decompensated heart failure (ADHF) patients at hospital admission present a differential proteomic urinary signature of 26 proteins, identified by two dimensional electrophoresis coupled to mass spectrometry.
2. *In silico* analysis identified the top molecular processes and functions related to the differential proteome in urine of ADHF patients. These are protein transport, coagulation and haemostasis, innate immunity and inflammation, and extracellular matrix remodelling.
3. Increased levels of transthyretin (TTR) and retinol binding protein 4 (RBP4) in urine of ADHF patients associate with renal dysfunction and with poor disease evolution within 18 months follow-up.
4. Antithrombin III (AT3) levels are increased in ADHF. AT3 associates with renal dysfunction and preserved/mildly reduced left ventricular ejection fraction. The role of AT3 in these patients is probably beyond its activity as a haemostatic factor.
5. ADHF patient showed an inflammatory background with increased levels of complement C3, which localises in the vascular extracellular matrix and stimulates cell functions such as adhesion, migration, and cytoskeletal reorganisation.
6. Vitamin D binding protein (VDBP) was found increased in urine of ADHF patients, with a differential evolution pattern at early stage of hospitalisation, which relates to subclinical renal dysfunction, in the absence of a pathological glomerular filtration rate.

General conclusions

In summary, all together, the results of this thesis provide evidence of a specific urinary protein signature in ADHF patients that associates with the underlying pathophysiology. The observed changes in the urinary proteome may contribute to a better understanding of mechanisms and triggers behind ADHF presentation and to a more accurate disease phenotyping.

CHAPTER VII: REFERENCES

8. References

1. McDonagh TA, Metra M, Adamo M, Gardner RS, Baumbach A, Böhm M, et al. 2021 ESC Guidelines for the diagnosis and treatment of acute and chronic heart failure. *Eur Heart J*. 2021;42(36):3599–726.
2. Yancy CW, Jessup M, Bozkurt B, Butler J, Casey DE, Drazner MH, et al. 2013 ACCF/AHA guideline for the management of heart failure: A report of the American college of cardiology foundation/american heart association task force on practice guidelines. *J Am Coll Cardiol*. 2013;62(16).
3. Mosterd A, Hoes AW. Clinical epidemiology of heart failure. *Heart*. 2007;93(9):1137–46.
4. Tanai E, Frantz S. Pathophysiology of heart failure. *Compr Physiol*. 2016;6(1):187–214.
5. Ponikowski P, Voors AA, Anker SD, Bueno H, Cleland JGF, Coats AJS, et al. 2016 ESC Guidelines for the diagnosis and treatment of acute and chronic heart failure. *Eur Heart J*. 2016;37(27):2129–2000.
6. Kurmani S, Squire I. Acute Heart Failure: Definition, Classification and Epidemiology. *Curr Heart Fail Rep*. 2017;14(5):385–92.
7. Sicras-Mainar A, Sicras-Navarro A, Palacios B, Varela L, Delgado JF. Epidemiology and treatment of heart failure in Spain: the HF-PATHWAYS study. *Rev Esp Cardiol*. 2022;75(1):31–8.
8. Sayago-Silva I, García-López F, Segovia-Cubero J. Epidemiology of Heart Failure in Spain Over the Last 20 Years.

- Rev Española Cardiol. 2013;66(8):649–56.
9. Maggioni AP, Dahlström U, Filippatos G, Chioncel O, Leiro MC, Drozd J, et al. EURObservational Research Programme: Regional differences and 1-year follow-up results of the Heart Failure Pilot Survey (ESC-HF Pilot). *Eur J Heart Fail.* 2013;15(7):808–17.
 10. Nieminen MS, Brutsaert D, Dickstein K, Drexler H, Follath F, Harjola V-P, et al. EuroHeart Failure Survey II (EHFS II): a survey on hospitalized acute heart failure patients: description of population. *Eur Heart J.* 2006;27:2725–36.
 11. Chioncel O, Mebazaa A, Harjola V-P, Coats AJ, Piepoli MF, Crespo-Leiro MG, et al. Clinical phenotypes and outcome of patients hospitalized for acute heart failure: the ESC Heart Failure Long-Term Registry. *Eur J Heart Fail.* 2017;19:1242–54.
 12. Miró Ò, García Sarasola A, Fuenzalida C, Calderón S, Jacob J, Aguirre A, et al. Departments involved during the first episode of acute heart failure and subsequent emergency department revisits and rehospitalisations: an outlook through the NOVICA cohort Methods and results. *Eur J Heart Fail.* 2019;21:1231–44.
 13. Farmakis D, Parissis J, Lekakis J, Filippatos G. Acute Heart Failure: Epidemiology, Risk Factors, and Prevention. *Rev Española Cardiol.* 2015;68(3):245–8.
 14. Buja A, Solinas G, Visca M, Federico B, Gini R, Baldo V, et al. Prevalence of heart failure and adherence to process indicators: Which socio-demographic determinants are involved? *Int J Environ Res Public Health.* 2016;13(2):1–12.
 15. Smeets M, Vaes B, Aertgeerts B, Raat W, Penders J,

- Vercammen J, et al. Impact of an extended audit on identifying heart failure patients in general practice: baseline results of the OSCAR-HF pilot study. *ESC Hear Fail.* 2020;7(6):3950–61.
16. Chioncel O, Tatu-Chițoiu G, Christodorescu R, Coman IM, Deleanu D, Vinereanu D, et al. Characteristics of patients with heart failure from Romania enrolled in - ESC-HF Long-Term (ESC-HF-LT) Registry. *Rom J Cardiol.* 2015;25(4):413–20.
 17. Conrad N, Judge A, Tran J, Mohseni H, Hedgecott D, Crespillo AP, et al. Temporal trends and patterns in heart failure incidence: a population-based study of 4 million individuals. *Lancet.* 2018;391:572–80.
 18. Danielsen R, Thorgeirsson G, Einarsson H, Ólafsson Ö, Aspelund T, Harris TB, et al. Prevalence of heart failure in the elderly and future projections: the AGES-Reykjavík study. *Scand Cardiovasc J.* 2017;51(4):183–9.
 19. Dansk selskab for almen medicin. Kronisk systolisk hjerteinsufficiens. 2013. 44 p.
 20. Değertekin M, Erol Ç, Ergene O, Tokgözoğlu L, Aksoy M, Erol MK, et al. [Heart failure prevalence and predictors in Turkey: HAPPY study]. *Turk Kardiyol Dern Ars.* 2012;40(4):298–308.
 21. Holstiege J, Akmatov MK, Steffen A, Bätzing J. Prävalenz der Herzinsuffizienz-bundesweite Trends, regionale Variationen und häufige Komorbiditäten. *Versorgungsatlas-Bericht.* 2018;18(9):1–22.
 22. Meems LMG, van Veldhuisen DJ, de Boer RA. Progress in heart failure management in the Netherlands and beyond: long-term commitment to deliver high-quality research and patient care.

- Netherlands Hear J. 2020;28(Suppl 1):31.
23. Santé publique France. Insuffisance cardiaque [Internet]. 2019 [cited 2022 Feb 12]. Available from: <https://www.santepubliquefrance.fr/maladies-et-traumatismes/maladies-cardiovasculaires-et-accident-vasculaire-cerebral/insuffisance-cardiaque>
 24. Murphy SP, Ibrahim NE, Januzzi JL. Heart Failure with Reduced Ejection Fraction: A Review. *J Am Med Assoc.* 2020;324(5):488–504.
 25. Roger VL. Epidemiology of Heart Failure. *Circ Res.* 2013;113(6):646–59.
 26. Lardizabal JA, Deedwania PC. Atrial Fibrillation in Heart Failure. *Med Clin North Am.* 2012;96(5):987–1000.
 27. Carlisle MA, Fudim M, DeVore AD, Piccini JP. Heart Failure and Atrial Fibrillation, Like Fire and Fury. *JACC Hear Fail.* 2019;7(6):447–56.
 28. Bouhairie VE, Goldberg AC. Familial Hypercholesterolemia. *Cardiol Clin.* 2015;33(2):169–79.
 29. Kenny HC, Abel ED. Heart Failure in Type 2 Diabetes Mellitus: Impact of Glucose Lowering Agents, Heart Failure Therapies and Novel Therapeutic Strategies. *Circ Res.* 2019;124(1):121–41.
 30. Mehta A, Bhattacharya S, Estep J, Faiman C. Diabetes and Heart Failure: A Marriage of Inconvenience. *Clin Geriatr Med.* 2020;36(3):447–55.
 31. Ingelsson E, Sundström J, Ärnlöv J, Zethelius B, Lind L. Insulin resistance and risk of congestive heart failure. *J Am Med Assoc.*

- 2005;294(3):334–41.
32. Anter E, Jessup M, Callans DJ. Atrial fibrillation and heart failure: Treatment considerations for a dual epidemic. *Circulation*. 2009;119(18):2516–25.
 33. Schefold JC, Filippatos G, Hasenfuss G, Anker SD, Von Haehling S. Heart failure and kidney dysfunction: Epidemiology, mechanisms and management. *Nat Rev Nephrol*. 2016;12(10):610–23.
 34. Mentz RJ, Felker GM. Noncardiac Comorbidities and Acute Heart Failure Patients. *Hear Fail Clin*. 2013;9(3):359–vii.
 35. Güder G, Störk S. COPD and heart failure: differential diagnosis and comorbidity. *Herz*. 2019;44:502–8.
 36. Hawkins NM, Petrie MC, Jhund PS, Chalmers GW, Dunn FG, McMurray JJ V. Heart failure and chronic obstructive pulmonary disease: diagnostic pitfalls and epidemiology. *Eur J Heart Fail*. 2009;11:130–9.
 37. de Miguel Díez J, Chancafe Morgan J, Jiménez García R. The association between COPD and heart failure risk: A review. *Int J COPD*. 2013;8:305–12.
 38. Badimon L, Padró T, Vilahur G. Atherosclerosis, platelets and thrombosis in acute ischaemic heart disease. *Eur Hear J Acute Cardiovasc Care*. 2012;1(1):60–74.
 39. Malakar AK, Choudhury D, Halder B, Paul P, Uddin A, Chakraborty S. A review on coronary artery disease, its risk factors, and therapeutics. *J Cell Physiol*. 2019;234(10):16812–23.

40. Snipelisky D, Chaudhry SP, Stewart GC. The Many Faces of Heart Failure. *Card Electrophysiol Clin*. 2019;11(1):11–20.
41. Hammond DA, Smith MN, Lee KC, Honein D, Quidley AM. Acute Decompensated Heart Failure. *J Intensive Care Med*. 2018;33(8):456–66.
42. Gheorghiade M, Follath F, Ponikowski P, Barsuk JH, Blair JEA, Cleland JG, et al. Assessing and grading congestion in acute heart failure: A scientific statement from the acute heart failure committee of the heart failure association of the European society of cardiology and endorsed by the European society of intensive care medicine. *Eur J Heart Fail*. 2010;12(5):423–33.
43. Gheorghiade M, Filippatos G, De Luca L, Burnett J. Congestion in Acute Heart Failure Syndromes: An Essential Target of Evaluation and Treatment. *Am J Med*. 2006;119(12 SUPPL.):3–10.
44. Mentz RJ, O CM. Pathophysiology and clinical evaluation of acute heart failure. *Nat Rev Cardiol*. 2015;(13):28–35.
45. Njoroge JN, Teerlink JR. Pathophysiology and Therapeutic Approaches to Acute Decompensated Heart Failure. *Circ Res*. 2021;128:1468–86.
46. Jackson G, Gibbs C, Davies M, Lip GYH. ABC of heart failure. Pathophysiology. *BMJ*. 2000;320(7228):167–70.
47. Arrigo M, Jessup M, Mullens W, Reza N, Shah AM, Sliwa K, et al. Acute heart failure. *Nat Rev Dis Prim*. 2020;6(16).
48. Summers RL, Amsterdam E. Pathophysiology of Acute Decompensated Heart Failure. *Heart Fail Clin*. 2009;5(1):9–17.

49. Sayer G, Bhat G. The Renin-Angiotensin-Aldosterone System and Heart Failure. *Cardiol Clin.* 2014;32(1):21–32.
50. Bock HA, Hermle M, Brunner FP, Thiel G. Pressure dependent modulation of renin release in isolated perfused glomeruli. *Kidney Int.* 1992;41(2):275–80.
51. Urata H, Healy B, Stewart RW, Bumpus FM, Husain A. Angiotensin II-forming pathways in normal and failing human hearts. *Circ Res.* 1990;66(4):883–90.
52. Peng JF, Gurantz D, Tran V, Cowling RT, Greenberg BH. Tumor necrosis factor- α -induced AT1 receptor upregulation enhances angiotensin II-mediated cardiac fibroblast responses that favor fibrosis. *Circ Res.* 2002;91(12):1119–26.
53. Weber KT. Extracellular Matrix Remodeling in Heart Failure. *Circulation.* 1997;96(11):4065–82.
54. Tan LB, Jalil JE, Pick R, Janicki JS, Weber KT. Cardiac myocyte necrosis induced by angiotensin II. *Circ Res.* 1991;69(5):1185–95.
55. Slavíková J, Kuncová J, Topolcan O. Plasma Catecholamines and Ischemic Heart Disease. *Clin Cardiol.* 2007;30:326–30.
56. Brilla C, Zhou G, Matsubara L, Weber K. Collagen metabolism in cultured adult rat cardiac fibroblasts: response to Angiotensin II and aldosterone. *J Mol Cell Cardiol.* 1994;26:809–20.
57. Yoshida M, Ma J, Tomita T, Morikawa N, Tanaka N, Masamura K, et al. Mineralocorticoid receptor is overexpressed in cardiomyocytes of patients with congestive heart failure. *Congest Heart Fail.* 2005;11(1):12–6.

58. Aronson D, Burger AJ. Neurohumoral Activation and Ventricular Arrhythmias in Patients with Decompensated Congestive Heart Failure: Role of Endothelin. *Pacing Clin Electrophysiol.* 2003;26(3):703–10.
59. Aronson D, Burger AJ. Neurohormonal prediction of mortality following admission for decompensated heart failure. *Am J Cardiol.* 2003;91(2):245–8.
60. Biegus J, Nawrocka-Millward S, Zymlński R, Fudim M, Testani J, Marciniak D, et al. Distinct renin/aldosterone activity profiles correlate with renal function, natriuretic response, decongestive ability and prognosis in acute heart failure. *Int J Cardiol.* 2021;345:54–60.
61. Gonzalez AA, Salinas-Parra N, Cifuentes-Araneda F, Reyes-Martinez C. Vasopressin actions in the kidney renin angiotensin system and its role in hypertension and renal disease. *Vitam Horm.* 2020;113:217–38.
62. Iovino M, Iacoviello M, De Pergola G, Licchelli B, Iovino E, Guastamacchia E, et al. Vasopressin in Heart Failure. *Endocrine, Metab Immune Disord - Drug Targets.* 2018;18(5):458–65.
63. Urbach J, Goldsmith SR. Vasopressin antagonism in heart failure: a review of the hemodynamic studies and major clinical trials. *Ther Adv Cardiovasc Dis Rev.* 2021;15:1–10.
64. Levine B, Kalman J, Mayer L, Fillit HM, Packer M. Elevated circulating levels of tumor necrosis factor in severe chronic heart failure. *N Engl J Med.* 1990;323(4):236–41.
65. Mann DL. Innate immunity and the failing heart: The cytokine hypothesis revisited. *Circ Res.* 2015;116(7):1254–68.

66. Murphy SP, Kakkar R, McCarthy CP, Januzzi JL. Inflammation in Heart Failure: JACC State-of-the-Art Review. *J Am Coll Cardiol*. 2020;75(11):1324–40.
67. Yang Y, Lv J, Jiang S, Ma Z, Wang D, Hu W, et al. The emerging role of toll-like receptor 4 in myocardial inflammation. *Cell Death Dis*. 2016;7(5):1–10.
68. Liu L, Wang Y, Cao ZY, Wang MM, Liu XM, Gao T, et al. Up-regulated TLR4 in cardiomyocytes exacerbates heart failure after long-term myocardial infarction. *J Cell Mol Med*. 2015;19(12):2728–40.
69. Torre-Amione G, Kapadia S, Lee J, Durand JB, Bies RD, Young JB, et al. Tumor Necrosis Factor- α and Tumor Necrosis Factor Receptors in the Failing Human Heart. *Circulation*. 1996;93(4):704–11.
70. Bartekova M, Radosinska J, Jelemensky M, Dhalla NS. Role of cytokines and inflammation in heart function during health and disease. *Heart Fail Rev*. 2018;23(5):733–58.
71. Sharma R, Coats AJS, Anker SD. The role of inflammatory mediators in chronic heart failure: Cytokines, nitric oxide, and endothelin-1. *Int J Cardiol*. 2000;72(2):175–86.
72. Meldrum DR. Tumor necrosis factor in the heart. *Am J Physiol*. 1998;274(3):R577-95.
73. Kalogeropoulos AP, Tang WHW, Hsu A, Felker GM, Hernandez AF, Troughton RW, et al. High-sensitivity C-reactive protein in acute heart failure: Insights from the ASCEND-HF trial. *J Card Fail*. 2014;20(5):319–26.
74. Lakhani I, Wong MV, Hung JKF, Gong M, Waleed K Bin, Xia Y,

- et al. Diagnostic and prognostic value of serum C-reactive protein in heart failure with preserved ejection fraction: a systematic review and meta-analysis. *Heart Fail Rev.* 2021;26(5):1141–50.
75. Zairis MN, Tsiaousis GZ, Georgilas AT, Makrygiannis SS, Adamopoulou EN, Handanis SM, et al. Multimarker strategy for the prediction of 31 days cardiac death in patients with acutely decompensated chronic heart failure. *Int J Cardiol.* 2010 Jun 11;141(3):284–90.
76. Kalogeropoulos AP, Georgiopoulou V V., Butler J. From Risk Factors to Structural Heart Disease: The Role of Inflammation. *Heart Fail Clin.* 2012;8(1):113–23.
77. Suleiman M, Aronson D, Reisner SA, Kapeliovich MR, Markiewicz W, Levy Y, et al. Admission C-reactive protein levels and 30-day mortality in patients with acute myocardial infarction. *Am J Med.* 2003;115(9):695–701.
78. Vistnes M, Høiseith AD, Røsjø H, Nygård S, Pettersen E, Søyseth V, et al. Lack of pro-inflammatory cytokine mobilization predicts poor prognosis in patients with acute heart failure. *Cytokine.* 2013;61(3):962–9.
79. Mann DL. Inflammatory mediators and the failing heart: Past, present, and the foreseeable future. *Circ Res.* 2002;91(11):988–98.
80. Mueller C, Laule-Kilian K, Christ A, Brunner-La Rocca HP, Perruchoud AP. Inflammation and long-term mortality in acute congestive heart failure. *Am Heart J.* 2006;151(4):845–50.
81. Dobaczewski M, Chen W, Frangogiannis NG. Transforming Growth Factor (TGF)- β signaling in cardiac remodeling. *J Mol Cell*

- Cardiol. 2011;51(4):600–6.
82. Li J-M, Brooks G. Differential Protein Expression and Subcellular Distribution of TGF 1 , 2 and 3 in Cardiomyocytes During Pressure Overload-induced Hypertrophy. *J Mol Cell Cardiol.* 1997;29(8):2213–24.
 83. Paulus WJ, Tschöpe C. A novel paradigm for heart failure with preserved ejection fraction: Comorbidities drive myocardial dysfunction and remodeling through coronary microvascular endothelial inflammation. *J Am Coll Cardiol.* 2013;62(4):263–71.
 84. Weerts J, Mourmans SGJ, Barandiarán Aizpurua A, Schroen BLM, Knackstedt C, Eringa E, et al. The Role of Systemic Microvascular Dysfunction in Heart Failure with Preserved Ejection Fraction. *Biomolecules.* 2022;12(2):278.
 85. Westermann D, Lindner D, Kasner M, Zietsch C, Savvatis K, Escher F, et al. Cardiac inflammation contributes to changes in the extracellular matrix in patients with heart failure and normal ejection fraction. *Circ Hear Fail.* 2011;4(1):44–52.
 86. Mohammed SF, Hussain S, Mirzoyev SA, Edwards WD, Maleszewski JJ, Redfield MM. Coronary Microvascular Rarefaction and Myocardial Fibrosis in Heart Failure with Preserved Ejection Fraction. *Circulation.* 2015;131(6):550–9.
 87. Master Sankar Raj V, Gordillo R, Chand DH. Overview of C3 Glomerulopathy. *Front Pediatr.* 2016;4(May):1–7.
 88. Frey A, Ertl G, Angermann CE, Hofmann U, Störk S, Frantz S. Complement C3c as a biomarker in heart failure. *Mediators Inflamm.* 2013;2013.
 89. Ahmad SB, Bomback AS. C3 Glomerulopathy: Pathogenesis and

- Treatment. *Adv Chronic Kidney Dis.* 2020;27(2):104–10.
90. Huber-Lang M, Sarma JV, Zetoune FS, Rittirsch D, Neff TA, McGuire SR, et al. Generation of C5a in the absence of C3: A new complement activation pathway. *Nat Med.* 2006;12(6):682–7.
 91. Aukrust P, Gullestad L, Lappegård KT, Ueland T, Aass H, Wikeby L, et al. Complement activation in patients with congestive heart failure: Effect of high-dose intravenous immunoglobulin treatment. *Circulation.* 2001;104(13):1494–500.
 92. del Balzo UH, Levi R, Polley MJ. Cardiac dysfunction caused by purified human C3a anaphylatoxin. *Proc Natl Acad Sci U S A.* 1985;82(3):886–90.
 93. Ricklin D, Reis ES, Lambris JD. Complement in disease: a defence system turning offensive. *Nat Rev Nephrol.* 2016;12(7):383–401.
 94. Gombos T, Förhécz Z, Pozsonyi Z, Széplaki G, Kunde J, Füst G, et al. Complement anaphylatoxin C3a as a novel independent prognostic marker in heart failure. *Clin Res Cardiol.* 2012;101(8):607–15.
 95. Silva N, Martins S, Lourenço P, Bettencourt P, Guimarães JT. Complement C3c and C4c as predictors of death in heart failure. *IJC Metab Endocr.* 2015;7:31–5.
 96. Zhang C, Li Y, Wang C, Wu Y, Cui W, Miwa T, et al. Complement 5a receptor mediates angiotensin II-induced cardiac inflammation and remodeling. *Arterioscler Thromb Vasc Biol.* 2014;34(6):1240–8.
 97. Mullick A, Tremblay J, Leon Z, Gros P. A novel role for the fifth

- component of complement (C5) in cardiac physiology. *PLoS One*. 2011;6(8).
98. Oliveira GHM, Brann CN, Becker K, Thohan V, Koerner MM, Loebe M, et al. Dynamic Expression of the Membrane Attack Complex (MAC) of the Complement System in Failing Human Myocardium. *Am J Cardiol*. 2006;97(11):1626–9.
 99. Lip GYH, Ponikowski P, Andreotti F, Anker SD, Filippatos G, Homma S, et al. Thromboembolism and antithrombotic therapy for heart failure in sinus rhythm: An executive summary# of a joint consensus document from the ESC heart failure association and the esc working group on thrombosis. *Thromb Haemost*. 2012;108(6):1009–22.
 100. Kim JH, Shah P, Tantry US, Gurbel PA. Coagulation Abnormalities in Heart Failure: Pathophysiology and Therapeutic Implications. *Curr Heart Fail Rep*. 2016;13(6):319–28.
 101. Zannad F, Stough WG, Regnault V, Gheorghide M, Deliargyris E, Gibson CM, et al. Is thrombosis a contributor to heart failure pathophysiology? Possible mechanisms, therapeutic opportunities, and clinical investigation challenges. *Int J Cardiol*. 2013;167(5):1772–82.
 102. Jug B, Vene N, Salobir BG, Šebeštjen M, Šabovič M, Keber I. Procoagulant state in heart failure with preserved left ventricular ejection fraction. *Int Heart J*. 2009;50(5):591–600.
 103. Wrigley BJ, Shantsila E, Tapp LD, Lip GYH. Increased Formation of monocyte-platelet aggregates in ischemic heart failure. *Circ Hear Fail*. 2013;6(1):127–35.
 104. Rajendran P, Rengarajan T, Thangavel J, Nishigaki Y,

- Sakthisekaran D, Sethi G, et al. The vascular endothelium and human diseases. *Int J Biol Sci.* 2013;9(10):1057–69.
105. Zuchi C, Tritto I, Carluccio E, Mattei C, Cattadori G, Ambrosio G. Role of endothelial dysfunction in heart failure. *Heart Fail Rev.* 2020;25(1):21–30.
106. Fischer D, Rossa S, Landmesser U, Spiekermann S, Engberding N, Hornig B, et al. Endothelial dysfunction in patients with chronic heart failure is independently associated with increased incidence of hospitalization, cardiac transplantation, or death. *Eur Heart J.* 2005;26(1):65–9.
107. McMurray JJV, Pfeffer M. Heart Failure. *Lancet.* 2005;365:1877–9.
108. Frangogiannis NG. The extracellular matrix in ischemic and non-ischemic heart failure. *Circ Res.* 2019;125(1):117–46.
109. Bonnans C, Chou J, Werb Z. Remodelling the extracellular matrix in development and disease. *Nat Rev Mol Cell Biol.* 2014;15(12):786–801.
110. Frangogiannis NG. Cardiac fibrosis: Cell biological mechanisms, molecular pathways and therapeutic opportunities. *Mol Aspects Med.* 2019;65(August 2018):70–99.
111. Martinez-Naharro A, Hawkins PN, Fontana M. Cardiac amyloidosis. *Clin Med (Northfield Il).* 2018;18(2):s30-35.
112. Ruberg FL, Grogan M, Hanna M, Kelly JW, Maurer MS. Transthyretin amyloid cardiomyopathy: JACC State of the Art Review. *J Am Coll Cardiol.* 2019;73(22):2872–2891.
113. Bainbridge P. Wound healing and the role of fibroblasts. *J Wound*

- Care. 2013;22(8):2013.
114. Kurose H. Cardiac Fibrosis and Fibroblasts. *Cells*. 2021;10(7):1716.
 115. Ma ZG, Yuan YP, Wu HM, Zhang X, Tang QZ. Cardiac fibrosis: new insights into the pathogenesis. *Int J Biol Sci*. 2018;14(12):1645–57.
 116. Volpe M, Carnovali M, Mastromarino V. The natriuretic peptides system in the pathophysiology of heart failure: From molecular basis to treatment. *Clin Sci*. 2016;130(2):57–77.
 117. Harjola V-P, Mullens W, Banaszewski M, Bauersachs J, Brunner-La Rocca HP, Chioncel O, et al. Organ dysfunction, injury and failure in acute heart failure: from pathophysiology to diagnosis and management. A review on behalf of the Acute Heart Failure Committee of the Heart Failure Association (HFA) of the European Society of Cardiology (ESC). *Eur J Hear Fail*. 2017;19(7):821–36.
 118. Damman K, Valente MAE, Voors AA, O'Connor CM, Van Veldhuisen DJ, Hillege HL. Renal impairment, worsening renal function, and outcome in patients with heart failure: An updated meta-analysis. *Eur Heart J*. 2014;35(7):455–69.
 119. Palazzuoli A, Ruocco G. Heart–Kidney Interactions in Cardiorenal Syndrome Type 1. *Adv Chronic Kidney Dis*. 2018;25(5):408–17.
 120. Correale M, Tarantino N, Petrucci R, Tricarico L, Laonigro I, Di Biase M, et al. Liver disease and heart failure: Back and forth. *Eur J Intern Med*. 2018;48(2018):25–34.
 121. Nikolaou M, Parissis J, Yilmaz MB, Seronde MF, Kivikko M, Laribi

- S, et al. Liver function abnormalities, clinical profile, and outcome in acute decompensated heart failure. *Eur Heart J*. 2013;34(10):742–9.
122. Biegus J, Hillege HL, Postmus D, Valente MAE, Bloomfield DM, Cleland JGF, et al. Abnormal liver function tests in acute heart failure: relationship with clinical characteristics and outcome in the PROTECT study. *Eur J Heart Fail*. 2016;18(7):830–9.
123. Xanthopoulos A, Starling RC, Kitai T, Triposkiadis F. Heart Failure and Liver Disease: Cardiohepatic Interactions. *JACC Hear Fail*. 2019;7(2):87–97.
124. Poelzl G, Ess M, Von Der Heidt A, Rudnicki M, Frick M, Ulmer H. Concomitant renal and hepatic dysfunctions in chronic heart failure: Clinical implications and prognostic significance. *Eur J Intern Med*. 2013;24(2):177–82.
125. Núñez J, Miñana G, Santas E, Bertomeu-González V. Síndrome cardiorenal en la insuficiencia cardiaca aguda: revisando paradigmas. *Rev Esp Cardiol*. 2015;68(5):426–35.
126. Lullo L Di, Bellasi A, Barbera V, Russo D, Russo L, Di Iorio B, et al. Pathophysiology of the cardio-renal syndromes types 1-5: An uptodate. *Indian Heart J*. 2017;69:255–65.
127. Aronson D. Cardiorenal syndrome in acute decompensated heart failure: A new approach. *Expert Rev Cardiovasc Ther*. 2012;177–89.
128. Ronco C, Haapio M, House AA, Anavekar N, Bellomo R. Cardiorenal Syndrome. *J Am Coll Cardiol*. 2008;52(19):1527–39.
129. Damman K, Testani JM. The kidney in heart failure: An update. *Eur Heart J*. 2015;36(23):1437–44.

130. Hillege HL, Girbes AR, de Kam PJ, van Vanelldhuisen DJ. Renal Function, Neurohormonal Activation, and Survival in Patients With Chronic Heart Failure. *Circulation*. 2000;102:203–10.
131. Ronco C, Bellasi A, Di Lullo L. Cardiorenal Syndrome: An Overview. *Adv Chronic Kidney Dis*. 2018;25(5):382–90.
132. Ronco C, McCullough P, Anker SD, Anand I, Aspromonte N, Bagshaw SM, et al. Cardio-renal syndromes: Report from the consensus conference of the acute dialysis quality initiative. *Eur Heart J*. 2010;31(6):703–11.
133. Cole RT, Masoumi A, Triposkiadis F, Giamouzis G, Georgiopoulou V, Kalogeropoulos A, et al. Renal Dysfunction in Heart Failure. *Med Clin North Am*. 2012;96(5):955–74.
134. Newsome BB, Warnock DG, McClellan WM, Herzog CA, Kiefe CI, Eggers PW, et al. Long-term risk of mortality and end-stage renal disease among the elderly after small increases in serum creatinine level during hospitalization for acute myocardial infarction. *Arch Intern Med*. 2008;168(6):609–16.
135. Krumholz HM, Chen YT, Vaccarino V, Wang Y, Radford MJ, Bradford WD, et al. Correlates and impact on outcomes of worsening renal function in patients ≥ 65 years of age with heart failure. *Am J Cardiol*. 2000;85(9):1110–3.
136. Damman K, Tang WHW, Testani JM, McMurray JJV. Terminology and definition of changes renal function in heart failure. *Eur Heart J*. 2014;35(48):3413–6.
137. Manguba AS, Vela Parada X, Coca SG, Lala A. Synthesizing Markers of Kidney Injury in Acute Decompensated Heart Failure: Should We Even Keep Looking? *Curr Heart Fail Rep*.

- 2019;16(6):257–73.
138. Metra M, Cotter G, Gheorghiade M, Cas LD, Voors AA. The role of the kidney in heart failure. *Eur Heart J*. 2012;33(17):2135–43.
 139. Chan D, Ng LL. Biomarkers in acute myocardial infarction. *BMC Med*. 2010;8.
 140. Vasan RS. Biomarkers of cardiovascular disease: Molecular basis and practical considerations. *Circulation*. 2006;113(19):2335–62.
 141. FDA-NIH Biomarker Working Group. BEST (Biomarkers, EndpointS, and other Tools) Resource. Silver Spring (MD): Food and Drug Administration (US); Bethesda (MD): National Institutes of Health (US). Food and Drug Administration (US); 2016.
 142. Gaggin HK, Januzzi JL. Biomarkers and diagnostics in heart failure. *Biochim Biophys Acta*. 2013;1832(12):2442–50.
 143. Fonarow GC, Peacock WF, Horwich TB, Phillips CO, Givertz MM, Lopatin M, et al. Usefulness of B-Type Natriuretic Peptide and Cardiac Troponin Levels to Predict In-Hospital Mortality from ADHERE. *Am J Cardiol*. 2008;101(2):231–7.
 144. Yu CM, Sanderson JE. Plasma brain natriuretic peptide - an independent predictor of cardiovascular mortality in acute heart failure. *Eur J Heart Fail*. 1999;59–65.
 145. Gegenhuber A, Mueller T, Dieplinger B, Poelz W, Pacher R, Haltmayer M. B-type natriuretic peptide and amino terminal proBNP predict one-year mortality in short of breath patients independently of the baseline diagnosis of acute destabilized heart failure. *Clin Chim Acta*. 2006;370(1–2):174–9.

146. Chen LJ, Hung CL, Yeh HI, Jeng MJ, Su CH, Wu TY, et al. The utilization and prognostic impact of B-type Natriuretic Peptide in hospitalized acute decompensated heart failure in an Asian population. *BMC Cardiovasc Disord.* 2016;16(1):1–8.
147. Januzzi JL, Van Kimmenade R, Lainchbury J, Bayes-Genis A, Ordonez-Llanos J, Santalo-Bel M, et al. NT-proBNP testing for diagnosis and short-term prognosis in acute destabilized heart failure: An international pooled analysis of 1256 patients: The international collaborative of NT-proBNP study. *Eur Heart J.* 2006;27(3):330–7.
148. Januzzi JL, Maisel AS, Silver M, Xue Y, Defilippi C. Natriuretic Peptide Testing for Predicting Adverse Events Following Heart Failure Hospitalization. *Congest Hear Fail.* 2012;18(SUPPL. 1):9–13.
149. Bachmann KN, Huang S, Lee H, Dichtel LE, Gupta DK, Burnett Jr JC, et al. Effect of Testosterone on Natriuretic Peptide Levels. *J Am Coll Cardiol.* 2019;73(11):1288–96.
150. Wang TJ, Larson MG, Levy D, Leip EP, Benjamin EJ, Wilson PWF, et al. Impact of age and sex on plasma natriuretic peptide levels in healthy adults. *Am J Cardiol.* 2002;90(3):254–8.
151. Kistorp C, Faber J, Galatius S, Gustafsson F, Frystyk J, Flyvbjerg A, et al. Plasma adiponectin, body mass index, and mortality in patients with chronic heart failure. *Circulation.* 2005;112(12):1756–62.
152. Balion CM, Santaguida P, McKelvie R, Hill SA, McQueen MJ, Worster A, et al. Physiological, pathological, pharmacological, biochemical and hematological factors affecting BNP and NT-proBNP. *Clin Biochem.* 2008;41(4–5):231–9.

153. Ibrahim NE, McCarthy CP, Shrestha S, Gaggin HK, Mukai R, Szymonifka J, et al. Effect of Neprilysin Inhibition on Various Natriuretic Peptide Assays. *J Am Coll Cardiol*. 2019;73(11):1273–84.
154. Schou M, Dalsgaard MK, Clemmesen O, Dawson EA, Yoshiga CC, Nielsen HB, et al. Kidneys extract BNP and NT-proBNP in healthy young men. *J Appl Physiol*. 2005;99(5):1676–80.
155. Daniels LB, Bayes-Genis A. Using ST2 in cardiovascular patients: A review. *Future Cardiol*. 2014;10(4):525–39.
156. Pourafkari L, Tajlil A, Nader ND. Biomarkers in diagnosing and treatment of acute heart failure. *Biomark Med*. 2019;13(14):1235–49.
157. Borovac JA, Glavas D, Susilovic Grabovac Z, Supe Domic D, Stanisic L, D’Amario D, et al. Circulating sST2 and catestatin levels in patients with acute worsening of heart failure: a report from the CATSTAT-HF study. *ESC Hear Fail*. 2020;7(5):2818–28.
158. Januzzi JL, Peacock WF, Maisel AS, Chae CU, Jesse RL, Baggish AL, et al. Measurement of the Interleukin Family Member ST2 in Patients With Acute Dyspnea. *J Am Coll Cardiol*. 2007;50(7):607–13.
159. Mueller T, Gegenhuber A, Leitner I, Poelz W, Haltmayer M, Dieplinger B. Diagnostic and prognostic accuracy of galectin-3 and soluble ST2 for acute heart failure. *Clin Chim Acta*. 2016;463:158–64.
160. Aimo A, Januzzi JL, Bayes-Genis A, Vergaro G, Sciarrone P, Passino C, et al. Clinical and Prognostic Significance of sST2 in

- Heart Failure: JACC Review Topic of the Week. *J Am Coll Cardiol.* 2019;74(17):2193–203.
161. Huang D-D, Shi J-P. Diagnostic Value of Soluble Suppression of Tumorigenicity-2 for Heart Failure. *Chin Med J.* 2016;129(5):570–7.
162. Lim W, Qushmaq I, Cook DJ, Crowther MA, Heels-Ansdell D, Devereaux PJ. Elevated troponin and myocardial infarction in the intensive care unit: a prospective study. *Crit Care.* 2005;9(6):636–44.
163. Xue Y, Clopton P, Peacock WF, Maisel AS. Serial changes in high-sensitive troponin i predict outcome in patients with decompensated heart failure. *Eur J Heart Fail.* 2011;13(1):37–42.
164. Pascual-Figal DA, Manzano-Fernández S, Boronat M, Casas T, Garrido IP, Bonaque JC, et al. Soluble ST2, high-sensitivity troponin T- and N-terminal pro-B-type natriuretic peptide: Complementary role for risk stratification in acutely decompensated heart failure. *Eur J Heart Fail.* 2011;13(7):718–25.
165. Aimo A, Januzzi JL, Vergaro GGV, Ripoli A, Latini R, Masson S, et al. Prognostic value of high-sensitivity troponin T in chronic heart failure an individual patient data meta-analysis. *Circulation.* 2018;137(3):286–97.
166. Zhong X, Qian X, Chen G, Song X. The role of galectin-3 in heart failure and cardiovascular disease. *Clin Exp Pharmacol Physiol.* 2019;46(3):197–203.
167. Sygitowicz G, Tomaniak M, Filipiak KJ, Kołtowski Ł, Sitkiewicz D. Galectin-3 in patients with acute heart failure: Preliminary report

- on first polish experience. *Adv Clin Exp Med*. 2016;25(4):617–23.
168. Stoica A, Şorodoc V, Lionte C, Jaba IM, Costache I, Anisie E, et al. Acute cardiac dyspnea in the emergency department: diagnostic value of N-terminal prohormone of brain natriuretic peptide and galectin-3. *J Int Med Res*. 2019;47(1):159–72.
169. Tarwater K. Estimated glomerular filtration rate explained. *Mo Med*. 2011;108(1):29–32.
170. Ferguson TW, Komenda P, Tangri N. Cystatin C as a biomarker for estimating glomerular filtration rate. *Curr Opin Nephrol Hypertens*. 2015;24(3):295–300.
171. Zhang Z, Lu B, Sheng X, Jin N. Cystatin C in prediction of acute kidney injury: A systemic review and meta-analysis. *Am J Kidney Dis*. 2011;58(3):356–65.
172. Manzano-Fernández S, López-Cuenca Á, Januzzi JL, Parra-Pallares S, Mateo-Martínez A, Sánchez-Martínez M, et al. Usefulness of β -trace protein and cystatin C for the prediction of mortality in non ST segment elevation acute coronary syndromes. *Am J Cardiol*. 2012;110(9):1240–8.
173. Breidthardt T, Sabti Z, Ziller R, Rassouli F, Twerenbold R, Kozhuharov N, et al. Diagnostic and prognostic value of cystatin C in acute heart failure. *Clin Biochem*. 2017;50(18):1007–13.
174. Bellos I, Fitrou G, Daskalakis G, Papantoniou N, Pergialiotis V. Serum cystatin-c as predictive factor of preeclampsia: A meta-analysis of 27 observational studies. *Pregnancy Hypertens*. 2019;16(August 2018):97–104.
175. Leto G, Sepporta MV. The potential of cystatin C as a predictive biomarker in breast cancer. *Expert Rev Anticancer Ther*.

- 2020;20(12):1049–56.
176. Akdağ T, Uca AU. Cystatin C as a potential biomarker to evaluate migraine. *Arq Neuropsiquiatr*. 2020;78(7):337–41.
177. Stephan Y, Sutin AR, Terracciano A. Subjective Age and Cystatin C among Older Adults. *Journals Gerontol - Ser B Psychol Sci Soc Sci*. 2019;74(3):382–8.
178. Al Musaimi O, Abu-Nawwas AH, Al Shaer D, Khaleel NY, Fawzi M. Influence of age, gender, smoking, diabetes, thyroid and cardiac dysfunctions on cystatin C biomarker. *Semergen*. 2019;45(1):44–51.
179. Maahs DM, Prentice N, McFann K, Snell-Bergeon JK, Jalal D, Bishop FK, et al. Age and sex influence cystatin C in adolescents with and without type 1 diabetes. *Diabetes Care*. 2011;34(11):2360–2.
180. Bonventre J V. Kidney injury molecule-1 (KIM-1): A urinary biomarker and much more. *Nephrol Dial Transplant*. 2009;24(11):3265–8.
181. Teo SH, Endre ZH. Biomarkers in acute kidney injury (AKI). *Best Pract Res Clin Anaesthesiol*. 2017;31(3):331–44.
182. Bouqueneau A, Krzesinski JM, Delanaye P, Cavalier E. Biomarkers and physiopathology in the cardiorenal syndrome. *Clin Chim Acta*. 2015;443:100–7.
183. Bonventre J V. Kidney injury molecule-1: a translational journey. *Trans Am Clin Climatol Assoc*. 2014;125:293–9.
184. Huang Y, Don-Wauchope AC. The clinical utility of kidney injury molecule 1 in the prediction, diagnosis and prognosis of acute

- kidney injury: A systematic review. *Inflamm Allergy - Drug Targets*. 2011;10(4):260–71.
185. Verbrugge FH, Dupont M, Shao Z, Shrestha K, Singh D, Finucan M, et al. Novel Urinary Biomarkers in Detecting Acute Kidney Injury, Persistent Renal Impairment and All-cause Mortality following Decongestive Therapy in Acute Decompensated Heart Failure Frederik. *J Card Fail*. 2013;19(9):621–8.
186. Atici A, Emet S, Toprak ID, Cakmak R, Akarsu M, Tukek T. The role of kidney injury molecule-1 in predicting cardiorenal syndrome type 1 after diuretic treatment. *Arch Med Sci - Atheroscler Dis*. 2019;4(1):208–14.
187. Buonafine M, Martinez-Martinez E, Jaisser F. More than a simple biomarker: The role of NGAL in cardiovascular and renal diseases. *Clin Sci*. 2018;132(9):909–23.
188. Smertka M, Chudek J. Using NGAL as an early diagnostic test of acute kidney injury. *Ren Fail*. 2012;34(1):130–3.
189. Liu F, Yang H, Chen H, Zhang M, Ma Q. High expression of neutrophil gelatinase-associated lipocalin (NGAL) in the kidney proximal tubules of diabetic rats. *Adv Med Sci*. 2015;60(1):133–8.
190. Borkham-Kamphorst E, Drews F, Weiskirchen R. Induction of lipocalin-2 expression in acute and chronic experimental liver injury moderated by pro-inflammatory cytokines interleukin-1 β through nuclear factor- κ B activation. *Liver Int*. 2011;31(5):656–65.
191. Savic-Radojevic A, Pljesa-Ercegovic M, Matic M, Simic D, Radovanovic S, Simic T. Novel Biomarkers of Heart Failure. *Adv*

- Clin Chem. 1st ed. 2017;79:93–152.
192. Legrand M, de Berardinis B, Gaggin HK, Magrini L, Belcher A, Zanca B, et al. Evidence of uncoupling between renal dysfunction and injury in cardiorenal syndrome: Insights from the BIONICS study. *PLoS One*. 2014;9(11):1–8.
 193. Breidthardt T, Socrates T, Drexler B, Noveanu M, Heinisch C, Arenja N, et al. Plasma neutrophil gelatinase-associated lipocalin for the prediction of acute kidney injury in acute heart failure. *Crit Care*. 2012;16(1):R2.
 194. Aghel A, Shrestha K, Mullens W, Borowski A, Wilson Tang WH. Serum Neutrophil Gelatinase-Associated Lipocalin (NGAL) in Predicting Worsening Renal Function in Acute Decompensated Heart Failure. *J Card Fail*. 2010;16(1):49–54.
 195. Ferrari F, Scalzotto E, Esposito P, Samoni S, Mistrorigo F, Topete LMR, et al. Neutrophil gelatinase-associated lipocalin does not predict acute kidney injury in heart failure. *World J Clin Cases*. 2020;8(9):1600–7.
 196. Chakraborty S, Kaur S, Guha S, Batra SK. The multifaceted roles of neutrophil gelatinase associated lipocalin (NGAL) in inflammation and cancer. *Biochim Biophys Acta*. 2012;1826(1):129–69.
 197. Wei CT, Tsai IT, Wu CC, Hung WC, Hsuan CF, Yu TH, et al. Elevated plasma level of neutrophil gelatinase-associated lipocalin (NGAL) in patients with breast cancer. *Int J Med Sci*. 2021;18(12):2689–96.
 198. Santiago-Sánchez GS, Pita-Grisanti V, Quiñones-Díaz B, Gumpfer K, Cruz-Monserrate Z, Vivas-Mejía PE. Biological

- functions and therapeutic potential of lipocalin 2 in cancer. *Int J Mol Sci.* 2020;21(12):1–15.
199. Charlton JR, Portilla D, Okusa MD. A basic science view of acute kidney injury biomarkers. *Nephrol Dial Transplant.* 2014;29(7):1301–11.
200. Okubo Y, Sairaku A, Morishima N, Ogi H, Matsumoto T, Kinoshita H, et al. Increased Urinary Liver-Type Fatty Acid–Binding Protein Level Predicts Worsening Renal Function in Patients With Acute Heart Failure. *J Card Fail.* 2018;24(8):520–4.
201. Ahmad T, Jackson K, Rao VS, Tang WHW, Brisco-Bacik MA, Chen HH, et al. Worsening renal function in patients with acute heart failure undergoing aggressive diuresis is not associated with tubular injury. *Circulation.* 2018;137(19):2016–28.
202. Virzi GM, Breglia A, Brocca A, De Cal M, Bolin C, Vescovo G, et al. Levels of Proinflammatory Cytokines, Oxidative Stress, and Tissue Damage Markers in Patients with Acute Heart Failure with and without Cardiorenal Syndrome Type 1. *CardioRenal Med.* 2018;8(4):321–31.
203. Schanz M, Shi J, Wasser C, Alscher MD, Kimmel M. Urinary [TIMP-2] × [IGFBP7] for risk prediction of acute kidney injury in decompensated heart failure. *Clin Cardiol.* 2017;40(7):485–91.
204. Fu K, Hu Y, Zhang H, Wang C, Lin Z, Lu H, et al. Insights of Worsening Renal Function in Type 1 Cardiorenal Syndrome: From the Pathogenesis, Biomarkers to Treatment. *Front Cardiovasc Med.* 2021;8(December):1–14.
205. Farley A, Hendry C, McLafferty E. Blood components. *Nurs Stand.* 2012;27(13):35–42.

-
206. Decramer S, de Peredo AG, Breuil B, Mischak H, Monsarrat B, Bascands JL, et al. Urine in clinical proteomics. *Mol Cell Proteomics*. 2008;7(10):1850–62.
 207. Harpole M, Davis J, Espina V. Current state of the art for enhancing urine biomarker discovery. *Expert Rev Proteomics*. 2016;9450(6):609–26.
 208. Gao Y. The Urine Proteome in Toxicology. *Chem Res Toxicol*. 2020;33(6):1281–3.
 209. Echeverry G, Hortin GL, Rai AJ. Introduction to Urinalysis: Historical Perspectives and Clinical Application. In: Rai AJ, editor. *The Urinary Proteome: Methods and Protocols*. Totowa, NJ: Humana Press; 2010. p. 1–12.
 210. Wu J, Li X, Zhao M, Huang H, Sun W, Gao Y. Early Detection of Urinary Proteome Biomarkers for Effective Early Treatment of Pulmonary Fibrosis in a Rat Model. *Proteomics - Clin Appl*. 2017;11(11–12).
 211. McArdle AJ, Menikou S. What is proteomics? *Arch Dis Child Educ Pract Ed*. 2020;178–81.
 212. Thomas A, Lenglet S, Chaurand P, Déglon J, Mangin P, Mach F, et al. Mass spectrometry for the evaluation of cardiovascular diseases based on proteomics and lipidomics. *Thromb Haemost*. 2011;106(1):20–33.
 213. Vlahou A, Fountoulakis M. Proteomic approaches in the search for disease biomarkers. *J Chromatogr B Anal Technol Biomed Life Sci*. 2005;814(1):11–9.
 214. Gao Y. Urine Is a Better Biomarker Source Than Blood Especially for Kidney Diseases. In: Gao Y, editor. *Urine Proteomics in*

- Kidney Disease Biomarker Discovery. Dordrecht: Springer Netherlands; 2015. p. 3–12.
215. Ho J, Lucy M, Krokhn O, Hayglass K, Pascoe E, Darroch G, et al. Mass Spectrometry-Based Proteomic Analysis of Urine in Acute Kidney Injury Following Cardiopulmonary Bypass: A Nested Case-Control Study. *Am J Kidney Dis.* 2009;53(4):584–95.
216. Zubiri I, Posada-Ayala M, Sanz-Maroto A, Calvo E, Martin-Lorenzo M, Gonzalez-Calero L, et al. Diabetic nephropathy induces changes in the proteome of human urinary exosomes as revealed by label-free comparative analysis. *J Proteomics.* 2014;96:92–102.
217. Orenes-Piñero E, Cortón M, González-Peramato P, Algaba F, Casal I, Serrano A, et al. Searching urinary tumor markers for bladder cancer using a two-dimensional differential gel electrophoresis (2D-DIGE) approach. *J Proteome Res.* 2007;6(11):4440–8.
218. Kohler M, Schänzer W, Thevis M. Effects of Exercise on the Urinary Proteome. In: Gao Y, editor. *Urine Proteomics in Kidney Disease Biomarker Discovery.* Dordrecht: Springer Netherlands; 2015. p. 121–31.
219. Castagna A, Channavajjhala SK, Pizzolo F, Olivieri O. Hormone-Dependent Changes in Female Urinary Proteome. In: Gao Y, editor. *Urine Proteomics in Kidney Disease Biomarker Discovery.* Dordrecht: Springer Netherlands; 2015. p. 103–20.
220. Virreira Winter S, Karayel O, Strauss MT, Padmanabhan S, Surface M, Merchant K, et al. Urinary proteome profiling for stratifying patients with familial Parkinson's disease. *EMBO Mol*

- Med. 2021;13(3):1–19.
221. Aragón CC, Tafúr RA, Suárez-Avellaneda A, Martínez MT, Salas A de las, Tobón GJ. Urinary biomarkers in lupus nephritis. *J Transl Autoimmun.* 2020;3(100042).
222. Raimondo F, Corbetta S, Chinello C, Pitto M, Magni F. The urinary proteome and peptidome of renal cell carcinoma patients: A comparison of different techniques. *Expert Rev Proteomics.* 2014;11(4):503–14.
223. Capolongo G, Zacchia M, Perna A, Viggiano D, Capasso G. Urinary proteome in inherited nephrolithiasis. *Urolithiasis.* 2019;47(1):91–8.
224. Seol W, Kim H, Son I. Urinary biomarkers for neurodegenerative diseases. *Exp Neurobiol.* 2020;29(5):325–33.
225. Farmakis D, Koeck T, Mullen W, Parissis J, Gogas BD, Nikolaou M, et al. Urine proteome analysis in heart failure with reduced ejection fraction complicated by chronic kidney disease: feasibility, and clinical and pathogenetic correlates. *Eur J Heart Fail.* 2016;18(7):822–9.
226. Templeton EM, Lassé M, Kleffmann T, Ellmers LJ, Palmer SC, Davidson T, et al. Identifying Candidate Protein Markers of Acute Kidney Injury in Acute Decompensated Heart Failure. *Int J Mol Sci.* 2022;23(2):1009.
227. Malagrino PA, Venturini G, Yogi PS, Dariolli R, Padilha K, Kiers B, et al. Proteome analysis of acute kidney injury – Discovery of new predominantly renal candidates for biomarker of kidney disease. *J Proteomics.* 2017;151:66–73.
228. Ferlizza E, Isani G, Dondi F, Andreani G, Vasylyeva K, Bellei E,

- et al. Urinary proteome and metabolome in dogs (*Canis lupus familiaris*): The effect of chronic kidney disease. *J Proteomics*. 2020;222:103795.
229. Hou LN, Li F, Zeng QC, Su L, Chen PA, Xu ZH, et al. Excretion of Urinary Orosomucoid 1 Protein Is Elevated in Patients with Chronic Heart Failure. *PLoS One*. 2014;9(9):107550.
230. Nguyen MT, Ross GF, Dent CL, Devarajan P. Early Prediction of Acute Renal Injury Using Urinary Proteomics. *Am J Nephrol*. 2005;25(4):318–26.
231. Kuznetsova T, Mischak H, Mullen W, Staessen JA. Urinary proteome analysis in hypertensive patients with left ventricular diastolic dysfunction. *Eur Heart J*. 2012;33(18):2342–50.
232. He T, Mischak M, Clark AL, Campbell RT, Delles C, Díez J, et al. Urinary peptides in heart failure: a link to molecular pathophysiology. *Eur J Heart Fail*. 2021;2.
233. He T, Siwy J, Metzger J, Mullen W, Mischak H, Schanstra JP, et al. Associations of urinary polymeric immunoglobulin receptor peptides in the context of cardio-renal syndrome. *Sci Rep*. 2020;10(1).
234. Melenovsky V, Cervenka L, Viklicky O, Franekova J, Havlenova T, Behounek M, et al. Kidney response to heart failure: Proteomic analysis of cardiorenal syndrome. *Kidney Blood Press Res*. 2018;43(5):1437–50.
235. Büttner P, Werner S, Baskal S, Tsikas D, Adams V, Lurz P, et al. Arginine metabolism and nitric oxide turnover in the ZSF1 animal model for heart failure with preserved ejection fraction. *Sci Rep*. 2021;11(1).

236. Baskal S, Büttner P, Werner S, Besler C, Lurz P, Thiele H, et al. Profile of urinary amino acids and their post-translational modifications (PTM) including advanced glycation end-products (AGEs) of lysine, arginine and cysteine in lean and obese ZSF1 rats. *Amino Acids*. 2021;1–10.
237. Rossing K, Bosselmann HS, Gustafsson F, Zhang ZY, Gu YM, Kuznetsova T, et al. Urinary proteomics pilot study for biomarker discovery and diagnosis in heart failure with reduced ejection fraction. *PLoS One*. 2016;11(6):1–15.
238. Zhang ZY, Ravassa S, Nkuipou-Kenfack E, Yang WY, Kerr SM, Koeck T, et al. Novel Urinary Peptidomic Classifier Predicts Incident Heart Failure. *J Am Heart Assoc*. 2017;6(8).
239. Cooper LB, Bruce S, Psocka M, Mentz R, Bell R, Seliger SL, et al. Proteomic differences among patients with heart failure taking furosemide or torsemide. *Clin Cardiol*. 2022;45(3):265–72.
240. McLafferty FW, Breuker K, Jin M, Han X, Infusini G, Jiang H, et al. Top-down MS, a powerful complement to the high capabilities of proteolysis proteomics. *FEBS J*. 2007;274(24):6256–68.
241. Aslam B, Basit M, Nisar MA, Khurshid M, Rasool MH. Proteomics: Technologies and their applications. *J Chromatogr Sci*. 2017;55(2):182–96.
242. Smith R. Two-Dimensional Electrophoresis: An Overview. *Methods Mol Biol*. 2009;519:2–17.
243. Smithies O, Poulik M. Two-dimensional electrophoresis of serum proteins. *Nature*. 1956;177(4518):1033.
244. Naryzhny S. Towards the full realization of 2DE power. *Proteomes*. 2016;4(4):1–15.

-
245. O'Farrell PH. High resolution two-dimensional electrophoresis. *J Biol Chem.* 1975;25(250):4007–21.
246. Rabilloud T, Vuillard L, Gilly C, Lawrence J. Silver-staining of proteins in polyacrylamide gels: a general overview. *Cell Mol Biol.* 1994;40(1):55–75.
247. Chevalier F, Centeno D, Rofidal V, Tauzin M, Martin O, Sonamerer N, et al. Different impact of staining procedures using visible stains and fluorescent dyes for large-scale investigation of proteomes by MALDI-TOF mass spectrometry. *J Proteome Res.* 2006;5(3):512–20.
248. Ünlü M, Morgan ME, Minden JS. Difference gel electrophoresis: A single gel method for detecting changes in protein extracts. *Electrophoresis.* 1997;18(11):2071–7.
249. Patton WF. Proteome analysis. II. Protein subcellular redistribution: Linking physiology to genomics via the proteome and separation technologies involved. *J Chromatogr B Biomed Sci Appl.* 1999;722(1–2):203–23.
250. Karas M, Bachmann D, Hillenkamp F. Influence of the Wavelength in High-Irradiance Ultraviolet Laser Desorption Mass Spectrometry of Organic Molecules. *Anal Chem.* 1985;57(14):2935–9.
251. Tanaka K, Waki H, Ido Y, Akita S, Yoshida Y, Yoshida T, et al. Protein and polymer analyses up to m/z 100 000 by laser ionization time-of-flight mass spectrometry. *Rapid Commun Mass Spectrom.* 1988;2(8):151–3.
252. Woods AG, Sokolowska I, Ngounou Wetie AG, Channaveerappa D, Dupree EJ, Jayathirtha M, et al. Mass Spectrometry for

- Proteomics-Based Investigation. In: Woods AG, Darie CC, editors. *Advancements of Mass Spectrometry in Biomedical Research*. Cham: Springer International Publishing; 2019. p. 1–26.
253. Cubedo Ràfols J. *Identificación de nuevos biomarcadores en los síndromes coronarios agudos*. Universitat de Barcelona; 2012.
254. Pais RJ, Iles RK, Zmuidinaite R. MALDI-ToF Mass Spectra Phenomic Analysis for Human Disease Diagnosis Enabled by Cutting-Edge Data Processing Pipelines and Bioinformatics Tools. *Curr Med Chem*. 2020;28(32):6532–47.
255. Duncan MW, Nedelkov D, Walsh R, Hattan SJ. Applications of MALDI mass spectrometry in clinical chemistry. *Clin Chem*. 2016;62(1):134–43.
256. Dudley E. MALDI Profiling and Applications in Medicine. In: Woods AG, Darie CC, editors. *Advancements of Mass Spectrometry in Biomedical Research*. Cham: Springer International Publishing; 2019. p. 27–43.
257. Alonso R, Defesche JC, Tejedor D, Castillo S, Stef M, Mata N, et al. Genetic diagnosis of familial hypercholesterolemia using a DNA-array based platform. *Clin Biochem*. 2009;42(9):899–903.
258. Cubedo J, Padró T, Alonso R, Mata P, Badimon L. ApoL1 levels in high density lipoprotein and cardiovascular event presentation in patients with familial hypercholesterolemia. *J Lipid Res*. 2016;57(6):1059–73.
259. García-Arguinzonis M, Padró T, Lugano R, Llorente-Cortes V, Badimon L. Low-density lipoproteins induce heat shock protein 27 dephosphorylation, oligomerization, and subcellular

- relocalization in human vascular smooth muscle cells. *Arterioscler Thromb Vasc Biol.* 2010;30(6):1212–9.
260. Lugano R, Peña E, Badimon L, Padró T. Aggregated low-density lipoprotein induce impairment of the cytoskeleton dynamics through urokinase-type plasminogen activator/urokinase-type plasminogen activator receptor in human vascular smooth muscle cell. *J Thromb Haemost.* 2012;10(10):2158–67.
261. Lugano R, Peña E, Casani L, Badimon L, Padró T. UPA promotes lipid-loaded vascular smooth muscle cell migration through LRP-1. *Cardiovasc Res.* 2013;100(2):262–71.
262. Padró T, Peña E, García-Arguinzonis M, Llorente-Cortes V, Badimon L. Low-density lipoproteins impair migration of human coronary vascular smooth muscle cells and induce changes in the proteomic profile of myosin light chain. *Cardiovasc Res.* 2008;77(1):211–20.
263. Padró T, Lugano R, García-Arguinzonis M, Badimon L. LDL-induced impairment of human vascular smooth muscle cells repair function is reversed by HMG-CoA reductase inhibition. *PLoS One.* 2012;7(6).
264. Benjamini Y, Krieger AM, Yekutieli D. Adaptive linear step-up procedures that control the false discovery rate. *Biometrika.* 2006;93(3):491–507.
265. Teerlink JR, Alburikan K, Metra M, Rodgers JE. Acute Decompensated Heart Failure Update. *Curr Cardiol Rev.* 2015;11:53–62.
266. Wu J, Wang W, Chen Z, Xu F, Zheng Y. Proteomics applications in biomarker discovery and pathogenesis for abdominal aortic

- aneurysm. *Expert Rev Proteomics*. 2021;18(4):305–14.
267. Laribi S, Mebazaa A. Cardiohepatic syndrome: Liver injury in decompensated heart failure. *Curr Heart Fail Rep*. 2014;11(3):236–40.
268. Biegus J, Zymlirski R, Sokolski M, Siwołowski P, Gajewski P, Nawrocka-Millward S, et al. Impaired hepato-renal function defined by the MELD XI score as prognosticator in acute heart failure. *Eur J Heart Fail*. 2016;18(12):1518–21.
269. McCullough PA, Kellum JA, Haase M, Müller C, Damman K, Murray PT, et al. Pathophysiology of the cardiorenal syndromes: Executive summary from the eleventh consensus conference of the acute dialysis quality initiative (ADQI). *Contrib Nephrol*. 2013;182:82–98.
270. Liu C, Lim ST, Teo MHY, Tan MSY, Kulkarni MD, Qiu B, et al. Collaborative Regulation of LRG1 by TGF- β 1 and PPAR- β/δ Modulates Chronic Pressure Overload-Induced Cardiac Fibrosis. *Circ Hear Fail*. 2019;12(12):1–16.
271. Sörensen-Zender I, Bhayana S, Susnik N, Rolli V, Batkai S, Baisantry A, et al. Zinc- α 2-Glycoprotein Exerts Antifibrotic Effects in Kidney and Heart. *J Am Soc Nephrol*. 2015;26:2659–68.
272. Lubrano V, Vergaro G, Maltinti M, Ghionzoli N, Emdin M, Papa A. α -1 Antitrypsin as a potential biomarker in chronic heart failure. *J Cardiovasc Med*. 2020;21(3):209–15.
273. Thomas AM, Chaban V, Pischke SE, Orrem HL, Bosnes V, Sunde K, et al. Complement ratios C3bc/C3 and sC5b-9/C5 do not increase the sensitivity of detecting acute complement activation systemically. *Mol Immunol*. 2022;141:273–9.

-
274. Holt MF, Michelsen AE, Shahini N, Bjørkelund E, Bendz CH, Massey RJ, et al. The Alternative Complement Pathway Is Activated Without a Corresponding Terminal Pathway Activation in Patients With Heart Failure. *Front Immunol.* 2021;12:800978.
275. Gao W, Wang H, Zhang L, Cao Y, Bao JZ, Liu ZX, et al. Retinol-binding protein 4 induces cardiomyocyte hypertrophy by activating TLR4/MyD88 pathway. *Endocrinology.* 2016;157(6):2282–93.
276. Bobbert P, Weithäuser A, Andres J, Bobbert T, Kühl U, Schultheiss HP, et al. Increased plasma retinol binding protein 4 levels in patients with inflammatory cardiomyopathy. *Eur J Heart Fail.* 2009;11(12):1163–8.
277. Cubedo J, Padró T, Cinca J, Mata P, Alonso R, Badimon L. Retinol-binding protein 4 levels and susceptibility to ischaemic events in men. *Eur J Clin Invest.* 2014;44(3):266–75.
278. Norden AGW, Lapsley M, Unwin RJ. Urine retinol-binding protein 4. A functional biomarker of the proximal renal tubule. 1st ed. Vol. 63, *Advances in Clinical Chemistry.* Elsevier Inc.; 2014. 85–122 p.
279. Ruberg FL, Berk JL. Transthyretin (TTR) Cardiac Amyloidosis. *Circulation.* 2012;126(10):1286–300.
280. Mohammed SF, Mirzoyev SA, Edwards WD, Dogan A, Grogan DR, Dunlay SM, et al. Left ventricular amyloid deposition in patients with heart failure and preserved ejection fraction. *JACC Hear Fail.* 2014;2(2):113–22.
281. Kapoor M, Rossor AM, Laura M, Reilly MM. Clinical presentation, diagnosis and treatment of TTR amyloidosis. *J Neuromuscul Dis.*

- 2019;6(2):189–99.
282. Vieira M, Saraiva MJ. Transthyretin: A multifaceted protein. *Biomol Concepts*. 2014;5(1):45–54.
283. Leite AR, Neves JS, Borges-Canha M, Vale C, Von Hafe M, Carvalho D, et al. Evaluation of thyroid function in patients hospitalized for acute heart failure. *Int J Endocrinol*. 2021;2021.
284. Schmidt-Ott UM, Ascheim DD. Thyroid Hormone and Heart Failure. *Curr Heart Fail Rep*. 2006;3:114–9.
285. Monu, Kharb R, Sharma A, Chaddar MK, Yadav R, Agnihotri P, et al. Plasma proteome profiling of coronary artery disease patients: Downregulation of transthyretin—an important event. *Mediators Inflamm*. 2020;2020:3429541.
286. Wang W, Wang CS, Ren D, Li T, Yao HC, Ma SJ. Low serum prealbumin levels on admission can independently predict in-hospital adverse cardiac events in patients with acute coronary syndrome. *Med (United States)*. 2018;97(30):1–5.
287. Cubedo J, Padró T, Alonso R, Cinca J, Mata P, Badimon L. Differential proteomic distribution of TTR (pre-albumin) forms in serum and HDL of patients with high cardiovascular risk. *Atherosclerosis*. 2012;222(1):263–9.
288. Raghu P, Sivakumar B. Interactions amongst plasma retinol-binding protein, transthyretin and their ligands: Implications in vitamin A homeostasis and transthyretin amyloidosis. *Biochim Biophys Acta - Proteins Proteomics*. 2004;1703(1):1–9.
289. Porcari A, Merlo M, Rapezzi C, Sinagra G. Transthyretin amyloid cardiomyopathy: An uncharted territory awaiting discovery. *Eur J Intern Med*. 2020;82:7–15.

290. Greve AM, Christoffersen M, Frikke-Schmidt R, Nordestgaard BG, Tybjaerg-Hansen A. Association of Low Plasma Transthyretin Concentration with Risk of Heart Failure in the General Population. *JAMA Cardiol.* 2021;6(3):258–66.
291. Judge DP, Heitner SB, Falk RH, Maurer MS, Shah SJ, Witteles RM, et al. Transthyretin Stabilization by AG10 in Symptomatic Transthyretin Amyloid Cardiomyopathy. *J Am Coll Cardiol.* 2019;74(3):285–95.
292. McComb S, Thiriot A, Akache B, Krishnan L, Stark F. Introduction to the Immune System. In: Fulton KM, Twine SM, editors. *Immunoproteomics: Methods and Protocols.* New York, NY: Springer New York; 2019. p. 1–24.
293. Dzik S. Complement and Coagulation: Cross Talk Through Time. *Transfus Med Rev.* 2019;33(4):199–206.
294. Hess K, Ajjan R, Phoenix F, Dobó J, Gál P, Schroeder V. Effects of MASP-1 of the complement system on activation of coagulation factors and plasma clot formation. *PLoS One.* 2012;7(4).
295. Krarup A, Wallis R, Presanis JS, Gál P, Sim RB. Simultaneous activation of complement and coagulation by MBL-associated serine protease 2. *PLoS One.* 2007;2(7):1–8.
296. Amara U, Flierl MA, Rittirsch D, Klos A, Chen H, Acker B, et al. Molecular Intercommunication between the Complement and Coagulation Systems. *J Immunol.* 2010;185(9):5628–36.
297. Irmischer S, Döring N, Halder LD, Jo EAH, Kopka I, Dunker C, et al. Kallikrein Cleaves C3 and Activates Complement. *J Innate Immun.* 2018;10(2):94–105.

298. Rezaie AR, Giri H. Anticoagulant and signaling functions of antithrombin. *J Thromb Haemost.* 2020;18(12):3142–53.
299. Suffritti C, Tobaldini E, Schiavon R, Strada S, Maggioni L, Mehta S, et al. Complement and contact system activation in acute congestive heart failure patients. *Clin Exp Immunol.* 2017;190(2):251–7.
300. Adamo L, Rocha-Resende C, Prabhu SD, Mann DL. Reappraising the role of inflammation in heart failure. *Nat Rev Cardiol.* 2020;17(5):269–85.
301. Shah AM. Ventricular Remodeling in Heart Failure with Preserved Ejection Fraction. *Curr Heart Fail Rep.* 2013;10(4):341–9.
302. Theocharis AD, Skandalis SS, Gialeli C, Karamanos NK. Extracellular matrix structure. *Adv Drug Deliv Rev.* 2016;97:4–27.
303. Latic N, Erben RG. Vitamin D and cardiovascular disease, with emphasis on hypertension, atherosclerosis, and heart failure. *Int J Mol Sci.* 2020;21(18):1–15.
304. Wu J, Garami M, Cheng T, Gardner DG. 1,25 (OH)₂ vitamin D₃ and retinoic acid antagonize endothelin-stimulated hypertrophy of neonatal rat cardiac myocytes. *J Clin Invest.* 1996 Apr 1;97(7):1577–88.
305. Rahman A, Hershey S, Ahmed S, Nibbelink K, Simpson RU. Heart extracellular matrix gene expression profile in the vitamin D receptor knockout mice. *J Steroid Biochem Mol Biol.* 2007;103(3–5):416–9.
306. Marshall Brinkley D, Ali OM, Zalawadiya SK, Wang TJ. Vitamin D and Heart Failure. *Curr Heart Fail Rep.* 2017;14(5):410–20.

-
307. Bouillon R, Schuit F, Antonio L, Rastinejad F. Vitamin D Binding Protein: A Historic Overview. *Front Endocrinol (Lausanne)*. 2020;10(January):1–21.
 308. Bagshaw SM, Bellomo R. Cystatin C in acute kidney injury. *Curr Opin Crit Care*. 2010;16(6):533–9.
 309. Nykjaer A, Dragun D, Walther D, Vorum H, Jacobsen C, Herz J, et al. An endocytic pathway essential for renal uptake and activation of the steroid 25-(OH) vitamin D3. *Cell*. 1999;96(4):507–15.
 310. Anderson JL, May HT, Horne BD, Bair TL, Hall NL, Carlquist JF, et al. Relation of vitamin D deficiency to cardiovascular risk factors, disease status, and incident events in a general healthcare population. *Am J Cardiol*. 2010;106(7):963–8.
 311. Teng M, Wolf M, Ofsthun MN, Lazarus JM, Hernán MA, Camargo CA, et al. Activated injectable vitamin D and hemodialysis survival: A historical cohort study. *J Am Soc Nephrol*. 2005;16(4):1115–25.
 312. Wolf M, Shah A, Gutierrez O, Ankers E, Monroy M, Tamez H, et al. Vitamin D levels and early mortality among incident hemodialysis patients. *Kidney Int*. 2007;72(8):1004–13.
 313. Figures 1, 3, 6-10, 12, and 14-16 created with Biorender.com

